Vol. 59 FEBRUARY, 1955 No. 2

THE JOURNAL OF PHYSICAL CHEMISTRY

(Registered in U. S. Patent Office)

SYMPOSIUM ON HIGH TEMPERATURE CHEMICAL REACTIONS, NEW YORK, N. Y., SEPTEMBER, 1954

Michael Hoch, Paul E. Blackburn, David P. Dingledy and Herrick L. Johnston: The Heat of Sublimation of Carbon. 97
William A. Chupka and Mark G. Inghram: Direct Determination of the Heat of Sublimation of Carbon with the Mass Spectrometer. 100
Leo Brewer and James S. Kane: The Importance of Complex Gaseous Molecules in High Temperature Systems. 105
A. E. Douglas: Recent Spectroscopic Studies of Simple Molecules. 109
N. W. Gregory and R. O. MacLaren: Vaporization Reactions: The Iron–Bromine System. 110
Gordon B. Skinner and Robert A. Ruehrwein: Thermodynamic Properties of the Titanium Chlorides. 113
E. R. Van Artsdalen and I. S. Yaffe: Electrical Conductance and Density of Molten Salt Systems: KCl–LiCl, KCl–NaCl and KCl–KI. 118
Warren O. Groves, Michael Hoch and Herrick L. Johnston: Vapor–Solid Equilibria in the Titanium–Oxygen System 127
John R. Soulen, Prasom Sthapitanonda and John L. Margrave: Vaporization of Inorganic Substances: B_2O_3, TeO_2 and Mg_3N_2. 132
H. R. Hoekstra, S. Siegel, L. H. Fuchs and J. J. Katz: The Uranium–Oxygen System: $UO_{2.5}$ to U_3O_8. 136
Ketil Motzfeldt: The Thermal Decomposition of Sodium Carbonate by the Effusion Method. 139
W. A. Weyl: Atomistic Interpretation of the Melting of Simple Compounds. 147
Tormod Forland: An Investigation of the Activity of Calcium Carbonate in Mixtures of Fused Salts. 152
Milton Farber and A. J. Darnell: The Disproportionation and Vapor Pressure of $TiCl_3$. 156

* * * * * * *

M. L. Lakhanpal, R. K. Sud and Balwant Rai Puri: Influence of Capillarity on the Boiling Point of Water. 160
Harold L. Friedman: On the Thermodynamics of the Interaction between the Solutes in Dilute Ternary Solutions. 161
George J. Levinskas and William F. Neuman: The Solubility of Bone Mineral. I. Solubility Studies of Synthetic Hydroxylapatite. 164
Hugo Fricke: The Complex Conductivity of a Suspension of Stratified Particles of Spherical or Cylindrical Form. 168
Reed M. Izatt, W. Conard Fernelius, C. G. Haas, Jr., and B. P. Block: Studies on Coördination Compounds. XI. Formation Constants of Some Tervalent Ions and the Thorium (IV) Ion with the Acetylacetonate Ion. 170
O. J. Kleppa: A New High Temperature Reaction Calorimeter: The Heats of Mixing of Liquid Lead–Tin Alloys. 175
Mark P. Freeman and G. D. Halsey, Jr.: The Interaction of Pairs of Gas Atoms with Surfaces. 181
R. O. MacLaren and N. W. Gregory: The Vapor Pressure of Iron(II) Bromide. 184
NOTE: **N. Krishnaswamy:** Chloride Uptake by Ion-exchange Membranes in Different Chloride Solutions. 187
NOTE: **G. J. Rotariu, D. W. Fraga and J. H. Hildebrand:** The Density of *n*-Octane and 2,2,3,3-Tetramethylbutane at Low Temperatures. 187
NOTE: **Thor L. Smith:** The Solubility of Chlorine in Carbon Tetrachloride. 188
NOTE: **Joseph A. Faucher and Henry C. Thomas:** Exchange between Heavy Water and Clay Minerals. 189
NOTE: **Fraser P. Price:** Light Scattering from Crystallizing Polymers. 191

THE JOURNAL OF PHYSICAL CHEMISTRY

(Registered in U. S. Patent Office)

Published monthly by the American Chemical Society at 20th and Northampton Sts., Easton, Pa.

Entered as second-class matter at the Post Office at Easton, Pennsylvania.

The *Journal of Physical Chemistry* is devoted to the publication of selected symposia in the broad field of physical chemistry and to other contributed papers.

Manuscripts originating in the British Isles, Europe and Africa should be sent to F. C. Tompkins, The Faraday Society, 6 Gray's Inn Square, London W. C. 1, England.

Manuscripts originating elsewhere should be sent to W. Albert Noyes, Jr., Department of Chemistry, University of Rochester, Rochester 3, N. Y.

Correspondence regarding accepted copy, proofs and reprints should be directed to Assistant Editor, Allen D. Bliss, Department of Chemistry, Simmons College, 300 The Fenway, Boston 15, Mass.

Business Office: American Chemical Society, 1155 Sixteenth St., N. W., Washington 6, D. C.

Advertising Office: Reinhold Publishing Corporation, 430 Park Avenue, New York 22, N. Y.

Articles must be submitted in duplicate, typed and double spaced. They should have at the beginning a brief Abstract, in no case exceeding 300 words. Original drawings should accompany the manuscript. Lettering at the sides of graphs (black on white or blue) may be pencilled in, and will be typeset. Figures and tables should be held to a minimum consistent with adequate presentation of information. Photographs will not be printed on glossy paper except by special arrangement. All footnotes and references to the literature should be numbered consecutively and placed in the manuscript at the proper places. Initials of authors referred to in citations should be given. Nomenclature should conform to that used in *Chemical Abstracts*, mathematical characters marked for italic, Greek letters carefully made or annotated, and subscripts and superscripts clearly shown. Articles should be written as briefly as possible consistent with clarity and should avoid historical background unnecessary for specialists.

Symposium papers should be sent in all cases to Secretaries of Divisions sponsoring the symposium, who will be responsible for their transmittal to the Editor. The Secretary of the Division by agreement with the Editor will specify a time after which symposium papers cannot be accepted. The Editor reserves the right to refuse to publish symposium articles, for valid scientific reasons. Each symposium paper may not exceed four printed pages (about sixteen double spaced typewritten pages) in length except by prior arrangement with the Editor.

Remittances and orders for subscriptions and for single copies, notices of changes of address and new professional connections, and claims for missing numbers should be sent to the American Chemical Society, 1155 Sixteenth St., N. W., Washington 6, D. C. Changes of address for the *Journal of Physical Chemistry* must be received on or before the 30th of the preceding month.

Claims for missing numbers will not be allowed (1) if received more than sixty days from date of issue (because of delivery hazards, no claims can be honored from subscribers in Central Europe, Asia, or Pacific Islands other than Hawaii), (2) if loss was due to failure of notice of change of address to be received before the date specified in the preceding paragraph, or (3) if the reason for the claim is "missing from files."

Subscription Rates: to members of the American Chemical Society, $8.00 for 1 year, $15.00 for 2 years, $22.00 for 3 years; to non-members, $10.00 for 1 year, $18.00 for 2 years, $26.00 for 3 years. Postage free to countries in the Pan American Union; Canada, $0.40; all other countries, $1.20. $12.50 per volume, foreign postage $1.20, Canadian postage $0.40; special rates for A.C.S. members supplied on request. Single copies, current volume, $1.00; foreign postage, $0.15; Canadian postage $0.05. Back issue rates (starting with Vol. 56): non-member, $1.50 per issue, foreign postage $0.15, Canadian postage $0.05.

The American Chemical Society and the Editors of the *Journal of Physical Chemistry* assume no responsibility for the statements and opinions advanced by contributors to THIS JOURNAL.

The American Chemical Society also publishes *Journal of the American Chemical Society*, *Chemical Abstracts*, *Industrial and Engineering Chemistry*, *Chemical and Engineering News*, *Analytical Chemistry*, and *Journal of Agricultural and Food Chemistry*. Rates on request.

THE JOURNAL OF PHYSICAL CHEMISTRY

(Registered in U. S. Patent Office)

VOLUME 59 FEBRUARY 21, 1955 NUMBER 2

THE HEAT OF SUBLIMATION OF CARBON[1]

BY MICHAEL HOCH, PAUL E. BLACKBURN, DAVID P. DINGLEDY AND HERRICK L. JOHNSTON

Contribution from The Cryogenic Laboratory and The Department of Chemistry, The Ohio State University, Columbus, Ohio

Received November 19, 1954

The heat of sublimation of carbon has been studied by measuring the partial pressure of carbon gas above graphite, tantalum carbide and tungsten carbide. The vacuum evaporation method of Langmuir was used; the temperature range investigated extended from 2170 to 2770°K. The partial pressures measured are of the same order of magnitude in all three cases. Therefore, the evaporation mechanisms of carbon from graphite and the carbides are identical. This implies that: (1) the accommodation coefficients of carbon gas on graphite and the carbides are closely the same and between 0.1 and unity; (2) the species in the gas are the same, the gas consisting to a considerable extent of C_1. Thus, the heat of sublimation of carbon is ΔH_0° = 170 kcal./mole at 0°K.

Introduction

The value for the heat of vaporization of carbon is not unequivocally determined, although much work has been done on the problem. From the interpretation of the CO spectrum (for detailed discussion see Gaydon[2b]) four values are possible for the heat of vaporization of graphite to C_1: 108.3, 124.7, 141.1 and 170.6 kcal./mole. To decide between these values, a thermodynamic determination is necessary. For the interpretation of the data, the following questions have to be taken into account: (1) electronic state and bonding of the carbon in the solid and gas phases, (2) molecular species in the gas, (3) accommodation coefficient of carbon gas on graphite surface.

The ground state of carbon is the ^3P state. Schmid and Gero[2] and Long and Norrish[3] postulated that in graphite the carbon is tetravalent and bound in the ^5S state, and vaporizes to the ^5S state. Herzberg[4] suggested that a large activation energy would be necessary to remove carbon from the solid ^5S state to the gaseous ^3P state. Herzberg, Herzfeld and Teller[5] showed that two C–C bonds have to be broken when removing the first carbon atom from a closed structure compound to $1^1/_2$ for the other carbons. This suggests that the dynamic value should be higher by 33% for ΔH_0° than the static value. Brewer, Gilles and Jenkins[6] concluded that C(g) is in the ^3P state. Chupka and Inghram[7] measured the ionization potential of C_1(g) and found it equal to the known value for the ^3P state. This proves conclusively that C(g) is in the ^3P state.

The molecular species in the gas are of importance because the spectroscopic values for the dissociation of CO have to be combined with the heat of vaporization of graphite to C_1(g) atoms. Brewer, Gilles and Jenkins[6] measured the intensity of the O–O head of the Swan band of the C_2 molecules, and found that below 3000°K., C_2(g) is negligible compared to C_1(g). Honig[8] and Chupka and Inghram[7] studied the gas by a mass spectrometer and found large amounts of C_3 and C_2 species. Honig[8] and Waelbroeck[9] state that, in accordance with the theory of Herzberg. Herzfeld and Teller,[5] the rate-determining step is the vaporization of C_2; therefore any rate method measures the heat of vaporization of C_2.

The accommodation coefficient enters in the determination of the heat of vaporization; a small accommodation coefficient will give a large apparent heat of sublimation. Brewer, Gilles and Jenkins, comparing their Knudsen effusion results with Langmuir method data, found that α is around 0.3. On the other hand, Doerhard, Goldfinger and Waelbroeck[10] and Waelbroeck[9] concluded that α is small,

(1) This work was supported in part by the Office of Naval Research under contract with The Ohio State University Research Foundation.

(2) (a) R. Schmid and L. Gero, *Z. physik. Chem.*, **B36**, 105 (1937); (b) A. G. Gaydon, "Dissociation Energies," 2nd Edition, Chapman and Hall, Ltd., London, 1953.

(3) L. H. Long and R. G. W. Norrish, *Nature*, **157**, 486 (1946).

(4) G. Herzberg, *Chem. Revs.*, **20**, 145 (1937).

(5) G. Herzberg, K. F. Herzfeld and E. Teller, *Z. physik. Chem.*, **41**, 325 (1937).

(6) L. Brewer, P. W. Gilles and F. A. Jenkins, *J. Chem. Phys.*, **16**, 797 (1948).

(7) W. A. Chupka and M. G. Inghram, *ibid.*, **21**, 371, 1373 (1953).

(8) R. E. Honig, *ibid.*, **22**, 126 (1954).

(9) F. Waelbroeck, *ibid.*, **20**, 751 (1952).

(10) T. Doerhard, P. Goldfinger and F. Waelbroeck, *ibid.*, **20**, 757 (1952).

less than 10^{-3}. Further, according to Doerhard, Goldfinger and Waelbroeck α varies with the temperature so that the method used to check α (constancy of ΔH_0° with temperature, $RT \ln \alpha = 0$, $\alpha = 1$) cannot be used. Furthermore, the spread in the values for ΔH_0° obtained over temperature range of 500° [11] is large, and it would mask any trend in ΔH_0°.

All the previous workers used graphite as starting material. In this work, we approached the problem by measuring the rate of evaporation of carbon from graphite and from two carbides, TaC and WC + W_2C. The rates of evaporation from the three materials were compared, and answers to the question of molecular species and accommodation coefficient obtained.

TaC is cubic, having a NaCl structure. WC is a simple hexagonal W lattice, having alternate layers of W and C. W_2C is, according to Westgren and Phragmen,[12] a closed packed hexagonal W lattice, the C atoms being placed interstitially as a solution of C_1.

From the heats of formation, TaC $\Delta H_{f298} = -38.6$ kcal./mole,[13] and WC $\Delta H_{f298} = -9.09$ kcal./mole,[14] we see that the activity of carbon in TaC is lowered, but in WC and W_2C is almost equal to that in graphite.

The explanation for the vaporization of graphite, given by Herzberg, Herzfeld and Teller,[5] requires a structure of odd coördination numbers, so that alternate atoms have different ease of removal. We have, according to this explanation, a hindrance, due to the structure of graphite, lowering the pressure measured dynamically by a factor of 10^4. By vaporizing carbon from TaC and W_2C, where this hindrance does not exist, we should get higher evaporation rates from TaC and W_2C than from graphite.

If, however, the rates of evaporation from graphite, TaC and WC + W_2C are of the same order of magnitude, then the evaporating mechanisms are the same on the three surfaces.

Apparatus and Experimental Procedure

The preparation of the carbides and the vaporization experiments were carried out in our new vapor pressure cell.[15] The temperature was measured with a disappearing filament optical pyrometer, calibrated against a standard lamp. The standard tungsten lamp had been calibrated by the National Bureau of Standards up to 2300°, where the uncertainty was 8°.

The graphite sample was turned from Acheson graphite into a cylinder, 1″ high, $^3/_4$″ o.d. and $^3/_{16}$″ wall thickness. The cell was degassed at 2800°K. for 20 minutes. The temperature was read on the surface; to obtain the true temperature, the emissivity values given by the "International Critical Tables" were used.

TaC and WC cells were prepared by carburizing Ta and W cells. Ta cells were made from Ta tubing 1″ high, $^1/_2$″ o.d. and 0.02″ wall thickness, and Ta sheet 0.010″ thick. Two holes, $^1/_{16}$″ diameter, were drilled into the top surface: one at the center, one at the edge. The W cells were made by bending a W ribbon 0.005″ thick, $^1/_4$″ wide into a cylinder, $^1/_2$″ diameter, welding the edges together, and welding a top and bottom to it. A hole, approximately $^1/_{16}$″ diameter, was ground in the top of the cell. These holes acted as the black bodies and were used to read the temperature. The Ta and W were obtained from the Fansteel Metallurgical Corporation. Before carburizing, the cells were degassed: Ta at 2600°K. for 0.5 hour, W at 2450°K. for 0.25 hour.

The cells were then packed with Acheson graphite in a tantalum container and heated for two hours at 2600°K. for TaC, and at 2350°K. for WC except for run 15, where the heating was only one hour. The use of different cells was necessitated by the fact that small cracks developed in them.

In the case of TaC, different cells were used for runs 6 and 7. The small cells were used for run 8 and 9, and another for 10 and 11. After run 8 and 10, the cells were re-carburized.

In the case of WC, three cells were used: one for run 12, one for runs 13 and 14, and one for run 15.

The composition of the sample was calculated from the weight-gain during carburization. To determine the solid phases present, X-ray diffraction patterns were taken with a Philips Norelco camera, using copper radiation, after runs 6, 9, 11 and 12, 14 and 15.

To account for the small temperature fluctuation during each run, for the evaporation during initial heating and for the small gradients in the sample, the averaging method[16] was used to calculate an "effective area" and an "effective time."

Experimental Results and Discussion of the Data

The experimental data are presented in Table I. The pressure was calculated from the rate of evaporation, using the equation $p = m/\alpha\sqrt{2\pi RT/M}$ where p is the pressure in atm., R is the molar gas constant, T is the absolute temperature, m is the rate of evaporation in g./sq. cm./sec. and M is the molecular weight of the vapor, and α is the accommodation coefficient.

For the case of TaC and WC, the composition of the solid phase is given in the second column. To prove that, in the case of the two carbides, only carbon and no metal was lost, the cells were re-carburized after runs 3 and 5. On re-carburization, only the vaporized carbon will be replaced, and not the vaporized metal. The weight gain corresponded, within experimental error, to the weight loss during the runs. This shows that only carbon was lost.

The X-ray diffraction pattern taken on TaC sample showed the TaC phase; for WC, in runs 1, 2 and 3 the solid phase consisted of WC and W_2C; whereas in run 4, due to the large W:C ratio, the W_2C phase only was present.

A comparison of the evaporation rates listed in Table I shows that they are of the same order of magnitude. The measured rates for TaC and WC + W_2C are not higher than those for graphite. This proves that there is no important structural hindrance inhibiting the vaporization of graphite by a factor of 10^3 or 10^4. The use of this mechanism to derive equations for the rate of evaporation[17] does not seem justified.

Due to the lower activity of carbon in TaC, the gas above TaC will contain more C_1 than above graphite and WC + W_2C. The rates measured for TaC are by a factor of 10 lower than those for graphite and WC + W_2C, which, within experimental error, are equal. From these results, we can

(11) (a) A. L. Marshall and F. J. Norton, *J. Am. Chem. Soc.*, **72**, 2166 (1950); (b) M. Farber and A. J. Darnell, *ibid.*, **74**, 3941 (1952).

(12) V. A. Westgren and G. Phragmen, *Z. anorg. allgem. Chem.*, **156**, 27 (1926).

(13) G. L. Humphrey, *J. Am. Chem. Soc.*, **76**, 978 (1954).

(14) F. D. Rossini, *et al.*, "Selected Values of Chemical Thermodynamic Properties," National Bureau of Standards, Circular No. 500.

(15) M. Hoch and H. L. Johnston, *J. Am. Chem. Soc.*, **76**, 4833 (1954).

(16) G. B. Skinner, J. W. Edwards and H. L. Johnston, *ibid.*, **73**, 174 (1951).

(17) T. Doerhard, P. Goldfinger and F. Waelbroeck, *Bull. soc. chim. Belges*, **62**, 498 (1953).

TABLE I

VAPOR PRESSURE OF CARBON

Run	Mole ratio metal to C	Temp., °K.	Wt. loss, g.	Effective time, sec.	Effective area, cm.²	Evaporation effusion rate, g./cm./sec. × 10⁷	P, atm. × 10⁷	−log P
				Above graphite				
5	..	2171	0.0009	14,286	17.6	0.0367	0.0111	8.954
2	..	2267	.0004	3,577	17.7	0.0649	0.0201	8.697
3	..	2482	.0139	3,764	17.6	2.098	0.680	7.167
4	..	2550	.0138	1,063	17.6	7.363	2.420	6.616
1	..	2743	.1866	983	17.6	108.1	36.85	5.434
				Above tantalum carbide				
9	1.00	2235	0.0009	26,956	11.7	0.0272	0.0084	9.077
6	1.11	2390	.0012	14,170	11.1	0.0776	0.0247	8.608
7	1.05	2495	.0017	6,013	11.4	0.2489	0.0809	8.092
8	1.00	2546	.0093	10,834	11.3	0.7611	0.250	7.602
10	1.00	2664	.0081	2,805	11.3	2.585	0.868	7.061
11	1.00	2765	.0067	955	10.9	6.465	2.213	6.677
				Above tungsten carbide				
13	1.96	2256	0.0014	30,827	5.0	0.0924	0.0286	8.544
12	1.81	2406	.0037	5,617	5.0	1.312	0.419	7.378
15	2.61	2743	.0076	436	4.9	35.57	12.13	5.916
14	1.96	2756	.0214	1,745	4.9	24.90	8.509	6.012

conclude that the accommodation coefficient of carbon on graphite and on the carbides cannot be greatly different, and probably lies between 0.1 and 1.0, and that monoatomic carbon must be an important species when all three vaporize.

In accordance with the above-mentioned facts in the calculation of the pressure, the accommodation coefficient was taken as unity and the molecular weight as 12, and the electronic state considered to be ^3P.

TABLE II

HEAT OF SUBLIMATION OF CARBON

Run	Temp., °K.	$-R \ln P$	$-\frac{\Delta F}{T}$	$\frac{\Delta H_0^\circ}{T}$	ΔH_0°
			From graphite		
5	2171	40.96	36.90	77.86	169.0
2	2267	39.78	36.91	76.69	173.9
3	2482	32.78	36.93	69.71	173.0
4	2550	30.26	36.94	67.20	171.4
1	2743	24.86	36.95	61.81	169.5
				Av. =	171.4 ± 2.2 kcal./mole
			From tantalum carbide		
9	2235	41.52	36.90	78.42	175.3
6	2390	39.37	36.92	76.29	182.3
7	2495	37.01	36.93	73.94	184.5
8	2546	34.77	36.93	71.70	182.5
10	2664	32.30	36.95	69.25	184.5
11	2765	30.54	36.96	67.50	186.6
				Av. =	182.6 ± 2.6 kcal./mole
			From tungsten carbide		
13	2256	39.08	36.91	75.99	171.4
12	2406	33.75	36.92	70.67	170.0
15	2743	27.06	36.95	64.01	175.6
14	2756	27.50	36.96	64.46	177.6
				Av. =	173.6 ± 2.8 kcal./mole

The pressures obtained are plotted in Fig. 1, together with the curves, which show what the pressure of C(g) would be if the heat of sublimation were 170.6, 141.7, 125.2, 108.7 kcal./mole. To obtain these curves, the free energy functions for C(g) and graphite given by the National Bureau of Standards were used.[18]

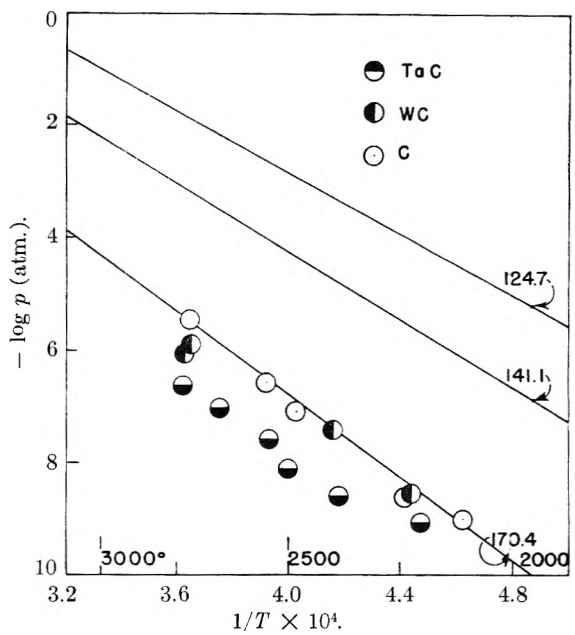

Fig. 1.—Vapor pressure of carbon.

It can be seen from Fig. 1 that all the points fall close to the curve, having $\Delta H_0^\circ = 170.6$ kcal.

To calculate the heat of sublimation of graphite, the free energy function of C(g) was used for the gas phase. As no free energy functions are available for TaC or WC, in all three cases we used the free energy function of graphite for the solid phase. This introduces a small error in the case of the carbides. Table II contains the data. These data show, as does Fig. 1, that the heat of sublimation of graphite to C(g) is $\Delta H_0^\circ = 170$ kcal./mole.

(18) "Selected Values of Chemical Thermodynamic Properties Series III," National Bureau of Standards.

DIRECT DETERMINATION OF THE HEAT OF SUBLIMATION OF CARBON WITH THE MASS SPECTROMETER[1]

BY WILLIAM A. CHUPKA[2] AND

Harvard University, Cambridge, Massachusetts

MARK G. INGHRAM[2]

University of Chicago, Chicago, Illinois

Received October 21, 1954

The vapor pressures and the temperature dependence of the vapor pressures of C, C_2 and C_3 above graphite have been measured. The experiment involved the use of a mass spectrometer to study separately the C, C_2 and C_3 effusing from a Knudsen cell. The measurements yield values of 170, 190 and 200 kcal./mole, respectively, for the heat of vaporization of these species. Conflicting results of other workers are discussed.

Introduction

The more recent attempts to determine the heat of sublimation of graphite directly have been of two types, namely, measurements of the rate of evaporation[3] and measurements of the equilibrium vapor pressure.[4] In addition, some experiments have employed mass spectrometric analysis of the vapor.[5,6] The rate of evaporation studies yield the activation energy of evaporation and various workers report values in the range 170–180 kcal./mole for this quantity. Studies employing mass spectrometric analysis show that C atoms and C_2 and C_3 molecules are present in comparable amounts. These mass spectrometric experiments give an activation energy for the sublimation of C atoms of about 177 kcal./mole. All these experiments are in agreement with $L(C) \leq 180$ kcal./mole.

Since rate of evaporation studies yield only the activation energy for evaporation, it has often been proposed that the heat of sublimation of carbon is considerably lower.[7] Spectroscopic studies of the CO molecule give several possible values for its dissociation energy.[8] When these are combined with other well-established thermochemical quantities, the values 170, 141 and 125 kcal./mole are obtained as possible values for the heat of sublimation of carbon. In order for one of the lower values to be correct, the evaporation of carbon atoms must take place with a low evaporation coefficient. Several mechanisms have been proposed which could cause such an effect.[7]

The measurements of the equilibrium vapor pressure of carbon, which are free of the effect of evaporation coefficient, have generally employed effusion from Knudsen cells. Experiments of this type have been carried out by Brewer, *et al.*,[4a] and by Goldfinger, *et al.*,[4b] and, as interpreted by these authors, indicated values of about 170 and 140 kcal./mole, respectively, for the heat of sublimation of carbon. Possible reasons for this discrepancy have been discussed.[9,10] Neither of these experiments employed analysis of the effusing vapor.

In the present work an apparatus has been developed which employs a Knudsen cell together with mass spectrometric analysis of the effusing vapor. The vapor pressures of C, C_2 and C_3 together with temperature dependences have been measured and heats of sublimation calculated.

Apparatus.—The mass spectrometer used was a single focusing 60°, 12″ radius of curvature instrument which had a resolving power of about $1/600$ for this experiment. The Knudsen cell assembly together with the mass spectrometer slit system is shown in Fig. 1. The three plates holding various components of the assembly are electrically insulated by quartz sleeves and spacers. The lowest plate supports the Knudsen cell by means of three tungsten rods and has provisions for precise alignment of the Knudsen cell by use of an auxiliary jig. The Knudsen cell itself is made of tantalum, has an effusion hole of 0.040″ diameter and is provided with a graphite liner. The inside area of the graphite liner is about 12 cm.^{2} so that σ, the ratio of effusion hole area to total inside area, is about $1/1500$. The middle plate of the assembly holds the tungsten support rods which support and provide electrical leads for two tungsten filaments. The temperature of the cell is measured with an optical pyrometer, which is sighted through a quartz window and a series of holes in the radiation shields. By means of electron bombardment from the tungsten filaments, cell temperatures somewhat greater than 2500°K. have been readily attained. It was found that the oven could be heated to about 1200°K. by radiation alone without any electron bombardment. To go to higher temperatures the filaments and radiation shields were kept at ground potential and the cell held in the range 500–1000 volts positive. The amount of bombardment current was adjusted by adjusting the filament heating current. A simple form of regulation resulted in cell temperatures being held constant to about $\pm 10°$ indefinitely.

A grounded plate containing a movable slit is positioned just above the radiation shields. The movable slit is actuated from outside through a flexible metal bellows and serves to sweep the effusing beam across the collimating slits before the ionization chamber. This slit thus serves as a shutter for the effusing vapor and provides a method of distinguishing between ions formed from the effusing vapor and those formed from residual gases in the source region of the mass spectrometer.

Above the shutter plate are two plates with collimating slits and following these the ionization chamber where the neutral atoms and molecules effusing from the Knudsen cell are bombarded with electrons of controlled energy and ionized. The ions are then focused and collimated by a series of plates and projected into the analyzer tube of the mass spectrometer. The geometry of the collimating slits and ionization chamber is such that practically all molecules

(1) This work was supported in large part by a grant from the National Science Foundation.

(2) Now with Argonne National Laboratory, Lemont, Ill.

(3) (a) A. Marshall and F. Norton, *J. Am. Chem. Soc.*, **72**, 2166 (1950); (b) O. Simpson, R. Thorne and G. Winslow, ANL-4264 (1949).

(4) (a) L. Brewer, P. Gilles and F. A. Jenkins, *J. Chem. Soc.*, **16**, 797 (1948); (b) Th. Doerhard, P. Goldfinger and F. Waelbroeck, *Bull. soc. chim. Belg.*, **62**, 498 (1953).

(5) W. A. Chupka and M. G. Inghram, *J. Chem. Phys.*, **21**, 371 (1953); **21**, 1313 (1953).

(6) R. E. Honig, *ibid.*, **22**, 126 (1954).

(7) For an excellent review, see H. B. Springall, *Research*, **3**, 260 (1950).

(8) A. G. Gaydon, "Dissociation Energies," Dover Publications, Inc., New York, N. Y., 1950, p. 175.

(9) P. Goldfinger and F. Waelbroeck, *Bull. soc. chim. Belg.*, **62**, 545 (1953).

(10) L. Brewer, *J. Chem. Phys.*, **20**, 758 (1952).

in the effusing beam make only one transit of the ionization chamber. A more detailed description of the apparatus will be published in another journal.

An electron multiplier was used for ion detection. Its output was measured by a vibrating reed electrometer and a strip chart recording potentiometer. Ion currents of 10^{-19} amp. were readily measured since the multiplier background corresponds to an ion current of about 10^{-20} amp.

Procedure.—A graphite liner made of very pure Acheson graphite was loaded into the tantalum Knudsen cell. In addition a weighed quantity of silver wire, usually about 10 mg., was placed inside that cell. The oven assembly was then mounted into position and the analyzer tube evacuated. The oven temperature was raised slowly by gradually increasing the current through the tungsten filaments surrounding the oven. The vacuum at all times was kept at 10^{-5} mm. or better.

When the temperature reached about 1250°K., Ag^+ and Ag^{++} ions were readily detected and a sensitivity calibration was begun. The purpose of the calibration was to determine the relation between the vapor pressure of a substance inside the Knudsen cell and the intensity of the corresponding ion. Two independent types of calibration were made. One consisted of measuring simultaneously the temperature of the oven and the intensity of the Ag^+ ion beam. The vapor pressure of silver at that temperature was then calculated from the data of K. K. Kelley,[11] and the sensitivity was expressed in terms of units of ion current per atmosphere of silver vapor in the cell. The other calibration consisted of integrating the Ag^+ ion intensity over the period of time required to vaporize the entire sample of silver out of the oven. Knowing the amount of silver sample evaporated and making use of Knudsen's effusion equation one can again calculate sensitivity. These two methods have generally yielded sensitivities agreeing within 50%. The integral calibration has been judged to be the more accurate. For convenience, the calibration was usually carried out by monitoring the Ag^{107++} ion beam since this occurs at a half-integer mass ($53^1/_2$) position which has almost no detectable background, whereas the mass 107 position has a considerably greater background due to a residual hydrocarbon peak. This background was easily subtracted by employing the shutter as will be described later, but it was simpler to determine the ratio Ag^+/Ag^{++} at the electron energy employed (150 volts) and thereafter monitor the Ag^{++} position without further use of the shutter.

During one of the calibrations a search was made for Ag_2^+ and Ag_3^+ ions in order to determine whether any significant amounts of silver evaporate as diatomic or triatomic molecules. No such ions were found and it was concluded that they were present in amounts less than 1% for the dimer and 5% for the trimer.

After the silver has been completely vaporized, the temperature of the oven was gradually raised. When the temperature finally reached about 2200°K., a search was made for C^+, C_2^+, C_3^+ and any other species which evaporate from the Knudsen cell. The intensities of these ions were then measured at various temperatures covering a range from about 2150°K. to about 2450°K.

The method of measuring ion intensities resulting from species evaporating from the Knudsen cell requires elaboration which must include a discussion of causes of difficulty with background. Background ions of the same mass as the species investigated result from residual gases present in the mass spectrometer. The total pressure of residual gas present in the mass spectrometer varied with the temperature of the cell due to outgassing. This pressure varied between about 10^{-5} mm. with the cell at the highest temperatures to about 10^{-8} mm. with the cell at room temperature. However, the effect of residual gas was practically negligible at the higher temperatures since the vapor pressure of the graphite rose much faster with temperature than did the residual gas pressure.

The operating procedure employed was designed to both minimize the amount of background and to make accurate corrections when the background was significant. The effect of background was minimized by using 17 volt electrons for ionization. This is roughly 6 volts above the ionization potentials of C, C_2 and C_3 as found earlier.[5] Since production of C^+, C_2^+ and C_3^+ ions by electron impact on residual hydrocarbons generally requires more energy than 17 volts, background from this source is greatly reduced.

(11) K. K. Kelley, Bureau of Mines Bulletin 383 (1935).

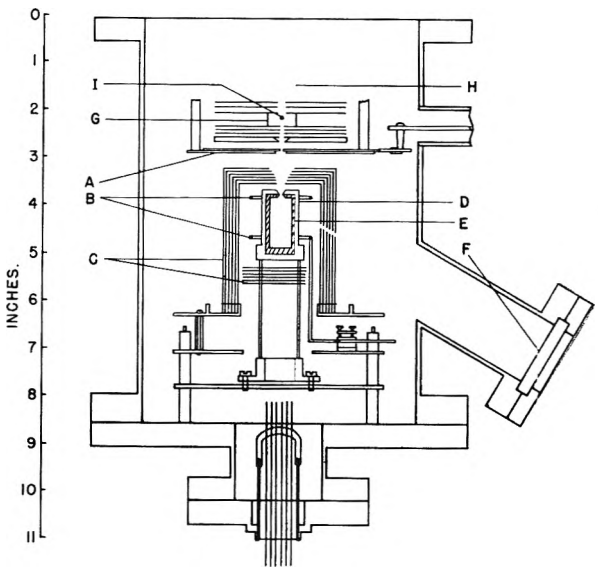

Fig. 1.—Knudsen cell for mass spectrometer: A, movable slit plate and mount; B, tungsten filaments; C, tantalum radiation shields; D, tantalum Knudsen cell; E, graphite liner; F, quartz window; G, ionization chamber; H, source focusing system; I, ionizing electron beam (cross-section).

The major background difficulty occurs for C^+ since C^+ can occur by electron impact on CO which is the major residual gas in the source. However, this process requires electron energies above 20.9 volts and is, therefore, absent when 17 volt electrons are used. Nevertheless, a very small amount of C^+ is still produced from CO at even these lower energies and is probably due to a second order process involving two electrons. Such a process was found to occur in CO at extremely low intensity in previous unreported work at this Laboratory. The C^+ intensity in this process was found to be proportional to the second power of the electron current and the appearance potential was about 14 volts. Since this is the ionization potential of CO, a possible mechanism which would fulfill requirements would be

$$CO + e^- \longrightarrow CO^+ + 2e^- \qquad E = 14 \text{ e.v.} \quad (1)$$

$$CO^+ + e^- \longrightarrow C^+ + O + e^- \qquad E \cong 8 \text{ e.v.} \quad (2)$$

Another source of background also was found. It is produced by an electrically neutral species which goes from the Knudsen cell into the ionization chamber. The evidence for its nature is the following. When the ionizing electron current is turned off completely, some small ion peaks are still observed. The peaks completely disappear when the shutter is moved to the "closed" position, and reappear when it is "opened." These peaks are unaffected by the electrostatic deflecting plates between the shutter and the ionization chamber. The ions are probably due to ionization by photoelectrons produced in the mass spectrometer slit system by radiation from the Knudsen cell. Since alkali metals are especially prominent in this background some of these ions may be formed by direct photoionization. Neutral excited species from the oven region may also play a part. For convenience, background of this nature will be referred to as due to the "photo" process.

The measurement of the ion intensity of a particular mass produced by electron bombardment of the neutral species evaporating from the Knudsen cell was made in the following manner (see Fig. 2). The magnetic field of the mass spectrometer was adjusted to focus the ion of interest into the collector. The deflection of the trace of the strip chart recording potentiometer gave a measure of the ion intensity. The ionizing electron voltage was adjusted to 17 volts. The shutter was adjusted to the "open" position. The ion current under these conditions included, in the case of C^+, ions formed from C atoms, from residual gases, and from the "photo" process. The shutter was then "closed." The remaining ion intensity was that due to the residual gas in the source region. The shutter was "opened" again

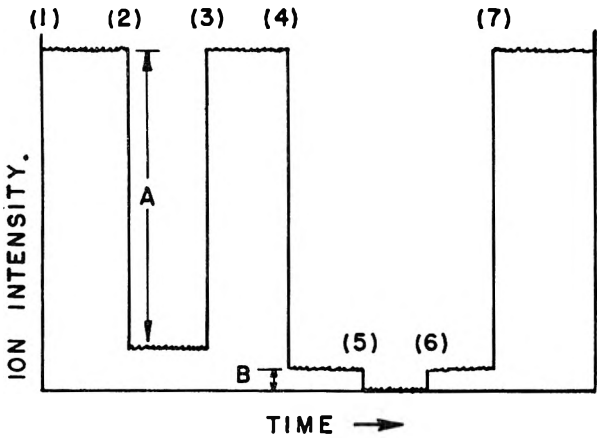

Fig. 2.—Recorder trace during C^+ measurement showing contributions of various backgrounds: (1) shutter open, 17 volts electron energy; (2) shutter closed; (3) shutter open; (4) electron beam off; (5) shutter closed; (6) shutter open; (7) electron beam on, C^+ formed from C atoms vaporizing from crucible is equal to $A - B$.

and the ionizing electron beam then turned off. The remaining ion intensity was that due to the "photo" process. The shutter was then "closed" to give the zero reading of the electrometer. The shutter was then again "opened," the electron beam turned on and the original intensity regained. A typical trace of the strip chart recorder made during this operation is shown in Fig. 2. This trace is typical of an intermediate temperature. At the highest temperatures, the total background amounted to only a few percentage of the entire ion intensity for C^+, C_2^+ and C_3^+. At the lowest temperatures, the background was of the order of half the total ion current. The amount of background depended on the residual gas pressure in the source region while the intensity of the ions formed from species evaporating from the cell was entirely independent of this.

In order to show that only ions formed from species evaporating from the cell were measured by this method, a rough measurement was carried out on the background peaks, which occurred at almost every mass number, in the range 10 to 80. When the backgrounds were subtracted as above, no detectable ion currents were measured except for masses 12, 24, 36 and a number of peaks from mass 48 to 65, the largest of which corresponded to V^+, Cr^+, Ti^+ (or C_4^+) VC^+ (or C_5^+). This latter group of peaks varied considerably in intensity in different runs. During some runs several of these peaks were not detectable. A more careful measurement was made on the H_2O^+ peak since this is one of the largest components of the residual gas. "Closing" and "opening" the shutter did not affect this ion intensity within a limit of accuracy of about 1%.

The measurement of the temperature dependence of the C^+, C_2^+ and C_3^+ intensities was made by the same procedure outlined above except that a rate of charge method was used to measure ion intensities. This method provided higher accuracy at low intensities and allowed a larger temperature range to be covered. In this method, the input resistor of the vibrating reed electrometer was disconnected and replaced by a 100 $\mu\mu$f. polystyrene capacitor. The ion intensity was then measured by the total deflection of the recording potentiometer after a measured period of time ranging from 30 seconds to 10 minutes, depending on the ion intensity. By this method, which still employed the electron multiplier, ion currents of 10^{-19} ampere were measured to an accuracy of $\pm 5\%$.

The temperature was measured by a Leeds and Northrup optical pyrometer. The effective emissivity of the tantalum cell was estimated to be 0.70, considering reflection and radiation back to it from the shields. The transmission of the quartz window was taken to be 0.9. The total temperature correction was taken from the graph of Benford[12] and amounted to 105 to 140°K. in the temperature range used.

Sensitivity Calibration.—The determination of the sensitivity of the mass spectrometer by the integration method gave an average of about 6.0×10^{11} intensity units (arbitrary) of Ag^{107++} formed by 150 volt electrons per atmosphere of Ag pressure inside the crucible. (The value of electron current was kept constant throughout these experiments.) This sensitivity was converted to sensitivity for C atoms by using the equation

$$I = \frac{6.0 \times 10^{11} \times C}{E} \times \frac{\text{Ag (total)}}{\text{Ag}^{107}} \times \frac{\sigma(\text{C})}{\sigma(\text{Ag})} \times \frac{T(\text{Ag})}{T(\text{C})} \times \frac{S(\text{C}^+)}{S(\text{Ag}^+)}$$

where

C = Ratio of Ag^+ produced by 80 volt electrons (at maximum ionization probability) to Ag^{++} produced by 150 volt electrons. This was measured directly and has the value 3.0.

E = Ratio of ionization probability of C atoms at maximum to that at 17 volts. This is estimated from the usual form of these curves to have the value 6.

$\frac{\text{Ag(total)}}{\text{Ag}^{107}}$ = Ratio of total amount of silver to that of the isotope of mass 107. This has the value 2.0

$\frac{\sigma(\text{C})}{\sigma(\text{Ag})}$ = Ratio of ionization cross-sections. This is estimated to be $1/4$.

$\frac{T(\text{Ag})}{T(\text{C})}$ = Ratio of average temperatures during evaporation. This is approximately 1400/2300 and is necessary since the vapor pressure is proportional to ion intensity times temperature.[5]

$\frac{S(\text{C}^+)}{S(\text{Ag}^+)}$ = Ratio of secondary electron efficiencies on the first plate of the electron multiplier. This is estimated to be 2.5 from the results of Inghram, Hayden and Hess.[13]

I = Sensitivity in intensity units of C^+ formed by 17 volt electrons per atmosphere of C (gas) in the Knudsen cell.

Inserting the values above, the average sensitivity of the spectrometer for C^+ formed by 17 volt electrons was 2.4×10^{11} intensity units of C^+ per atmosphere of C pressure inside the Knudsen cell. The measured intensity of C^+ was then divided by this quantity to give the pressure in atmospheres of C (gas) inside the Knudsen cell.

The major uncertainty in the above calculation is in the estimate of the relative ionization cross sections of carbon and silver atoms. The available data in the literature[14] indicate that ionization cross sections are roughly proportional to gas-kinetic cross-sections. The gas-kinetic cross-sections for carbon and silver atoms are taken as proportional to the squares of the interatomic distances in diamond and silver crystals, respectively. These distances are 1.54 and 2.88 Å., respectively, and the ratio of cross sections is taken to be $(2.88)^2/(1.54)^2$, which is approximately 3.5. Since the ionization potential of carbon (11.2 e.v.) is higher than that of silver (7.0 e.v.), this ratio of cross-sections will be somewhat higher and the value 4.0 is used in this calculation. By comparison with data on the ionization cross sections of mercury and the rare gases,[14] it is estimated that the probable error of this crude estimate is about a factor of two. The error is certainly less than a factor of four, since the ratio of ionization cross sections of Hg and He is about 16 and in this case the disparity in both geometrical cross sections and ionization potential is considerably larger than in the case of Ag and C.

Results

A total of six runs, each including a sensitivity calibration, have been made. The first two runs were terminated by short circuits before any C^+ ions were detectable and yielded only lower limits on ΔH (0°K.) of about 155 and 160 kcal./mole, re-

(12) F. Benford, *J. Opt. Soc. Am.*, **29**, 162 (1939).

(13) M. G. Inghram, R. J. Hayden and D. C. Hess, "Mass Spectroscopy in Physics Research," NBS Circular 522, p. 257, 1953.

(14) H. S. W. Massey and E. J. S. Burhop, "Electronic and Ionic Impact Phenomena," Oxford University Press, London, 1952, p. 30.

spectively. The next four runs were successful in measuring the vapor pressure of C atoms and the results are given in Table I. In calculating ΔH (0°K.) from the measured vapor pressure of C, the procedure of Brewer[3] was used.

TABLE I

ABSOLUTE PRESSURE MEASUREMENTS ON C(GAS)

Run	Temp., °K.	Pressure of C, atm.	ΔH (0°K.), kcal.
3	2400	4.0×10^{-8}	170
4[a]	2437	1.3×10^{-7}	166
5	2384	1.8×10^{-8}	171
6	2427	0.9×10^{-7}	168

[a] In run 4, a shutter protecting the quartz window from evaporating materials became stuck in the open position so that the window became progressively coated. Over a period of a week during which the Knudsen cell was kept at about 2000°K. or higher, the measured ΔH (0°K.) dropped steadily to 158 kcal./mole when no correction was made for the lower transmission of the window.

The temperature dependence of the intensities of C^+, C_2^+ and C_3^+ were also measured and the data plotted on the graph of Fig. 3. An inspection of the graph indicates that the ratios of intensities were quite accurately measured at all but the lowest temperature, since the departure of the experimental points from the straight lines at a particular temperature is about the same for each ionic species. The scatter is evidently due to slight errors in the temperature measurements.

The ΔH of vaporization of the three species as calculated from the slopes of Fig. 3 is given in Table II, together with values of ΔH calculated from the vapor pressures. The vapor pressures of C_2 and C_3 were obtained by comparison of the respective ion intensities with that of C^+ using relative ionization cross sections of 1, 2 and 3 for C, C_2 and C_3, respectively. The free energy functions given by Brewer[3] were used for C_2 and those estimated by Glockler were used for C_3.[15]

TABLE II

HEATS OF VAPORIZATION OF CARBON SPECIES

Species	ΔH (0°K.) kcal./mole From slope	From pressure
C	171 ± 10	170 ± 7
C_2	183 ± 10	197 ± 7
C_3	200 ± 10	199 ± 7

The evaporating species of mass 48 and higher have not yet been fully investigated. However, several of them were considerably higher in intensity than C^+ at the beginning of a run. In one run even after keeping the cell at 2000°K. or higher for 24 hours, the mass 51 and 52 intensities, probably V^+ and Cr^+, were 3.5 and 7.5 times higher than C^+. The appearance potentials of these two masses were both about 6 volts, suggesting the assignment to metals. The ions of mass 48 and 60 were also prominent but were not constant with time. Our earlier assignment[16] of the mass 60 peak to a C_5 molecule must be regarded as uncertain until further data are obtained. The mass 48 and 50 peaks have not been studied sufficiently to decide whether any appreciable fraction of them might be C_4^+ or C_5^+.

(15) G. Glockler, *J. Chem. Phys.*, **22**, 159 (1954).

(16) W. A. Chupka and M. G. Inghram, *ibid.*, **22**, 1472 (1954).

The high intensity of these species emphasizes the care that must be taken in experiments in which no analysis of effusing material is made.

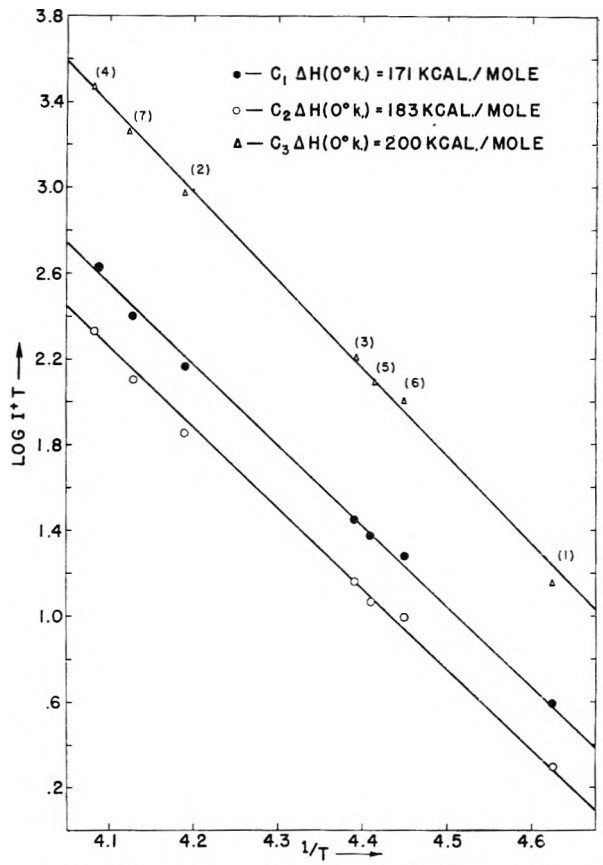

Fig. 3.—Temperature dependence of C^+, C_2^+ and C_3^+ ion intensities. The points are numbered in the order measured: points 1 to 5 were measured during one day and points 6 and 7 on the following day after keeping the temperature at about 2100°K. overnight.

Discussion of Errors

The major sources of error in the absolute pressure measurements of this experiment are the estimated ratio of ionization cross-sections and the estimated optical emissivity of the Knudsen cell. The probable error is estimated to be about a factor of two for the cross-section ratio and about 30°K. for the emissivity correction. Together with smaller errors estimated for the other factors used in the calibration calculation, these give a probable error in ΔH (0°K.) of C equal to about 7 kcal./mole. The low value of ΔH (0°K.) = 140 kcal./mole is clearly well outside the probable error.

If it is assumed that about one-half of the carbon measured in surface evaporation experiments[3] is due to C atoms, then either 125 or 141 kcal./mole for ΔH would lead to a pressure of C atoms under the conditions of this experiment roughly 200 times the amount measured. If it is also assumed that the ratio of ionization cross-sections used in calibration is too small by a factor of four and that temperature measurements are too high by about 100°K. (corresponding to no correction for emissivity), an error of a factor of 20 is expected. This is clearly an upper limit for these errors. No combination of other errors which can produce more

than an addition factor of 2 or 3 is apparent. Thus the low value is outside the range of systematic errors we have considered.

A major source of error in the values of ΔH determined from the slopes of Fig. 3 is the possibility of small amounts of impurity of the same mass as C, C_2 and C_3 evaporating from the oven. These impurities are negligible at higher cell temperatures, otherwise they would be easily detectable from appearance potential curves and also from their isotopes at other masses. Thus, they cannot contribute any appreciable error in the determination of the vapor pressures of the carbon species at intermediate and high temperatures. However, they would be more important at lower temperatures, where they would also be more difficult to detect. Consequently, they could lower appreciably the ΔH obtained from the slope measurements. Thus an Mg^+ ion may be the reason for the apparently low slope of the C_2^+ line of Fig. 3. If this is true, more careful study at mass 25 should indicate the presence of another isotope of this impurity. Therefore, the value of ΔH for C_2 calculated from its measured vapor pressure is considered to be more reliable.

Conclusions

This work very strongly supports a value of 170.4 kcal./ mole for the heat of sublimation of carbon. The lower values are well outside the probable error of the vapor pressure measurement and are also outside the limits of the systematic errors which we have considered. It should be possible in the near future to reduce considerably the possibility of systematic error. The high value is also suggested by the temperature dependence of the C^+ ion intensity and by the fact that the C_3^+/C^+ ratio from the Knudsen cell is about four times larger than that from surface evaporation. The latter indicates that the C atom vapor pressure has already reached its equilibrium value at values of σ at least one-fourth that of the 1/1500 used in this work. This is inconsistent with the very low evaporation coefficient suggested by Goldfinger, *et al.*[9]

The heats of vaporization of C_2 and C_3 are found to be 190 ± 10.0 and 200 ± 6.0 kcal./mole, respectively. The dissociation energy of C_2 is then calculated to be 150 kcal./mole.

Discussion

The major experimental support for a lower value of the heat of sublimation of carbon comes from the effusion work of Goldfinger, *et al.*,[4b] and the electron impact work of Hagstrum.[17] The effusion experiments of Goldfinger give results which are directly contradictory to those of this work. There appear to be several reasons for the discrepancy. In Goldfinger's work, the vaporization of impurities in the graphite may be significant. Also, it appears possible that some significant amount of the carbon may effuse as negative ions under his conditions. The possible role of the high electron pressure in the Knudsen cell is not understood. If large electron currents are allowed to flow from the cell, some carbon vapor may be swept out of the cell rather than effuse out. In our experiment, negative ions can have no effect since they are repelled by the potential of the radiation shields, while the electron pressure, except possibly at the higher temperatures, is too low to have any effect on the normal effusion of molecules from the cell. The importance of larger carbon molecules such as C_5 has not been satisfactorily evaluated. Since Goldfinger worked at considerably higher temperatures and lower σ than did the authors, these molecules could be important in his studies. Our work, on the other hand, is not considered complete as yet. Further work is planned in order to decrease the various possible errors and attempt to detect higher molecular weight species.

The experiments of Hagstrum[17] on CO appear to be the most thorough and complete of the electron impact experiments. These experiments support a value of 9.6 e.v. for the dissociation energy of CO which corresponds to 136 kcal./mole for the heat of sublimation of carbon. The value of 9.6 e.v. for the dissociation energy now appears to be very improbable.[18] If errors of 0.5 to 0.7 e.v. are allowed, Hagstrum's data on three processes in CO can be made to agree with the value 11.1 e.v. for the dissociation energy. The fourth process, as interpreted by Hagstrum, would require 1.5 volts error. However, there appears to be some possibility that the interpretation of this process may be incorrect. Incomplete work in this Laboratory indicates that Hagstrum's process A may be

$$CO \longrightarrow C^- + O^+$$

instead of

$$CO \longrightarrow C + O^+$$

The C^- ions detected from electron impact on CO have an appearance potential approximately equal to that of O^+ and have a large kinetic energy spectrum similar to that of O^+ ions. They appear to be of considerably lower intensity than O^+ but this has not yet been thoroughly established. If the first interpretation above is correct, either a value of about 11.1 or 9.6 e.v. is possible depending on whether the O^- ion is in the ground state or in an excited state which must be near its continuum. It may also be pointed out that recent work[19] indicates that the dissociation energy of N_2 is very probably 9.8 e.v. If this is true, then Hagstrum's appearance potential studies on NO gas are in error by as much as 1.1 e.v.

In view of the results of our experiments and of the uncertainties in the work supporting a low value, it appears very probable that the heat of sublimation of carbon is 170.4 kcal./mole.

(17) H. Hagstrum, *Rev. Mod. Phys.*, **23**, 185 (1951).

(18) A. E. Douglas, paper delivered at 126th Natl. ACS Meeting, New York, N. Y., 1954.

(19) A. E. Douglas, *Can. J. Phys.*, **30**, 302 (1952).

THE IMPORTANCE OF COMPLEX GASEOUS MOLECULES IN HIGH TEMPERATURE SYSTEMS[1]

BY LEO BREWER AND JAMES S. KANE

Department of Chemistry and Chemical Engineering and Radiation Laboratory, University of California, Berkeley 4, California

Received December 6, 1954

The influence of polymerized gaseous molecules upon equilibrium pressure measurements and upon measurements of rate of vaporization is discussed. Vaporization data for red phosphorus and arsenic are presented and the existence of catalytic effects upon rates of vaporization is demonstrated.

Introduction

Recent mass spectrometer measurements[2,3] have demonstrated that complex polymeric gaseous molecules are rather common in high temperature vapors. In a saturated vapor in equilibrium with a condensed phase, it can be demonstrated that the vapor becomes more complex as the temperature is raised, and the various possible minor species in a vapor have their greatest importance at the boiling point. This may be illustrated by the well-known example of saturated sodium vapor, which consists of 99.9% atomic sodium and 0.1% Na_2 at 400°K., but which contains about 12 mole % Na_2 at 1100°K.[4] Brewer[5] has shown that a simple relationship exists between the heats of vaporization of monomeric and dimeric species and the heat of dissociation of the dimer. When the heat of dissociation of the dimer, ΔH_D, is equal to the heat of vaporization of the monomer, ΔH_1, both the monomer and the dimer have equal heats of vaporization, and their proportion remains unchanged as the temperature is changed. It can be shown that the entropies of vaporization will not differ greatly. Thus monomer and dimer species will be of the same order of concentration when ΔH_D is equal to ΔH_1. If the heat of dissociation of the dimer is less than ΔH_1, which is the usual case, the vapor will consist largely of the monomer at low temperatures, but as the temperature is increased, a larger and larger proportion of the saturated vapor will consist of dimeric species with a maximum of dimer at the boiling point. The same is true of higher polymers. In the rarer situation where the heat of dissociation of the dimer is greater than the heat of vaporization of the monomer, the dimer will be the main species at low temperatures, while the percentage of monomer and higher polymers in the saturated vapor will increase as the temperature is increased. Brewer[5] has illustrated this behavior by examining the stability of dimers of the halides of the elements. A similar behavior is to be expected for the elemental vapors and other saturated vapor systems. Thus if one wishes to study the various minor polymeric gaseous species of a substance, it is usually easier to detect them at higher temperatures where these polymers comprise a higher proportion of the vapor.

When one is studying slightly volatile substances, the Langmuir method, which consists of the measurement of the rate of vaporization in a low pressure system, is commonly used for the determination of the vapor pressure. The rate of vaporization can normally be measured with a high accuracy and with much less difficulty due to the reaction of the vapor with containers and with much less chance of contamination by gaseous impurities than one encounters with other vapor pressure methods. However, the determination of the equilibrium pressure by this method requires the equating of the rate of vaporization to the rate of condensation. The rate of condensation can be calculated accurately from kinetic theory if the assumption is made that every molecule striking the surface condenses without rebounding. When this condition is met, it corresponds to a unit sticking or condensation coefficient and a unit vaporization coefficient. In the literature, both of these coefficients are commonly called accommodation coefficients. The vaporization coefficients of many materials have been checked, and virtually all materials that have been investigated have been found to have unit vaporization coefficients.[6] That is, the rates of vaporization are found within experimental error, to be those expected from the equilibrium pressures and the kinetic theory of gases. From experience to date, one can predict that all molecular lattices that consist of the main gaseous molecular species held together by van der Waals forces or weak forces of any type will have vaporization coefficients close to unity. However, as indicated in the recent report by Guthrie, Scott and Waddington[7] for rhombic sulfur, minor species that are not present in the molecular lattice and which are not readily formed from the main gaseous species may not be present in the gas vaporizing from a surface under reduced pressures, and thus the rate of vaporization will be slightly lower than that expected from the total equilibrium pressure, since the rate will correspond only to the partial pressure of the main species. All elements that vaporize predominantly to atomic species have been found to have unit vaporization coefficients whenever checked.[8] All ionic salts such

(1) Abstracted from the thesis to be submitted by James S. Kane in partial satisfaction of the requirements for the degree of Doctor of Philosophy in Chemistry at the University of California.

(2) (a) R. E. Honig, *J. Chem. Phys.*, **21**, 373 (1953); (b) **22**, 1610 (1954).

(3) W. A. Chupka and M. G. Inghram, ACS High Temperature Symposium, New York City, Sept. 1954; THIS JOURNAL, **59**, 100 (1955).

(4) National Bureau of Standards, "Selected Values of Thermochemical Properties," Series 3.

(5) L. Brewer, Paper 7, National Nuclear Energy Series, Vol. 19B, edited by L. L. Quill, McGraw-Hill Book Co., New York, N. Y., 1950.

(6) S. Dushman, "Vacuum Technique," John Wiley and Sons, Inc., New York, N. Y., 1949.

(7) G. B. Guthrie, D. W. Scott and G. Waddington, *J. Am. Chem. Soc.*, **76**, 1488 (1954).

(8) R. S. Bradley and P. Volans, *Proc. Roy. Soc. (London)*, **217**, 508 (1953).

as the alkali halides that vaporize predominantly to a monomeric gaseous molecule are believed to have vaporization coefficients close to unity, the measured values ranging as low as 0.5.[8] There have been some accurate measurements indicating slightly low values, but there are no indications that vaporization coefficients below the range 0.5–1.0 are to be expected for any ionic substance where the ions required for a gaseous molecule are in contact. Hydrogen-bonded substances have been found to have unit accommodation coefficients whenever checked.[9-11]

The only clearly demonstrated examples of low vaporization coefficients occur when the main molecular gaseous specie does not occur as such in the condensed phase. The investigation of Stranski and Wolff[12] on the rate of vaporization of two crystalline modifications of As_2O_3, arsenolite and claudetite, serves to illustrate this point. The crystal structure of arsenolite is known to be a molecular lattice of As_4O_6 molecules, while the structure of claudetite does not consist of a molecular lattice. In both cases, the saturated equilibrium vapor consists primarily of As_4O_6 molecules. The rate of vaporization of arsenolite is observed to be 10^6 times greater than that of claudetite. There are other examples such as the ammonium halides which vaporize to ammonia and hydrogen halide,[13] neither of which is present in the condensed phase. Elemental phosphorus is another clear example. White phosphorus, which is a molecular lattice of P_4 molecules, the main gaseous species, has a unit vaporization coefficient, while red phosphorus which is not believed to contain P_4 molecular units has a vaporization coefficient of about 10^{-6}. Similarly, arsenic, whose lattice is known not to contain As_4 units, has a low vaporization coefficient.[13]

Experimental

In an effort to elucidate the mechanism of vaporization when one has a barrier against vaporization as indicated by a low vaporization coefficient, a study has been made of the vaporization of arsenic under a variety of conditions, and a similar study is under way for red and black phosphorus. Melville and Gray[14] attributed the anomalously low rate of vaporization of red phosphorus to the existence of P_2 units in the solid lattice, and they hypothesized that P_2 was vaporizing with unit vaporization coefficient from the solid, but, because of the small partial pressure of P_2 compared to P_4, a very low rate of vaporization was obtained. To check this hypothesis for red phosphorus, we have repeated their Langmuir measurements and have obtained results agreeing within an order of magnitude. We have evaluated the data in the literature on the equilibrium between P_4 and P_2 in the gaseous phase and agree with Yost and Russell[15] that the measurements of Preuner and Brockmoller[16] must be in error, and that the measurements of Stock, Gibson and Stamm[17] appear to be reliable. Thus from the known equilibrium pressure of P_4 over red phosphorus as determined by static methods[18] and the equilibrium between P_4 and P_2, we have been able to calculate the equilibrium partial pressure of P_2 in equilibrium with solid red phosphorus. We find that the rate of vaporization of red phosphorus is smaller than what would be expected from the equilibrium pressure of P_2. This would indicate that even P_2 has a vaporization coefficient less than unity. Thus the limiting rate of vaporization in a Langmuir experiment is not necessarily fixed by the P_2 vapor pressure as proposed by Melville and Gray. For arsenic where equilibrium data are not available to determine the pressure of As_2 in equilibrium with the solid, we have examined the vapor from a Langmuir type experiment in a mass spectrometer, and have found the vapor to be predominantly As_4.

To check the correlation between vaporization coefficients and sticking or condensation coefficients, molecular beams of phosphorus and arsenic vapor were impinged upon various targets that had been cooled to a sufficiently low temperature so that any phosphorus or arsenic that would condense upon the target would be incapable of revaporizing. It was found that virtually all of the vapor rebounded without condensation from most target materials. Copper cooled to a low temperature appeared to be the most efficient target.

As the equilibrium pressure of As_4 over arsenic did not appear to be completely established by means of static measurements,[16,19,20] the vapor pressure of arsenic was evaluated by the Knudsen method using orifice area to vaporizing area ratios ranging from 1.0 to 1.6×10^{-4}. It was found that the orifice to vaporizing area had to be less than 10^{-3} before a vapor pressure near to the equilibrium value and independent of orifice size was reached. Comparison of Langmuir results with the equilibrium pressures indicated vaporization coefficients of about 5×10^{-4}. Some measurements were also made with red phosphorus and with the smallest orifice to vaporizing area tried, 1.33×10^{-4}, the vapor pressure in the Knudsen cell was still only 10^{-3} times the equilibrium value.

From the results obtained to date, it appears clear that it will be extremely difficult to obtain any reliable vapor pressure results for red phosphorus by the conventional Knudsen method. The orifice size required for any reasonable cell must be so small that cracks and fissures and porosity of the cell material will become comparable to the orifice area. To eliminate this difficulty, an attempt to find a catalyst for the vaporization reaction was made. It had been observed that fresh samples of phosphorus and arsenic gave abnormally high rates of vaporization which decreased as vaporization proceeded. This might be attributed to impurities such as oxides, etc., but the effect seemed larger than might be attributed to impurities. Our hypothesis was that fresh material contained many distorted or defective crystals in which the atoms were not so rigidly fixed. Thus they could reorganize to form P_4 or As_4 molecules whereas in a perfect lattice, it would be extremely difficult to distort the rigid lattice to produce a P_4 or an As_4 molecule. Thus we believed that the abnormal vaporization rate was due to the distorted crystals that were soon removed. The effect of the nature of the material was also apparent in the reproducibility of Langmuir type measurements or Knudsen measurements with large orifice. The results appeared to vary from sample to sample for no obvious reason, whereas measurements with the same materials made by the Knudsen method with small enough orifices to produce the equilibrium pressure of As_4 were much more reproducible. It thus appeared that we might be able to catalyze the rate of vaporization by loosening up the lattice. A simple procedure to accomplish this would be to add some non-volatile liquid which would not react chemically with phosphorus or arsenic to form any intermediate phases, but which would dissolve some of these elements. In the mobile liquid, it should be possible for the atoms to rearrange to form the P_4 and As_4 aggregates necessary for attainment of equilibrium pressures. Thallium and lead appeared to be liquids that would meet the requirements. Thallium was added to phosphorus and arsenic in Knudsen cells with relatively large orifices, and heated above the melting point of thallium. The pressures observed were 30 times greater than those observed without addition of the liquid catalyst, all other experimental conditions being the same. Upon

(9) R. S. Bradley, *J. Chem. Soc.*, 1681 (1953).

(10) R. S. Bradley, *ibid.*, 1684 (1953).

(11) R. S. Bradley, *ibid.*, 1688 (1953).

(12) I. N. Stranski and G. Wolff, *Research*, **4**, 15 (1951).

(13) F. Metzger, *Helv. Phys. Acta*, **16**, 323 (1943).

(14) H. W. Melville and S. C. Gray, *Trans. Faraday Soc.*, **32**, 1026 (1936).

(15) D. M. Yost and H. Russell, "Systematic Inorganic Chemistry," Prentice-Hall, Inc., New York, N. Y., 1946, pp. 166–168.

(16) G. Preuner and I. Brockmoller, *Z. physik. Chem.*, **81**, 129 (1912).

(17) A. Stock, G. E. Gibson and E. Stamm, *Ber.*, **45**, 3527 (1912).

(18) C. C. Stephenson, Dept. of Chemistry, Mass. Institute of Technology (private communication).

(19) G. E. Gibson, Diss., Breslau, 1911, "see Landolt Bornstein-Roth Physikalisch-Chemische Tabellen," Vol. 2, Julius Springer, Berlin, 1923, p. 1332.

(20) S. Horiba, *Proc. Acad. Sci. Amsterdam*, **25**, 387 (1923).

further heating the same sample, the pressure steadily decreased, although the quantity of arsenic present was still sufficient to maintain a solid arsenic phase. Examination of the system upon cooling indicated that the phosphorus or arsenic in contact with the liquid had dissolved, leaving very few points of contact between the solid and liquid. Thus the transfer of material between the solid and liquid became slower and slower. To minimize this, mixtures of thallium and arsenic were heated in sealed quartz tubes to 1000°K. and then chilled, resulting in a fine intermixture of arsenic and thallium. When these mixtures were again heated in Knudsen cells with large orifices, the pressures were again about 30 times higher than observed without the catalyst present, and in fact were very close to the extrapolation of the equilibrium vapor pressure curve determined at higher temperatures by static methods. Further, continued heating of the samples gave consistent results, showing that slowness in transfer between the liquid and solid has been greatly reduced. The main experimental results demonstrating the effects are given in Fig. 1. The small dependence upon orifice size even in the presence of thallium liquid shows that the transfer from solid to liquid still limits the rate of evaporation to some extent, however. Because of the large arsenic pressure when liquid thallium was present, large Knudsen orifices or a Langmuir type measurement would have given too rapid a loss of material for accurate measurements. Extrapolation of the thallium results to unit orifice to surface area ratio shows that addition of thallium has increased the rate of vaporization of arsenic almost 100-fold. Thus by means of the thallium catalyst it is possible to accelerate the rate of vaporization sufficiently to allow the determination of pressures closely approaching the equilibrium values using a Knudsen cell of comparatively large orifice. To ensure that the effusate in these runs was arsenic only, spectroscopic analyses were utilized; the quantity of thallium found being much less than in a standard alloy mixture containing 1% thallium, 99% arsenic. Similar experiments are now in progress with red and black phosphorus.

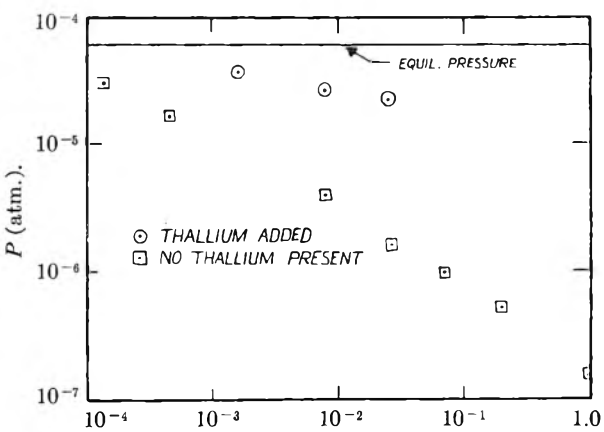

Fig. 1.—Knudsen cell data for arsenic at 575°.

Although it appears possible to saturate the liquid metal with arsenic or phosphorus by obtaining a large surface contact between the solid and liquid, the resulting vapor pressures for arsenic appear to be about 40% lower than the extrapolation of the equilibrium curve obtained from static methods.[16,19,20] With regard to these static measurements, consideration of the data in the literature does not enable the equilibrium pressure to be fixed precisely. A considerable variation is found between different investigators in the values given for the equilibrium vapor pressures and, since the molecular constants are not known for the As_4 molecule, one is not able to subject the data to a third law check. Therefore, for this work, a heat capacity for the gas was estimated, a constant ΔC_p was assumed over the temperature range of the experiments, and the "best" line was drawn through the experimental points. The equilibrium pressures calculated in this manner are therefore uncertain to a relatively large degree. The Σ plot of the data is shown in Fig. 2: $\Sigma = -R \ln P + \Delta C_p \ln t$. The ΔC_p used over this range was -8.6.

In addition to the fact that the equilibrium pressure is uncertain, the difference between the pressures of the arsenic–thallium experiments and the equilibrium values may be attributed to another factor. Thallium undoubtedly forms a solid solution with arsenic to some extent and the saturated solution of arsenic in liquid thallium may not be quite at unit activity with respect to pure arsenic solid. In the phosphorus–thallium system there is a solid solubility of thallium in phosphorus of 25 atomic %.[21] The results using liquid lead will give us a check on reduction of activity due to solid solubility.

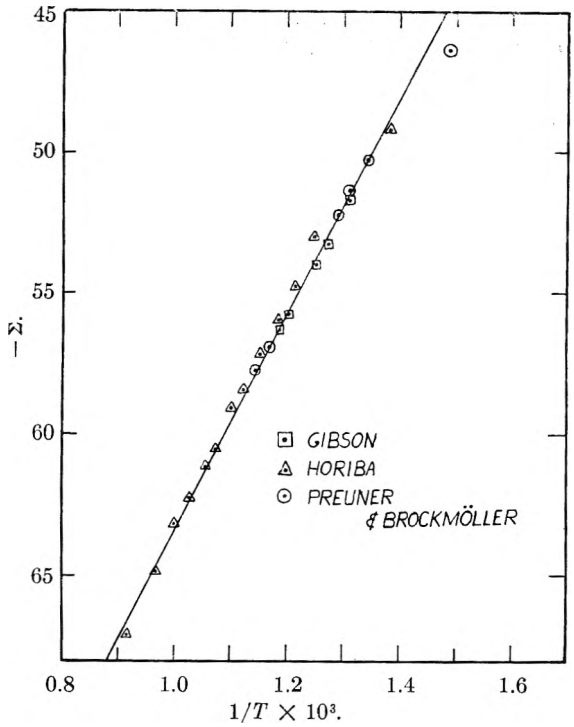

Fig. 2.—Plot of vapor pressure data of arsenic.

It is of interest to compare the equilibrium heat of vaporization of 33 ± 1 kcal. at 550°K. with the heat of 43 ± 3 kcal. obtained from the temperature coefficient of Langmuir type measurements for arsenic. The barrier of 10 kcal. indicated by these data should correspond to a vaporization coefficient of $\exp^{-10000/2 \times 550}$ or a factor of about 10^{-4}. The observed accommodation coefficients were of this order of magnitude, although a distinct trend to smaller accommodation coefficients was observed with the smaller orifices.

Discussion

It is believed that some generalization can be made about systems with low vaporization coefficients. From the available data, low vaporization coefficients can be expected whenever the main vaporizing gaseous species are not present as such in the condensed phase and the atoms or molecules in the condensed phase are held so rigidly that they cannot readily reorganize to form the main gaseous species. It appears very unlikely that materials vaporizing predominantly to atomic gaseous species will have low vaporization coefficients. Further, it is reasonable to expect that materials vaporizing to predominantly diatomic gaseous species will have low vaporization coefficients in cases where the two component atoms are so separated in the condensed phase that they cannot readily contact each other. Thus Margrave[22] reports a low vaporization coefficient for the vaporization of

(21) M. Hansen, "Der Aufbau der Zweistofflegierungen," Julius Springer, Berlin, 1936.

(22) J. R. Soulen, P. Sthapitanonda and J. Margrave, THIS JOURNAL, **59**, 132 (1955).

magnesium nitride that vaporizes under equilibrium conditions to Mg atoms and N_2 molecules because of the separation of nitrogen atoms in the rigid magnesium nitride lattice. In general we would expect low vaporization coefficients when the main gaseous species is a polyatomic molecule that does not exist as such in the condensed phase and because of the rigidity of the lattice cannot readily form within the lattice. The examples of red phosphorus, arsenic, arsenic oxide, ammonium halides, etc., fall in this class. For a similar reason, materials that vaporize predominantly to atomic species with a vaporization coefficient close to unity may produce a different vapor when vaporizing in a Langmuir type experiment compared to the equilibrium vapor. This is due to low vaporization coefficients for the various complex polymeric species that do not affect the observed rate of vaporization materially because of their small percentage contribution, particularly at low temperatures. However, at higher temperatures where they become more important the effect of the polymeric species may become noticeable. Also mass spectrometer studies that can detect these minor polymeric species may yield different results with vapors produced in a Langmuir type experiment in contrast to a vapor obtained from a Knudsen cell with a small orifice. Although liquids generally would be expected to yield vaporization coefficients close to unity because of a better chance of rearrangement to produce the desired molecule species, two interesting examples giving evidence to the contrary may be noted. In the study by Motzfeldt[23] of the vaporization of liquid sodium carbonate to produce sodium atoms, oxygen molecules and carbon dioxide molecules, he found a low vaporization coefficient which he attributed to the difficulty of bending a triangular carbonate ion in the liquid to form a linear carbon dioxide molecule. Also Stranski[12] in his study of the arsenic oxides, observes that although the vaporization coefficient from the molecular lattice modification (arsenolite) is unity, measurements made on the supercooled liquid show the vaporization coefficient to be considerably less. In this case the attraction between adjacent As_4O_6 molecules is apparently stronger in the liquid than in the solid.

It is of interest to apply these generalizations to the rate of vaporization of graphite for which vaporization coefficients less than unity are known to exist. One may note that black phosphorus and arsenic have structures that are closely related to the graphite structure and that red phosphorus is believed also to have a similar structure.[24,25] Goldfinger, Waelbroeck and Doerhard[26] have presented a model for the vaporization of graphite based on the Herzberg–Herzfeld–Teller model which would require a low vaporization coefficient for monoatomic carbon, a unit vaporization coefficient for C_2, and a much larger than unit vaporization coefficient for C_3. Although their model is self-consistent and quite conceivable, it would be much more reasonable on the basis of experience with other systems that the atomic products would vaporize with a high vaporization coefficient while more complex molecules might have a low vaporization coefficient. The more recent mass spectrometer results of Inghram and Chupka[3] and Hoch, Blackburn, Dingledy and Johnston[27] now clearly demonstrate that monatomic carbon must have a vaporization coefficient between 0.1 and 1 and could not have a vaporization coefficient of 10^{-3} as has been proposed. Their results together with the Langmuir method measurements would be consistent with a vaporization coefficient for C_2 between 0.5 and 1, a coefficient for C around 0.3, and a coefficient for C_3 of about 0.1. Thus none of these species could account for the high vapor pressure observed by Goldfinger, Doerhard and Waelbroeck using Knudsen cells with extremely small orifices, and one is forced to attribute their results to a more complex species. Chupka and Inghram have reported observations that indicate that the C_5 molecule has an extremely low vaporization coefficient and becomes very important in a Knudsen cell measurement. Although these measurements require verification before they can be fully accepted, such a species would adequately explain Goldfinger's results as well as the various static determinations of the total vapor pressure of graphite. Examination of the structure of graphite shows that it would be extremely difficult to form a C_5 molecule from the graphite structure and one would expect a low vaporization coefficient for such a molecule. From its required high stability, it must be a ring or other compact structure. It is of interest to note that Brewer, Gilles and Jenkins[28] report that graphite powder gives an abnormally high vapor pressure upon first heating that gradually decreases just as observed with phosphorus and arsenic, and the same explanation might apply. Thus imperfect or strained graphite crystals might allow the necessary distortion to form C_5 molecules and thus would vaporize more rapidly than the more perfect crystals from which it would be very difficult to form C_5 molecules. If the mass spectrometer observations of C_5 can be verified, a ready reconciliation of all the apparently contradictory data on the vapor pressure of graphite can be made. With C_5 the main species under true equilibrium conditions, one would expect high vapor pressures under static conditions or with Knudsen cells with extremely small orifices as used by Goldfinger, Doerhard and Waelbroeck. However with the very small vaporization coefficient of probably 10^{-4} or smaller for C_5, other kinetic methods of determining the vapor pressure would give little indication of C_5, and the measured vapor pressures would correspond mainly to C and C_3, as the C_2 pressure is considerably smaller. As both C and C_3 are present in comparable amounts, third law calculations using total vapor pressure measurements obtained by the usual

(23) K. Motzfeldt, THIS JOURNAL, **59**, 139 (1955).

(24) N. S. Gingrich and C. O. Thomas, *J. Chem. Phys.*, **6**, 659 (1938).

(25) R. Hultgren, N. S. Gingrich and B. E. Warren, *ibid.*, **3**, 351 (1935).

(26) T. Doerhard, P. Goldfinger and F. Waelbroeck, *Bull. soc. chim. Belges.*, **62**. 498 (1953).

(27) M. Hoch, P. Blackburn, D. Dingledy and H. Johnston, THIS JOURNAL, **59**, 97 (1955).

(28) L. Brewer, P. Gilles and F. Jenkins, *J. Chem. Phys.*, **16**, 797 (1948).

Langmuir and Knudsen methods will give the heat of sublimation of graphite to monatomic carbon within a few kilocalories. It should be possible to check the importance of C_5 by using a catalyst as has been done with phosphorus and arsenic. A suitable liquid that would dissolve graphite without forming an intermediate phase or without reducing the carbon activity would be liquid platinum or another relatively non-volatile platinum group metal. Preliminary experiments with platinum and graphite have indicated that liquid platinum will dissolve appreciable amounts of carbon at 2100°. If the same effect is obtained as has been observed with phosphorus and arsenic, one should observe high pressures similar to those observed by Goldfinger, Doerhard and Waelbroeck, even with Knudsen cells of large orifice.

Further experiments are in progress to combine mass spectroscopic examination with Langmuir and Knudsen type experiments to establish the vaporization coefficients of the minor species as well as of the major species of systems like phosphorus and arsenic and to check some of the generalizations made above.

This work was performed under the auspicies of the United States Atomic Energy Commission.

RECENT SPECTROSCOPIC STUDIES OF SIMPLE MOLECULES[1]

By A. E. Douglas

Division of Physics, National Research Council, Ottawa, Canada

Received November 19, 1954

This paper gives a summary of some recent work on the dissociation energies of O_2, N_2, CO and CN.

The problems involved in the spectroscopic determination of dissociation energies of molecules have been adequately discussed by Herzberg[2] and by Gaydon.[3] A review of the state of our knowledge of the dissociation energies of diatomic molecules at the beginning of 1952 has been given by Gaydon.[3] The following paragraphs give a brief summary of the work done on this problem at the Division of Physics of the National Research Council of Canada since that time.

O_2.—From the measurements of the Schumann–Runge bands by Knauss and Ballard,[4] a reasonably accurate value of $D(O_2)$ has been known for many years. Recently Herzberg[5] from measurements of the $^3\Sigma_u^+ - {}^3\Sigma_g^-$ bands and Brix and Herzberg[6] from more accurate and extensive measurements of the Schumann–Runge bands have considerably reduced the error in the value of $D(O_2)$. For the oxygen molecule, the positions of two dissociation limits are now accurately known and the states of the atoms at these limits are known with certainty. The new value of 41260 ± 15 cm.$^{-1}$ for $D(O_2)$ is one of the most accurate and reliable dissociation energies now known.

N_2.—Gaydon[3] has discussed the problem of the dissociation energy of N_2 and has pointed out that there is a good deal of evidence pointing to a value of 9.756 e.v. It has, however, been difficult to reconcile the observed spectrum of N_2^+ with this value of $D(N_2)$ unless one assumed that the $B^2\Sigma$ state of N_2^+ has quite an anomalous potential curve. Recently it has been shown experimentally that the $B^2\Sigma$ state does indeed have such an anomalous curve.[7] Furthermore the new spectroscopic data on N_2^+ gives very strong support to the value of 9.756 e.v. for the dissociation energy of N_2.

The spectra of N_2 and related molecules, unlike the spectrum of O_2, do not supply us with a direct and simple proof of the dissociation energy of nitrogen. These spectra do, however, supply us with a good deal of data which can be readily interpreted if a value of 9.756 e.v. is assumed for the dissociation energy. Any other value of $D(N_2)$ finds no positive support from the observed spectra and requires a number of drastic assumptions regarding the nature of the potential curves of N_2, N_2^+ and NO. Thus the data now available are overwhelmingly in favor of a value of 9.756 e.v. for $D(N_2)$.

CO.—The dissociation energy of CO is related directly to the latent heat of sublimation of carbon and has been the subject of much controversy. The known spectrum of CO has not provided data from which an unequivocal value for $D(CO)$ can be derived. Predissociations have been reported in the CO spectrum in the $B^1\Sigma$ and $B^3\Sigma$ states at a little over 11 e.v. above the ground state and in the $A^1\Pi$ state near 9.6 e.v.[3]. The fact that there is a predissociation in the $v = 0$ level of the $B^1\Sigma$ state has been almost universally accepted. It has also been widely accepted that the $v = 1$ level of the $B^1\Sigma$ state is predissociated and that from the two predissociations it can be established that a dissociation limit exists at 11.11 e.v. Hagstrum,[8] in order to bring the spectroscopic results into agreement with his electron impact work, has endeavored to show that no dissociation limit exists at this energy. Recent[9] work in which the $B^1\Sigma - A^1P$ (ångström) bands of $C^{12}O$ and $C^{13}O$ were photographed at high dispersion has shown that predissociations do exist in the $v = 0$ and in the $v = 1$ levels of the B state and there is very good evidence that a dissociation limit does exist at 89,595 ± 30 cm.$^{-1}$ (11.1078 ±

(1) Contribution No. 3517 from the National Research Laboratories, Ottawa, Canada.

(2) G. Herzberg, "Spectra of Diatomic Molecules," D. Van Nostrand Company, Inc., New York, N. Y., 1950.

(3) A. G. Gaydon, "Dissociation Energies and Spectra of Diatomic Molecules," Chapman and Hall, London, England, 1953.

(4) H. P. Knauss and S. S. Ballard, *Phys. Rev.*, **48**, 796 (1935).

(5) G. Herzberg, *Can. J. Phys.*, **30**, 185 (1952).

(6) P. Brix and G. Herzberg, *ibid.*, **32**, 110 (1954).

(7) A. E. Douglas, *ibid.*, **30**, 302 (1952).

(8) H. D. Hagstrum, *Phys. Rev.*, **72**, 947 (1947).

(9) A. E. Douglas and C. Møller, to be published.

0.0037 e.v.) above the $v = 0$ level of the ground state.

If it is assumed that at this dissociation limit the resulting atoms are in the ground state [$C(^3P_0) + O(^3P_2)$], then it follows that the dissociation energy of CO is 89,595 ± 30 cm.$^{-1}$. It should be pointed out, however, that even if it is assumed that the molecule dissociates into $C(^3P) + O(^3P)$, it is not possible to be certain which components of the triplet state are involved. Since the combination $C(^3P_2) + O(^3P_0)$ lies 270 cm.$^{-1}$ above $C(^3P_0) + O(^3P_2)$, the dissociation energy is still uncertain to this extent.

The predissociations in the $A^1\Pi$ state reported by Gerö[10] have never been accepted without reservations. They are, however, most significant predissociations since, if they are real, the dissociation energy of CO cannot exceed 9.60 e.v. High dispersion (0.23 Å./mm.) photographs of $A^1\Pi - X^1\Sigma$ bands have recently been obtained.[9] On none of the spectra has it been possible to find the predissociation reported by Gerö. Furthermore, bands in which the predissociation is reported to occur have been shown to be quite normal. There therefore appears no basis for believing that any predissociation exists in the electronic states of CO below 11.1 e.v. It should be emphasized, however, that this new work has not established the dissociation energy of CO and from the spectrum alone no unequivocal value can be derived.

CN.—The dissociation energy of the CN molecule is related to those of N_2 and CO by the work of Brewer, Templeton and Jenkins.[11] An accurate determination of D(CN) would not only be of significance for its own intrinsic value, but also would be very useful in establishing D(CO). An extensive investigation of the spectrum of CN from 2000 to 10,000 Å. has recently been completed.[12] A large number of new bands has been found and analyzed. It was found, however, that even with this expanded knowledge of the spectrum, no reliable value of D(CN) could be determined. Though in the past there have been estimates of D(CN) based on spectroscopic data, it appears that none of these estimates have a firm foundation.

(10) L. Gerö, *Z. Physik*, **100**, 374 (1936).

(11) L. Brewer, L. K. Templeton and F. A. Jenkins, *J. Am. Chem. Soc.*, **73**, 1462 (1951).

(12) A. E. Douglas and P. M. Routly, *Ap. J. Supplement*, **1**, No. 9 (1954).

VAPORIZATION REACTIONS. THE IRON-BROMINE SYSTEM[1]

BY N. W. GREGORY AND R. O. MACLAREN

Contribution from the Department of Chemistry at the University of Washington, Seattle, Washington

Received September 28, 1954

The reaction between bromine and $FeBr_2$ has been studied between 200 and 400° using the transpiration technique with the aid of a colorimetric analytical procedure which permits convenient determination of pressures as low as 10^{-3} mm. Fe_2Br_6 (with Br_2) is the principal constituent in the vapor phase. Dissociation of the dimer has been measured between 500 and 680° in a quartz diaphragm gage. Appreciable solubility of the iron(III) phase in liquid $FeBr_2$ is observed.

The study of vapor–solid equilibria constitutes one of the most useful methods of gaining thermodynamic information concerning reactions at high temperatures. Experimental procedures commonly employed are effusion, transpiration or direct measurement of the total pressure with a device such as a diaphragm or sickle gage. The effusion method is restricted to pressures sufficiently low to permit molecular flow, generally less than 10^{-2} mm., and is subject to uncertainties associated with the kinetics of vaporization and condensation processes; the last two methods have not generally been applied at pressures lower than 1–10 mm. The region between 10^{-2} and 1 mm. has frequently been referred to as the difficult range.

In a study of the iron–bromine system, it has been found convenient to extend the transpiration method to measure pressures as low as 10^{-3} mm. All three procedures have been used to determine the vapor pressure of iron(II) bromide, described in an earlier paper.[2] The transpiration technique is well suited for study of the rather unstable iron(III) bromide. The decomposition pressure of bromine above solid $FeBr_3$ reaches one atmosphere at 139°,[3] when its vapor pressure is only 0.014 mm. However, by using bromine both as reactant and carrier gas the equilibrium between $FeBr_2$, bromine and gaseous iron(III) bromide has been characterized between 200 and 400°. The method is feasible at these temperatures largely because of an accurate colorimetric procedure for determination of milligram quantities of iron(II). The molecular form of the iron(III) vapor phase is principally Fe_2Br_6 below 400°; dissociation of the dimer between 500 and 800° has been studied in a quartz diaphragm gage; above the melting point of $FeBr_2$, appreciable solubility of the vapor phase in the liquid is observed.

Experimental

Transpiration Experiments.—The apparatus is shown in Fig. 1. $FeBr_2$ was sublimed in high vacuum onto the walls of the reaction chamber at B and the end bulb sealed off; three independent samples were used for 33 measurements. Prior to each experiment the entire system was evacuated except A which contained anhydrous liquid bromine. Bromine gas was introduced into the reactor in one of three pressure ranges; *ca.* 200 mm. by keeping A in a water-bath at 25°, 70 mm. with A in an ice-bath, or between 25 and 30 mm. by bleeding bromine into the system through

(1) Presented at the Symposium on High Temperature Chemical Reactions, 126th National ACS meeting at New York, Sept. 15, 1954.

(2) R. O. MacLaren and N. W. Gregory, THIS JOURNAL, **59**, 184 (1955).

(3) N. W. Gregory and B. A. Thackrey, *J. Am. Chem. Soc.*, **72**, 3176 (1950).

a partially opened stopcock. The actual pressure was measured with a differential sulfuric acid manometer E; the flow of bromine, induced by condensation in D with liquid oxygen, was controlled between 2 and 28 cc./min. (volume calculated at 250°) by a series of interchangeable capillaries at C. Bromine collected in D was dissolved in KI solution and the iodine liberated titrated with standard thiosulfate.

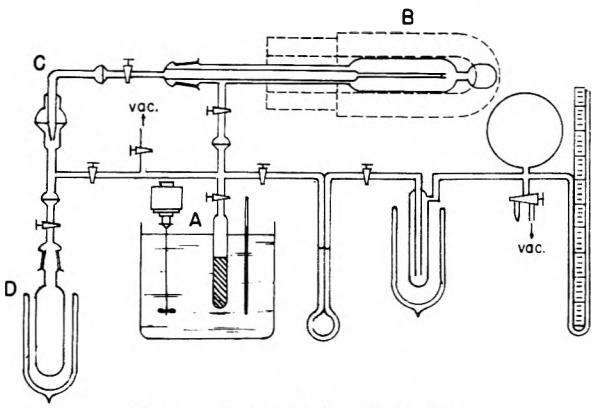

Fig. 1.—Transpiration apparatus.

Before introduction of bromine the temperature of B was raised (electric furnace) to the desired value, regulated within ±2°, and measured with three calibrated chromel–alumel thermocouples spaced around the reactor. The preheater was kept within 10° of the main furnace; variation of its temperature in this range had no observable effect.

Iron(III) bromide vapor, formed by reaction of bromine and $FeBr_2$ and transported by bromine down the inner tube of B, condensed and decomposed to $FeBr_2$ in the cool region outside the furnaces. At the completion of an experiment (one to two hours) the inner tube was removed in a dry-box and the $FeBr_2$, in amounts varying from 0.8 to 40 mg., dissolved in water and determined colorimetrically as the iron(II) complex of 1,10-(ortho)-phenanthroline by a method similar to that described by Hiskey.[4,5] A Beckman (DU) spectrophotometer was used at wave length 510 mμ, an absorption maximum of the complex. The accuracy of the analysis was found to be ±0.5%. This technique permitted study of the equilibrium with Fe_2Br_6 pressures as low as 10^{-3} mm.

Diaphragm Gage Measurements.—The dimer–monomer equilibrium was studied by measuring the total pressure developed in the system $FeBr_2(s)$–Br_2–Fe_2Br_6–$FeBr_3$ between 500 and 750°, using a thin quartz membrane manometer of the Daniels type.[6] Deflections of a slender quartz pointer (20 cm. long) sealed to the diaphragm were observed through a 40-power microscope. The gage, with volume approximately 35 ml., was connected by graded quartz–Pyrex seals and waxed ground-glass ball joints to the vacuum line, mercury manometer and bromine source. The gage was used as a null point instrument; the zero position was determined before and after a series of measurements by freezing out the bromine with liquid oxygen. No irreversible shift in the null point was noted; appreciable pressure differentials were not allowed to develop at high temperatures. The uncertainty of a pressure measurement was of the order of ±1 mm.

$FeBr_2$ was sublimed into the gage after the apparatus had been outgassed at 900°, the sublimation tube sealed off and a side arm also sealed after introduction of a known amount of bromine. The latter was obtained by thermal decomposition of $FeBr_3$,[4] a convenient method for producing small quantities of high purity. The apparatus was heated with an electric furnace with three separate nichrome windings. The current in the main winding was controlled with a thermal regulator to maintain the temperature in the center of the tube within ±1° of the desired value; currents in the smaller windings at the top and bottom of the furnace were adjusted independently so the temperatures indicated by five calibrated chromel–alumel thermocouples spaced all along the gage were within 1°.

(4) C. F. Hiskey, *Anal. Chem.*, **21**, 1440 (1949).
(5) C. F. Hiskey, J. Rabinowitz and I. G. Young, *ibid.*, **22**, 1464 (1950).
(6) F. Daniels, *J. Am. Chem. Soc.*, **50**, 1115 (1928).

Results and Discussion

Transpiration Study.—Equilibrium constants for the reaction of bromine with $FeBr_2(s)$ to give iron(III) bromide vapor are shown in Fig. 2. The solid circles correspond to constants calculated if the iron(III) vapor is assumed to be $FeBr_3$; the open circles for Fe_2Br_6. No trend on either basis was apparent with variation in flow rate; however, the solid circles are observed to fall roughly on three parallel lines, corresponding to the three ranges of bromine pressure used. The open circles show no such dependence on bromine pressure; it is concluded that the equilibrium characterized is

$$2FeBr_2(s) + Br_2(g) = Fe_2Br_6(g) \qquad (1)$$

with negligible amounts of $FeBr_3(g)$ present. The solid line represents the least squares analysis of the data in the form $\log K_1 = -3565/T + 3.943$. The average deviation of $\log K_1$ (expt.) from calculated values is 0.8%. The mean heat of reaction is 16.3 ± 0.3 kcal.

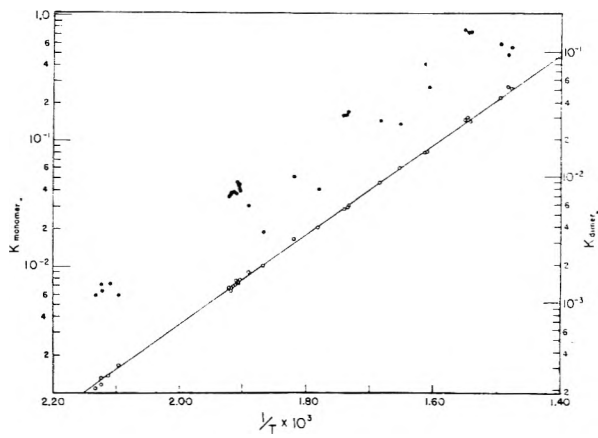

Fig. 2.—The system $2FeBr_2(s) + Br_2(g) \rightleftarrows Fe_2Br_6(g)$.

Taken with results of a previous study[3] of the thermal dissociation of solid $FeBr_3$, an expression for the vapor pressure of dimer above the solid may be derived; $\log P_{mm} = -7044/T + 15.24$, assuming a constant heat of sublimation, 32.3 kcal. Obviously this equation applies only if sufficient bromine is present in the system; solid $FeBr_3$ cannot exist above *ca.* 257° as the necessary bromine pressure exceeds the vapor pressure of bromine above this point; the hypothetical sublimation pressure of Fe_2Br_6 reaches one atmosphere at 297°.

The Monomer–Dimer Equilibrium.—Six independent series of measurements, each with different initial amounts of $FeBr_2$ and bromine, were made in quartz diaphragm gages. Three distinct regions were apparent in each series. A low temperature region (100–450°) exhibited ideal gas behavior and afforded a check on the quantity of bromine introduced. Between 500 and 670° apparent deviation from perfect gas behavior occurred which may be correlated with the dissociation of Fe_2Br_6. Beyond 670° a sudden decrease in pressure and subsequent rise with increasing temperature demonstrated solubility of the vapor phase in liquid $FeBr_2$. The behavior above 500° is shown for four of the series in Fig. 3. Equilibrium was verified in all regions by approaching a given point from both higher and lower temperatures.

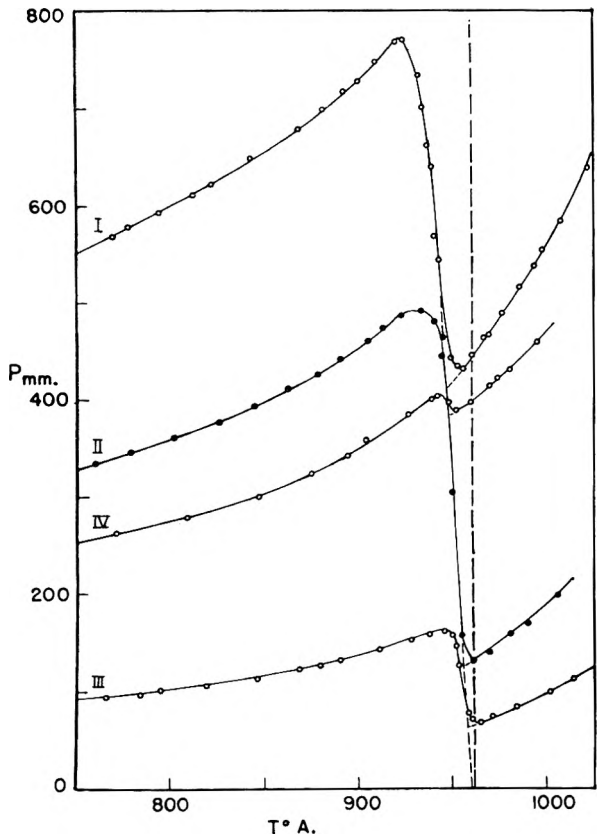

Fig. 3.—Equilibrium pressures in the $FeBr_3$–Br_2 system.

The pressure of $FeBr_3$ in the dissociation range can be determined from the total pressure and its deviation from the extrapolated line characterizing the lower region, with a small correction for the vapor pressure of $FeBr_2$. The proportion of Fe_2Br_6 and Br_2 can be calculated by extrapolation of results for equilibrium (1). Hence knowing the initial amount of bromine introduced, equilibrium constants for the reaction

$$Fe_2Br_6(g) = 2FeBr_3(g) \qquad (2)$$

may be evaluated and are shown in Fig. 4; the size of the circles indicates the effect of an uncertainty in the measured pressure of 1 mm. The solid line represents the equation $\log K_2 = -7268/T + 9.900$ (pressures in mm.), determined by least squares treatment of the data with the more uncertain points (K_2 less than 10) weighted one-half. The heat of dissociation is 33.2 ± 0.8 kcal.

Thermodynamic properties calculated from results of the present work, recent low temperature heat capacity studies on $FeBr_2$,[7] and other references indicated are given in Table I. Some of the values involve an estimate of heat capacities above room temperatures; ΔC_P has been taken as -8 cal./deg., for (1) and -1 cal./deg. for (2). Previously reported constants for the chlorides are listed for comparison.

A rough confirmation of the composition of the vapor phase was made in one of the diaphragm gage studies. The initial amounts of $FeBr_2$ and bromine were adjusted so only the gas phase would be present at higher temperatures. A change in slope on a P–T plot was observed at 662° and was taken to be the highest temperature at which solid $FeBr_2$ was present. The average molecular weight of the gas based on the weight of reactants introduced and the volume of the apparatus, 383, compared favorably with 368, calculated from the equilibrium constants given above and the vapor pressure of $FeBr_2$.[2]

(7) Private communication from Professor E. F. Westrum, Jr., Department of Chemistry, University of Michigan, Ann Arbor, Michigan.

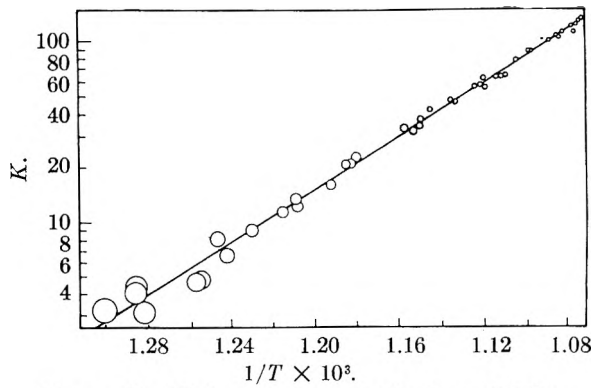

Fig. 4.—Equilibrium constants for $Fe_2Br_6 \leftrightarrows 2FeBr_3$.

TABLE I

THERMODYNAMIC PROPERTIES OF ANHYDROUS IRON CHLORIDES AND BROMIDES AT 25°

Standard state for halogens: gas at one atmosphere.

Substance	$\Delta H°$, kcal.	$\Delta F°$, kcal.	$S°$, e.u.
$FeBr_2(s)$[6,8]	− 66.0	− 56.6	33.62
$FeCl_2(s)$[6,8]	− 81.5	− 72.1	28.19
$FeBr_3(s)$[2]	− 74.0	− 58.9	43.9
$FeCl_3(s)$[8,11]	− 93.4	− 78.6	36.9
$FeBr_3(g)$	− 39.7	− 38.7	91.1
$Fe_2Br_6(g)$	−113.5	−101.8	149.2
$FeCl_3(g)$[9,10]	− 58.1	− 58.3	86.9
$Fe_2Cl_6(g)$[11,12]	−149.0	−139.9	142.2

The solubility effects (Fig. 3) may be correlated by assuming, in regions where the pressure decreases with increasing temperature, solid $FeBr_2$ is in equilibrium with a solution of iron(III) bromide in liquid $FeBr_2$, the solubility varying with pressure of iron(III) vapor and with temperature. From the equilibrium data and the amount of reactants initially introduced, the composition of the liquid can be approximated at the temperature which corresponds to melting of the last trace of solid $FeBr_2$. A slight rounding at these minima was corrected by extrapolating the vertical and higher temperature portions of the curves. The solubility of bromine was assumed negligible in comparison to the solubility of iron(III) bromide and the latter to be in the form of the monomer in solution. Hence a plot of $\log N_{FeBr_2}$ *vs.* the freezing point may be constructed, which on the basis of ideal solution behavior, gives the heat of fusion and freezing point of $FeBr_2$ (the latter shown by the dotted

(8) J. C. M. Li and N. W. Gregory, *J. Am. Chem. Soc.*, **74**, 4670 (1952).

(9) W. Kangro and H. Bernstorff, *Z. anorg. allgem. Chem.*, **263**, 316 (1950).

(10) H. Schäfer, *Z. anorg. Chem.*, **259**, 53 (1949).

(11) W. Kangro and E. Peterson, *ibid.*, **261**, 157 (1952).

(12) K. K. Kelley, Bureau of Mines Bulletin 383, U. S. Gov't Pr. Office, Washington, D. C., 1935, p. 59.

line in Fig. 3). The heat of fusion obtained, 10 kcal./mole, is somewhat lower than that determined in vapor pressure studies (15.5 kcal.[2]); the freezing point, 686°, is also slightly below that of 689°, determined by a cooling curve study of pure $FeBr_2$.[2] However, in view of the necessary assumptions, the agreement is felt to be as good as could be expected.

It has been demonstrated that the transpiration method may be conveniently extended to determine equilibrium pressures in the low region usually studied by the effusion technique, provided suitable analytical procedures are available. This not only extends the usefulness of the method in thermodynamic studies but enables a direct check of the effusion method, and evaluation of the importance of kinetic factors in the latter, in cases where the two may be applied to the same system. The success of the effusion method in the study of vaporization reactions is largely dependent on the accommodation coefficient for the condensation process. This is generally assumed to be sufficiently near unity so the rate of effusion for small orifices will be negligible compared with the rates of vaporization and condensation. However, caution should be exercised in the investigation of systems in which the molecular nature of the vapor is materially different from the building units in the crystal. In some preliminary studies conducted in this Laboratory on the decomposition of chromium(III) iodides, accommodation coefficients appear to be very small, 10^{-3} to 10^{-6}; in the latter case it is impractical to attempt to use an effusion cell with a sufficiently small orifice to keep the steady state pressure near the equilibrium pressure. Comparison of the steady state pressures for various orifices with the true equilibrium pressure offers interesting possibilities for the examination of the kinetics of vaporization reactions in such cases. We are proceeding with research along these lines.

We are pleased to acknowledge support of this work by the Office of Ordnance Research, U. S. Army.

THERMODYNAMIC PROPERTIES OF THE TITANIUM CHLORIDES

BY GORDON B. SKINNER AND ROBERT A. RUEHRWEIN

Monsanto Chemical Company, Chemical Research Department, Dayton, Ohio

Received November 23, 1954

The heat of formation at 25° of liquid titanium tetrachloride has been found to be -191 ± 3 kcal. mole^{-1}, and that of solid titanium trichloride, -170.0 ± 0.8 kcal. mole^{-1}. Experimental determinations have been made of the total disproportionation pressures of titanium trichloride and dichloride, the vapor pressure of titanium trichloride, and the molecular weight of titanium trichloride. Equilibria in the reactions between titanium tetrachloride vapor and titanium carbide, and between sodium chloride and titanium metal, were also investigated. Some estimates of thermal functions of the titanium chlorides were made to permit thermodynamic calculations relating the various experiments.

Introduction

The literature contains very few references to the thermodynamic properties of the titanium chlorides. The heat of formation of titanium tetrachloride has been calculated[1] from an approximate measurement by Thomsen[2]; Latimer[3] has measured the heat capacity of titanium tetrachloride at low temperatures; and Kelley[4,5] has calculated the thermal properties of gaseous titanium tetrachloride from the molecular constants.

We have made several measurements of thermal properties of the titanium chlorides, which, taken together, provide a fairly complete set of thermal data. While the accuracy of many of the figures may be improved by more careful work, we feel that, in the general absence of other experimental data, these will be of value.

Experimental

Materials.—Titanium prepared by the "iodide" process, of 99.9% purity, was used in measurements of the heat of formation of $TiCl_4$. A titanium rod made from du Pont sponge of about 99.7% purity was turned on a lathe to give fine turnings for measurements of the heat of formation of $TiCl_3$. A piece of this rod was used to make the reactor to study the reaction of sodium chloride with titanium.

Titanium tetrachloride was obtained from the Stauffer Chemical Company, and fractionally distilled several times before use. It contained less than 0.1% impurity. Titanium trichloride for disproportionation experiments was prepared by the National Research Corporation by the Sherfey[6] process from pure $TiCl_4$ and hydrogen, and contained only a little $TiCl_4$ as impurity. Trichloride for other experiments was made by reaction of $TiCl_4$ with du Pont sponge titanium at about 800°. This material was found to contain about 1% titanium dichloride.

Titanium carbide was made by heating titanium dioxide and carbon *in vacuo* to about 1800°. Chemical analysis gave 18.90% carbon, 78.86% titanium. The remaining 2.24% was likely oxygen. Other chemicals were standard reagent grade products.

Heat of Formation of Titanium Tetrachloride.—After a number of unsuccessful trials with other methods, direct chlorination was used to measure this property. The strongly-built Pyrex bomb of Fig. 1 could withstand a pressure of several atmospheres—experimentally three atmospheres of chlorine were used to speed up the reaction. The apparatus came apart in the middle, where a Teflon gasket was used to make a seal, and the two pieces were held together by a commercial pipe coupling. Titanium turnings were placed in the silica sample container, along with a little red phosphorus to start combustion. The sample container had a few small holes in the bottom, to aid in the circulation of the chlorine. The assembled apparatus was placed inside a conventional combustion calorimeter which was used to measure the heat given out by the chlorination. Before the chlorination was carried out, the apparatus was evacuated, and the reaction took place as soon as the chlorine was admitted. The chlorine was

(1) F. D. Rossini, D. D. Wagman, W. H. Evans, S. Levine and I. Jaffe, U. S. Dept. of Commerce, Natl. Bur. of Standards Circ. No. 500 (1952).

(2) J. Thomsen, "Thermochemical Investigations," Barth, Leipzig, 1882-86.

(3) W. M. Latimer, *J. Am. Chem. Soc.*, **44**, 90 (1922).

(4) K. K. Kelley, U. S. Bureau of Mines, Bulletin **476** (1949).

(5) K. K. Kelley, U. S. Bureau of Mines, Bulletin 477 (1950).

(6) J. M. Sherfey, *J. Research Natl. Bur. Standards*, **46**, 299 (1951).

dried with phosphorus pentoxide before use, and a pressure gage in the line made it possible to maintain a constant pressure of chlorine during the reaction. The chlorine was kept at its full vapor pressure at room temperature in the drying cylinder, and before entering the calorimeter it passed through a long coil of copper tubing (also at room temperature) so that it could warm up after any cooling on expansion when it was released from the cylinder. Room temperature at the time of the experiment was noted in order to make a correction for the heat capacity of the chlorine. The calorimeter was calibrated electrically to 0.2%. Its heat capacity was 2811 cal./deg. C. Experiments were done at about 29°.

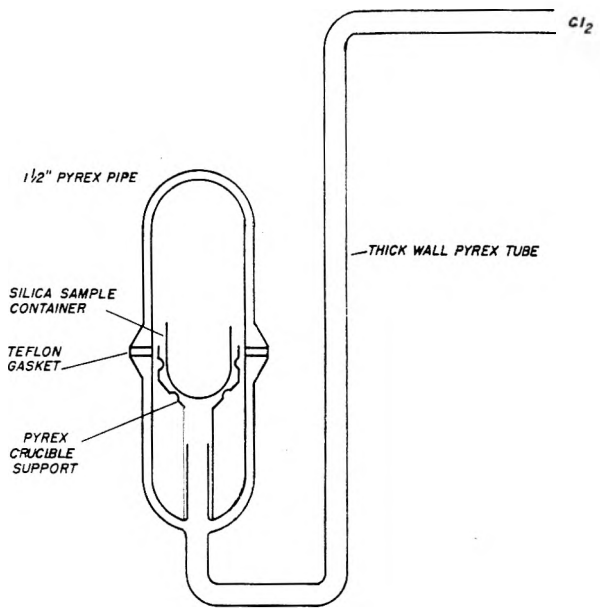

Fig. 1.—Apparatus for measuring the heat of formation of titanium tetrachloride.

The experiments are described in Table I. A correction was made for the change in heat content of chlorine with pressure, on the assumption that it obeyed the Berthelot equation. Another correction was made for the solubility of chlorine in the liquid titanium tetrachloride, assuming that chlorine and titanium tetrachloride form an ideal solution. While the average value from Table I is −189.0 kcal., it seems that the value for the largest sample is most accurate, since several of the sources of error in the determination are independent of the amount of sample used, and hence proportionately larger for the smaller samples. This gives the value −190 ± 3 kcal. for the heat of formation of titanium tetrachloride at 25°.

TABLE I

EXPERIMENTAL DATA FOR THE HEAT OF FORMATION OF $TiCl_4$ (l)

Run no.	1	2	3
Wt. of titanium (g.)	0.2473	0.7474	0.5199
Wt. of phosphorus (g.)	0.0040	0.0040	0.0040
Total heat evolved, cal.	997.9	3,021.3	2,093.5
Heat capacity corrn., cal.	+1.6	+4.1	+2.9
Corrn. for chlorination of P, cal.	−13.7	−13.7	−13.7
Corrn. for $TiCl_4$ vaporization, cal.	+0.7	+0.7	+0.7
Corrn. for soln. of Cl_2 in $TiCl_4$, cal.	−17.6	−48.5	−33.7
Pressure corrn. for heat content of Cl_2, cal.	+0.8	+2.4	+1.6
Net heat of chlorination to $TiCl_4$(l), cal.	969.6	2,966.3	2,051.3
Heat of formation of $TiCl_4$(l), kcal./mole	187.8	190.2	189.0

Heat of Formation of Titanium Trichloride.—This property was measured by dissolving samples of titanium metal and titanium trichloride in a dilute solution of hydrofluoric acid. The solutions were made in a polyethylene-coated Dewar flask fitted with a stirrer, calibrating heater and resistance thermometer, and the samples were contained in thin-walled Pyrex bulbs which were broken on the bottom of the Dewar flask at the proper time. In the solution of the titanium metal, in which hydrogen was produced, a layer of C_{15}-C_{17} paraffin oil was spread on the surface of the solution to prevent splashing. Corrections were made for its heat capacity and for the heat of vaporization of the water vapor carried away by the hydrogen.

The heat of formation of titanium trichloride was obtained by combining the heats of the reactions

$$Ti(s) + (3HCl + 11.96HF + 1322H_2O) \longrightarrow (\text{final soln.}) + 3/2H_2(g)\ \Delta H_1 \quad (1)$$

$$TiCl_3(s) + (11.96HF + 1322H_2O) \longrightarrow (\text{final soln.})\ \Delta H_2 \quad (2)$$

$$(3HCl + 30H_2O) + (11.96HF + 1292H_2O) \longrightarrow (3HCl + 11.96HF + 1322H_2O)\ \Delta H_3 \quad (3)$$

$$3/2\ H_2(g) + 3/2\ Cl_2(g) + 30H_2O(l) \longrightarrow (3HCl + 30H_2O)\ \Delta H_4 \quad (4)$$

$$(11.96HF + 1292H_2O) + 30H_2O(l) \longrightarrow (11.96HF + 1322H_2O)\ \Delta H_5 \quad (5)$$

Adding up these five reactions, the result is

$$Ti(s) + 3/2\ Cl_2(g) \longrightarrow TiCl_3(s)$$
$$\Delta H = \Delta H_1 - \Delta H_2 + \Delta H_3 + \Delta H_4 - \Delta H_5$$

The first three reactions were measured experimentally, and the last two taken from the literature. The small amount of $TiCl_2$ in the $TiCl_3$ introduced an uncertainty estimated at 1% in the measured heat of solution of titanium trichloride.

Care was taken to ensure that the "final solutions" of equations (1) and (2) were identical. It was established by titration with $K_2Cr_2O_7$ that solutions of both $TiCl_3$ and Ti in HCl–HF solutions give trivalent titanium, within 1%. Moreover Latimer[7] points out that "it is impossible to have appreciable concentrations of +2 titanium in solutions which have an acidity greater than 0.1 N H^+." There is, therefore, little doubt that titanium metal is oxidized quantitatively to Ti^{+3}. A solution of $TiCl_3$ in HCl solution is pink, but when HF is added there is an immediate change in color to green. This same green color is apparent when titanium is dissolved in HF or HCl–HF solutions so that whatever the reason is for the color change, it occurs in both reactions. Argon was bubbled through the acid solutions before the experiments, and an argon atmosphere kept over the solutions during experiments, to reduce oxidation of the solutions by the air.

Two determinations of the heat of solution of titanium metal in the HF–HCl solution gave ΔH_1's of −106.88 and −107.03 kcal. per gram-atom of titanium, or an average of −106.96 ± 0.2 kcal. Two determinations of the heat of solution of titanium trichloride gave ΔH_2's of −55.61 and −55.41 kcal. per mole of titanium trichloride, or an average of −55.51 ± 0.7 kcal. This large uncertainty, as mentioned above, is to allow for impurities in the trichloride. Two determinations of ΔH_3 gave −2.61 and −2.69 kcal., or an average of −2.65 ± 0.1 kcal. The values of ΔH_4 and ΔH_5, respectively,[1] are −115.88 + 0.05 kcal., and −0.01 ± 0.00 kcal. Accordingly, the final $\Delta H°$ for the heat of formation of solid titanium trichloride is −170.0 ± 0.8 kcal. This figure was determined at about 24.2°, but should not be appreciably different at 25°.

Vapor Pressure of Titanium Trichloride.—This vapor pressure was measured by the transfer method, with titanium tetrachloride as carrier gas. The tetrachloride prevented the disproportionation of the trichloride (see below). The tetrachloride was boiled at about one atmosphere pressure in a Pyrex flask, and the vapor passed over the heated trichloride which was contained in a silica tube connected to the Pyrex flask by a graded seal. The trichloride was solid at the experimental temperatures. The trichloride and tetrachloride vapors were condensed in different parts of the exit tube, and the amount of each was meas-

(7) W. M. Latimer, "The Oxidation States of the Elements and their Potentials in Aqueous Solutions," Second Edition, Prentice-Hall Inc., New York, N. Y., 1952.

ured. From these and the measured total pressure in the apparatus, the vapor pressure of titanium trichloride was calculated on the assumption that the vapors behave ideally.

Six experiments gave vapor pressures ranging from 0.7 mm. at 528° to 66 mm. at 641°. However, after the experiments were done, it became apparent that the tetrachloride had not been saturated with trichloride vapor, particularly at the lower temperatures, and it had to be concluded that the measured vapor pressures were all low. The vapor pressure of trichloride was estimated to be about 80 mm. at 641°, instead of 66 mm. as found experimentally. This is the figure which has been used in thermodynamic calculations.

Disproportionation of Titanium Trichloride.—The apparatus of Fig. 2 was used to measure the total pressure in the reaction

$$2TiCl_3 \longrightarrow TiCl_4 + TiCl_3 \qquad (I)$$

A sample of titanium trichloride was put into the apparatus and the seal-off made as shown. The apparatus was then evacuated through the U-tube. The sample tube on the left was heated in an electric tube furnace, with a heavy copper block surrounding it to maintain an even temperature, which was measured with a chromel–alumel thermocouple and Brown potentiometer to 1°. Much of the other part of the apparatus was immersed in an oil-bath to keep the titanium tetrachloride from condensing, and the part between the oil-bath and the furnace was also heated by chromel heater wire.

The pressures measured by the manometer were exerted entirely by titanium tetrachloride vapor, but it is considered that back in the furnace the pressures are the totals of the partial pressures of tetrachloride, trichloride and dichloride. These pressures are accurate to about 1 mm. Some of them were obtained twice on the same sample of titanium trichloride, after pumping out the system, and the equilibrium was approached from both high and low temperatures in some cases.

The experimental total pressures are given in column 2 of Table II. The next two columns give the vapor pressures of titanium trichloride and dichloride at the respective temperatures, calculated as described in the Discussion. The net disproportion pressures of titanium trichloride are given in the last column of Table II.

TABLE II

DISPROPORTIONATION OF TITANIUM TRICHLORIDE

T, °K.	Total P, mm.	$P(TiCl_3)$, mm.	$P(TiCl_2)$, mm.	$P(TiCl_4)$, mm.
802	16.1	4.0	0.0	12.1
849	54.1	15.2	0.2	38.7
863	75.5	21.9	0.4	53.2
900	182	58	1	123
928	339	105	2	232

Disproportionation of Titanium Dichloride.—A sample of titanium dichloride was made by heating titanium trichloride at 600° *in vacuo*. The sample was put into the apparatus of Fig. 2, and the procedure described above was used to obtain the total pressure over the solids. Titanium dichloride disproportionates according to the reactions

$$3TiCl_2 \longrightarrow Ti + 2TiCl_3 \qquad (II)$$

and

$$2TiCl_2 \longrightarrow Ti + TiCl_4 \qquad (III)$$

Therefore the furnace contained titanium dichloride, trichloride and tetrachloride vapors, and the tetrachloride again served to transmit the pressure to the manometer. The total pressures measured are listed in the second column of Table III. The pressures are accurate to about 1 mm.

TABLE III

DISPROPORTIONATION OF TITANIUM DICHLORIDE

T°, K	Total P, mm. (obsd.)	$P(TiCl_3)$, mm. (calcd.)	$P(TiCl_2)$, mm. (calcd.)	$P(TiCl_4)$, mm. (calcd.)	Total P, mm. (calcd.)
977	16.3	6	8	1	15
1009	36.3	11	18	1	30
1041	66.7	23	36	3	62
1071	125.2	41	66	5	112

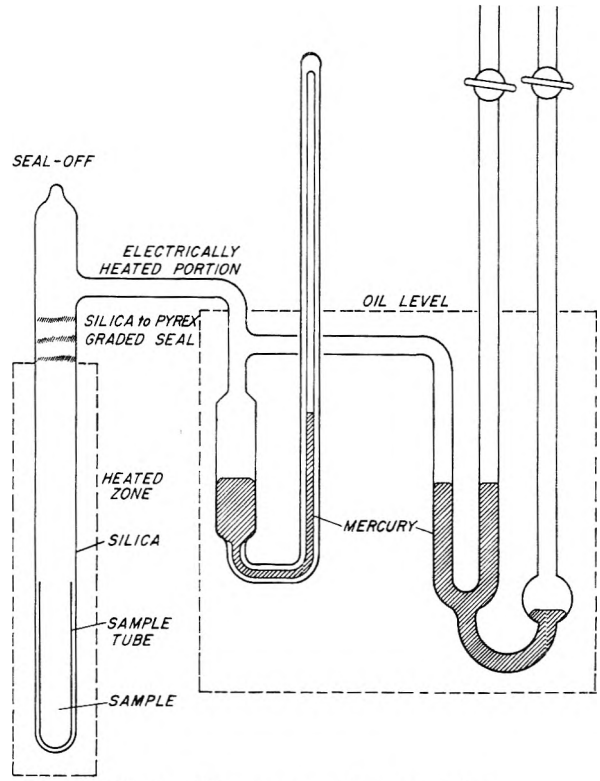

Fig. 2.—Disproportionation apparatus.

Molecular Weight of Titanium Trichloride.—It seemed possible that titanium trichloride might resemble aluminum chloride and ferric chloride in having a dimeric vapor at temperatures just above the boiling point and monomeric vapor at higher temperatures. If it were dimeric, the actual vapor pressure would be half that given in the previous section. The disproportionation reaction complicates vapor density measurements, and a rather roundabout way had to be used to get at the problem.

A silica apparatus of the Victor Meyer type was used, with a long tube furnace to heat the bulb. The apparatus was flushed with argon before each experiment, and the furnace heated to 750°, at which temperature the vapor pressure of titanium trichloride was expected to be over one atmosphere. An experimental sample consisted of a mixture of titanium trichloride and tetrachloride contained in a small silica bottle with a ground stopper. The sample was dropped into the heated apparatus and the volume of argon displaced was measured. After the experiments the sample bottle was removed and a small amount of titanium dichloride in it was weighed. It seemed that the tetrachloride

TABLE IV

CALCULATION OF MOLECULAR WEIGHT OF TITANIUM TRICHLORIDE

Starting material: $TiCl_3$, 0.0654 g., 0.423 mmole
$TiCl_4$, 0.0834 g., 0.440 mmole

Final state: 0.773 mmole argon displaced ($TiCl_4$ + $TiCl_3$ vapor)
0.0138 g. $TiCl_2$ left in bottle (0.116 mmole)

Disproportionation reaction

$2TiCl_3$	$\longrightarrow$	$TiCl_4$	+	$TiCl_2$
0.232 mmole		0.116 mmole		0.116 mmole
0.0358 g.		0.0220 g.		0.0138 g.

Thus, total mmole of $TiCl_4$ present (0.440 + 0.116) = 0.556
total mmole of $TiCl_3$ present (0.773 − 0.556) = 0.217
total wt. of $TiCl_3$ in vapor (0.0654 − 0.0358) = 0.0296 g.

$$\therefore \text{ mol. wt. of } TiCl_3: \frac{0.0296}{0.000217} = 137$$

vaporized very rapidly, and did not prevent some disproportionation of the trichloride from occurring in the sample bottle.

Three experiments of this type were carried out, and a typical one is described in Table IV. This molecular weight of 137, with the others of 163 and 134, give a mean value of 145, not far from the titanium trichloride monomer value of 154, and a long way from the dimer value of 308. This result strongly suggests that titanium trichloride vapor is mostly monomeric at 750°. If comparisons with aluminum chloride and ferric chloride hold, titanium trichloride stays monomeric at higher temperatures.

Reaction between Titanium Carbide and Titanium Tetrachloride.—This reaction was studied since it gave equilibrium data at a moderately high temperature. Titanium tetrachloride vapor was passed over heated titanium carbide in a silica tube, and titanium trichloride was formed and separated out in a cooler part of the tube. This reaction was run at several different rates of flow of tetrachloride, so that the approach to equilibrium could be studied. The reaction involved is

$$3TiCl_4 + TiC \longrightarrow 4TiCl_3 + C \qquad (IV)$$

Ehrlich[8] has shown that TiC and C are the only two phases present in the composition range TiC–C. These experiments were all done at 1050°. An extrapolation of the experiments to an infinitely slow rate of tetrachloride flow showed that 8.2 weight per cent. trichloride would be present in the vapor. If an equilibrium constant K_p is written as

$$K_p = [P(TiCl_3)]^4/[P(TiCl_4)]^3$$

then at 1050°, the logarithm of this K_p is −3.9.

Reaction between Titanium and Sodium Chloride.—This reaction was studied to obtain equilibrium data at still higher temperatures. The disproportionation experiments described above suggested that at the boiling point of sodium chloride, the reaction

$$2NaCl(g) + Ti(s) \longrightarrow 2Na(g) + TiCl_2(g) \qquad (V)$$

would proceed to a measurable extent. Experimentally, a closed-end titanium tube of $^1/_2$-inch outside diameter, $^3/_8$-inch inside diameter and 5-inch length, containing sodium chloride and titanium turnings, was heated inductively in an argon atmosphere so that the sodium chloride boiled and passed over the titanium turnings and then out of the tube. The salt condensed on the walls of the silica tube inside which the titanium tube was heated, and was collected and analyzed for titanium. The temperature of the tube was measured with an optical pyrometer, but since the sodium chloride vapor interfered with the measurements, the temperatures are accurate to only about ±30°. Experiments were done at about one atmosphere and one-half atmosphere.

The equilibrium constant for the reaction of sodium chloride with titanium was written

$$K_p = \frac{[P(Na)]^2\,[P(TiCl_2)]}{[P(NaCl)]^2}$$

where the pressures are expressed in atmospheres. An approximate calculation showed that titanium dichloride is the only titanium chloride present in an appreciable amount. The experimental data are listed in Table V, while the equilibrium constants and other thermodynamic data are listed in Table VI. These calculations will be discussed below.

TABLE V

EXPERIMENTAL DATA FOR REACTION OF NaCl VAPOR WITH TITANIUM

T, °K. ±30	Pressure, mm.	Time at high temp., min. ±1	Wt. of NaCl evap., g. ±0.02	Wt. of Ti in vapor, g. ±0.004
1830	780 ± 10	6	2.00	0.0905
1780	780 ± 10	3	0.95	.0395
1810	780 ± 10	8	1.99	.0862
1810	780 ± 10	4	1.31	.0585
1670	360 ± 5	10	1.17	.0370
1690	370 ± 5	10	1.50	.0428
1690	360 ± 5	14	2.16	.0706

(8) P. Ehrlich, *Z. anorg. allgem. Chem.*, **259**, 1 (1949).

TABLE VI

THERMODYNAMIC CALCULATIONS FOR REACTION OF NaCl VAPOR WITH TITANIUM

T, °K.	$K \times 10^3$, atm.	$\Delta F°$, cal.	$\Delta(F° - H_0°)$, cal.	$\Delta H_0°$, cal.
1830	0.833	25,800	−42,600	68,400
1780	.474	27,100	−41,600	68,700
1810	.719	26,000	−42,200	68,200
1810	.781	25,700	−42,200	67,900
1670	.106	30,400	−39,200	69,600
1690	.091	31,200	−39,600	70,800
1690	.139	29,800	−39,600	69,400
Mean				69,000

Discussion

The experiments described above have not, unfortunately, determined all of the unknown thermal properties of the titanium chlorides. Therefore, when an attempt is made to relate the various experiments by thermodynamic calculations, several estimates have to be made. The most important estimates are of the heat capacities and related functions of the dichloride and trichloride. Once these functions are established, complete thermodynamic calculations can be made since thermal functions of titanium tetrachloride can be calculated from the molecular constants,[5] Latimer[3] has measured the heat capacity of solid and liquid tetrachloride at low temperatures, and Schafer and Zeppernick[9] have measured the vapor pressure of titanium tetrachloride.

In this work estimates of the thermal properties of the lower chlorides were made by comparisons with other molecules whose properties are known. The details of the methods of estimating are too tedious for a complete discussion here, although they are simple enough in principle. The results are given in Tables VII and VIII. Values for NaCl and $TiCl_4$ are included since they have been changed from the literature values to include allowances for vibrational anharmonicities and rotation–vibration interactions. The uncertainties assigned to these estimates are considered to be maximum uncertainties, with the probability of 1 in 25 that the actual values lie outside the given ranges of uncertainty.

TABLE VII

FREE ENERGY FUNCTIONS, $-(F° - H_0°)/T$, IN CAL. DEG.$^{-1}$ MOLE^{-1}

Substance	298°K.	500°K.	1000°K.	1500°K.	2000°K
$TiCl_2$(s)	12.7	19.7	30.7 ± 5		
$TiCl_2$(g)	58.5	64.1	72.4	77.6	81.3 ± 4
$TiCl_3$(s)	19.4	28.2	42.2 ± 5		
$TiCl_3$(g)	63.7	71.4	82.9	90.1 ± 4	
$TiCl_4$(l)	29.3 ± 2				
$TiCl_4$(g)	67.0	76.8	92.0	102.6 ± 2	
NaCl(g)				61.7	63.2 ± 0.2

TABLE VIII

HEAT CONTENTS, $H_0 - H_0°$, IN CAL. MOLE^{-1}

Substance	298°K.	500°K.	1000°K.	1500°K.
$TiCl_2$(s)	3,800	7,500	17,000 ± 600	
$TiCl_2$(g)	3,000	5,600	12,700	20,400 ± 1200
$TiCl_3$(s)	4,500	9,200	21,800 ± 800	
$TiCl_3$(g)	4,200	8,000	17,700	27,600 ± 1500
$TiCl_4$(l)	9,100 ± 300			
$TiCl_4$(g)	5,100	10,100	22,800	35,600 ± 800

(9) H. Schafer and F. Zeppernick, *ibid.*, **272**, 274 (1953).

The authors have recently learned that Johnson, Nelson and Prosen[10] have found the heat of formation of liquid titanium tetrachloride to be -192.9 ± 0.6 kcal./mole (compared to our value of -190 ± 3 kcal./mole). While the two values agree within the experimental errors assigned, Johnson, Nelson and Prosen's value seems to be the more accurate. Therefore, it has been used in the calculations described below.

Thermodynamic calculations were made as follows. Free energy functions of solid and gaseous $TiCl_3$ were combined with the vapor pressure (80 mm.) at 914°K., to give the heat of sublimation at 0°K. (42.4 kcal.). Heat contents of solid and gaseous $TiCl_3$ then gave the heat of sublimation at 900°K. as 38.8 kcal. Then the vapor pressure equation of $TiCl_3$ was written in the form

$$\log P = \frac{\Delta H}{2.303RT} + B$$

The constant B was obtained from ΔH and the known value of the vapor pressure (P) at 914°K. From this equation, vapor pressures of $TiCl_3$ were calculated at each of the experimental disproportionation temperatures. These are listed in column 3 of Table II. These pressures were subtracted from the total experimental pressures to give the net $TiCl_4$ pressures (as in column 5 of Table II, except that the small $TiCl_2$ vapor pressure at this point was neglected). From the $TiCl_4$ pressure ΔH for the disproportionation of $TiCl_3$ (34.7 kcal. at about 900°K., 38.5 kcal. at 0°K.) was calculated. At this point an important check on the estimates could be made, by calculating ΔH_0 for the disproportionation reaction using one experimental pressure and free energy functions of $TiCl_2$(s), $TiCl_3$(s) and $TiCl_4$(g). Needless to say, this didn't come out exactly right the first time and the estimates were adjusted until it did.

From the ΔH_0 of the disproportionation measurements and the measured heats of formation of $TiCl_3$ and $TiCl_4$, the heat of formation of solid $TiCl_2$ (Table IX) was calculated. Further data on $TiCl_2$ were obtained from the study of reaction V. Calculations using free energy functions to give ΔH_0° are given in Table VI. Since the heat of formation of NaCl(g) is known,[1] ΔHf_0° of $TiCl_2$(g) was obtained (Table IX), although not with the highest accuracy. The difference in the ΔHf_0°'s of solid and gaseous $TiCl_2$ gives, of course, its heat of sublimation. The vapor pressures of $TiCl_2$ given in column 4 of Table II were obtained by combining this ΔH_0° with free energy functions of solid and gaseous $TiCl_2$.

TABLE IX

HEATS OF FORMATION OF THE TITANIUM CHLORIDES

Substance	State	$-\Delta Hf^\circ$, at 0°K., kcal. mole^{-1}	$-\Delta Hf^\circ$, at 298.16°K., kcal. mole^{-1}
$TiCl_2$	s	118.7 ± 2.9	118.3 ± 3.0
	g	69.1 ± 3.0	69.5 ± 3.0
$TiCl_3$	s	170.1 ± 1.0	170.0 ± 0.8
	g	127.7 ± 2.2	128.0 ± 2.3
$TiCl_4$	s	196.4 ± 0.7	
	l		192.9 ± 0.6
	g	182.6 ± 0.8	183.0 ± 0.8

The equilibrium measurements of the reaction between titanium carbide and titanium tetrachloride gave an important check on the estimates and the other experiments. The thermal properties listed in Tables VII, VIII and IX, combined with those of titanium carbide and carbon,[4,5,11] yield a value of log K_p equal to -3.5, quite close to the experimental value of -3.9. The same sort of thing holds with the measurements of the disproportionation pressures of $TiCl_2$. Observed and calculated pressures are shown in Table III. According to these calculations, $TiCl_2$ disproportionates mostly to $TiCl_3$, only a small amount of $TiCl_4$ being formed.

While no great accuracy is claimed for these estimates, they are consistent with all the experiments and seem reasonable in comparison with known thermal functions for other compounds. They have served a useful purpose in relating our experiments, and in giving values for quantities which were not directly measured, such as the heat of formation of $TiCl_2$. It is hoped that the estimates can soon be eliminated as new experimental measurements are made.

(10) W. H. Johnson, R. A. Nelson and E. J. Prosen, unpublished results, reported to the Office of Naval Research in National Bureau of Standards Report No. 3663 (1954).

(11) G. L. Humphrey, *J. Am. Chem. Soc.*, **73**, 2261 (1951).

ELECTRICAL CONDUCTANCE AND DENSITY OF MOLTEN SALT SYSTEMS: KCl–LiCl, KCl–NaCl AND KCl–KI[1]

BY E. R. VAN ARTSDALEN AND I. S. YAFFE

Chemistry Division, Oak Ridge National Laboratory, Oak Ridge, Tennessee

Received October 8, 1954

Electrical conductance and density have been determined as functions of temperature for the fused, binary salt systems potassium chloride–lithium chloride, potassium chloride–sodium chloride and potassium chloride–potassium iodide. Specific conductance increases with temperature, and is generally more temperature-dependent immediately above the melting point than at higher temperatures. Molar volumes have been computed from density data; they are very closely additive for the chloride mixtures, but deviate slightly in a positive direction for the chloride-iodide system. On the other hand, equivalent conductance isotherms for all three systems studied show quite marked negative deviations from additivity, with certain mixtures being less conducting than either pure component. Conductance has been treated as a rate process and values have been calculated for the heat of activation and the entropy of activation. In general, it was found that the heat of activation is temperature dependent, although lithium chloride appears to be an exception. Both heat and entropy of activation tend to maximum values for those mixtures which exhibit minimum conductance. Qualitative explanations are presented to account for the various effects in terms of charge density, internuclear distance and short range order within the melts.

In recent years our lack of knowledge concerning the fundamental properties of molten salt systems has been accentuated by the greater emphasis now being placed on high temperature processes. Notwithstanding the need for specific data concerning particular fused systems for specific industrial processes, such as electrolytic production of aluminum, etc., a greater need exists for obtaining fundamental data about molten salts in general so that there may be a better understanding of the properties of the fused state. It was with these thoughts in mind that we have embarked upon a program of study of the basic physical chemistry of molten salts.

Molar volume and electrical conductance are among the fundamental properties of liquid systems, and well-established experimental techniques for measurement of these physical characteristics of aqueous solutions are applicable with slight modification to use at higher temperatures. So it was decided to initiate our program with a study of these two quantities. Furthermore, a considerable amount of previous work concerning these properties of pure fused salts furnishes a firm foundation for our work on mixtures.

A number of prior publications[2,3] have pointed out that various maxima, minima and other points of inflection can be found in molar volume and conductance isotherms for molten salt mixtures. Such points of inflection have frequently been considered to indicate the existence of complex ions in melts. It was our hope that our studies might give us some reliable information about the existence, stability and reactions of complex ions which certainly exist in numerous molten salts at high temperatures. In order to lay a satisfactory foundation for more complicated systems, it was decided to investigate first some halide mixtures in which there appeared little likelihood of the formation of complexes. Therefore, the molten systems potassium chloride–lithium chloride, potassium chloride–sodium chloride and potassium chloride–potassium iodide were chosen for our initial investigations. Although the first system had been studied previously by Karpachev, Stromberg and Padchainova,[4] and the second by Ryschkewitsch,[5a] and Barzokowsky, [5b] we thought them worthy of reinvestigation. The possibility of complex formation in the chloride–iodide system was not overlooked.

The more recent work on conductance and molar volume of molten salts is listed in references 2 through 14. These papers contain references to earlier work.

Experimental

The furnace assembly used for these measurements is shown in Fig. 1. The furnace, 3.5″ inner diameter by 16″ long, was provided with shunts for removing or imposing thermal gradients. A platinum–rhodium crucible, which contained the melt, was inside a heavy-walled nickel tube, which, in turn, was enclosed by an outer inconel tube. The crucible was placed inside an alumina crucible in order to insulate the melt from electrical contact with the assembly. Appropriate heat baffles were inserted as illustrated. In order to provide an inert atmosphere, argon was admitted to the assembly through the hollow nickel support rod. The temperature of the furnace was controlled to 0.2° by an anticipating thermocouple which operated a zero-suppression-type, 6-millivolt range, Leeds and Northrup Speedomax Type S recorder-controller in conjunction with a Leeds and Northrup "DAT" controller. The actual temperature within the melt was measured with a calibrated platinum, 87% platinum–13% rhodium thermocouple by means of a Rubicon precision potentiometer. By appropriate adjustment of furnace shunts and with the described control equipment, the temperature of the molten salt, which

(1) Presented at the Symposium on High Temperature Chemical Reactions at the 126th Meeting of the American Chemical Society, New York, N. Y., Sept. 15, 1954.

(2) (a) H. Bloom, J. W. Knaggs, J. J. Molloy and D. Welch, *Trans. Faraday Soc.*, **49**, 1458 (1953); (b) Y. V. Baimakov and S. P. Samusenko, *Trans. Leningrad Industrial Inst.*, 3 (1938).

(3) V. A. Izbekov, *Ukrain. Akad. Nauk. Institut Khim.* (Proc. 1st. All-Union Conf. Non-aqueous Solutions), p. 142 (1935).

(4) S. V. Karpachev, A. G. Stromberg and N. Padchainova, *Zhur. Obshchei Khim.*, **5**, 1517 (1935).

(5) (a) E. Ryschkewitsch, *Z. Elektrochem.*, **39**, 531 (1933); (b) B. P. Barzokowsky, *Bull. Acad. Sci. URSS, Class Chim.*, no. 5, 825 (1940).

(6) J. O. Edwards, C. S. Taylor, A. S. Russell and L. F. Maranville, *J. Electrochem. Soc.*, **99**, 527 (1952).

(7) P. W. Huber, E. V. Potter and H. W. St. Clair, U. S. Bureau Mines, Report of Invest. 4858 (1952).

(8) R. C. Spooner and F. E. W. Wetmore, *Can. J. Chem.*, **29**, 777 (1951).

(9) J. Byrne, H. Fleming and F. E. W. Wetmore, *ibid.*, **30**, 922 (1952).

(10) H. Bloom and E. Heymann, *Proc. Roy. Soc. (London)*, **188A**, 392 (1947).

(11) W. J. Davis, S. E. Rogers and A. R. Ubbelohde, *ibid.*, **220A**, 14 (1953).

(12) A. E. van Arkel, E. A. Flood and N. F. H. Bright, *Can. J. Chem.*, **31**, 1009 (1953).

(13) J. S. Peake and M. R. Bothwell, *J. Am. Chem. Soc.*, **76**, 2653 (1954).

(14) J. O'M. Bockris, J. A. Kitchener, S. Ignatowicz and J. W. Tomlinson, *Trans. Faraday Soc.*, **48**, 75 (1952), *et seq.*

fluctuated less than the furnace temperature, could be maintained to better than ±0.1° at temperatures up to 1000° with a thermal gradient of no more than 0.2° over the height of the melt (usually about 2.5″).

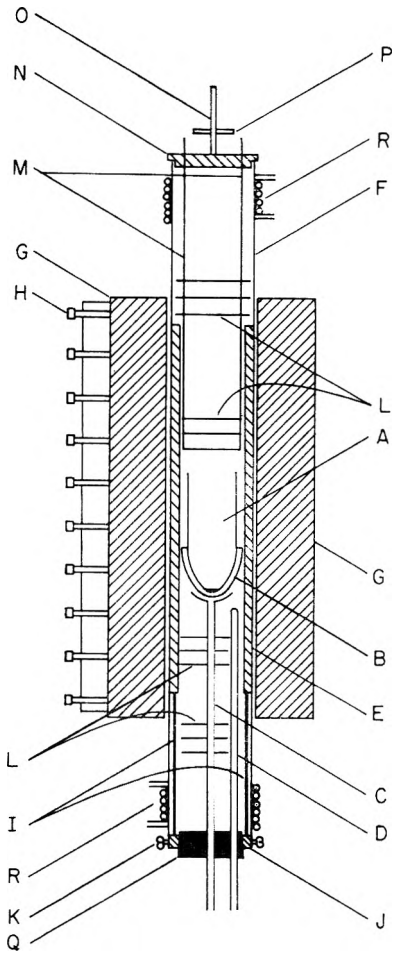

Fig. 1.—Furnace assembly: A, Pt crucible; B, Alundum crucible; C, Ni support tube; D, quartz thermocouple sheath; E, heavy-walled Ni tube; F, inconel tube; G, furnace; H, external taps for shunts; I, stainless steel support rods; J, bottom ring; K, wing nuts; L, radiation shields; M, radiation shield support; N, brass top plate; O, cell support; P, cell yoke; Q, rubber stopper; R, cooling coils.

Figure 2 is a diagram of the quartz dip-type capillary conductance cell used. Cylindrical platinum electrodes rest on the shelf at the top of the capillary tubing. Resistance measurements were made with a Leeds and Northrup precision "Jones" bridge. In order to eliminate the mutual inductance caused by the close proximity to each other of the electrode leads, it was found necessary to make resistance measurements from 2000 to 20,000 c.p.s. (The measured resistance varied less than 0.5% in this range.) A linear extrapolation to infinite frequency of measured resistance *versus* (frequency)$^{-2}$ was then made so that the inductance-free resistance could be obtained. The conductance cells were calibrated in demal aqueous potassium chloride solution at 25.00° using platinized electrodes according to the method of Jones and Bradshaw.[15] Allowance can be made for expansion of the quartz cells on raising the temperature, but such correction amounts to less than 0.05% and was therefore considered unnecessary. The cell constants were of the order of 300 to 500 cm.$^{-1}$ and were of the proper order of magnitude to agree with the conclusion that the resistance of the cell was determined almost exclusively by the salt melt within the capillary. Recalibration of the cells following two or three days use in the molten salt mixtures showed that the cell constants did not change by more than 0.3%, and, on the average, about 0.1%, although the platinum black of the electrodes was converted to platinum grey by the melts.

(15) G. Jones and B. C. Bradshaw, *J. Am. Chem. Soc.*, **55**, 1780 (1933).

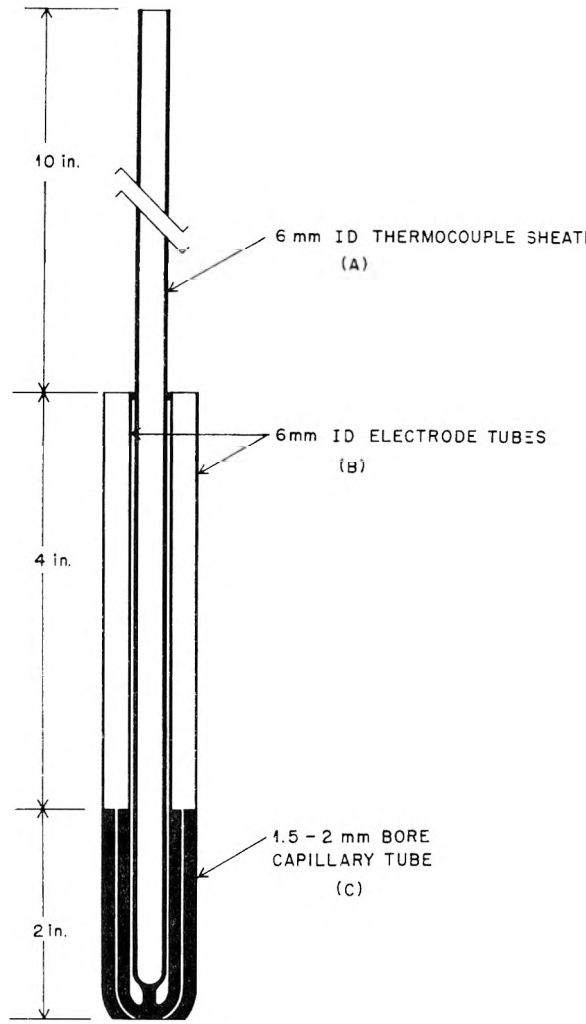

Fig. 2.—Capillary conductance cell.

Density measurements were made by weighing submerged within the melt a calibrated platinum bob suspended by a thin (36 gage) Pt–Rh wire from an analytical balance. The expansion of the platinum bob was computed[16] in order to obtain the volume of the bob at each temperature.

For both conductance and density measurements, data were taken going up and down the temperature scale; no difference was observed in the measurements upon this temperature cycling. During temperature changes, the conductance cell and the density bob were raised out of the melt. Duplicate measurements were made at each temperature in order to assure thermal equilibrium. Normally, the same melt was used for both types of measurements.

Mixtures were made by weighing appropriate amounts of carefully purified and dried reagents[17] into the platinum–rhodium crucible which was then placed in the furnace. With dry purified argon flowing through the assembly, the temperature was slowly raised above the melting point of the salt mixture. Such precautions were necessary in order to prevent hydrolysis of the salts by traces of moisture. At the conclusion of an experiment, samples of the melt were removed and checked for neutrality in aqueous solution. The data from a few melts which showed evidence of

(16) L. Holborn and A. L. Day, *Ann. Physik*, **4**, 104 (1901); cited by R. F. Vines, "The Platinum Metals and Their Alloys," The International Nickel Company, Inc., New York, N. Y., 1941, p. 17.

(17) Analytical grade materials were recrystallized and premelted under an atmosphere of hydrogen or argon to dry them and then cooled to room temperature, crushed roughly and stored in a dry atmosphere.

TABLE I

SPECIFIC CONDUCTANCE OF KCl, LiCl, NaCl, KI AND MIXTURES

Compn., mole %	t, °C.	κ, mho cm.$^{-1}$	Compn., mole %	t, °C.	κ, mho cm.$^{-1}$	Compn., mole %	t, °C.	κ, mho cm.$^{-1}$
100 KCl	778.9	2.1628		738.0	1.4041		551.8	3.2440
	782.4	2.1816		739.5	1.4132		562.6	3.3054
	787.0	2.1984		745.7	1.4207		579.0	3.4006
	790.0	2.2074		754.3	1.4395		599.7	3.5121
	799.0	2.2342		768.2	1.4639		612.2	3.5708
	800.5	2.2407		770.1	1.4643		622.5	3.6268
	804.1	2.2478		783.2	1.4955		626.4	3.6438
	823.0	2.3020		785.7	1.4970		642.5	3.7214
	846.0	2.3507		791.1	1.5022		670.8	3.8492
	850.9	2.3609		815.7	1.5440		671.2	3.8500
	851.2	2.3618		830.7	1.5637	79.60 KCl	718.4	1.8246
	865.0	2.3901		847.4	1.5905	20.40 NaCl	718.9	1.8344
	877.5	2.4174		877.2	1.6232		730.5	2.1446
	889.0	2.4476		897.6	1.6555		730.9	2.1453
	892.5	2.4484		910.7	1.6664		766.3	2.2466
	905.5	2.4745	80.04 KCl	706.9	2.0765		789.7	2.3180
	906.7	2.4777	19.96 LiCl	707.2	2.0773		815.1	2.3784
	925.1	2.5156		726.5	2.1331		839.0	2.4379
100 LiCl	622.8	5.6923		760.0	2.2529		853.7	2.4638
	634.4	5.8262		765.0	2.2634		868.4	2.4958
	643.9	5.8922		765.4	2.2644		889.8	2.5422
	667.8	6.0083		804.0	2.3735		930.1	2.6109
	691.1	6.1185		807.6	2.3842	59.00 KCl	673.5	1.5316
	712.5	6.2253		832.3	2.4397	41.00 NaCl	679.0	1.9085
	741.0	6.3704		855.7	2.4975		692.1	2.1766
	760.3	6.4626	59.55 KCl	589.0	1.8480		708.3	2.2370
	783.3	6.5399	40.45 LiCl	634.2	2.0726		734.9	2.3393
(N.B. considerable corrosion of cell occurred at higher temp.)				641.6	2.1144		740.7	2.3639
				657.5	2.1783		740.9	2.3643
100 NaCl	802.3	3.0887		662.6	2.2028		769.8	2.4472
	804.6	3.4497		685.8	2.2864		794.5	2.5196
	806.4	3.5804		701.2	2.3602		822.8	2.5848
	806.5	3.5821		737.5	2.4734		853.0	2.6634
	808.0	3.6057	41.20 KCl	389.8	1.1819		853.7	2.6641
	808.2	3.6060	58.80 LiCl	394.0	1.2040		881.5	2.7223
	817.8	3.6431		441.5	1.5162		907.9	2.7725
	817.9	3.6441		443.0	1.5314	48.77 KCl	665.9	2.1986
	827.4	3.6601		476.1	1.7290	51.23 NaCl	674.4	2.2523
	839.8	3.7145		483.8	1.7811		679.2	2.2789
	857.8	3.7662		486.0	1.7964		706.2	2.3687
	871.4	3.8041		514.8	1.9524		726.8	2.4374
	892.7	3.8502		522.2	1.9987		738.7	2.4695
	899.4	3.8637		535.2	2.0655		769.5	2.5633
	911.5	3.9154		553.5	2.1638		788.9	2.6107
	913.3	3.9129		588.3	2.3375		818.8	2.6914
	922.4	3.9416	29.64 KCl	450.1	1.9074		843.4	2.7523
	933.3	3.9680	70.36 LiCl	450.4	1.9123		846.7	2.7569
	933.8	3.9701		450.7	1.9239		875.1	2.8273
	947.3	4.0151		465.5	2.0773		887.6	2.8533
	971.5	4.0653		502.2	2.3222		912.5	2.9019
	972.0	4.0616		507.3	2.3580	34.85 KCl	690.7	2.3236
	972.3	4.0719		509.8	2.3722	65.15 NaCl	695.4	2.5049
	1006.9	4.1595		544.1	2.5765		709.1	2.5562
	1010.1	4.1701		547.5	2.5954		736.7	2.6556
	1021.4	4.1861		563.9	2.6881		756.8	2.7175
100 KI	685.4	1.2440		585.1	2.7969		783.6	2.7971
	689.0	1.2613		586.6	2.8073		823.6	2.9210
	697.5	1.2940		608.6	2.9130		825.0	2.9254
	698.5	1.2961	18.23 KCl	521.1	3.0443		825.5	2.9281
	708.6	1.3234	81.77 LiCl	529.4	3.1075		853.4	3.0066
	718.5	1.3546		529.7	3.1087		898.4	3.1139

TABLE I (*Continued*)

Compn., mole %	t, °C.	κ, mho cm.$^{-1}$	Compn., mole %	t, °C.	κ, mho cm.$^{-1}$	Compn., mole %	t, °C.	κ, mho cm.$^{-1}$
	919.7	3.1611		817.8	1.9998		903.7	1.3815
	944.2	3.2163		845.6	2.0559	25.67 KCl	634.9	1.2578
27.06 KCl	708.0	2.5583		865.0	2.0843	74.33 KI	644.8	1.2837
72.94 NaCl	717.1	2.6866		875.1	2.0985		667.8	1.3369
	735.1	2.7591		883.3	2.1130		698.0	1.4114
	750.5	2.8160		903.1	2.1402		722.3	1.4683
	773.9	2.8977	61.12 KCl	642.3	1.0824		745.8	1.5115
	788.8	2.9472	38.88 KI	643.5	1.1932		759.9	1.5400
	819.5	3.0365		645.3	1.3418		779.6	1.5777
	841.0	3.0947		649.6	1.3868		810.8	1.6347
	857.7	3.1397		660.0	1.4395		829.0	1.6547
	876.4	3.1914		664.0	1.4500		856.9	1.7012
	899.4	3.2344		692.7	1.5350		876.4	1.7296
	927.9	3.2864		713.1	1.5982		904.5	1.7631
15.23 KCl	758.0	2.9859		732.6	1.6446	15.30 KCl	668.4	1.3069
84.77 NaCl	759.6	3.0827		759.2	1.7120	84.70 KI	686.0	1.3493
	762.7	3.1085		783.8	1.7596		709.1	1.3961
	767.2	3.1237		817.3	1.8321		730.5	1.4316
	773.2	3.1444		843.6	1.8806		737.6	1.4439
	789.4	3.1938		873.2	1.9252		742.2	1.4585
	795.2	3.2092		905.7	1.9725		766.3	1.5024
	811.2	3.2607					772.2	1.5089
	816.8	3.2787	45.15 KCl	607.8	1.2450		787.8	1.5429
	817.3	3.2803	54.85 KI	612.6	1.2585		794.9	1.5517
	835.0	3.3309		624.2	1.2896		822.9	1.6051
	852.4	3.3784		646.1	1.3500		847.5	1.6440
	875.3	3.4415		658.4	1.3834		870.2	1.6772
	895.5	3.4885		682.1	1.4398		904.0	1.7282
	909.2	3.5233		691.6	1.4666			
	927.2	3.5609		707.3	1.5004	6.04 KCl	690.5	1.2913
				724.6	1.5376	93.96 KI	719.8	1.3612
80.22 KCl	711.8	1.7043		739.7	1.5732		750.4	1.4307
19.78 KI	726.8	1.7530		754.7	1.6055		769.8	1.4701
	741.6	1.7936		781.5	1.6654		799.1	1.5239
	745.4	1.8071		807.5	1.7141		830.4	1.5759
	761.2	1.8517		808.7	1.7208		857.0	1.6126
	767.4	1.8712		825.1	1.7441		877.4	1.6388
	790.2	1.9243		839.5	1.7715		878.4	1.6402
	797.6	1.9500		861.0	1.8128		902.1	1.6663
	814.9	1.9905		875.8	1.8332		902.7	1.6666

hydrolysis were discarded. Samples of the melts also were analyzed gravimetrically to determine the exact composition of the mixtures. In the case of the chloride mixtures analysis was for total chloride by precipitation as silver chloride, while the analysis of the potassium chloride–potassium iodide mixtures was for total potassium as potassium sulfate by fuming with excess sulfuric acid and drying at 550°.

Results and Discussion

The specific conductance of various compositions of the systems KCl–LiCl, KCl–NaCl and KCl–KI was measured, in general, from a few degrees above the melting point to over 900°. These data are listed in Table I. Figure 3 shows our data on the four pure salts and their comparison with other published work. In general, our results agree reasonably well with the more recent determinations by other investigators. Representative isotherms at 800° showing the variation of specific conductance with composition are illustrated in Fig. 4. Except for the data within 10 or 20° of the melting point, the specific conductance data could be represented quite exactly by quadratic equations in temperature, $\kappa = a + bt + ct^2$; where κ is specific conductance, t is temperature in degrees centigrade and a, b and c are constants for any particular composition. Values of the constants for these equations have been derived by the method of least squares and are listed in Table III, along with the applicable temperature range. These equations were used for subsequent calculations.

Densities of the pure salts and of their mixtures were determined as functions of temperature. The data which are given in Table II are represented very precisely by linear equations, $\rho = a - bt$, from a few degrees above the melting point to the highest temperature at which measurements were made (usually the same temperature range as for specific conductance). In this equation ρ is density in g./cc., t is temperature in degrees centigrade and a and b are constants for any given salt or mixture. Numerical values of the constants for all mixtures studied were derived by the method of least squares and are listed in Table III. The density data for molten potassium chloride are in good agreement (0.3%) with the data reported by

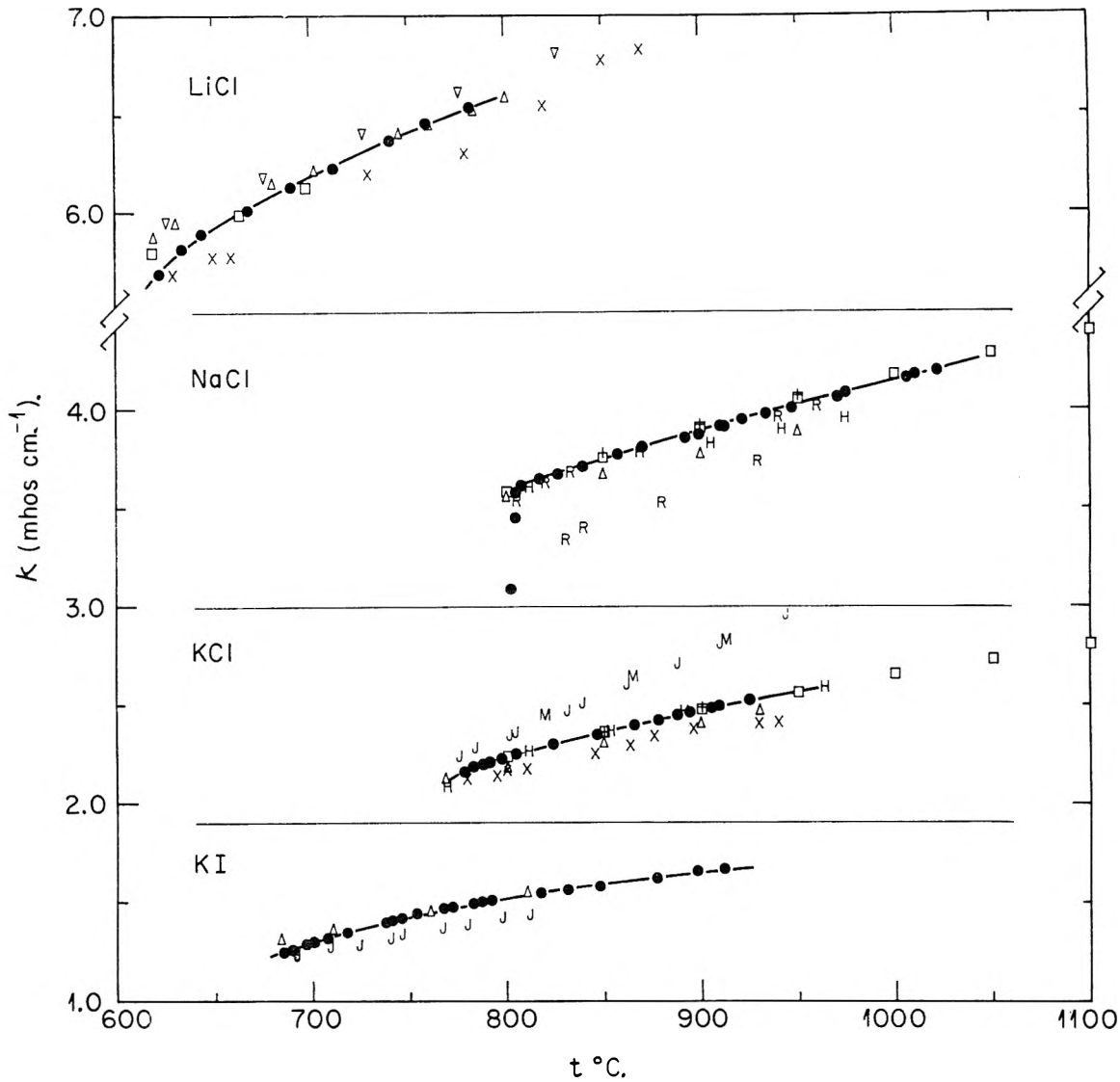

Fig. 3.—Specific conductance of pure salts: ●, this work; □, Edwards, Taylor, Russell and Maranville[6]; H, Huber, Potter and St. Clair[7]; X, Karpachev, Stromberg and Padchainova[4]; ▽, Bloom, Knaggs, Molloy and Welch[2a]; J, Jaeger and Kampa[18]; R, Ryschkewitsch[5]; +, E. K. Lee and E. P. Pearson, *Trans. Electrochem. Soc.*, **88**, 171 (1945); △, W. Biltz and W. Klemm, *Z. anorg. Chem.*, **152**, 267 (1926); M. E. Mantzell, *Z. Elektrochem.*, **49**, 283 (1943).

Edwards, *et al.*,[6] Jaeger and Kampa[18] and Jaeger[19] and are within 0.5% of the values reported by Huber, Potter and St. Clair[7] and by Peake and Bothwell.[13] For lithium chloride, the density data are within 0.2% of those reported by the "International Critical Tables,"[20] and within 0.5% of the data of Bloom, Knaggs, Molloy and Welch.[2a] The data for sodium chloride are slightly higher than previously reported data for this salt, varying approximately 0.5% from those of Edwards, *et al.*,[6] and of Huber, *et al.*,[7] and are 1% higher than the early work of Jaeger.[19] Densities of sodium chloride were determined using four different salt melts purified by various methods, including a sample of the salt purified by J. W. Johnson.[21] The potassium iodide density data are within 0.2% of the values reported by Jaeger and Kampa.[18]

The equivalent volumes of the pure salts and of the mixtures were computed by use of the equation $V = (\sum_i X_i E_i)/\rho$, in which X_i is the mole fraction of the ith component of equivalent weight E_i. Figure 5 shows the equivalent volume isotherms at 800° for the systems KCl–LiCl, KCl–NaCl and KCl–KI. The system KCl–LiCl is strictly linear in composition to within at least 0.1% while in the case of the system KCl–NaCl there is a slight positive deviation from additivity, which, however, at the maximum deviation at 50 mole % KCl, does not exceed 0.6%. The KCl–KI system shows a distinct positive deviation from additivity close to the KI side of the diagram. This bears out the phase equilibrium data[22] which show that KCl–LiCl forms a simple eutectic with no solid solution, KCl–NaCl

(18) F. M. Jaeger and B. Kampa, *Z. anorg. Chem.*, **113**, 27 (1920).

(19) F. M. Jaeger, *ibid.*, **101**, 175 (1917).

(20) "International Critical Tables," Vol. III, McGraw-Hill Book Co., New York, N. Y., 1928, p. 14.

(21) M. A. Bredig, J. W. Johnson and W. T. Smith, *J. Am. Chem. Soc.*, **77**, 307 (1955).

(22) Reference 20, Vol. IV, 1928; see also E. Elchardus and P. Laffitte, *Bull soc. chim., France*, **51**, 1572 (1932).

TABLE II

DENSITIES OF KCl, LiCl, NaCl, KI AND MIXTURES

Compn., mole %	Temp., °C.	Density, g./cc.	Compn., mole %	Temp., °C.	Density, g./cc.	Compn., mole %	Temp., °C.	Density, g./cc.
100 KCl	779.5	1.5219		967.6	1.4653		783.4	1.5235
	781.8	1.5211		986.0	1.4566		801.8	1.5130
	809.4	1.5058		995.8	1.4494		802.3	1.5127
	827.4	1.4943		1004.9	1.4468		835.1	1.4932
	870.4	1.4688		1014.1	1.4403		855.0	1.4819
	907.2	1.4479		1027.5	1.4322		855.4	1.4816
	939.0	1.4292					878.2	1.4685
			80.04 KCl	690.0	1.5614		878.4	1.4683
100 LiCl	620.3	1.4975	19.96 LiCl	719.2	1.5439		905.7	1.4525
	631.6	1.4924		761.2	1.5196		927.8	1.4397
	638.2	1.4899		795.1	1.4998		928.2	1.4395
	638.6	1.4898		795.8	1.4994			
	655.9	1.4821		834.6	1.4773	59.00 KCl	685.0	1.5837
	676.9	1.4730		844.9	1.4715	41.00 NaCl	685.1	1.5836
	685.9	1.4689		845.5	1.4711		704.0	1.5729
	713.6	1.4570		853.3	1.4670		740.7	1.5514
	737.8	1.4468	59.55 KCl	585.0	1.5958		748.6	1.5465
	752.5	1.4403	40.45 LiCl	588.3	1.5932		766.5	1.5363
	754.1	1.4396		613.4	1.5794		783.4	1.5267
	780.5	1.4282		645.4	1.5610		796.2	1.5195
				648.5	1.5592		826.0	1.5022
100 KI	681.9	2.4467		686.5	1.5378		838.1	1.4955
	706.3	2.4242		746.0	1.5054		875.6	1.4738
	730.1	2.4009					908.2	1.4556
	745.0	2.3865	41.20 KCl	395.0	1.6766			
	752.3	2.3795	58.80 LiCl	395.3	1.6764	48.77 KCl	670.0	1.5956
	767.7	2.3645		440.0	1.6528	51.23 NaCl	710.9	1.5728
	786.5	2.3472		445.0	1.6505		752.1	1.5493
	789.9	2.3434		445.2	1.6503		794.6	1.5250
	809.4	2.3245		477.7	1.6331		817.5	1.5118
	819.9	2.3145		481.7	1.6313		842.2	1.4981
	825.6	2.3090		482.7	1.6308		871.5	1.4814
	847.6	2.2887		504.5	1.6188		909.0	1.4600
	847.7	2.2886		518.2	1.6119			
	878.6	2.2590		538.0	1.6012	34.85 KCl	705.5	1.5886
	903.4	2.2355		555.2	1.5922	65.15 NaCl	758.5	1.5587
				579.8	1.5791		758.7	1.5586
100 NaCl	803.1	1.5560		593.1	1.5722		779.0	1.5471
	816.4	1.5467					803.5	1.5333
	819.7	1.5457	29.64 KCl	455.9	1.6245		818.4	1.5251
	826.0	1.5425	70.36 LiCl	456.7	1.6242		823.0	1.5229
	826.1	1.5424		471.0	1.6171		855.8	1.5042
	829.3	1.5401		495.2	1.6046		885.1	1.4883
	830.0	1.5397		516.4	1.5942		886.2	1.4877
	840.3	1.5362		533.6	1.5850		924.7	1.4662
	840.6	1.5361		534.3	1.5847			
	845.1	1.5317		560.5	1.5715	27.06 KCl	707.5	1.5895
	859.2	1.5242		577.0	1.5633	72.94 NaCl	739.6	1.5711
	866.6	1.5200		602.1	1.5504		777.9	1.5504
	867.2	1.5198					802.3	1.5358
	870.9	1.5184	18.23 KCl	532.6	1.5751		823.2	1.5241
	889.2	1.5086	81.77 LiCl	561.7	1.5605		859.4	1.5041
	890.3	1.5074		577.2	1.5529		893.7	1.4854
	890.4	1.5073		589.7	1.5466		915.6	1.4730
	891.6	1.5071		592.0	1.5458			
	898.9	1.5031		605.8	1.5390	15.23 KCl	780.6	1.5568
	916.9	1.4928		626.3	1.5291	84.77 NaCl	781.3	1.5564
	918.2	1.4921		647.5	1.5187		807.1	1.5414
	922.5	1.4909		660.5	1.5123		829.8	1.5288
	939.9	1.4812		660.6	1.5122		849.9	1.5180
	940.8	1.4798	79.25 KCl	717.0	1.5622		850.1	1.5178
	942.2	1.4793	20.75 NaCl	738.6	1.5498		875.3	1.5037
	953.6	1.4743		758.8	1.5380		898.3	1.4916
	967.2	1.4661		759.0	1.5378		921.2	1.4787

TABLE II (*Continued*)

Compn., mole %	Temp., °C.	Density, g./cc.	Compn., mole %	Temp., °C.	Density, g./cc.	Compn., mole %	Temp., °C.	Density, g./cc.
80.22 KCl	711.8	1.7825	45.15 KCl	618.8	2.1742		756.9	2.1994
19.78 KI	728.2	1.7719	54.85 KI	650.2	2.1474		790.3	2.1698
	728.5	1.7716		665.2	2.1348		818.7	2.1443
	751.2	1.7550		690.2	2.1135		846.6	2.1198
	775.2	1.7392		735.7	2.0755		879.0	2.0906
	793.7	1.7253		735.8	2.0754		914.1	2.0595
	823.8	1.7056		762.3	2.0537			
	847.0	1.6890		806.7	2.0171	15.96 KCl	706.0	2.3536
	870.2	1.6735		809.6	2.0146	84.04 KI	763.0	2.3055
	904.6	1.6501		828.4	1.9991		820.9	2.2540
61.12 KCl	679.5	1.9856		874.4	1.9621		874.2	2.2081
38.88 KI	694.6	1.9744		902.3	1.9397		901.2	2.1856
	736.5	1.9426		902.7	1.9394	6.04 KCl	682.1	2.3962
	784.1	1.9069				93.96 KI	726.6	2.3550
	805.9	1.8900	25.67 KCl	640.3	2.3033		778.6	2.3063
	829.0	1.8730	74.33 KI	675.4	2.2718		813.5	2.2739
	855.1	1.8535		700.6	2.2499		845.4	2.2440
	881.9	1.8327		728.4	2.2244		869.5	2.2215
	911.9	1.8103		729.1	2.2237		904.4	2.1900

TABLE III

SPECIFIC CONDUCTANCE AND DENSITY EQUATIONS FOR KCl, LiCl, NaCl, KI AND MIXTURES

	Specific conductance $\kappa = a + bt + ct^2$ (mho cm.$^{-1}$)					Density $\rho = a - bt$ (g./cc.)			
Compn., %	a	$b \times 10^2$	$c \times 10^6$	Standard dev. (mho cm.$^{-1}$)	Temp. range, °C.	a	$b \times 10^3$	Standard dev. (g./cc.)	Temp. range, °C.
100 KCl	−1.7491	0.7383	−3.000	0.003	790–930	1.9767	0.5831	0.0003	780–940
100 LiCl	+0.5282	1.125	−4.554	.008	630–790	1.7660	.4328	.0001	620–780
100 NaCl	−0.1697	0.6259	−1.953	.006	810–1030	1.9911	.5430	.0007	803–1030
100 KI	−1.7100	0.6408	−2.965	.003	720–920	3.0985	.9557	.0003	682–904
				KCl–LiCl System					
mole % KCl									
80.04	−3.159	1.115	−5.310	0.005	700–860	1.9892	0.5781	0.0003	690–853
59.55	−4.142	1.488	−8.009	.004	580–740	1.9234	.5610	.0004	585–746
41.20	−2.273	1.084	−5.100	.003	380–600	1.8851	.5275	.0002	395–593
29.64	−2.966	1.465	−8.200	.001	460–620	1.8559	.5074	.0002	456–602
18.23	−2.261	1.401	−7.312	.002	525–680	1.8354	.4893	.0002	532–661
				KCl–NaCl System					
79.25						1.9793	0.5815	0.0001	717–929
79.60	−2.0578	0.8429	−3.665	0.003	730–930				
59.00	−2.8540	1.0750	−5.018	.005	690–910	1.9774	.5750	.0002	685–908
48.77	−1.2908	0.7179	−2.828	.002	680–920	1.9764	.5680	.0002	670–909
34.85	−1.6108	0.8194	−3.267	.003	695–950	1.9815	.5574	.0002	705–925
27.06	−2.5493	1.0770	−4.825	.003	715–930	1.9851	.5595	.0003	707–916
15.23	−1.3731	0.8458	−3.383	.002	760–930	1.9891	.5542	.0003	780–921
				KCl–KI System					
80.22	−3.8914	1.2226	−6.144	0.003	710–910	2.2736	0.6897	0.0005	711–905
61.12	−2.2493	0.8067	−3.761	.002	655–910	2.4985	.7546	.0002	679–912
45.15	−1.0837	0.4976	−1.873	.003	600–910	2.6838	.8257	.0008	618–903
25.67	−1.3927	0.5790	−2.542	.003	630–910	2.8730	.8899	.0003	640–914
15.96						2.9143	.8645	.0005	706–901
15.30	−0.8419	0.4291	−1.605	0.003	685–910				
6.04	−2.2372	0.7654	−3.688	0.001	690–910	3.0305	0.9300	0.0003	682–904

forms mixed crystals as well as a eutectic and KCl–KI forms rather simple solid solutions with a minimum melting point. Despite these small deviations from additivity, it is nevertheless evident that these three systems are reasonably ideal in their equivalent volume (molar volume) relationships.

The equivalent conductance was calculated from the specific conductance and the equivalent volume by the relationship, $\Lambda = \kappa V$, where Λ is equivalent conductance and V is equivalent volume. Isotherms at 800° for the three systems are illustrated in Fig. 6. In contrast to the equivalent volume behavior, it is evident that these systems are far from additive with respect to conductance.

The pronounced minimum in equivalent con-

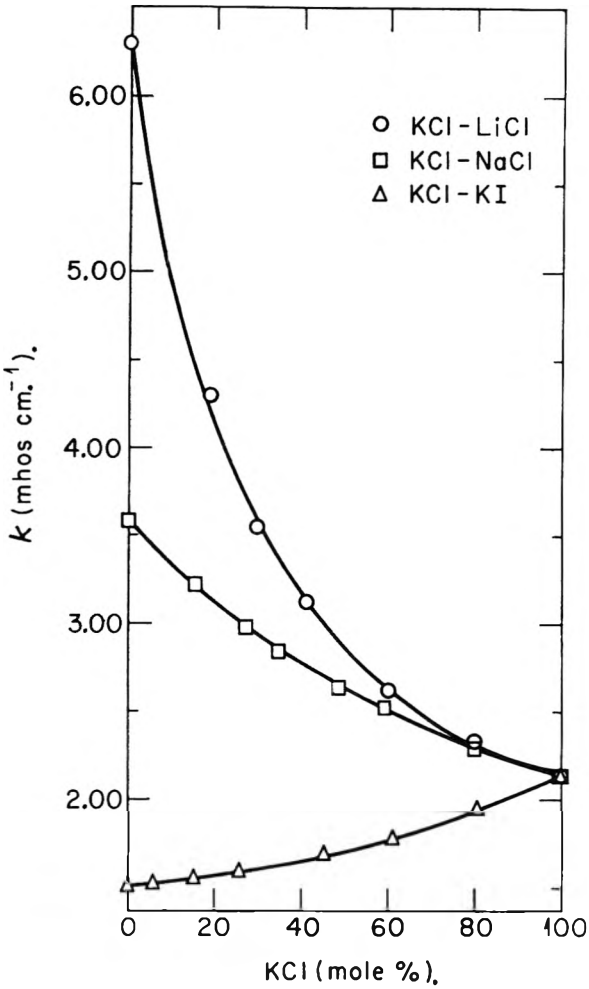

Fig. 4.—Specific conductance *vs.* composition at 800°.

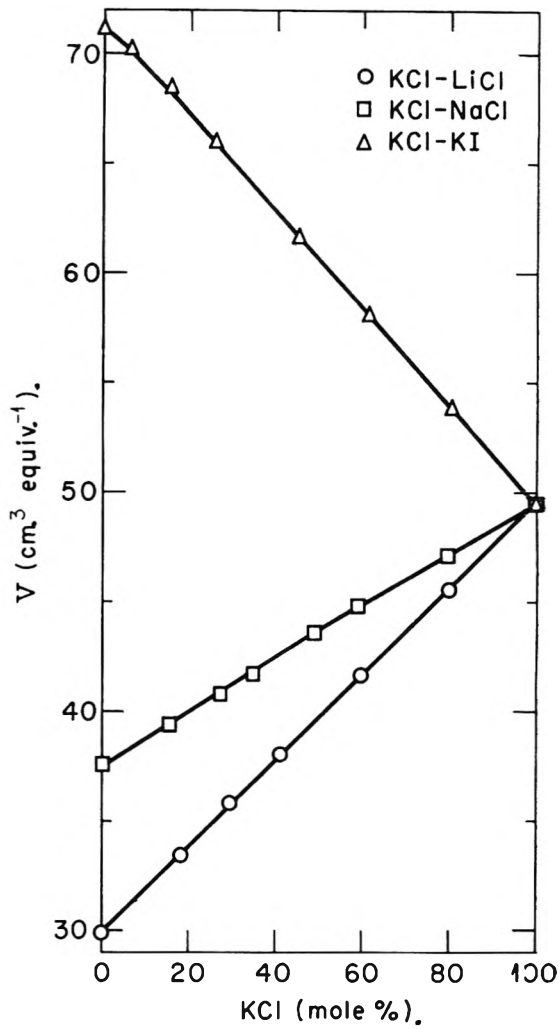

Fig. 5.—Equivalent volume *vs.* composition at 800°.

ductance in the KCl–LiCl system is particularly noteworthy. A tentative, qualitative explanation may be attempted in terms of the following model. It is assumed that the liquid salts possess short range order similar to that of the crystalline solids, while the long range order of the crystal has been largely destroyed during melting. We envision the melt as consisting of a sort of semi-lattice of chloride ions with smaller cations occupying positions much as in the crystal. The size of this chloride semi-lattice will be a direct reflection of the molar (equivalent) volume and so it is a linear function of composition for the KCl–LiCl system, being smallest for pure LiCl. The Li^+ ions, which are smaller and have a higher charge density than K^+ ions, may be considered a better glue for holding together the Cl^- anion semi-lattice of the liquid. One calculates that the chlorine–chlorine internuclear distance in molten LiCl is about 12% less than in molten KCl at 800°. We further assume that the small cations, Li^+ and K^+, do practically all of the conducting with essentially no contribution from the larger chloride anions.[23] Upon substituting some Li^+ ions for K^+ ions in a KCl melt the chloride semi-lattice will be somewhat shrunken, the net effect of which will be to make migration of K^+ ions more difficult by raising the restricting potentials. Alternatively we may consider that all cation sites in pure KCl will be approximately equivalent, but when the melt contains some Li^+ not all cation sites will be equivalent and it will be more difficult for a K^+ to migrate into an Li^+ type site than into a K^+ type site, thereby making migration of K^+ more difficult than in pure KCl. When only a small amount of lithium has been substituted for potassium, most of the electrical conduction will be by K^+ in view of our model of the melts, and so, it is not surprising that equivalent conductance decreases. Clearly as the percentage of Li^+ ions increases, the higher mobility of Li^+ becomes predominant and the conductance rises to that of pure LiCl. This explanation suggests the possibility of positive deviations from additivity of the equivalent conductance at high LiCl composition because of expansion of the semi-lattice which might be expected to make migration of Li^+ easier than in pure LiCl. While the data do not exclude this possibility, they seem to deny it. It may well be that the expansion of the chloride lattice does not make it appreciably easier for the Li^+ ion to migrate, since, as will be shown later, the potentials restricting it are much less than in the case of K^+.

(23) This concept is supported by other types of experimental approach and was advanced by J. Frenkel (for review see, Frenkel, "Kinetic Theory of Liquids," Oxford University Press, Oxford, 1946; p. 439 *et seq.*).

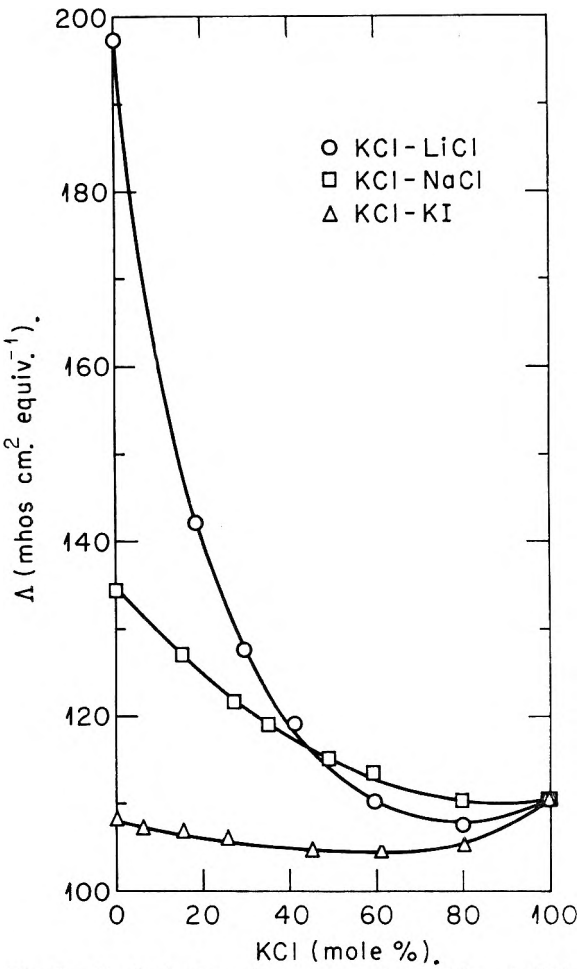

Fig. 6.—Equivalent conductance *vs.* composition at 800°.

If this explanation is correct, the KCl–NaCl system should be expected to behave in a similar manner to the KCl–LiCl system but the minimum should be less pronounced because Na^+ is larger than Li^+ and, therefore, should exert a smaller modifying influence upon the chloride semi-lattice of the melt. This is the case, as may be seen in Fig. 6.

The 800° equivalent conductance isotherm for the KCl–KI system is likewise in Fig. 6. Work is in progress on other systems of this type and an explanation will be attempted after more data are available.

Minima in equivalent conductance for these simple systems indicate conclusively the great danger inherent in ascribing them to the formation of complexes or compounds within a melt, unless other confirming evidence is at hand.

Application of Rate Theory.—If electrical conductance is considered as a rate process, one may write the equation[2,8–11,14]

$$\Lambda_i = A_i e^{-\Delta H_i \ddagger / RT} \qquad (1)$$

in which $\Delta H_i^{\pm}$ is the heat of activation of the conduction process, A_i is a constant of the system and T is degrees Kelvin. Values of the heat of activation were computed from the equivalent conductance, and, for the pure salts, are shown in Fig. 7. Apparent or average heats of activation for conductance in the salt mixtures have been calculated according to equation 1; in general $\Delta H^{\pm}$ tends to a maximum for those mixtures which show minimum conductance. However, in the case of a mixture such as KCl and LiCl where two cations conduct, it seems clear that there will be two separate heats of activation, one for each ion. This point is discussed later. With the exception of pure LiCl, $\Delta H^{\pm}$ for all compositions studied was found to be temperature dependent, decreasing fairly rapidly in the first 20 to 50° above the melting point and then varying linearly at higher temperatures. A similar variation of $\Delta H^{\pm}$ with temperature has previously been reported by Wetmore[8,9] and Ubbelohde.[11] It seems reasonable to expect that as the liquid expands with rising temperature, the restricting potentials for migration would be lowered and this effect would be reflected in the heat of activation. In the case of LiCl, where there is essentially chloride–chloride contact in the crystal and presumably also in the liquid on a short range basis, such an effect should be at a minimum, and, in fact, no temperature dependence of $\Delta H^{\pm}$ is observed. The initial rapid decrease in $\Delta H^{\pm}$ as the temperature rises just above the melting point may be attributed to rapidly decreasing order of the melt. The increase of $\Delta H^{\pm}$ with temperature in the case of pure NaCl is unexplainable at this time. It seems reasonable that $\Delta H^{\pm}$ should be greater for KCl than for LiCl, since we expect the potentials restricting migration to be larger for the much larger K^+ than Li^+ in the chloride semi-lattice, even though the chlorine–chlorine internuclear distance decreases from KCl to LiCl. Likewise, the fact that $\Delta H^{\pm}$ for conductance by KI is less than by KCl is in agreement with the concept that the charge density of I^- is less than Cl^- and so restricting potentials are smaller for K^+ conductance in KI than in KCl.

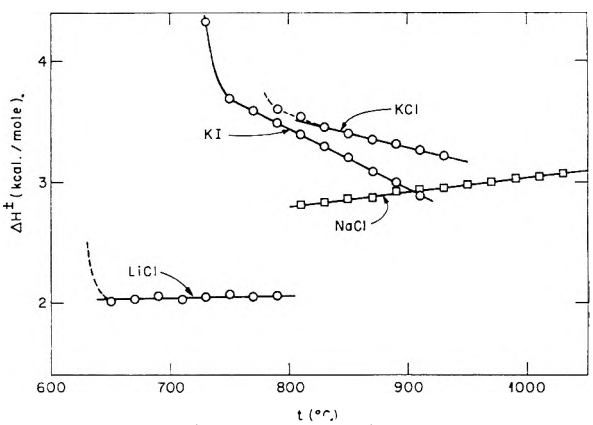

Fig. 7.—Variation of $\Delta H \ddagger$ with temperature.

As $\Delta H^{\pm}$ was found to vary linearly with temperature, the differential equation

$$\frac{\partial \ln \Lambda}{\partial (1/T)} = B' + C'T$$

can be written and hence the equation

$$\log \Lambda = A + B(1000/T) + C \log (1000/T) \qquad (2)$$

can be derived in which T is in degrees Kelvin. This equation reproduces exceedingly well the variation of equivalent conductance with temperature for all salts and mixtures studied. Table IV lists the constants of this equation for the pure salts. It is,

however, difficult to ascribe any physical significance to the values of these constants.

TABLE IV

EQUIVALENT CONDUCTANCE EQUATIONS FOR KCl, LiCl, NaCl AND KI

$\log \Lambda = A + B(1000/T) + C \log (1000/T)$ (mho cm.^{2} equiv.$^{-1}$)

Compn.	A	B	C
100% KCl	3.34204	−1.35302	+1.24340
100% LiCl	2.63987	−0.37505	−0.16694
100% NaCl	2.42522	−0.33686	−0.59108
100% KI	3.91176	−1.93237	+2.53113

By making use of absolute reaction rate theory, the following equation can be derived from equation 1

$$\Lambda_i = 5.18 \times 10^{18} (D + 2) d_i^2 e^{\Delta S_i^{\mp}/R} e^{-\Delta H_i^{\mp}/RT} \quad (3)$$

in which D is the dielectric constant and d_i is the half-migration distance for the conducting ion. This is analogous to the case for hydrogen ion in aqueous solution given by Glasstone, Laidler and Eyring[24] and is identical with the equation of Bockris,[14] *et al.*, for molten silicates. Entropies of activation for conductance in the three systems have been calculated by equation 3. The values of d_i were estimated for the pure salts from the equation

$$\left(\frac{\rho(c)_{25}}{\rho(l)_t}\right)^{1/3} d(c)_{25} = d_i(l)_t \quad (4)$$

where (c) refers to crystal, (l) to liquid and the subscripts denote the temperature. Values of d_i for mixtures were obtained by interpolation since molar volumes are nearly additive. The dielectric constants for the molten salts are unknown, so we have used an estimate of $D = 3$ for all.[25] In any case small differences in D will introduce almost negligible differences in $\Delta S^{\mp}$. All entropies of activation were negative and had the value −6.1 e.u. for LiCl at 700° and −6.4, −6.7 and −7.4 e.u. for NaCl, KCl and KI, respectively, at 850°. The values for mixtures lay close to those of the component pure salts (deviations generally less than 0.5 e.u.) with a tendency to a maximum negative value in the region of minimum equivalent conductance. The entropy of activation is only very slightly temperature dependent, varying perhaps 0.1 e.u. per 100 or 150°. We believe that the values of $\Delta S^{\mp}$ calculated by this method are reasonable and that probably the differences for the pure salts are real. The close similarity of $\Delta S^{\mp}$ for all salts and mixtures studied bespeaks a similar conduction mechanism for all.

A more refined method is desirable for calculating the heat and entropy of activation for conductance in mixtures. When two cations are the major conducting species there must be two rate processes, each with its own characteristic composition-dependent heat of activation, both of which will be of the same order of magnitude. We are in the process of testing equations which we have derived for binary mixtures. They express equivalent conductance as the sum of exponential terms involving heats of activation in which interaction is considered between the two salts.

We have in progress in this Laboratory further work including other experimental approaches in attempts to elucidate in greater detail physical-chemical behavior of molten salts and to test more exactly some of the ideas presented in this paper.

(24) S. Glasstone, K. V. Laidler and H. Eyring, "The Theory of Rate Processes," McGraw-Hill Book Co., Inc., New York, N. Y., 1943.

(25) Bockris, *et al.*,[14] assumed $D = 5$ for a series of molten silicates which are rather poorer conductors than the molten halide cases.

VAPOR–SOLID EQUILIBRIA IN THE TITANIUM–OXYGEN SYSTEM[1]

BY WARREN O. GROVES,[2] MICHAEL HOCH AND HERRICK L. JOHNSTON

Contribution from The Cryogenic Laboratory and the Department of Chemistry, The Ohio State University, Columbus, Ohio

Received November 23, 1954

The vaporization of TiO, Ti_2O_3, Ti_3O_5 and TiO_2 has been studied by the Knudsen effusion method, and the solid phases investigated by high temperature X-ray diffraction technique. TiO, TiO_2 (rutile) and Ti_2O_3 do not undergo any structural change up to their melting points. Ti_3O_5 has a low temperature structure and a high temperature structure (above 1600°K.). TiO(s) vaporizes to TiO(g), ΔH_0° = 134.6 kcal./mole, TiO_2(s) to TiO_2(g), ΔH_0° = 138.9 kcal./mole. Ti_2O_3 decomposes on vaporization to TiO(g) + TiO_2(g), the heat of reaction being ΔH_0° = 296.0 kcal./mole.

Introduction

The purpose of this research is to determine the nature of the vaporization processes of the titanium oxides, to measure the equilibria between the solid and the vapor, and to derive the related thermodynamic properties.

The compositions and solid-phase equilibria of the titanium oxide system together with the vaporization processes have been discussed briefly by Brewer[3] in his recent review of the thermodynamic properties of the oxides. Skinner, Johnston and Beckett[4] reviewed the literature up to 1951. Kubaschewski and Dench[5] constructed the partial free energy of oxygen *vs.* composition diagram at 1000 and 1200°.

No direct determination of any of the vapor pressures or dissociation pressures have been pub-

(1) This work was supported in part by the Office of Naval Research under contract with the Ohio State University Research Foundation.

(2) General Electric Fellow, 1953–1954. Present Address: New Mexico A. and M., State College, N. M.

(3) L. Brewer, *Chem. Revs.*, **52**, 1 (1953).

(4) G. B. Skinner, H. L. Johnston and C. Beckett, "Titanium and Its Compounds," Herrick L. Johnston Enterprises, Columbus, Ohio, 1954.

(5) O. Kubaschewski and W. A. Dench, *J. Inst. Metals*, **82**, 87 (1953).

lished except that of TiO by Gilles and Wheatley, reported by Brewer[3] and Skinner.[4] Starodubtsev and Timokhina,[6] using a mass spectrometer, observed Ti^+, TiO^+, Ti, TiO and TiO_2 ions and molecules in the vapor of TiO_2 heated *in vacuo*.

As we have seen,[5] the solid phases in the titanium–oxygen system are characterized by wide homogeneity ranges. In vaporization experiments, the solid phase has to be characterized as to whether or not it can form an invariant system with the gas. In the case of an invariant system, the vapor and solid composition are equal, and the pressure will remain constant at constant temperature as vaporization proceeds. If no invariant system can be formed the composition of the solid will change continuously as vaporization proceeds, and the vapor pressure will decrease until a two phase system is reached. An intermediate possibility, which is very commonly found, is a pseudo-invariant system. The composition of vapor and solid are not equal, but the difference is so small that the decrease in vapor pressure and change in composition of the solid are imperceptible.

Apparatus and Experimental Procedure

The high temperature X-ray diffraction patterns were taken in our camera.[7,8] When the desired temperature had been reached, the temperature was maintained for an hour to allow equilibrium to be attained. Following this equilibration period, the X-ray beam was turned on, and exposures for one hour were taken. The temperature interval in which X-ray diffraction patterns were taken extended from 1600–2100°K.

The metal vapor pressure cell was similar to the one described previously.[9] The power was supplied by a 15 kw. General Electric heater. The temperature was controlled with a motor-driven variometer[10] in series with the work coil, the variometer being operated manually. The temperature was measured with a Leeds and Northrup disappearing filament optical pyrometer, the pyrometer being calibrated against a standard tungsten-ribbon lamp which has been calibrated at the National Bureau of Standards.

The Knudsen cells used in the vapor pressure measurements were either drawn from 0.010 inch tantalum or molybdenum sheet or were constructed of seamless tubing the tops and bottoms being drawn. The cells used in the measurement of the vapor pressure of TiO were drawn from tantalum 1″ in diameter $^1/_2$–$^3/_4$″ high. For the first series on Ti_2O_3, cells, drawn from molybdenum, $^1/_2$″ high, $^3/_4$″ diameter were used. For the other series on Ti_2O_3, and for TiO_2 and Ti_3O_5, molybdenum cells, made of molybdenum tubing $^1/_4$–$^1/_2$″ o.d., were used. These cells were enclosed into tantalum cells, $^1/_2$–$^3/_4$″ o.d., the top of the molybdenum cells being flush with the top of the tantalum cell. The tantalum cell had a hole $^1/_2$″ diameter, concentric with the effusion hole in the molybdenum cell, in the top. By this method, the molybdenum weight loss was reduced to a minimum, and the path of the effusing molecules was not obstructed by the tantalum cell.

The tantalum cells were degassed at 2000°; for the cells containing molybdenum, blank runs were carried out, to determine the weight loss. The weight losses obtained with the titanium oxides were corrected for the small, less than 10%, molybdenum weight loss.

To correct for temperature fluctuations the effective time, t_{eff}, was calculated by the averaging method.[11,12] The effective orifice area was obtained by correcting the measured area for thermal expansion and for the effect of the non-ideal conditions, finite size and depth. The thermal expansion data for tantalum and molybdenum obtained in this Laboratory[13] were used. The correction for the non-idealized effusion conditions was applied according to the equation derived by Whitman.[14]

In order to determine the composition of the effusing vapor and the composition of the solid from which it evaporated, the material was vaporized from an open molybdenum crucible, and a portion of the vapor condensed on a collector disk. A portion of the solid was analyzed for the Ti:O ratio before and after each vaporization and an X-ray diffraction pattern taken of the material collected.

The analyses of the oxides were carried out by igniting samples in air at 800 to 900° in a platinum crucible. From the weight gain, due to oxidation to TiO_2, the titanium to oxygen ratio could be calculated.

Materials.—The titanium dioxide used in this research was "Baker's Analyzed," C.P. grade, the following analysis being given: water soluble salts, 0.04%; arsenic, 0.00000%; iron, 0.003%; lead, 0.01%; zinc, 0.002%. The iodide process titanium had been donated by the New Jersey Zinc Company, Palmerton, Pennsylvania. Its analysis was: manganese, 0.0082%; silicon, 0.007%; aluminum, 0.0066% nitrogen, tellurium, lead and copper, 0.02%.

Intermediate oxides of titanium were prepared by heating together equivalent amounts of titanium and titanium dioxide in molybdenum or tantalum crucibles, the reaction being carried out under high vacuum in the vapor pressure apparatus. Weighed amounts of the oxide and metal were intimately mixed, placed in the crucible and heated to 1500° *in vacuo* for one hour. The solid was then removed, reground in a mortar and replaced in the crucible for a further heating period of several hours at 1500°. Following this treatment, the samples appeared homogeneous, but to ensure complete reaction, the regrinding and heating processes were repeated. At this temperature the reaction of any of the oxides with the crucible appeared to be negligible, although the dioxide and the sesquioxide attacked tantalum at 1700°. If any tantalum or molybdenum oxides had been formed, they should have been volatile.

The following materials were prepared and used:

Oxide	Batch	Mole ratio TiO_x
TiO	1	1.075
	2	1.029
Ti_2O_3	1	1.503
	2	1.491
Ti_3O_5	1	1.667

Experimental Results and Discussion of the Data

X-Ray Diffraction Data.—TiO has the same NaCl-type structure at elevated temperatures, as at room temperatures. Rutile, TiO_2, maintains its structure up to its melting point. A series of patterns of oxygen deficient rutile were obtained. A one-phase system, having a distorted rutile structure, was obtained as low as $TiO_{1.82}$ at room temperature. Ti_2O_3 does not undergo any structural changes up to 2100°K. The pattern taken at 2100°K. showed the corundum-type lattice strongly, but also six faint lines, which corresponded to lines found in the high temperature form of Ti_3O_5. This may indicate a slight disproportionation of Ti_2O_3 into TiO(g) and Ti_3O_5(s) near its melting point: but it is not impossible that some oxygen was picked up during the exposure.

(6) S. V. Starodubtsev and Y. I. Timokhina, *Zhur. Tekh., Fiz.*, **19**, 606 (1949); *C. A.*, **44**, 8223f (1950).

(7) J. W. Edwards, H. L. Johnston and R. Speiser, *Rev. Sci. Instr.*, **20**, 343 (1949).

(8) M. Hoch and H. L. Johnston, *J. Am. Chem. Soc.*, **76**, 2560 (1954).

(9) M. Hoch and H. L. Johnston, *ibid.*, **76**, 4833 (1954).

(10) R. Speiser, G. W. Ziegler, Jr., and H. L. Johnston, *Rev. Sci. Instr.*, **20**, 385 (1949).

(11) J. W. Edwards, H. L. Johnston and P. E. Blackburn, *J. Am. Chem. Soc.*, **73**, 172 (1951).

(12) G. B. Skinner, J. W. Edwards and H. L. Johnston, *ibid.*, **73**, 174 (1951).

(13) J. W. Edwards, R. Speiser and H. L. Johnston, *J. Appl. Phys.*, **22**, 343 (1949).

(14) G. I. Whitman, *J. Chem. Phys.*, **20**, 161 (1952).

The room temperature patterns of Ti_3O_5 did not correspond to that described by Rusakov and Zhdanov,[15] nor could the lines be indexed into the Ti_2O_3, rutile or anatase pattern. The pattern might be considered a very strongly distorted (much more than the above-mentioned $TiO_{1.82}$) rutile structure. At high temperatures, we obtained a new diffraction pattern for Ti_3O_5, different from the room temperature form, and from TiO_2 and Ti_2O_3.

Vapor Pressure Data.—1. The experiments carried out to determine the composition of the solid and vapor are given in Table I.

TABLE I

VAPORIZATION EXPERIMENTS

Material	Vaporization: Amount original, g.	Vaporization: Amount vaporized, g.	Analysis: Amount, g.	Analysis: Wt. gain, g.	Composition, TiO_x
TiO	1.3244	0.04631			
Original			0.25206	0.06084	1.0290
Residue			.10632	.02562	1.0302
Ti_2O_3	1.58643	.2797			
Original			.24634	.02792	1.4916
Residue			.16359	.01851	1.4924
Ti_3O_5	1.2300	.3412			
Original			.19596	.01401	1.6668
Residue			.15406	.01101	1.6669
TiO_2	0.23895	.15825			
Original			.29578	.00340	1.9432
Residue			.03612	.00114	1.8472

To check our vaporization experiments, material was collected during several vapor pressure runs. The amount was too small to be analyzed, and X-ray diffraction patterns were taken.

For TiO and Ti_2O_3 the collected vapor showed the TiO and Ti_2O_3 structures, agreeing well with the vaporization measurements. For Ti_3O_5 the collected vapor showed a rutile structure, similar to the one when TiO_2 is vaporized.

TiO will not vaporize stoichiometrically, the vapor containing Ti and TiO, and very small amounts of TiO_2. The solid therefore will steadily become richer in oxygen. Our vaporization measurements and X-ray data indicate that the TiO/Ti ratio is larger than 10:1. The correction for Ti is smaller using $TiO_{1.029}$ as a solid phase, than if $TiO_{1.000}$ would have been used. The activity of TiO over the homogeneity range is almost constant.[5] The TiO system is a pseudo-invariant system, and the measured pressures may be taken as the partial pressure of TiO in equilibrium with $TiO_{1.000}$, the composition for which thermodynamic data are available.

The vaporization and X-ray data on Ti_2O_3 indicate that Ti_2O_3 vaporizes stoichiometrically within 10%. The TiO to TiO_2 ratio must be between 0.9 and 1.1. The data were treated according to stoichiometric vaporization: the Ti_2O_3 system, even with only one solid phase present, is an invariant system.

The vaporization and X-ray data on Ti_3O_5 are contradictory. Vaporization and analysis of the residue indicate stoichiometric vaporization; the X-ray data from the collected vapor show that vapor contained only TiO_2. This discrepancy could be caused by an oxidation of the solid during the single vaporization run, or the oxidation of the collected vapor, during the vapor pressure runs. The TiO_2 pressure above Ti_3O_5 must be at least equal to the TiO_2 pressure above Ti_2O_3. Inspecting the measured rates of evaporation we see that this is only possible if almost all the material vaporized was TiO_2. Our data were therefore treated as $Ti_3O_5(s) \rightarrow Ti_2O_3(s) + TiO_2(g)$.

TiO_2 showed on the first heating a high evaporation rate, until the composition of the solid dropped to $TiO_{1.943}$. At this point the rate of evaporation became constant, and the collected vapor showed the rutile structure. After the vapor pressure measurements the solid analyzed $TiO_{1.847}$. The vaporization of TiO_2 takes place under invariant conditions, the reaction occurring being

$$1.206\ TiO_{1.943}(s) \longrightarrow 0.206\ TiO_{1.667}(s) + TiO_2(g) \quad (A)$$

The reaction

$$TiO_{1.943}(s) \longrightarrow TiO_{1.667}(s) + 0.138\ O_2(g) \quad (B)$$

will take place simultaneously.

To obtain the free energy of formation of $TiO_{1.943}$, and for all the subsequent calculations we used the data compiled by Skinner, Beckett and Johnston.[4]

To obtain the free energy function of TiO_2 gas, we assumed that the addition of an oxygen to TiO to form TiO_2 will increase the free energy by an amount which is 75% of the increase due to the addition of an oxygen to Ti to form TiO. Thus

$$\left(\frac{F^0 - H_0^\circ}{T}\right)_{TiO_2(g)} = \left(\frac{F^0 - H_0^\circ}{T}\right)_{TiO(g)} + 0.75\left[\left(\frac{F^0 - H_0^\circ}{T}\right)_{TiO(g)} - \left(\frac{F^0 - H_0^\circ}{T}\right)_{Ti(g)}\right]$$

The oxygen pressure for reaction B must be smaller than the pressure for

$$TiO_2(s) \longrightarrow TiO_{1.667} + 0.167\ O_2(g)$$

which at 2000°K. is $10^{-8.3}$ atm.

The oxygen loss is negligible compared to the TiO_2 loss in the two phase region $TiO_{1.943} - Ti_3O_5$. The oxygen pressure for reaction B must be larger than the pressure for

$$Ti_3O_5 \longrightarrow 1.5\ Ti_2O_3 + 0.25\ O_2(g)$$

which at 2000°K. is 10–11.5 atm.

The oxygen pressure for reaction B must be between $10^{-11.5}$ and $10^{-8.3}$ atm., ΔF^0 at 2000°K. for reaction B is between 14.5 and 10.5 kcal. Thus ΔF^0 of formation of $TiO_{1.943}(s)$ at 2000°K. is between −141.7 and −137.7 kcal., and we can fix it as -140 ± 1 kcal. For the reaction

$$1.206\ TiO_{1.943}(s) \longrightarrow 0.206\ TiO_{1.667}(s) + TiO_2(s)$$

we obtain at 2000°K., $\Delta F^0 = 2.5$ kcal.; that means the activity of TiO_2 in the $TiO_{1.943}/Ti_3O_5$ two phase mixture is $10^{-0.273}$ or 0.53 at 2000°K. We assume that this activity does not vary over our experimental temperature range. To obtain the pressure of $TiO_2(g)$ above $TiO_{2.0}$ solid, the experimental pressure was multiplied by $1/0.53 = 1.885$, and this corrected pressure used in connection with the free energy functions to calculate the heat of vaporization of TiO_2.

The vapor pressures were calculated from the rate of effusion, using the equation

$$P = m\sqrt{2\pi RT/M} \quad (1)$$

(15) A. A. Rusakov and G. S. Zhdanov, *Doklady Akad. Nauk S.S.S.R.*, **17**, 411 (1951); *C. A.*, **45**, 6452 (1951).

where P is the pressure in atmospheres, R is the molar gas constant, T is the absolute temperature, m is the rate of effusion in g./sq. cm./sec. and M is the molecular weight of the vapor.

In the presence of more than one species in the gas, the measured total rates of effusion were divided according to the ratio of molecular weight of the components, multiplied by the composition of the gas phase, and the pressure calculated for each

TABLE II

VAPOR PRESSURE ABOVE TiO[a]

Temp., °K.	Eff. time, sec.	Eff. area, cm.²	Wt. loss, g. × 10³	Evap. rate, g./cm.²/ sec. × 10⁵	Pressure, atm. × 10⁶ (calcd. as TiO)	−log₁₀ P
1847	109080	0.01524	2.79	0.1678	0.2035	6.691
1880	57694	.01709	3.85	.3905	.4778	6.321
*1908	36875	.01710	3.91	.6201	.7643	6.117
1913	29275	.01525	3.17	.7101	.876	6.058
1920	117378	.01526	13.04	.7280	.900	6.046
1934	28721	.01710	5.27	1.073	1.332	5.876
*1960	28868	.01709	8.03	1.628	2.034	5.692
1968	14382	.01711	5.38	2.186	2.736	5.563

[a] For the runs marked with a * the solid had the composition $TiO_{1.075}$; for all the others $TiO_{1.029}$.

TABLE III

VAPOR PRESSURE OVER TiO_{2-x}

Temp., °K.	Eff. time, sec.	Eff. area, cm.²	Wt. loss, g. × 10³	Evap. rate, g./cm.²/ sec. × 10⁵	Pressure, atm. × 10⁶ (calcd. as TiO_2)	−log P
1849	28872	0.01379	1.45	0.364	0.395	6.403
1867	28800	.01379	1.94	0.488	0.533	6.273
1916	12960	.01380	1.98	1.107	1.223	5.913
1918	14400	.01381	2.45	1.232	1.362	5.866
1936	14400	.01353	3.33	1.709	1.899	5.721
1943	10800	.01381	2.96	1.985	2.207	5.656
1949	28800	.01381	11.06	2.808	3.098	5.509
1954	18072	.01382	6.03	2.414	2.693	5.570
1956	14472	.01382	5.29	2.645	2.953	5.530
1958	14400	.01382	6.29	3.161	3.529	5.452
1966	14400	.01353	4.93	2.530	2.831	5.548
1972	14400	.01353	4.67	2.397	2.686	5.571
1982	14400	.01354	5.98	3.067	3.446	5.463
2010	14400	.01354	8.90	4.565	5.164	5.287

TABLE IV

VAPOR PRESSURE ABOVE Ti_2O_3

Temp., °K.	Eff. time, sec.	Eff area, cm.²	Wt. loss, g. × 10³	Evap. rate, g./cm.²/ sec. × 10⁵	$\sqrt{p_{TiO}p_{TiO_2}} = \sqrt{K \times 10^6}$	$-\frac{1}{2}\log K_p$
1971	14400	0.01749	0.66	0.262	0.154	6.812
1990	25030	.04351	5.75	.528	.312	6.506
1992	21600	.01750	1.21	.320	.189	6.724
2008	13380	.04031	1.82	.337	.200	6.699
2010	37400	.04031	5.80	.385	.229	6.640
2017	29220	.01751	3.49	.682	.406	6.392
2022	10800	.04354	6.06	1.289	.769	6.114
2023	7301	.04354	3.67	1.155	.689	6.162
2029	7441	.04354	4.30	1.327	.793	6.101
2030	28560	.01751	4.17	0.834	.498	6.303
2035	15930	.04355	6.61	0.953	.570	6.244
2059	7409	.04357	5.42	1.679	1.010	5.996
2064	19770	.04357	13.91	1.615	0.973	6.012
2076	14760	.01753	4.07	1.573	.950	6.022
2085	6998	.04038	3.41	1.207	.731	6.136
2097	20040	.01404	2.73	0.970	.589	6.230
2101	14400	.01404	2.09	1.034	.629	6.201
2102	12600	.01754	3.31	1.498	.911	6.040
2106	6545	.04361	14.28	5.003	3.044	5.516
2106	14400	.01404	2.46	1.217	0.741	6.130
2108	14400	.01754	6.25	2.475	1.507	5.822
2113	6959	.04040	5.16	1.835	1.119	5.951
2116	13740	.01754	6.53	2.710	1.653	5.782
2120	14040	.01754	6.09	2.743	1.510	5.821
2122	41400	.01754	18.84	2.594	1.585	5.800
2151	10860	.01405	3.04	1.992	1.225	5.911

TABLE V

VAPOR PRESSURE ABOVE Ti_3O_5

Temp., °K.	Eff. time, sec.	Eff. area, cm.²	Wt. Loss, g. × 10³	Evap. rate, g./cm.²/ sec. × 10⁵	Pressure, atm. × 10⁶ (calcd. as TiO_2)	−log P
2068	59260	0.01767	6.72	0.642	0.740	6.131
2070	14340	.01767	1.54	.608	.700	6.155
2076	28660	.01767	3.63	.717	.826	6.083
2078	29020	.01767	2.98	.581	.669	6.175
2078	14460	.01767	1.67	.654	.753	6.123
2088	6660	.01768	1.16	.985	1.135	5.945
2099	11820	.01768	1.67	.799	0.920	6.036
2122	14400	.01769	4.96	1.947	2.243	5.649

TABLE VI

HEAT OF SUBLIMATION OF TiO

Temp., °K.	$-R \ln P$	$-\Delta\left(\frac{F - H_0^\circ}{T}\right)$	$\frac{\Delta H_0^\circ}{T}$	ΔH_0°, kcal./mole
1847	30.605	42.78	73.382	135.54
1880	28.912	42.69	71.600	134.61
1908	27.979	42.61	70.593	134.69
1913	27.709	42.61	70.314	134.51
1920	27.655	42.59	70.240	134.86
1934	26.877	42.55	69.423	134.26
1960	26.035	42.48	68.513	134.28
1968	25.445	42.45	67.898	133.62

Av. = 134.55 ± 0.52

TABLE VII

HEAT OF SUBLIMATION OF TiO_2

Temp., °K.	$-R \ln P$	$-\Delta\left(\frac{F^\circ - H_0^\circ}{T}\right)$	$\frac{\Delta H_0^\circ}{T}$	ΔH_0° kcal./mole
1849	28.03	47.0	75.0	138.7
1867	27.43	46.9	74.3	138.7
1916	25.79	46.8	72.6	139.1
1918	25.57	46.8	72.4	138.9
1936	24.91	46.8	71.7	138.8
1943	24.61	46.8	71.4	138.7
1949	23.94	46.8	70.7	137.8
1954	24.22	46.7	70.9	138.5
1956	24.03	46.7	70.7	138.3
1958	23.68	46.7	70.4	137.8
1966	24.12	46.7	70.8	139.2
1972	24.22	46.7	70.9	139.8
1982	23.73	46.7	70.4	139.5
2010	22.92	46.6	69.5	139.7

Av. = 138.9 ± 0.5

TABLE VIII

HEATS OF REACTION FOR Ti_2O_3

Temp., °K.	$-R \ln K_p$	$-\Delta\left[\frac{F^\circ - H_0^\circ}{T}\right]$	$\frac{\Delta H_0^\circ}{T}$	ΔH_0°, kcal./mole
1971	62.32	87.7	150.0	295.6
1990	59.52	87.6	147.1	292.7
1992	61.51	87.6	149.1	297.0
2008	61.28	87.5	148.8	298.8
2010	60.74	87.5	148.2	297.9
2017	58.47	87.4	145.9	294.3
2022	55.93	87.4	143.3	289.8
2023	56.37	87.4	143.8	290.9
2029	55.81	87.4	143.2	290.6
2030	57.66	87.4	145.1	294.6
2035	57.12	87.3	144.4	293.9
2059	54.85	87.2	142.0	292.4
2064	55.00	87.2	142.2	293.5
2076	55.09	87.1	142.2	295.2
2085	56.13	87.1	143.2	298.6
2097	56.99	87.0	144.0	302.0

TABLE VIII (*Continued*)

Temp., °K.	$-R \ln K_p$	$-\Delta\left[\frac{F^0 - H}{T}\right]$	$\frac{\Delta H_0^\circ}{T}$	ΔH_0°, kcal./mole
2101	56.73	87.0	143.7	301.9
2102	55.25	87.0	142.2	298.9
2106	50.46	86.9	137.4	289.4
2106	56.08	86.9	143.0	301.2
2108	53.26	86.9	140.2	295.5
2113	54.44	85.9	141.3	298.6
2116	52.89	86.9	139.8	295.8
2120	53.25	86.8	140.0	296.8
2122	53.06	86.8	139.9	296.9
2151	54.07	86.7	140.8	302.9
			Av. =	296.0 ± 3.6

TABLE IX

HEATS OF REACTION FOR Ti_3O_5

Temp., °K.	$-R \ln K_p$	$-\Delta\left(\frac{F^0 - H_0^\circ}{T}\right)$	$\frac{H_0^\circ}{T}$	ΔH_0°, kcal./mole
2068	28.05	43.6	71.7	148.3
2070	28.16	43.6	71.8	148.6
2076	27.83	43.5	71.3	148.0
2078	28.25	43.5	71.8	149.2
2078	28.01	43.5	71.5	148.6
2088	27.20	43.5	70.7	147.6
2099	27.61	43.5	71.1	149.2
2112	25.84	43.4	69.2	146.2
			Av.	148.2 ± 0.7.

TABLE X

Heats of dissociation of TiO(g) and TiO_2(g)

$TiO(g) \rightarrow Ti(g) + O(g)$ $\quad \Delta H_0^\circ = 159.9$ kcal/mole

$TiO_2(g) \rightarrow Ti(g) + 2O(g)$ $\quad \Delta H_0^\circ = 315.2$ kcal./mole

component according to equation 1. The use of the rates of effusion instead of the pressures introduces a small error in the calculations because the molecular weight of TiO and TiO_2 are different. In the case of Ti_2O_3, we assumed that the rate of effusion of TiO is equal to that of TiO_2: the value for the equilibrium constant K, will be changed by only 0.47% if it is assumed that the pressures of TiO and TiO_2 are equal. This difference is much smaller than the experimental error.

The calculations of the pressures and equilibrium constants are given in Tables II–V, whereas the calculations of the heats of sublimation and heats of reaction are given in Tables VI–IX. Table X contains the heats of dissociation of gaseous molecules to gaseous atoms.

After expanding the free energy function as a linear function of the temperature, we obtain the equilibrium constants and pressure of TiO and TiO_2 above the four oxides investigated. The results are given in Table XI. The values for titanium are given to complete the table. In the last column, the pressures are given at 2000°K., for better comparison.

The heat of vaporization of TiO, agrees very well with the value found by Gilles and Wheatley and given by Brewer.[3] The heat of dissociation of TiO is in very good agreement with the spectroscopic value of 158.8 kcal./mole quoted by Herzberg.[16]

The value obtained for the heat of vaporization of TiO_2 is in good agreement with $\Delta H_{1900} = 138$ kcal./mole, which is obtained from our data using the Clausius–Clapeyron equation. The heat of dissociation of TiO_2 is 4.6 kcal. or 1.4% smaller than twice the heat of dissociation of TiO, which is about the amount one would expect.

To check the data, and to resolve the discrepancy in the vaporization of Ti_3O_5, further experiments are under way at other compositions.

TABLE XI

EQUILIBRIUM CONSTANTS AND PRESSURES ABOVE TiO, TiO_2, Ti_2O_3 AND Ti_3O_5

Solid phase	Eq. constant	Vapor pressure equation	$-\log P$ at 2000°K.
TiO	$K_p = p_{TiO}$	$\log K_p = \log p_{TiO} = -\frac{29421}{T} - 0.583 \times 10^{-3}T + 10.43$	5.44
TiO_2	$K_p = p_{TiO_2}$	$\log K_p = \log p_{TiO_2} = -\frac{30361}{T} - 0.492 \times 10^{-3}T + 11.19$	4.97
Ti_2O_3	$K_p = p_{TiO}p_{TiO_2}$	$\log K_p = -\frac{64700}{T} - 1.26 \times 10^{-3}T + 21.65$	
		$\log p_{TiO} = \log p_{TiO_2} = -\frac{32350}{T} - 0.63 \times 10^{-3}T + 10.83$	6.61
Ti_3O_5/Ti_2O_3	$K_p = p_{TiO_2}$	$\log K_p = \log P_{TiO_2} = -\frac{32393}{T} - 0.48 \times 10^{-3}\,T + 10.51$	6.64
Ti	$K_p = p_{Ti}$	$\log K_p = \log p_{Ti} = -\frac{24644}{T} - 0.227 \times 10^{-3}\,T + 7.796$	4.97

(16) G. Herzberg, "Spectra of Diatomic Molecules," Second Edition, D. Van Nostrand Company, Inc., New York, N. Y., 1950, p. 576.

VAPORIZATION OF INORGANIC SUBSTANCES: B_2O_3, TeO_2 AND Mg_3N_2[1]

BY JOHN R. SOULEN, PRASOM STHAPITANONDA AND JOHN L. MARGRAVE

Department of Chemistry, University of Wisconsin, Madison, Wisconsin

Received October 12, 1954

The necessity for auxiliary experiments in the study of vaporization of substances at high temperatures is discussed. Earlier work pertaining to the vaporization of B_2O_3 and TeO_2 is reviewed and new vapor pressure determinations are presented which extend the temperature ranges of the measurements. In the temperature ranges studied B_2O_3 and TeO_2 are found to vaporize as $B_2O_3(g)$ and $TeO_2(g)$ molecules, and vapor pressure equations are given. ΔH°_0 of sublimation has been calculated from vapor pressure data for B_2O_3 with the aid of free energy functions, and the heats of sublimation, vaporization and fusion are given for TeO_2. Vapor pressure measurements have been supplemented by spectroscopic observations and bands attributable to the $B_2O_3(g)$ molecule have been found. The vaporization of Mg_3N_2 has also been studied and found to be more complex. It is found that the $Mg_2(g)$ molecule is involved in the process of vaporization of Mg_3N_2. From the $Mg_2(g)$ band spectrum the dissociation energy of the molecule has been estimated. Final products of Mg_3N_2 vaporization are $Mg(g)$ and $N_2(g)$.

In most cases where vaporization or evaporation processes at high temperatures have been studied carefully by modern techniques, the reactions have been found to be more complex than formerly believed. The idea that stable species at high temperatures are necessarily simple is found not to be true, and many indications of large and/or new molecules are found through careful interpretation of vapor pressure, spectroscopic and mass spectrographic data.

Because of this possibility of a complex vaporization process, it is usually necessary to perform several different experiments to establish without doubt the vaporization equilibrium species and equilibrium constant, and even more data may be necessary to establish the mechanism of a vaporization reaction. A systematic vapor pressure study of any material may well be accompanied by the following auxiliary studies besides the standard flow, effusion, or other type of vapor pressure measurement.

(1) Identification of all solid phases present at all temperatures of interest. This can best be done with the aid of low and high temperature X-ray diffraction studies.

(2) Analysis of the compound before and after several vaporization runs to determine whether or not one constituent is being lost preferentially. Use of the same sample for several consecutive runs might also show this effect through changing analyses.

(3) A search by spectrographic means for emission or absorption spectra of gaseous molecules and atoms being formed. This method is very sensitive, and may detect partial pressures down to about 10^{-6} atm.

(4) A search with a mass spectrograph to identify important vapor species.

(5) A determination of the vapor density to confirm vapor composition and indicate whether dimers, trimers or other complex species are important in vaporization.

(6) Calculation of the equilibrium pressure of the elements over a compound assuming decomposition only to the elements. This will give the lowest possible pressure over a compound at equilibrium in a vacuum. If there are any other species important in the vapor, or if a reactive atmosphere is used, vaporization may be greater than calculated.

(7) Comparison of flow, effusion, static and other vapor pressure measurements should be made to see if they all agree, since molecular species are often incorrectly assumed in effusion and flow calculations and erroneous pressures calculated. One *must* know what atoms or molecules are coming out of an effusion cell before the equilibrium pressure inside the cell can be calculated from weight loss or gain alone.

In this work we have used flow and effusion vapor pressure measurements, and spectroscopic observations in the visible and ultraviolet regions to elucidate the vaporization processes for three inorganic compounds: B_2O_3, TeO_2 and Mg_3N_2.

Vapor Pressure of B_2O_3.—Liquid boric oxide begins to vaporize appreciably at temperatures above 1000°. The logical possibilities for the vaporization reaction are

$$B_2O_3(l) = B_2O_3(g)$$
$$xB_2O_3(l) = (B_2O_3)_x(g)$$
$$B_2O_3(l) = 2BO(g) + {}^1/_2O_2(g)$$

Purified boric oxide from Baker and Adamson was prepared for vapor pressure runs by slow heating of samples in a platinum boat up to 1000° and maintaining this temperature for an hour or more to remove all traces of water. Two series of flow vapor pressure studies were carried out, both with dry, oxygen-free nitrogen as the carrier gas. In one series of runs a platinum boat containing B_2O_3 was placed in the flow stream and in the hot zone of a McDanel high temperature porcelain tube heated in a SiC hollow tube furnace. In the other series of runs the porcelain tube was lined with platinum foil, and the vaporization carried out essentially in a platinum system.

The runs made in the unprotected tube gave weight losses per mole of flow gas similar to those predicted from the early work of Cole and Taylor[2] and much higher than expected on the basis of the effusion vapor pressure studies of Speiser, Naiditch and Johnston.[3] Runs in the platinum foil protected tube agreed closely with those of Speiser, Naiditch and Johnston in regions where experimental temperatures allowed direct comparison.

(1) Presented at the Symposium on High Temperature Chemical Reactions at the 126th Meeting of the American Chemical Society, New York, N. Y., September 15, 1954.

(2) S. S. Cole and N. W. Taylor, *J. Am. Cer. Soc.*, **18**, 82 (1935).

(3) R. Speiser, S. Naiditch and H. L. Johnston, *J. Am. Chem. Soc.*, **72**, 2578 (1950).

Treatment of the weight loss type of vapor pressure data obtained in these measurements requires knowledge of the gaseous species present, and Bradt[4] has recently shown in a mass spectrographic study of the vapor effusing from a Knudsen cell containing $B_2O_3(l)$ at about 1300° that monomeric $B_2O_3(g)$ is the only important vapor species under these conditions. In part (a) of Table I are listed the pressures of $B_2O_3(g)$ from Speiser, Naiditch and Johnston calculated with the assumption of monomeric $B_2O_3(g)$, the change of free energy function for vaporization, $\Delta F/T$, $\Delta H^\circ_0/T$ and ΔH°_0, the heat of sublimation of B_2O_3 at 0°K. Free energy functions for gaseous and liquid B_2O_3 were computed from the tables of Huff, Gordon and Morrell.[5]

Values of ΔH°_0 are seen to be essentially constant, and the average is 89.4 kcal./mole. An uncertainty of at least 0.5 kcal./mole should be allowed because of the doubt about the true structure of $B_2O_3(g)$. If one corrects this calculated heat up to 1500°K., the middle of the experimental range studied by Speiser, Naiditch and Johnston, by means of the heat content functions of Huff, Gordon and Morrell, one obtains $\Delta H_{1500} = 77.6$ kcal./mole, which is exactly the slope of the log p *vs.* $1/T$ plot of their data.

TABLE I

VAPORIZATION OF B_2O_3

T, °K.	$p_{B_2O_3}$, atm.	$-\Delta\left(\frac{F-H^\circ_0}{T}\right)_{vap}$, e.u.	$\frac{\Delta F}{T}$, e.u.	$\frac{\Delta H^\circ_0}{T}$, e.u.	ΔH°_0, kcal./mole
(a) Effusion vapor pressure data (from ref. 3)					
1331	7.74×10^{-7}	39.80	27.96	67.76	90.2
1350	1.88×10^{-6}	39.68	26.20	65.88	88.9
1369	2.46×10^{-6}	39.58	25.67	65.25	89.3
1380	5.02×10^{-6}	39.52	24.25	63.77	88.0
1390	4.00×10^{-6}	39.47	24.70	64.17	89.2
1449	9.90×10^{-6}	39.14	22.90	62.04	89.2
1476	1.59×10^{-5}	39.00	21.96	60.96	90.0
1490	2.25×10^{-5}	38.92	21.27	60.19	89.7
1497	2.88×10^{-5}	38.89	20.78	59.67	89.3
1510	4.25×10^{-5}	38.80	20.00	58.80	88.8
1540	6.53×10^{-5}	38.65	19.15	57.80	89.0
1550	7.36×10^{-5}	38.61	18.91	57.52	89.2
1569	7.21×10^{-4}	38.51	18.95	57.46	90.1
1631	2.31×10^{-4}	38.21	16.64	54.85	89.5
1642	2.87×10^{-4}	38.15	16.20	54.35	89.2
(b) Flow vapor pressure data					
1567	3.6×10^{-4}	38.51	15.74	54.25	85.0
1579	3.1×10^{-4}	38.47	16.08	54.55	86.2
1772	4.1×10^{-3}	37.72	10.90	48.62	86.3
1806	3.5×10^{-3}	37.44	11.22	48.66	88.0
1808	2.6×10^{-3}	37.44	11.82	49.26	89.0

Part (b) of Table I includes calculations similar to those above but based on our flow vapor pressure measurements in platinum, and again assumes the vapor to consist of monomeric $B_2O_3(g)$. ΔH°_0 values calculated here agree fairly well with the results of the effusion measurements.

Figure 1 shows that, over the range 1331 to 1808°K., one can satisfactorily describe the vaporization of B_2O_3 by assuming monomeric $B_2O_3(g)$ as the main vapor species. The older data of Cole and Taylor[2] are also shown. The vapor pressure is given by the equation

$$\log p_{atm} = 6.742 - \frac{16960}{T} \qquad (1331 < T < 1808°K.)$$

The molecule $B_2O_3(g)$ is not well known. Various spectra from flames and electrical discharges into which boric acid has been introduced show BO(g) bands as well as the so-called "boric acid fluctuation bands."[6] By heating B_2O_3 in porcelain tubes to 1400–1700° we have obtained emission and absorption spectra of the gas over $B_2O_3(l)$ with a small Hilger quartz spectrograph. These are shown in Fig. 2. The bands are the same as the "fluctuation bands," but do not have the BO background spec-

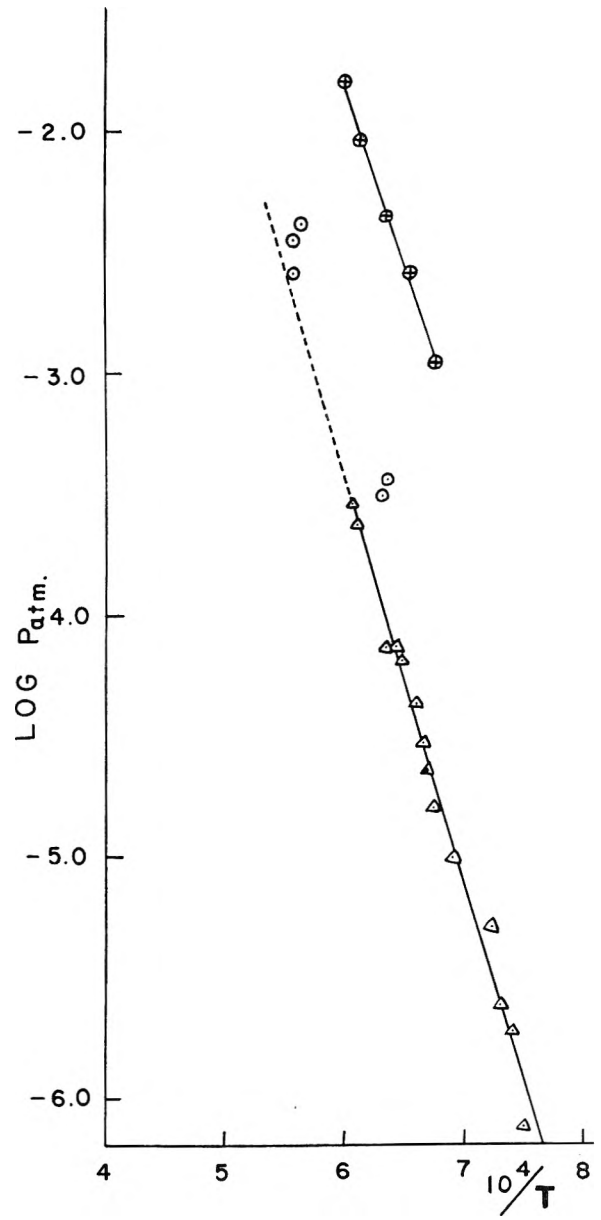

Fig. 1.—Log p *vs.* $1/T$ plot for B_2O_3 vaporization: △, Speiser, Naiditch and Johnston[3]; ⊕, Cole and Taylor[2]; ⊙, this work.

(4) P. Bradt, NBS Report 3016, January, 1954.

(5) V. N. Huff, S. Gordon and V. E. Morrell, National Advisory Committee for Aeronautics Report 1037 (1951). These authors assume $B_2O_3(g)$ to be a symmetrical molecule in which the oxygen atoms form an equilateral triangle, and the boron atoms lie on each side of the plane of this triangle and are both singly bonded to each of the three oxygen atoms. This structure was suggested by P. F. Wacker, H. W. Wooley and M. F. Fair in a Technical Report to the Bureau of Aeronautics, Navy Department, January 25, 1945.

(6) R. W. B. Pearse and A. G. Gaydon, "The Identification of Molecular Spectra," John Wiley and Sons, Inc., New York, N. Y., 1950, p. 60.

trum. From the analysis of the vapor pressure data, they must be associated with an electronic transition for the $B_2O_3(g)$ molecule. We are now re-photographing these spectra with a high resolution grating, and hope to obtain more information about the structure of the molecule.

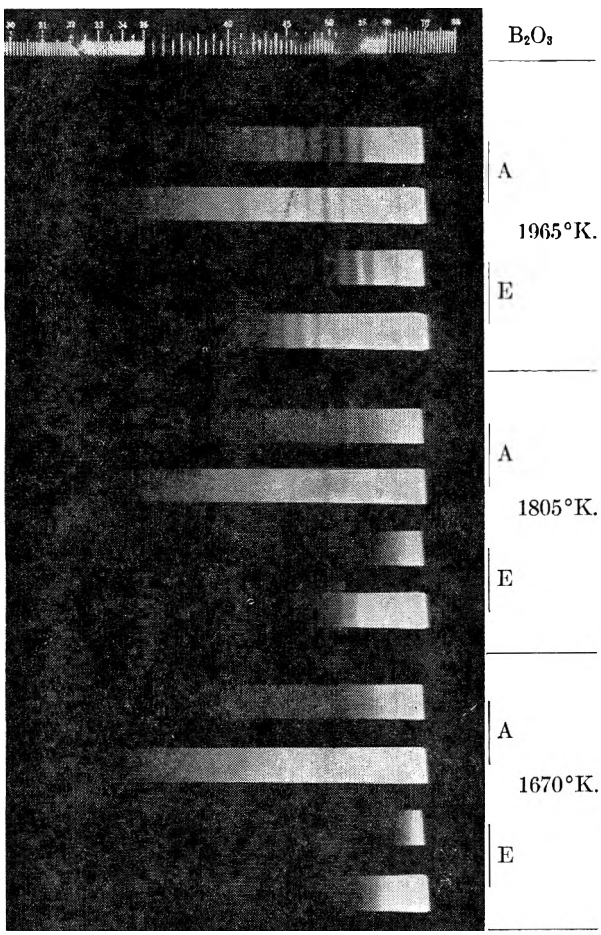

Fig. 2.—Absorption (A) and emission (E) spectra of gas over $B_2O_3(l)$ at various temperatures. Exposure times for the absorption photographs were 0.1 sec. (upper) and 1 sec. (lower). For emission, exposure times of 1 sec. (upper) and 10 sec. (lower) were used.

Vapor Pressure of TeO_2.—The vapor pressure of solid and liquid TeO_2 has been measured over the range 846 to 1211°K. by effusion and flow vapor pressure studies. The main species in equilibrium with both solid and liquid TeO_2 in this range is $TeO_2(g)$ as established by spectroscopic observations.[7] TeO(g) is observed at still higher temperatures.

Spectroscopically pure TeO_2 was used. It was checked by X-ray diffraction, and showed the desired powder pattern with no impurity lines. Samples were vaporized from porcelain, quartz and MgO containers and no signs of attack were observed for any of these materials. The melting point of TeO_2 was determined in a quartz capillary tube, and found to be 733 ± 1°, in good agreement with previous work.[8]

(7) (a) C. S. Piaw, *Ann. Phys.*, **10**, 173 (1935); (b) J. Duschesne and B. Rosen, *J. Chem. Phys.*, **15**, 631 (1947).

(8) A. Simek and B. Stehlik, *Collection Czechov. Chem. Communs.*, **2**, 447 (1930).

The flow vapor pressure measurements were carried out with five flow rates of either nitrogen or oxygen: 559, 340, 155, 80.2 and 34.4 ml./min. Graphical extrapolation to zero flow rate gave the extrapolated vapor pressures at the various experimental temperatures as shown in part (a) of Table II. Effusion vapor pressure data are given in part (b) of Table II. A graph showing the log of the vapor pressure in atm. *vs.* $1/T$ is given in Fig. 3.

TABLE II

VAPORIZATION OF TeO_2

(a) Flow vapor pressure data (both N_2 and O_2 as carrier gases)

T, °K.	$-\log p$, atm. (extrapd. to zero flow rate)
1064	3.30
1100	2.93
1151	2.38
1211	1.90

(b) Effusion vapor pressure data

T, °K.	Total wt. loss, mg.	Area of effusion hole, cm.²	Time, min.	$-\log p$, atm.
846	0.2	8.58×10^{-3}	35	6.07
888	1.0	8.58×10^{-3}	60	5.60

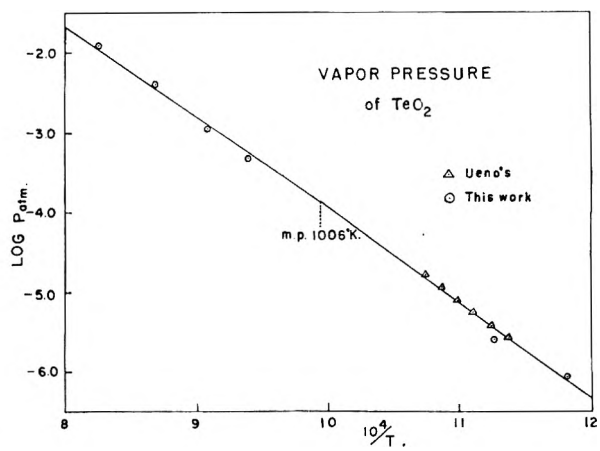

Fig. 3.—Log p *vs.* $1/T$ plot for TeO_2 vaporization.

Also shown here are the effusion data of Ueno[9] for solid TeO_2. From the difference in the slopes of the vapor pressure curves for liquid and solid, one evaluates the heat of fusion of TeO_2 as 3.2 ± 0.5 kcal./mole. The vapor pressure equations are

$$TeO_2(s) = TeO_2(g);\ \Delta H_{sub} = 54.9 \text{ kcal./mole}$$

$$\log p_{atm} = 8.067 - \frac{12000}{T} \qquad (846 < T < 1006°K.)$$

$$TeO_2(l) = TeO_2(g);\ \Delta H_{vap} = 51.7 \text{ kcal./mole}$$

$$\log p_{atm} = 7.367 - \frac{11300}{T} \qquad (1006 < T < 1211°K.)$$

Vapor Pressure of Mg_3N_2.—Vaporization of solid nitrides is of interest because of the possibility of forming gaseous metal nitrides. We have studied the vaporization of Mg_3N_2 by both flow and effusion techniques, and also examined the vapors over this compound spectroscopically. The various possible vaporization processes for magnesium nitride include

$$Mg_3N_2(s) = Mg_3N_2(g)$$
$$Mg_3N_2(s) = 2MgN(g) + Mg(g)$$
$$Mg_3N_2(s) = 3Mg(g) + N_2(g)$$

(9) K. Ueno, *J. Chem. Soc. Japan*, **62**, 990 (1941).

Samples of magnesium nitride were prepared from high purity Mg by reaction with N_2 as suggested by Mitchell.[10] X-Ray diffraction patterns showed only the Mg_3N_2 phase to be present.

When Mg_3N_2(s) contained in a refractory oxide container was heated rapidly to 1200–1400° in either N_2 or He atmospheres and a series of absorption spectra taken, spectra like those shown in Fig. 4 were obtained. The narrow Mg absorption line

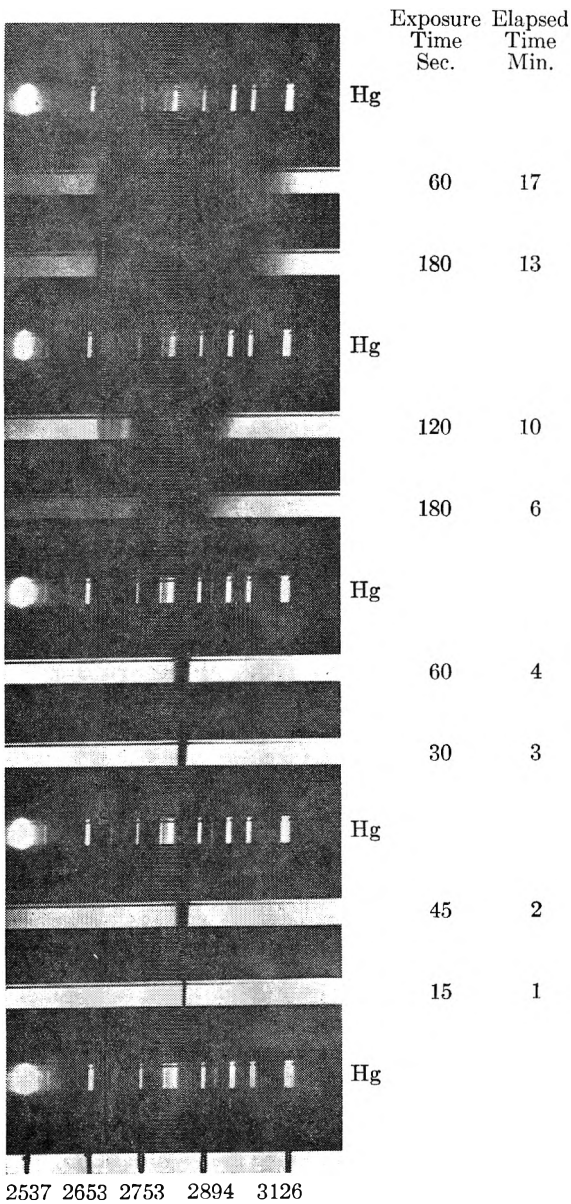

Fig. 4.—Absorption spectra taken at various intervals after placing a Mg_3N_2 sample in a furnace at 1400°. The Mg (I) resonance line ($^1P_1 - {}^1S_0$) is at 2852 Å. (Hg reference spectra are also shown.)

which first appeared at 2852 Å. was found to broaden into a continuum plus several absorption bands as vaporization took place. These absorption bands correspond exactly to certain of the emission bands which were observed by Hamada[11] in electrical discharges through highly concentrated Mg vapor in a hollow cathode, and which have been attributed to Mg_2(g).

From the position of the sharp cut-off of the observed absorption at 2661 Å. and the known energies of excitation of Mg atoms, one may deduce potential energy curves describing the interactions of Mg atoms.[12] The Mg_2 molecule appears to be relatively weakly bound, much like the similar molecules Zn_2, Cd_2 and Hg_2, which are held together mainly by a van der Waals type of bond. The dissociation energy of Mg_2(g) is estimated as 7.2 ± 0.2 kcal./mole. Mg_2(g) spectra were not observed in the recent absorption studies of Ditchburn and Marr[13] because they studied Mg vapor at low pressures (<1.3 mm.) where the Mg_2 molecules would be dissociated.

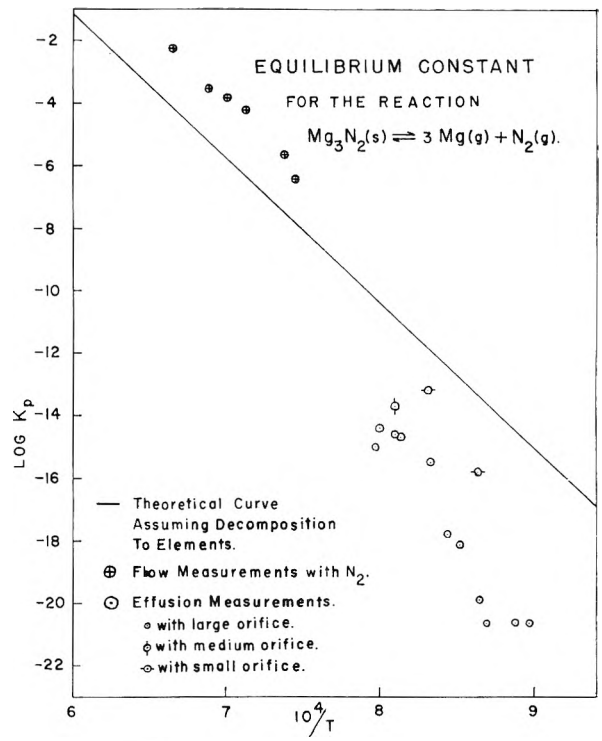

Fig. 5.—Log K_p *vs.* $1/T$ plot for the reaction $Mg_3N_2(s) = 3Mg(g) + N_2(g)$.

Equilibrium studies of the vapor over Mg_3N_2 have also been carried out. The experimental data for our flow vapor pressure measurements, in which Mg_3N_2(s) was heated in Coors porcelain boats and high purity N_2 was used as the flow gas, are given in part (a) of Table III. In part (b) of Table III are the data for some of our effusion vapor pressure studies made in MgO containers with three sizes of effusion holes. The equilibrium constants for decomposition to the elements as calculated from these data are compared with the theoretical values in Fig. 5. The theoretical curve was computed with data from NBS Circular 500, and free energy functions based on the high temperature heat capacity

(10) D. W. Mitchell, *Ind. Eng. Chem.*, **41**, 2027 (1949).

(11) H. Hamada, *Phil. Mag.*, **12**, 50 (1931).

(12) These Mg_3(g) spectra are presently being carefully examined and will be described more fully in a later publication. The authors wish to acknowledge the aid of Professor J. G. Winans of the Physics Department, University of Wisconsin, in interpreting these spectra.

(13) R. W. Ditchburn and G. V. Marr, *Proc. Phys. Soc.*, **66A**, 655 (1953).

data of Mitchell[10] along with an estimated entropy at 298°K. of 22 e.u. for Mg_3N_2(s).

TABLE III
VAPORIZATION OF Mg_3N_2

(a) Flow vapor pressure data (N_2 as carrier gas)

T, °K.	Total wt., loss,[a] mg.	Time, min.	− log K[b]
1337	44–64	60–66	6.41
1355	75–103	60–100	5.67
1403	114–225	38–68	4.22
1426	143–232	32–62	3.84
1452	155–180	30–42	3.52
1506	262–317	18–23	2.29

(b) Effusion vapor pressure data[c]

T, °K.	Total wt. loss, mg.	Area of effusion hole, cm.²	Time, min.	− log K[d]
1118	4.7	1.26×10^{-2}	90	20.7
1158	8.8	2.39×10^{-3}	60	15.8
1184	28.6	1.26×10^{-2}	105	17.8
1203	38.6	2.39×10^{-3}	60	13.2
1229	123.7	1.26×10^{-2}	80	14.7
1248	85.9	8.58×10^{-3}	60	13.7
1254	150.2	1.26×10^{-2}	90	15.0

[a] Measured at three flow rates: 340, 155 and 80 ml./min. [b] Calculated assuming zero flow rate and decomposition to the elements. [c] Eleven additional runs with the large orifice are shown in Fig. 5. [d] Calculated assuming decomposition to the elements and including corrections for difference in molecular weights of effusing species and the non-ideal knife edge of the effusion hole.

The high points observed in the flow measurements can be explained by assuming a small amount of oxygen in the flow gas which reacted with Mg(g) formed in vaporization and thus caused excessive vaporization of the sample and an apparently high equilibrium constant. Also, slight reaction of the sample with the porcelain boats may contribute to this deviation.

The effusion measurements scatter below the theoretical curve but approach it more closely in those studies in which small effusion holes were used. This behavior is characteristic of a molecule or atom with a low accommodation coefficient being present in the effusion cell. N_2(g) would appear likely to have a very low accommodation coefficient on Mg_3N_2(s). N_2(g) is an extremely stable molecule and practically no N(g) atoms would be formed at 1400° by thermal dissociation; yet, in Mg_3N_2(s), which crystallizes in an anti-Tl_2O_3 arrangement, N atoms are distributed one at a time through the lattice.

Thus, one concludes that Mg_3N_2(s) vaporizes by a complex mechanism which apparently involves Mg_2(g) in one of the early steps; at equilibrium, the vaporization products are Mg(g) and N_2(g).

Acknowledgments.—We wish to thank Mr. George Leroi who carried out most of the B_2O_3 vapor pressure runs in the platinum system. This research was in part conducted under contract No. AF 33(616)-338, with the United States Air Force, the sponsoring agency being the Aeronautical Research Laboratory of the Wright Air Development Center, Air Research and Development Command.

THE URANIUM–OXYGEN SYSTEM: $UO_{2.5}$ TO U_3O_8

BY H. R. HOEKSTRA, S. SIEGEL, L. H. FUCHS AND J. J. KATZ

Chemistry Division, Argonne National Laboratory, Lemont, Illinois

Received October 28, 1954

Investigations under way on the uranium-oxygen system in the composition range $UO_{2.5}$ to U_3O_8 indicate that U_2O_5 does not exist; $UO_{2.56}$ represents the lower limit of the monophasic region below U_3O_8. Composition limits of the orthorhombic $UO_{2.6}$ phase appear to be $UO_{2.56}$ to $UO_{2.65}$. Transition to the U_3O_8 phase occurs above the composition $UO_{2.65}$. Single crystals of the $UO_{2.6}$ phase and U_3O_8 have been prepared. A metastable (β) modification of U_3O_8 has been observed on oxidation of the $UO_{2.6}$ phase. High temperature X-ray studies have not as yet shown the existence of βU_3O_8 as a high temperature form of U_2O_5, but do show the formation of a hexagonal structure above 400°.

Oxide systems of metals which exhibit variable valency are often complicated by the occurrence of non-stoichiometric compounds and the existence of more or less extensive regions of solid solution. One of the more complex of such systems is that formed between oxygen and uranium. Three oxides of the element have been known for many years: UO_2, U_3O_8 and UO_3. In recent years UO, β-UO_2 ($UO_{2.25}$), U_2O_5 and U_6O_{17}, as well as at least three compounds in the region $UO_{2.3}$–$UO_{2.4}$ have been claimed, although the existence of some of these has not been definitely established. In addition UO_3 has been shown to exist in four crystalline modifications. Extensive regions of solid solution are encountered between UO_2 and UO_3.

One of the areas in which conflicting results are encountered is in the composition range $UO_{2.5}$ to U_3O_8. Tensimetric work by Biltz and Müller[1] on the thermal decomposition of uranium oxides indicated that $UO_{2.6}$ represents the lower limit of the one phase area extending from UO_3, since equilibrium oxygen pressures were found to be constant from that point to the composition $UO_{2.3}$. They found no evidence for the existence of a compound at U_2O_5. The results obtained by Rundle, *et al.*,[2] however, seemed to show conclusively that U_2O_5 does exist, and that its structure is closely related to that of U_3O_8, but with a larger unit cell. Ignited mixtures of UO_2 and U_3O_8 having the empirical composition $UO_{2.52}$ or above showed no trace of the fluorite uranium dioxide phase on X-ray films. This work was carried out with small quantities of the oxides (in X-ray capillaries) and there may have been some doubt as to the exact composition of the ignited mixture. Grønvold and Haraldsen[3] re-

(1) W. Biltz and H. Müller, *Z. anorg. allgem. Chem.*, **163**, 257 (1927).

(2) R. E. Rundle, N. C. Baenziger, A. S. Wilson and R. A. McDonald, *J. Am. Chem. Soc.*, **70**, 99 (1948).

(3) F. Grønvold and H. Haraldsen, *Nature*, **162**, 69 (1948).

ported the lower limit of the monophasic region at $UO_{2.56}$, while Alberman and Anderson,[4] as well as Hering and Perio,[5] confirmed Rundle's result. More recently Milne[6] reported that his single crystal studies on U_3O_8 showed that its structure was hexagonal rather than orthorhombic as Zachariasen[7] and Grønvold[8] had found (see also Brooker and Nuffield[9]). The value of Milne's work is somewhat in doubt since no complete chemical analysis was reported, and the source of the U_3O_8 crystals was unknown.

This paper is a preliminary report in our investigation of the phase relationships of the uranium–oxygen system between $UO_{2.5}$ and U_3O_8.

Experimental

Determination of Oxygen–Uranium Ratio.—As indicated by the previous discussion, an accurate determination of the oxygen–uranium ratio of the compounds under investigation is required. The composition of the compounds prepared in our work has been determined by two methods. The first involves decomposition of the oxide with bromine trifluoride, *i.e.*

$$UO_2 + 2BrF_3 \longrightarrow UF_6 + Br_2 + O_2$$

The apparatus and procedure involved have been described in detail elsewhere.[10] Results of several hundred runs on uranium oxides, as well as a number of other metal oxides, have shown that the composition may be determined to the nearest 0.01 atom of oxygen.

The composition of uranium oxides may also be determined accurately by oxidation to U_3O_8 at 750°. Repeated observations indicate that the product formed when a lower oxide is heated to this temperature in air or in oxygen at a pressure of 150 mm. or above is exactly U_3O_8. At lower oxygen pressures the composition will be slightly low in oxygen depending on the previous history of the sample and the oxygen pressure utilized. A reaction system similar to that described for work on the thermal stability of alkaline earth diuranates[11] will permit determination of composition to better than the nearest 0.01 atom of oxygen.

The $UO_{2.6}$ Phase.—As was shown above, previous investigations had indicated that a monophasic region extended $UO_{2.5}$ and $UO_{2.6}$. The structure at the composition below U_3O_8 to somewhere between the composition range $UO_{2.5}$ was found to be related to the U_3O_8 structure, but the point at which the change from one to the other took place was unknown. Clarification of these items was undertaken by heating mixtures of UO_2 and U_3O_8 at approximately 0.02 oxygen atom intervals between $UO_{2.5}$ and $UO_{2.65}$ to 1200° for several weeks in evacuated quartz tubes. The samples were weighed into platinum cups which slipped into the quartz tubes thus preventing the possibility of contamination of the sample by contact with the quartz tube. Samples having the composition $UO_{2.55}$ (as confirmed by subsequent analysis) showed traces of the fluorite phase, while $UO_{2.57}$ did not, thus placing the lower limit of the monophasic region at $UO_{2.56}$ in agreement with Grønvold's results. It must be remembered that these are X-ray observations at room temperature—the phase may extend to lower compositions at 1200° with the apparent limit of solubility depending upon the sample cooling rate. Only high temperature X-ray work can give a definite answer to this question.

The upper limit of the $UO_{2.6}$ phase was determined by heating U_3O_8 in the evacuated tensimetric apparatus. Quenching of the oxide from 1000° to room temperature gave oxide compositions ranging down to $UO_{2.64}$. X-Ray films of these samples showed the upper limit of the $UO_{2.6}$ phase to be at $UO_{2.65}$. Above this composition X-ray patterns show line shifts and intensity changes in the maxima suggesting that this represents the transitional region to U_3O_8. Although there is an indication that the cell size of the $UO_{2.6}$ phase increases with increasing oxygen content from $UO_{2.56}$ to $UO_{2.65}$, the errors of measurement are sufficiently high to preclude a quantitative measurement. A comparison of calculated lattice dimensions by several observers is given in Table I for U_3O_8 and the $UO_{2.6}$ phase (Rundle's U_2O_5). Good agreement is obtained in all instances except for Milne's U_3O_8 (recalculated for orthorhombic symmetry) thus strengthening the belief that his sample was not pure U_3O_8.

TABLE I

LATTICE DIMENSIONS

	a, kX.	b, kX.	c, kX.	X-Ray density, g./cc.
U_3O_8: 2 molecules per unit cell.				
Zachariasen	6.70	11.94	4.14	8.39
Grønvold	6.703	11.91[a]	4.136	8.40
Hering and Perio	6.708	11.94[a]	4.141	8.39
Milne[b]	6.69	11.79	4.14	8.51
This work	6.704	11.95	4.142	8.39
$UO_{2.6}$ phase: 32 uranium atoms per unit cell.				
Rundle	6.72	31.65	8.26	8.35
This work	6.738	31.70	8.269	8.38

[a] Reported as pseudo-cell, 1/3 of true cell. [b] Converted from hexagonal to orthorhombic symmetry.

Preparation of Single Crystals of U_3O_8.—Single crystals of uranium oxide having the composition $UO_{2.64}$ were prepared by heating U_3O_8 in air at 1100–1500°. At the higher temperature some volatilization occurred with condensation at the cooler portion of the tube (~1100°). Material suitable for single crystal studies was obtained in several hours at the higher temperatures, while several weeks of heating was required at 1100–1200°. The crystals were sometimes obtained as needle-shaped laths, and sometimes as hexagonal blocks. A serious barrier to the study of these crystals was the fact that they were invariably twinned. Single crystals of U_3O_8 were obtained from $UO_{2.64}$ by heating the $UO_{2.64}$ in oxygen to 750°. In performing this oxidation it was observed that the structure of the U_3O_8 as given by powder photographs was not always identical with the conventional orthorhombic pattern. The structure of the new U_3O_8, as tentatively indexed, has orthorhombic symmetry with the lattice constants a = 7.04 kX., b = 11.40 kX., and c = 8.27 kX. This leads to 4 molecules in the unit cell and an X-ray density of 8.38 g./cc. Work is continuing in order to assure that the symmetry has been assigned correctly and to locate the uranium positions. The new form of U_3O_8 (β) was converted to the conventional (or α) structure by repeating the temperature cycle (to 750°).

High Temperature X-Ray Studies.—With the knowledge that the β-form of U_3O_8 and the $UO_{2.6}$ phase could be produced by suitable quenching from elevated temperatures, experiments were started to determine the phase transformation temperature (α to β) and the decomposition temperature (β to $UO_{2.6}$) by means of high temperature X-ray studies. For purposes of technique it was desirable to confine the U_3O_8 in a closed and evacuated capillary. However, since it was known that α-U_3O_8 loses oxygen below 750° under these conditions, a second set of data was obtained using an open-ended capillary, thus permitting the sample to equilibrate with atmospheric oxygen.

Upon heating the α-U_3O_8 to 975° in either an open or a closed capillary, the β-U_3O_8 form was not observed and the decomposition to $UO_{2.64}$ was never detected. Apparently, the β-U_3O_8 must appear near the decomposition temperature of U_3O_8 (approximately 1150°) which is beyond the heating range of the X-ray camera. However, some surprising pattern changes were observed in the high temperature runs, and these indicate that the uranium–oxygen phase diagram in the region U_3O_8 is quite complicated. We are currently studying the patterns, and, although the results are very incomplete, we wish to indicate some of these findings at present.

(4) K. B. Alberman and J. S. Anderson, *J. Chem. Soc. Suppl.*, **2**, 303 (1949).

(5) H. Hering and P. Perio, *Bul. soc. chim. France*, 351 (1952).

(6) I. H. Milne, *Am. Mineral.*, **36**, 415 (1951).

(7) W. H. Zachariasen, Manhattan Project Report, CP1249.

(8) F. Grønvold, *Nature*, **162**, 70 (1948).

(9) E. J. Brooker and E. W. Nuffield, *Am. Mineral.*, **37**, 363 (1952).

(10) H. R. Hoekstra and J. J. Katz, *Anal. Chem.*, **25**, 1608 (1953).

(11) H. R. Hoekstra and J. J. Katz, *J. Am. Chem. Soc.*, **74**, 1683 (1952).

In the temperature range 25 to 365°, the a-axis increases in value and the b- and c-axes decrease in value with increasing temperature as indicated by Fig. 1. If the ratio a/b for U_3O_8 is plotted as a function of temperature, this ratio increases, so that at 365° the value is very near 0.577. For hexagonal symmetry, $a/b = \sqrt{3}/3$; hence the U_3O_8 is approaching hexagonal or pseudo-hexagonal symmetry. From 445° up to approximately 600°, there is a noticeable sharpening of the diffraction pattern, especially at large angles. Furthermore, the a value has now dropped slightly, and increases slowly with temperature. The c value has not changed, but it too increases with temperature. Thus, there is every indication that a phase transformation has taken place. This new phase can be indexed on a hexagonal basis with $a = 6.801 \pm 0.001$ kX., $c = 4.128 \pm 0.001$ kX. The cell contains one molecule and the calculated X-ray density is 8.41 g./cm.^{3}.

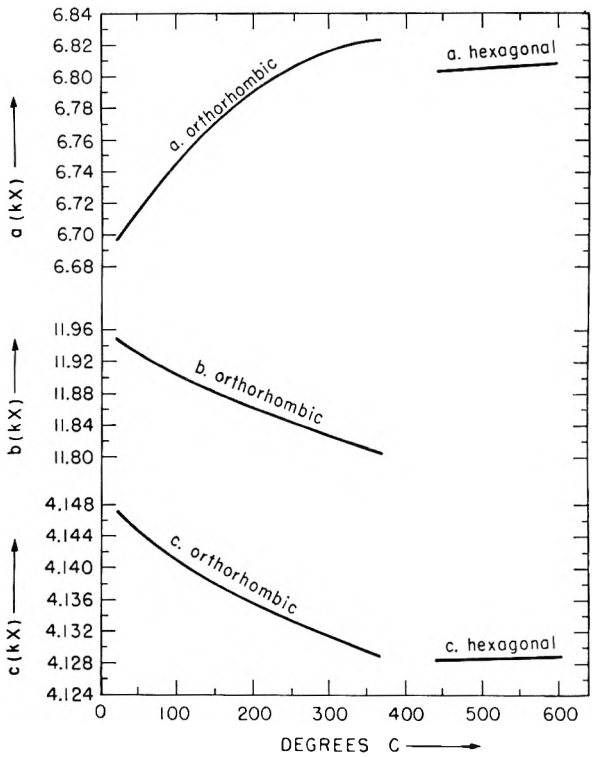

Fig. 1.—Variation of U_3O_8 unit cell parameters with temperature.

The main features of the X-ray diffraction pattern of this phase can be accounted for by replacing the uranium atoms at

0	0	0
1/3	2/3	0
2/3	1/3	0

The relationship of the hexagonal U_3O_8 to the conventional U_3O_8, and the α-UO_3 structures may be shown by reference to Fig. 2.

The structure of α-UO_3 has been reported by Zachariasen.[12] The α-UO_3 is given by the small hexagonal cell. An extended array of these cells produces the distribution of uranium atoms (black circles) and the oxygen atoms (large open circles) as shown. For α-UO_3 the atomic positions are

1 U at 0 0 0
1_I O at 0 0 1/2
2_{II} O at $1/3\ 2/3\ z$, $2/3\ 1/3\ \bar{z}$ with $z = 0.17$

(12) W. H. Zachariasen, *Acta Cryst.*, **1**, 268 (1948).

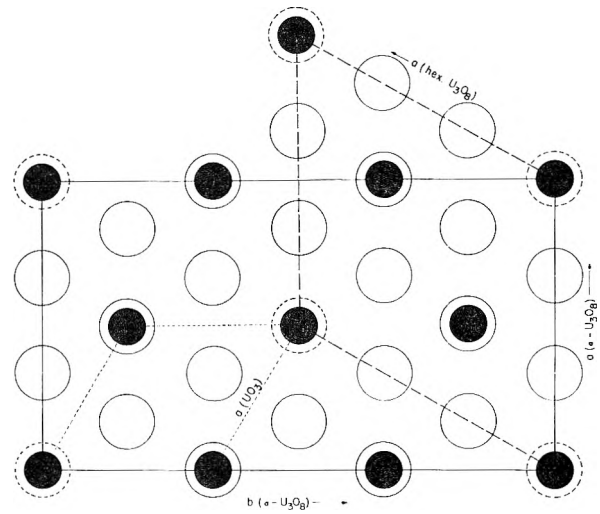

Fig. 2.—Structural relationship, α-UO_3, orthorhombic U_3O_8, and hexagonal U_3O_8.

Zachariasen considers that the U_3O_8 structure can be derived from α-UO_3 by referring the UO_3 to orthohexagonal axes and choosing an axis three times longer than required.[13] He suggests that the oxygen positions in the two structures must be similar except that there are no oxygens at 0 0 1/2 and 1/2 1/2 1/2 in U_3O_8. These atoms indicated by open dashed circles represent oxygens which must therefore be removed from UO_3 to derive the U_3O_8 structure.

The transfer from α-U_3O_8 to hexagonal U_3O_8, the large hexagonal cell, involves only slight shifts in the uranium positions. If one places oxygen atoms in the structure by analogy with α-UO_3, these positions are

$$1/3\ 0\ z;\ 0\ 1/3\ z;\ 1/3\ 1/3\ \bar{z};\ 1/3\ 2/3\ 1/2$$
$$2/3\ 0\ \bar{z};\ 0\ 2/3\ \bar{z};\ 2/3\ 2/3\ z;\ 2/3\ 1/3\ 1/2$$

With $z = 0$, the agreement between observed and calculated intensities becomes very reasonable. However, a few weak lines are observed for which the uranium contribution is zero, and these cannot be accounted for by the oxygen contributions alone. Furthermore, for the 6-fold coördination of the oxygen atoms around the uraniums, the observed U–O distance of 2.27 Å. is small. Hence, it is possible that the cell has been chosen incorrectly or that the structure remained orthorhombic and the transition which has occurred corresponds to an ordering (or disordering) process. The latter suggestion is reasonable in the light of the observation that oxygen can be driven off continuously by heat. We are now studying these possibilities.

If a freshly prepared sample is pre-heated to 675°, a room temperature photograph reveals the typical α-U_3O_8 pattern, with the exception that a few lines, normally weak, or not present, become very pronounced in intensity. In a high temperature run, there may be a transition near 375°, but the above lines of pronounced intensity persist and the pattern cannot be indexed on a hexagonal basis. Above this temperature, up to 975°, the patterns become very complex and have not been studied in any detail. Hence it appears that a transition may occur at approximately 400°, but the transition temperature and nature of the transformation may depend on the preheat history of the sample. The β-phase was not observed.

In an open capillary, the results are different. No measurements have been made, but it appears that a minor transformation has occurred at about 300°. Again the β-phase was not observed.

Acknowledgment.—We wish to acknowledge the aid of Miss Lila Wiersema who prepared many of the X-ray photographs and assisted in the calculations.

(13) W. H. Zachariasen, Manhattan Project Report, CK-2667.

THE THERMAL DECOMPOSITION OF SODIUM CARBONATE BY THE EFFUSION METHOD[1]

BY KETIL MOTZFELDT

Institute of Silicate Science, Norwegian Institute of Technology, Trondheim, Norway

Received December 16, 1954

A formal treatment of the effusion method, including cases with low accommodation coefficient is presented. The thermal decomposition of sodium carbonate has been investigated by the effusion method. The decomposition becomes appreciable only above the melting point of the carbonate. Starting with pure carbonate, the oxide formed by the evolution of carbon dioxide will be present in solution in the melt, hence the process is not monovariant. As the oxide concentration in the melt builds up, the evaporation of sodium oxide (as sodium gas and oxygen) becomes increasingly important, and finally a steady state is reached. The oxide concentration in the melt at steady state is of the order of magnitude of 1%. The formal treatment of this type of process is presented. The accommodation (evaporation) coefficient of carbon dioxide on the melt appears to be rather low, with the consequence that both observed pressure and composition of the melt at steady state depend on the size of the effusion orifice. A discussion of these factors is included.

Part One. On the Effusion Method

The effusion method, usually named after Knudsen,[2] has become one of the classical methods for measuring low vapor pressures. Due to the simplicity of the method, it is particularly suited for the study of high-temperature phenomena. There are, however, certain problems connected with this method which deserve attention.

Consider an effusion cell such as outlined in Fig. 1. Assume that we observe the weight of gas that leaves the cell per unit time. (The use of a cooled target or other types of molecular beam detectors will not be considered here.) In order to interpret the weight loss in terms of the equilibrium vapor pressure of the evaporating substance, the following factors have to be considered: (1) the possible resistance to evaporation represented by a low accommodation (or evaporation) coefficient α for the evaporating surface; (2) the resistance exerted on the effusing gases by the main body of the cell, expressed in terms of the cross-section area A and the Clausing probability factor[3] W_A for this cell; (3) the resistance represented by the hole with area B and Clausing factor W_B.

The well-known effusion equation may be written

$$P_m = \frac{q}{W_B B t}\sqrt{\frac{2\pi RT}{M}} = \frac{3.760 \times 10^{-4} q}{W_B B t}\sqrt{\frac{T}{M}} \quad (1)$$

where (for the right-hand expression) P_m is pressure in atm., q is mass of effused gas in grams, t the corresponding time in minutes, B area of the orifice in cm.^{2}, T absolute temperature and M the molecular weight of the effusing species. With the Clausing factor W_B omitted, this expression is strictly valid only for an "ideal" hole, *i.e.*, a hole in a sheet of infinitely small thickness. Any real hole will have the character of a short canal. Clausings calculations (ref. 3) are concerned with cylindrical canals. The quantity W is the fraction of the gas molecules entering the canal which really comes through. Clearly, then, $(1 - W)$ is the fraction of the entering amount which is reflected back again by the walls of the canal.

In practice, the ideal hole has often been approximated by a "knife edge hole," *i.e.*, a canal that widens rapidly outward. Unfortunately, no calculation exists for this shape, and we will therefore be concerned only with the straight cylindrical hole in the present treatment. It should be noted, however, that the treatment in the following is equally applicable to any type orifice, provided its factor W_B is known. It is the product of area and Clausing factor which is of importance, rather than the two quantities separately. The product $W_B B$ may be termed the effective orifice area and enters also into the ratio between orifice area and evaporating surface area, *viz.*, $f = W_B B/A$.

Whitman[4] was the first to take into account the influence of the main cell body. Through a procedure involving infinite series he obtained a solution which, however, was left in a shape rather cumbersome for practical use. It will be shown that a solution for the general case can be obtained in a simpler way by employing the conditions for steady state in the cell.

In the cell Fig. 1 we will consider the pressure in plane 1 close above the evaporating surface and in plane 2 close below the lid of the cell. At steady state and with no hole, the pressure will be evenly distributed throughout the cell. With a finite hole size, this will no longer be the case. The upward pressure u will be different from the downward pressure d for each plane, and the pressures will be different in the different planes. But the pressures will be related through the following equations (for explanation, see below)

$$\alpha P_{eq} = \alpha d_1 + f u_2 \quad (I)$$

$$u_1 = \alpha P_{eq} + (1 - \alpha) d_1 \quad (II)$$

$$d_2 = (1 - f) u_2 \quad (III)$$

$$u_2 = W_A u_1 + (1 - W_A) d_2 \quad (IV)$$

Equation I expresses that the rate of evaporation, which is proportional to[5] $\alpha P_{equilibrium}$, must be equal to the rate of recondensation plus the rate of escape through the hole. Equation II expresses that the upward pressure u_1 above the surface is made up of the evaporation from this surface plus the rebouncing of molecules coming from above. Equation III expresses that the downward pres-

(1) Work done at the Department of Chemistry and Chemical Engineering, University of California, Berkeley, Calif.

(2) M. Knudsen, *Ann. Phys.*, **28**, 75 (1909); *ibid.*, **28**, 999 (1909); *ibid.*, **29**, 179 (1909); see also R. G. J. Fraser, "Molecular Rays," Cambridge University Press, 1931.

(3) P. Clausing, *Ann. Phys.*, **12**, 961 (1932); see also S. Dushman, "Scientific Foundations of Vacuum Technique," John Wiley and Sons, New York, N. Y., 1949, p. 96.

(4) C. I. Whitman, *J. Chem. Phys.*, **20**, 161 (1952).

(5) I. Langmuir, *Phys. Rev.*, **2**, 329 (1913).

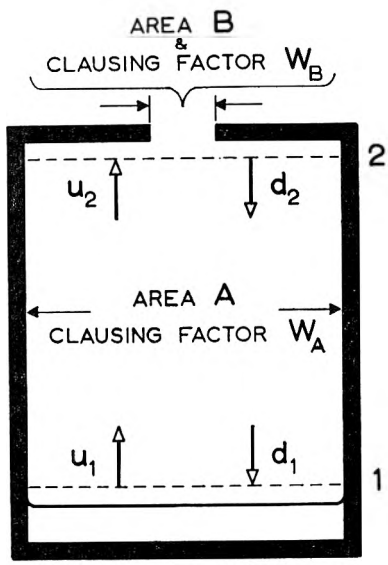

Fig. 1.—Diagram of effusion cell.

sure closely below the lid is due to reflection of the upward molecules minus the fraction that escapes through the hole. Equation IV is possibly the least obvious of the four, expressing that the upward pressure u_2 at the top of the cell is due to the fraction W_A of the molecules that are heading upward from the bottom of the cell, plus the fraction $(1 - W_A)$ of the molecules heading downward from the top of the cell, because this fraction is reflected upwards again by the walls of the cell.

The pressure u_2 is equal to the pressure P_m of eq. 1 and hence may be considered as known. There are then as many equations as unknowns (u_1, d_1, d_2 and P_{eq}). The solution is

$$P_{eq} = \left[1 + f\left(\frac{1}{\alpha} + \frac{1}{W_A} - 2\right)\right] P_m \qquad (2)$$

The derivation of this expression rests on some assumptions which are not rigidly valid. For one thing, the pressures were considered as uniform across any one of the horizontal planes, notably for plane 2 this cannot be strictly true. Also, the calculations by Clausing presuppose a truly random scattering of the molecules at the walls, which may not always be the case. A discussion of these factors has been given by Whitman (ref. 4, p. 162). It may only be suggested here that the inaccuracies are too small to impair the general validity of eq. 2.

Several limiting cases may be considered. $f \to 0$ gives $P_{eq} \to P_m$ which is the correct Knudsen equation for sufficiently small hole sizes irrespective of α. $f = W_A = W_B = 1$ gives $P_{eq} = P_m/\alpha$ which is the equation for evaporation from a free surface (Langmuir experiment). $\alpha = 1$ gives $P_{eq} = [1 + f((1/W_A) - 1)]P_m$. This looks quite different from the expression given by Whitman for this case, but a bit of rearrangement will show that the two expressions are identical. (Note that Whitman's ratio $f = B/A$, *i.e.*, the W_B appears separately. Also, in his notation, A is the area of the *orifice* with factor W_B.) It can also be shown that the combination of equations 5, 8 and 9 in Whitman's paper (after correcting for an obvious misprint in equation 8) ultimately yields our equation 2.[5a]

Rearrangement of eq. 2 suggests a graphical method for getting at both P_{eq} and α

$$P_m = P_{eq} - \left(\frac{1}{\alpha} + \frac{1}{W_A} - 2\right) P_m f \qquad (2a)$$

By plotting P_m *versus* $P_m f$ for constant temperature and varying ratio f (*i.e.*, different hole sizes), a straight line should result, with slope $-(1/\alpha + 1/W_A - 2)$ and with intercept for $f = 0$ equal to P_{eq}.

For a cell of about equal diameter and height (*i.e.*, rather normal shape), W_A is about 0.5, so that $1/W_A$ and 2 will tend to cancel. This represents a justification for the use of the simpler equation given by Speiser and Johnston.[5b] Particularly for small values of α, then, the expression for the slope may be simplified to $-1/\alpha$.

A problem of a more practical nature is connected with keeping the effusion cell at a uniform temperature, and with measuring this temperature. The requirement of open space for the effusing gas above the cell may lead to a lid temperature considerably lower than the temperature of the charge, unless special provisions are made to counteract this effect. Radiation shields above the lid may, on the other hand, seriously obstruct the free passage of the gas. Various experimental solutions to this problem may be thought of. The simple arrangement chosen for the carbonate work consisted essentially of a resistance wound furnace with both diameter and length rather large compared to the dimensions of the cell (Fig. 2). The resistance wire[6] was more closely spaced toward the ends of the furnace than in the middle, to compensate for the extra heat loss at the ends. Furthermore, the middle section (as well as the lower) was shunted with variable resistance. A thermocouple sliding through a Wilson seal[7] was used to scan the temperature along the furnace, and the input to the various sections of the furnace was adjusted to give optimum conditions as shown by this thermocouple. For illustration, power input per cm. furnace length and the corresponding temperature distribution are given in Fig. 3 for a typical run. It should be noted that the scanning thermocouple, strictly speaking, gives information only about the temperature on its own hot junction, not on the effusion cell. With this in mind, the temperature distribution was made slightly saddle-shaped and slightly top heavy (Fig. 3).

(5a) NOTE ADDED IN PROOF.—Recently, M. G. Rossman and J. Yarwood (*Brit. J. Appl. Phys.*, **5**, 7 (1954)) have presented a rather elaborate mathematical treatment for the case of a straight cylindrical crucible without lid, and accommodation coefficient $\alpha < 1$, their derivation being independent of Clausing's work.[3] A numerical comparison of Rossman and Yarwood's expression with our equation 2 applied to the same case will show that the difference is negligible for very low crucibles. For crucibles of greater height, Rossman and Yarwood's expression becomes increasingly inexact due to certain approximations inherent in their derivation. The same authors state that by heating a liquid in a vacuum, bubble formation will be significant at vapor pressures of 10^{-4} mm. or greater. Their reasoning does not, however, take into account the surface tension of the liquid (even though the authors mention this property in a less significant connection). By a reasoning similar to the authors' own but with the surface tension taken into account it can be shown that a bubble cannot be stable in any molten material unless the vapor pressure is of the order of magnitude 1 mm. or higher. The supersaturation required for the nucleation of the bubble will increase this figure. It can thus be concluded that bubble formation is highly improbable in any effusion experiment. The earlier letter by Rossman and Yarwood (*J. Chem. Phys.*, **21**, 1406 (1953)) on the Knudsen effusion method has been amply commented by C. I. Whitman (*ibid.*, **21**, 1407 (1953)).

(5b) R. Speiser and H. L. Johnston, *Trans. Am. Soc. Metals*, **42**, 283 (1950), equation X.

(6) Kanthal A, obtained from the Kanthal Corporation, Amelia Place, Stamford, Connecticut.

(7) See, *e.g.*, W. E. Bush, in "N.N.E.S. Div. I," Vol. 1, A. Guthrie and R. K. Wakerling, Eds., McGraw-Hill Book Co., New York, N. Y., 1949, p. 166.

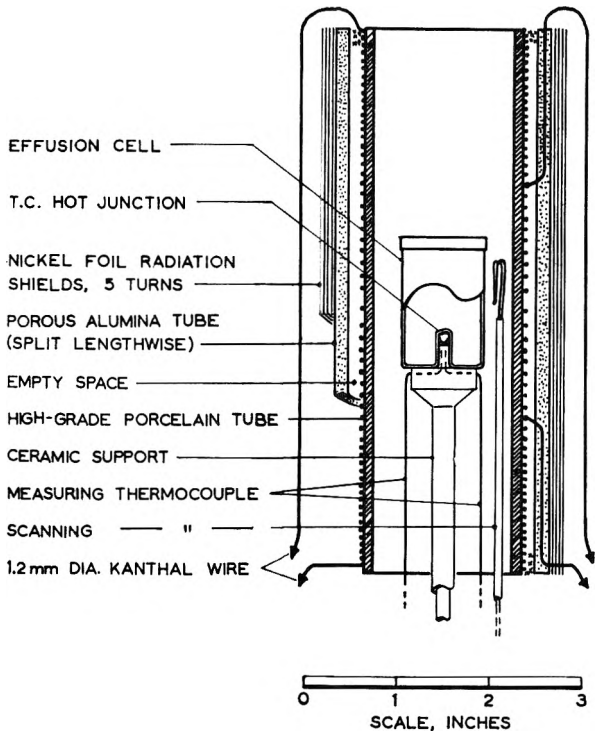

Fig. 2.—Furnace and cell for weight-loss effusion experiments.

An effusion cell is quite well suited for the use of an optical pyrometer. But in the range where a thermocouple can be used, this must be considered more accurate, provided it is brought to indicate the true temperature of the cell. To make the temperature of the hot junction equal to that of the object in question requires considerably more care in a vacuum than at atmospheric pressure. Consequently, the platinum effusion cell was provided with a thermocouple well protruding from the bottom, into which the enlarged hot junction of the measuring thermocouple fitted snugly. Still it was found that distinct halts at the melting point of sodium sulfate (which was used as a standard substance) were obtained only when the cell was resting solidly on the hot junction bead, rather than on the support platform. A check by means of the simple laws of radiation and heat conduction shows that metal-to-metal contact is imperative to the successful application of thermocouples in a vacuum.

Part Two. On Sodium Carbonate Decomposition

I. Introduction.—The thermal decomposition of sodium carbonate has been dealt with in a number of publications, the first of these dating at least a hundred years back. The most recent study appears to be given by Howarth and Turner.[8] They have essentially treated the process as corresponding to the thermal decomposition of the Group II carbonates. For the general process

$$M_{(2)}CO_3 = M_{(2)}O + CO_2(g)$$

the Group II carbonates and oxides will be solid (and with negligible solid solubility) up to the temperature for $P_{CO_2} = 1$ atm. Thus to each temperature corresponds a definite carbon dioxide pressure. For the alkali carbonates, however, the melting occurs before any appreciable dissociation, and the oxide which is formed will be present in the melt at a concentration which in the beginning increases as the dissociation proceeds. In view of this, it is quite puzzling that Howarth and Turner found

(8) J. T. Howarth and W. E. S. Turner, *Glastechn. Ber.*, **9**, 218 (1931).

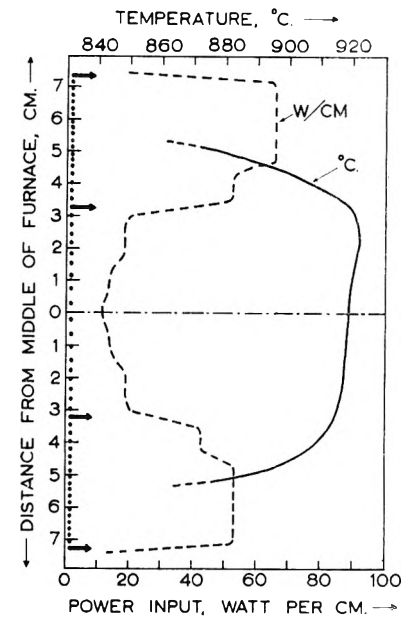

Fig. 3.—Power input per cm. furnace length (as calculated from the current, resistance and spacing for each winding) and temperature distribution (as measured with the scanning thermocouple) *versus* position in the furnace (data from run N3-a).

good reproducibility of the carbon dioxide pressure as a function of temperature only. It is, however, hard to tell exactly what the over-all process has been in their experiments, so that the quantitative interpretation of their data appears to be impossible.

Earlier investigations[9,10] led to values still higher than those of Howarth and Turner. It is also interesting to note that, more recently, a couple of physicists[11] have been working with alkali carbonates evaporated in a vacuum, apparently with the assumption that the carbonates evaporate as molecules.

In connection with the use of sodium carbonate as a primary standard in acid–base titrations, quite divergent results have been reported as to the maximum allowable temperature for drying the carbonate. According to Kolthoff[12] "the controversy still continues." As will appear from the present discussion, there should be no chance for significant dissociation at any temperatures below some 800° at least. The discrepant results may, however, partly find their explanation by assuming reaction with the moisture of the air (or the water content of the sodium bicarbonate, which is the usual starting material) to form sodium hydroxide and carbon dioxide. The equilibrium constant for this reaction is greater than the constant for the dry dissociation by a factor of about 10^4 at 900° and about 10^8 at 500°.

The interest of the present author in this matter stems primarily from the use of sodium carbonate in connection with electrometric measurements by means of an oxygen electrode.[13] The use of concentration cells with molten

(9) P. Lebeau, *Compt. rend.*, **137**, 1255 (1903).

(10) J. Johnston, *Z. physik. Chem.*, **62**, 330 (1908).

(11) R. Suhrmann and W. Berger, *Z. Physik*, **123**, 73 (1944).

(12) I. M. Kolthoff and V. A. Stenger, "Volumetric Analysis," Vol. II, Interscience Publishers, Inc., New York, N. Y., 1947, p. 80.

(13) H. Flood, T. Förland and K. Motzfeldt, *Acta Chem. Scand.*, **6**, 257 (1952).

electrolytes and different anion systems in the two half-cells seems to have potentialities, due to the fact that the transference number of the anion in melts of oxygen acids has been found close to zero in the cases hitherto studied.

II. Thermodynamic Calculations.—High-temperature data for sodium carbonate are not available. Heat capacity was estimated according to Kopp's rule as follows: for the solid 34 ± 4 (average for 298–1127°K.), for the liquid 41 ± 4 cal./degree. The heat of melting was taken as 7 ± 1 kcal.[14] It should be noted that three solid state transitions have been reported for sodium carbonate,[15] but the heats of transition are not known and hence have not been taken into account in the present calculations. Room temperature data for sodium carbonate, and data for sodium oxide, carbon dioxide, sodium gas and oxygen are available in the literature.[16–20]

For the reaction

$$Na_2CO_3(l) = Na_2O(l) + CO_2(g) \qquad (R1)$$

the calculated equilibrium constant is

$$\log K_1 = 6.4 - \frac{16{,}600}{T} \pm 1.2 \text{ (around 1200°K.)}$$

(The result is expressed directly in terms of the equilibrium constant instead of the more customary thermodynamic functions because the equilibrium constant enters into the succeeding calculations.)

The calculations by Brewer and Mastick[21] made it likely that all the alkali oxides except possibly Li_2O volatilize to the elements rather than to any gaseous molecules. For sodium oxide, this has been experimentally verified by Brewer and Margrave[22] by effusion experiments. For the reaction

$$Na_2O(l) = 2Na(g) + \frac{1}{2}O_2(g) \qquad (R2)$$

one calculates the equilibrium constant

$$\log K_2 = 14.7 - \frac{20{,}900}{T} \pm 0.5 \quad \text{(around 1200°K.)}$$

The calculated values check with the experiments[22] within the experimental accuracy.

III. Expected Behavior of Sodium Carbonate in an Effusion Experiment.—Assume that a steady state is reached, with mole fraction of sodium oxide in the melt, $N_{Na_2O} = b$. The evaporation process can then be written

$$(1-b)Na_2CO_3 + bNa_2O = 2Na + (1-b)CO_2 + \frac{1}{2}O_2 \qquad (R3)$$

This equation gives the relation between the losses in moles

$$n_{Na} = 4n_{O_2} = \frac{2}{1-b}n_{CO_2}$$

By introducing the molecular weights M for the different species, we get the total weight loss

$$q = q_{Na} + q_{O_2} + q_{CO_2} = q_{Na}\left[1 + \frac{M_{O_2}}{4M_{Na}} + \frac{(1-b)M_{CO_2}}{2M_{Na}}\right]$$

By introducing numerical values for the molecular weights, this gives

$$q_{Na} = \frac{q}{2.31 - 0.96b}$$

Similarly one can solve for q_{O_2} and q_{CO_2} in terms of the observable quantities q and b.

The three gas species are assumed to effuse independently. For the time being, we will also assume that the ratio f is small enough, or the accommodation coefficients large enough, so that we do not have to take these factors into account. Equation 1 will then be valid for each of the species This gives for the three partial pressures

$$P_{CO_2} = \frac{5.67(1-b)Q}{2.41 - b} \qquad (3)$$

$$P_{O_2} = \frac{6.65Q}{6.63 - 2.75b} \qquad (4)$$

$$P_{Na} = \frac{7.84Q}{2.31 - 0.96b} \qquad (5)$$

where

$$Q = \frac{q\sqrt{T}}{W_B B t} \times 10^{-5}$$

In order to estimate $b = N_{Na_2O}$ we will assume that $b << 1$, *i.e.*, $N_{Na_2CO_3} \cong 1$. We will furthermore assume ideal behavior of the molten mixture sodium carbonate–sodium oxide. This assumption is rather plausible in view of the information regarding molten salts which has been accumulating in recent years. The equilibrium constants for the two reactions (R1) and (R2), written in terms of mole fractions, together with equations 3–5, constitute five equations with five unknowns, *viz.*, N_{Na_2O}, P_{CO_2}, P_{O_2}, P_{Na} and Q. By elimination one finds

$$N_{Na_2O} = 1.09\left[\frac{K_1^6}{K_2^2}\right]^{1/7}$$

By introduction of the calculated values of the equilibrium constants, this gives

$$\log N_{Na_2O} = 0.41 - \frac{3310}{T}$$

i.e., at *e.g.*, 1200°K.: $N_{Na_2O} \cong 0.45\%$. It is thus seen that the concentration of oxide in the melt at steady state will be rather small, as we assumed.

We may put the expression for N_{Na_2O} thus obtained back into the expression for K_1 and solve for P_{CO_2}, this gives

$$\log P_{CO_2} = 6.0 - \frac{13{,}300}{T} \pm 1.2$$

i.e., at *e.g.*, 1200°K.: $P_{CO_2} \cong 10^{-5}$ atm.

Only sodium carbonate will be dealt with in this paper. It may be mentioned in passing that the stability of the carbonate increases with increasing size of the cation (due to the lessened polarizing effect of the larger cation on the oxygen ion of the

(14) K. K. Kelley, U. S. Bur. of Mines Bull. 393, Washington, 1936.
(15) S. Z. Makarov and M. P. Shul'gina, *Bull. Acad. Sci. U. R. S. S. Classe Sci. Chim.*, 691 (1940); *C. A.*, **35**, 3154 (1941).
(16) F. D. Rossini, *et al.*, "Selected Values of Chemical Thermodynamic Properties," National Bureau of Standards, Washington, 1952.
(17) Fumihiko Saegusa, *Science Rept. Tohoku Univ., First Ser.*, **34**, 104 (1950); *C. A.*, **46**, 811 (1952).
(18) K. K. Kelley, U. S. Bur. of Mines Bull. 476, Washington 1949; Bull. 477, Washington 1950.
(19) L. Brewer, *Chem. Revs.*, **52**, 1 (1953).
(20) L. Brewer, paper 5 in "N.N.E.S. Div. IV," Vol. 19B, L. L. Quill, Ed., McGraw-Hill Book Co., New York, N. Y., 1950.
(21) L. Brewer and D. F. Mastick, *J. Am. Chem. Soc.*, **73**, 2045 (1951).
(22) L. Brewer and J. Margrave, *U. Cal. Rad. Lab. Report*, 1864 (1952).

$CO_3^=$ group) whereas the stability of the oxide decreases. Thus the oxide concentration at steady state will be highest for lithium carbonate and decrease down the group.

So far, this discussion has been concerned only with the conditions at steady state. This might suffice as a basis for the experimental work; by repeated heating and weighing of the cell one may assure that the weight loss per unit time has become constant and consequently a steady state has been reached. This procedure, however, appears rather tedious, and in course of the work interest arises in the behavior of the carbonate right from the start onwards. The carbon dioxide pressure will in the beginning be rather high, diminishing as the oxide concentration builds up toward the steady state. This results in an excess weight loss at start, the quantitative knowledge of which would permit the interpretation of observations from one single heating in terms of steady state values.

The basic effusion equation will be valid for each of the three species, but must be applied in a differential form. Arranged to give the weight loss explicitly, it can be written

$$\mathrm{d}q = C\sqrt{M}\,P\,\mathrm{d}t$$

where

$$C = \frac{2660 W_B B}{\sqrt{T}}$$

(*cf.* equation 1. It is assumed here that $P_m \leqq P_{eq} = P$.)

It will be noted that C is a constant for one particular run. It may also be anticipated that the resulting differential equations are difficult to solve analytically. The result of this discussion will therefore appear as a graphical integration of the equations for one given set of experimental conditions.

On the assumption that the sodium oxide dissolved in the melt will retain its stoichiometric composition at all times, we have a relationship which can be used to eliminate P_{O_2} right away

$$\mathrm{d}q_{O_2} = \frac{1}{4}\frac{M_{O_2}}{M_{Na}}\,\mathrm{d}q_{Na} = \frac{1}{4}\frac{M_{O_2}}{M_{Na}}\,C\sqrt{M_{Na}}P_{Na}\,\mathrm{d}t$$

Further relationships are furnished by the equilibrium constants[23]

$$K_1 = \frac{P_{CO_2} n_{Na_2O}}{n_{Na_2CO_3}}$$

$$K_2 = \frac{P^2_{Na}\sqrt{P_{O_2}}[n_{Na_2CO_3} + n_{Na_2O}]}{n_{Na_2O}}$$

From the first of these two expressions, P_{CO_2} can be substituted in the effusion equation for this species. By so doing, and simultaneously introducing weight w instead of number of moles, and introducing the numerical values for the molecular weights, one arrives at

$$\frac{\mathrm{d}q_{CO_2}}{\mathrm{d}t} = 3.88 C K_1 \frac{w_{Na_2CO_3}}{w_{Na_2O}} \qquad (6)$$

In the second of the two equilibrium constants, P_{O_2} can again be eliminated by the same relationship as before. This results in

$$K_2 = \frac{P^{5/2}_{Na}\left(\frac{M_{O_2}}{M_{Na}}\right)^{1/4}(n_{Na_2CO_3} + n_{Na_2O})}{2n_{Na_2O}}$$

Changing from moles n to weight w and introducing numerical values as before, plus rearranging, gives an expression for P_{Na}. This expression, when introduced into the equation for the weight loss of sodium oxide

$$\mathrm{d}q_{Na_2O} = \mathrm{d}q_{Na} + \mathrm{d}q_{O_2} = CM_{Na}\left(1 + \frac{1}{4}\frac{M_{O_2}}{M_{Na}}\right)P_{Na}\mathrm{d}t$$

finally gives the second differential equation

$$\frac{\mathrm{d}q_{Na_2O}}{\mathrm{d}t} = 10.23C\left[\frac{K_2}{\frac{w_{Na_2CO_3}}{w_{Na_2O}} + 1.71}\right]^{2/5} \qquad (7)$$

The last two equations express the material balances

$$w_{Na_2CO_3} = w^\circ_{Na_2CO_3} - \frac{M_{Na_2CO_3}}{M_{CO_2}}\,q_{CO_2} \qquad (8)$$

and

$$w_{Na_2O} = \frac{M_{Na_2O}}{M_{CO_2}}\,q_{CO_2} - q_{Na_2O} \qquad (9)$$

where w° represents the weight of the charge at time zero.

In graphical integration of the equations 6–9 one runs into the trouble that the carbon dioxide pressure is theoretically infinite at the very start. The trouble can be circumvented by noting that the behavior closely after the start will be similar to what one would get if sodium oxide were non-volatile. For this case, the equation for $\mathrm{d}q/\mathrm{d}t$ can be solved analytically. Denoting the number of moles of carbon dioxide effused with $\mathrm{d}z$, we have

$$\mathrm{d}z = \frac{C}{\sqrt{M_{CO_2}}}P_{CO_2}\,\mathrm{d}t$$

and

$$P_{CO_2} = K_1\frac{n_{Na_2CO_3}}{n_{Na_2O}}$$

as before. But the expressions for the number of moles in the melt are now very simple

$$n_{Na_2O} = z \quad \text{and} \quad n_{Na_2CO_3} = n^\circ_{Na_2CO_3} - z$$

This can be combined to

$$\mathrm{d}t = \frac{M_{CO_2}\,\mathrm{d}z}{CK_1(n^\circ_{Na_2CO_3} - z)}$$

This equation can be integrated, with $z = 0$ for $t = 0$ it gives

$$t = -\frac{\sqrt{M_{CO_2}}}{CK_1}\left[z + n^\circ \ln\left(1 - \frac{z}{n^\circ}\right)\right] \qquad (10)$$

For small values of z/n°, the logarithm can be approximated by expanding in series. The first power terms cancel; retaining only the second power term the equation can be made explicit in z. Simultaneously changing from moles to weight and introducing the numerical value of the molecular weight as before, one arrives at the expression for the weight loss of carbon dioxide shortly after start

$$q_{CO_2} = 2.35\sqrt{CK_1 w^\circ_{Na_2CO_3} t} \qquad (10a)$$

where everything on the right-hand side but t is constant for one particular run.

Next, the conditions from run N2 were chosen as a basis for a plot of the functions. Values from run N2: B = 0.0327 cm.², W_B = 0.890, T = 1276°K., which gives C = 2.16. The run started with w° = 15.20 g. and gave as result[24]: $K_1 = 6.16 \times 10^{-7}$, $K_2 = 1.00 \times 10^{-9}$. With these numerical values, equation (10a) gives the dashed curve in Fig. 4. The same numerical values were introduced into equations 6–9, and the value of q_{CO_2} after five minutes was taken from the dashed curve and used as starting point (with assumed $q_{Na_2O} = 0$ at this point) for the graphical integration which yielded the solid curves for q_{CO_2} and q_{Na_2O} and consequently for their sum, and also the curve for N_{Na_2O}. The small circles are the experimental points. The fact that the straight portion of the curve for q_{total} falls very well in line with these points is not surprising, because these experimental values formed the basis for the calculation of the curve. For the same reason, the calculated values for N_{Na_2O} converge toward the experimental value 1.49 mole % obtained by analysis after the end of run N2c. The main point of interest established by the plot is the magnitude of the "total excess weight loss" Δq. It should also be noted that the slope of the straight portion for q_{total} depends mainly on the product K_1K_2 which in turn is nearly independent of the analytical value for N_{Na_2O}, whereas the fact that the line for q_{total} not only goes parallel to, but through the experimental points, indicates that also the separate values for K_1 and K_2 as found by means of the analytical value for N_{Na_2O} must be largely correct (and that the charge at start consisted of pure stoichiometric Na_2CO_3).

The value of Δq is seen to be rather small, only about six tenths of the weight increase of the melt by carbon dioxide

(23) In the following, n is number of moles in the melt, w is number of grams in the melt, z is number of moles evaporated and q is, as before, weight evaporated.

(24) The results given here are not yet corrected for the influence of the accommodation coefficient of carbon dioxide, see later.

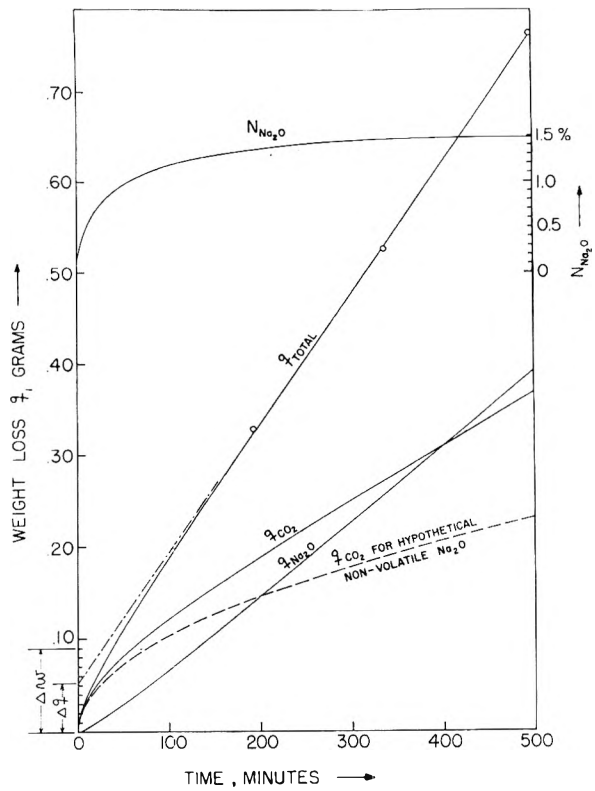

Fig. 4.—Weight loss of carbon dioxide and of sodium oxide, total weight loss, and mole fraction of sodium oxide, as functions of time, calculated from equations 6 to 9. Experimental values from run N2-a-b-c: T, 1276°K.; $W_B \times B = 0.0291$ cm.²; $w = 15.203$ g. (see text).

absorption after the end of the run, given as Δw in the figure. (This Δw is corrected upwards to what it would have been for the weight of the charge at start, a detail of more importance for some of the other runs.) It seems reasonable to assume, without going into further graphical solutions, that Δq and Δw will remain roughly proportional at different temperatures. Thus the correction $\Delta q = 0.6\Delta w$ has been used to evaluate the results of runs with only a single observation of the weight loss, as given in Table I. The accuracy of the correction suffices because the "excess weight loss" is only a small fraction of the observed weight loss in all of the runs.

IV. Flow Methods and Analytical

When hunting for the equilibrium constant for a reaction such as (R1), the most obvious procedure would seem to be the equilibration of the molten sodium carbonate with a fixed carbon dioxide partial pressure in a flow-type experiment. The trouble is of a practical nature. In the first part of Section III we calculated the limiting sodium oxide concentration attainable in a vacuum to be of the order of magnitude 1%. Any applied carbon dioxide pressure would greatly offset this concentration, and thus makes the analytical problems almost insurmountable.

On the contrary, this situation has been utilized for the analysis of the melts from the effusion runs. The cell plus content was heated to 900–930° in a controlled atmosphere of dry carbon dioxide with a small percentage oxygen added. Generally one hour or somewhat more was required to attain constant weight. The cell was cooled to below 300° in the furnace before removal. In terms of the weight of the melt before carbon dioxide absorption w and the weight gain Δw, the mole fraction of oxide is

$$N_{Na_2O} = 2.41 \frac{\Delta w}{w + \Delta w}$$

Some attempts were made at a flow method with a fixed oxygen partial pressure and absorption of the carbon dioxide evolved. This case may be formally treated by an equation analogous to equation 10, because of the retarding effect of the oxygen on the evaporation of sodium oxide. This effect was found all right, but the method presented a number of practical difficulties. This is mentioned to indicate that, in spite of the somewhat unconventional formal treatment involved, the effusion method appears to be the easiest way to the goal of the present work.

V. Experimental.—The first three runs reported here were done with high-frequency induction heating. The temperature was measured by an optical pyrometer. Neither the measurement nor the control of the temperature was very accurate in these runs. Radiation shields on top of the effusion cell also made the total resistance for the effusing gases somewhat uncertain. These uncertainties were abolished as far as possible by changing to the resistance heated furnace described in Part One (see Fig. 2). This furnace was mounted on a movable brass bottom fitting on to a water-cooled brass can which was attached to the vacuum system in a fixed, vertical position.[25] The temperature control was effected by a Brown ElectroniK potentiometer recorder connected to the scanning thermocouple, which was left in middle position except for the brief periods of gradient investigation. By thus having the controlling thermocouple (with bare leads at the hot-junction end) closer to the source of heat (the furnace wall) than to the heated object (the effusion cell), the oscillations in temperature on the cell were less than ±0.1° although the temperature on the controller oscillated a couple of degrees. The long-time variations were also less than one degree when the controller was operating properly. The temperature reported in Table I for each run was obtained by graphical averaging on a time–temperature plot. The vacuum during a run was about 5×10^{-5} mm. or better, reading about the same on a McLeod and a Philips gage.

The analysis of the oxide content after the HF runs was done by titration according to Winkler (see, *e.g.*, ref. 12, p. 109). The titration volumes were rather small and the end-point sluggish and hard to see in the white slush of precipitate, so that it may be regarded as partly fortuitous when these results fall quite well in line with the rest. The melts from the resistance-heated runs were analyzed in the way outlined in Section IV.

The effusion cell was made of platinum for all the runs. A note on the behavior of this metal in the basic melts may be added at this point. After an effusion run, the melt was always dark-brown to black (with the exception of run N6). Upon absorption of carbon dioxide, the melt turned to pure white again. After dissolving in water, small, gray, loosely coherent flakes, presumably of metallic platinum were found at the bottom. In the cases where the melt was dissolved in water, without preceding carbon dioxide absorption, the insoluble matter was present in the form of a reddish brown precipitate, presumably $PtO_2 \cdot nH_2O$. Spectroscopic analyses of the insoluble matter from a number of the runs showed platinum as the major constituent, with minor impurities of alkaline earths and silica.

It is suggested that the platinum is oxidized (by simultaneous reduction of sodium oxide) to PtO_2 which dissolves in the basic melt to form platinate ions. The carbon dioxide acts as an acid on this ion, precipitating the oxide again. The behavior thus far is quite analogous to an amphoteric oxide in aqueous solution. But the precipitated platinum oxide is unstable at higher temperatures and decomposes yielding the metal.

The weights of the precipitates checked fairly well with the weight loss of the cell itself during the corresponding

(25) A fixed bottom (base plate) and a movable bell jar would have been a more convenient arrangement in use.

TABLE I

Run[a]	B, cm.²	W_B	$f = W_B \times B/A$	T, °K.	t, min	w°	Δw	q	Δq	N_{Na_2O}, %	$P_{CO_2(m)}$, atm. × 10^{-5}
						gram					
HF 2	0.0779	0.949	0.023	1380	54	2.489	....	1.0451	0.013	1.36	22.0
HF 3	.0779	.949	.023	1323	111	1.693	....	0.7655	.008	1.14	7.91
HF 4	.0779	.949	.023	1302	76	3.988	....	.2948	.016	...	4.24
N1-a	.0327	.890	.0074	1292	137	11.734	....	.5991	.050	..	11.6
b	.0327	.890	.0074	1283	188	....	0.0769	.3881	...	1.70	5.94
N2-a	.0327	.890	.0074	1275.9	193	15.203	....	.3289	.052	...	
b	.0327	.890	.0074	1277.4	143	....	....	.1975	...	...	4.08
c	.0327	.890	.0074	1276.4	163	....	.0903	.2369	...	1.49	(mean)
N3-a	.1225	.940	.0294	1189.0	436	15.200	....	.4624	.021	...	0.690
b	.1225	.940	.0294	1189.3	1382	....	.0336	.7337	...	0.58	.362
N4-a	.1225	.940	.0294	1154.0	1357	14.784	....	.3668	.024	...	.176
b	.1225	.940	.0294	1154.8	2023	....	.0374	.6797	...	0.65	.232
N5	.1225	.940	.0294	1341.0	242	12.528	.0493	2.3600	.029	1.16	7.15
N6-a	2.92[b]	.70[c]	.522	1211.2	133	12.360	....	0.2493	.002	...	0.075
b	2.92[b]	.70[c]	.522	1211.5	333	....	.0031	0.8698	...	0.066	0.104

[a] For HF runs: $A = 3.2$ cm.²; $W_A \cong 0.6$. For N runs: $A = 3.92$ cm.²; $W_A \cong 0.5$. The value of W_A varies somewhat with the level of the melt in the cell. [b] The effusion "hole" was smaller than the area A even with no lid due to a thickened rim on the crucible. [c] A correction for the "effusion resistance" of the furnace is included in this figure.

run. These weights respectively weight losses were around 0.05 g. or less, so that the reaction with the platinum cannot in any event have influenced the results significantly.

The results of all runs are given in Table I and in Figs. 5 and 6 (except that the result from run N1a is omitted in the plot Fig. 5, the high result being ascribed to impurities in the new platinum cell). The hole sizes used increase in the order N1,2–HF2,3,4–N3,4,5. It was noted in course of the work that the results for the pressure,[26] when extrapolated to a common temperature, decrease in the same order, suggesting that at least one of the species has a low accommodation coefficient. Consequently Run N6 was done without any lid on the cell, the result confirming this supposition.

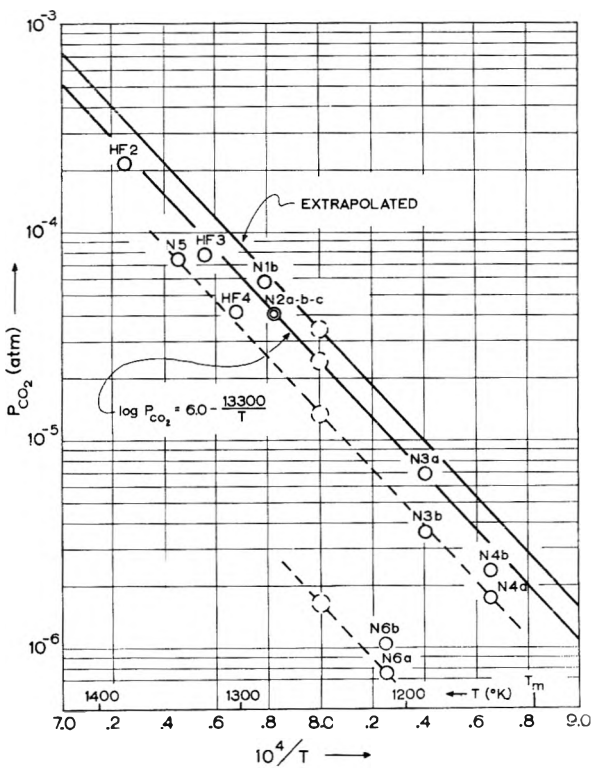

Fig. 5.—Carbon dioxide pressure (according to equation 3) *versus* inverse temperature. The uppermost dashed point is the result of extrapolation on Fig. 7 to $f = 0$. The double point for run N2 is the mean value, taken from Fig. 4.

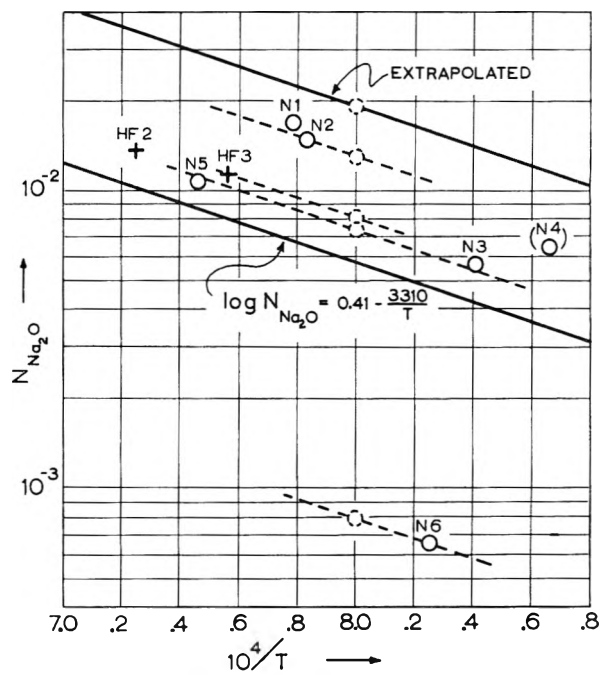

Fig. 6.—Sodium oxide concentration *versus* inverse temperature. The uppermost dashed point is the result of extrapolation on Fig. 8 to $f = 0$.

It will be noted that the agreement between the different parts a and b of the same run is rather poor for most of the runs. A discrepancy of some 50% is way outside the experimental accuracy that was expected. No definite explanation for the deviations can be offered, but it is known that rate-controlled processes such as the evaporation from a surface with low evaporation coefficient are less reproducible than true equilibrium processes. The excellent agreement between Run N2a, -b and -c (Fig. 4) is probably due to the smaller hole size than in the following runs.

(26) The results for the pressures of the three species are all very closely proportional to the observed weight loss (*cf.* eq. 3–5), with small b, consequently the pressure is reported for only one of the species (carbon dioxide) in the table and in Fig. 5.

There are probably more sources of error that may give rise to a too high weight loss than to a too low one, hence the lowest observed value for each temperature was considered the correct one.

VI. Discussion of the Results.—The monatomic Na or the diatomic O_2 would not be expected to have a particularly low accommodation (or, here, really evaporation) coefficient. However, too little is known as yet about this type of process. In the work on sodium oxide, Brewer and Margrave[22] varied the hole size over a too narrow range for any effect to show up, in view of the appreciable experimental uncertainty. Above the melting point of the oxide, only one hole size was used.

The evaporation of the carbon dioxide involves a reaction of the trigonal $CO_3^=$ to form a linear CO_2. This reaction appears to have a relatively high activation energy. The low accommodation coefficient of the carbon dioxide will also make the composition of the melt at steady-state dependent upon the size of the hole. Opening up the hole has a relatively larger effect on the rate of escape of sodium oxide than on the rate of escape of the carbon dioxide. Consequently the melt at steady state will contain less oxide the bigger the hole, as borne out by the analyses (*cf.* Fig. 6).

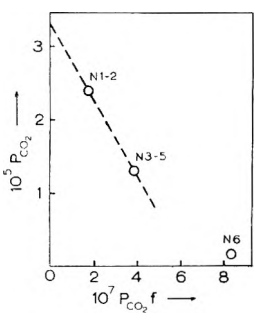

Fig. 7.—Carbon dioxide pressure P_{CO_2} adjusted to 1250°K., *versus* the product $P_{CO_2}f$.

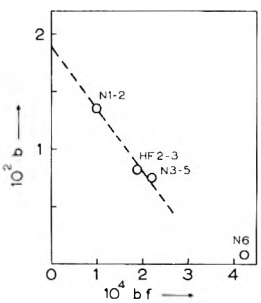

Fig. 8.—Sodium oxide concentration b adjusted to 1250°K., *versus* the product bf.

The low accommodation coefficient was (without much justification) not expected at the outset of this work. As a consequence, the orifice to surface ratios used are not sufficiently small for a valid approach to equilibrium.[27] The most obvious procedure then is to plot the observed pressure P_m *versus* the ratio f and extrapolate to $f = 0$. But this plot is curved to such an extent that an extrapolation is highly uncertain. The method suggested in Part One in connection with equation 2a affords a more reliable way of extrapolation. In the present case, the shorter form of this equation will suffice

$$P_m = P_{eq} - \frac{1}{\alpha} P_m f \qquad (2b)$$

Now, this should be valid for simple evaporation processes like those of most metallic elements or molecular compounds. The case of the carbonate is somewhat more complex. Equations 3 to 5 will still be valid, but it should be remembered that the weight loss of each of the species is related to the actual pressure (generally denoted P_m) of that species inside the cell. We may try a correlation between P and f by assuming that the actual pressure is equal to the equilibrium pressure for sodium and oxygen, while the carbon dioxide pressure satisfies equation 2b. This gives for the first equilibrium constant

$$K_1 = \frac{P_{CO_2(m)} \left[1 + \frac{f}{\alpha}\right] N_{Na_2O}}{N_{Na_2CO_3}}$$

where N_{Na_2O} ($= b$) is also the actual value during the run at steady state. By going through the derivation in the same way as outlined in the first part of Section III, one obtains

$$P_{CO_2}^{7/2} = P_{CO_2(eq)}^{7/2} - \frac{1}{\alpha} P_{CO_2}^{7/2} f \qquad (11)$$

where the subscript m has been omitted; furthermore

$$b^{7/6} = b_{eq}^{7/6} - \frac{1}{\alpha} b^{7/6} f \qquad (12)$$

From the first of these two equations it follows that a plot of $P_{CO_2}^{7/2}$ *versus* $P_{CO_2}^{7/2} f$ should give a straight line. But this turns out not to be the case for the present data. On the contrary, a simple, first-power plot gives a fairly reasonable picture (Fig. 7) whereas the exponent 3.5 applied to the pressures gives a plot which points upwards to the right (towards "one o'clock") for decreasing f-values, *i.e.*, it does not point toward any finite equilibrium value. Also for the b values, the first-power plot looks the most reasonable (Fig. 8); the exponent 1.4 does not make as big a difference as the exponent 3.5, but causes the point for run N6 to fall completely out of line to the left.

The plots Fig. 7 and 8 have been made by adjusting the values of P_{CO_2} (Fig. 5), respectively, b (Fig. 6) to a common temperature, *viz.*, 1250°K., by (dashed) lines drawn through experimental points of the same f-value, parallel to the theoretical (calculated) slope. The isothermal values thus obtained are marked with dashed circles on the graphs. These values are necessarily somewhat uncertain; furthermore it would have been a distinct advantage to have data for more than three (or four) different f-values, particularly for smaller f-values.[28] Still it may be concluded from the present data and their disagreement with Equations 11 and 12 that the rate of evaporation is, for the larger orifice sizes, not directly proportional to the activity of the species in the melt. Qualitatively speaking, the observed pressure drop upon opening the orifice is too large to be compatible with the simultaneously observed drop in oxide content, because this latter effect would increase the (equilibrium) carbon dioxide pressure.

Tentatively one might try an explanation by assuming a very low accommodation coefficient α for the carbon dioxide together with a medium low accommodation coefficient β as an average for Na and O_2. The β can be eliminated by multiplication of

(27) A note on the reason for using fairly large orifices: If a comparable weight loss is wanted with a much smaller orifice, time, temperature, or both, will have to be higher. This results in increased corrosion of the platinum cell. In view of some previous experience with a pinhole developing in the bottom of the cell, this corrosion was considered rather undesirable.

(28) Complementary work will be attempted in the author's present laboratory when a suitable vacuum set-up has been completed.

the resulting expressions for P_{CO_2} and b, this giving an equation

$$bP_{CO_2} = b_{eq}P_{CO_2(eq)} - \frac{1}{\alpha} bP_{CO_2}$$

The experimental data do not, however, fit particularly well with such a treatment. The author is inclined to leave the question open until more exhaustive experimental data become available. It is clear that the mechanism of vaporization will be rather complex.

It may be noted that for carbon dioxide onto pure water, an accommodation coefficient equal to 4×10^{-6} has been calculated by Danckwerts[29] from data given by Highbie in 1933.

The empirical extrapolation to equilibrium values may be brought about in two ways; one may use the points for the two lowest f-values, as indicated in Figs. 7 and 8 by dashed lines, on the presumption that these are closest to equilibrium measurements, or one may apply a suitable exponent (close to 1.2 for both P_{CO_2} and b) to make the plots truly linear. The two methods give just about identical results, which are then accepted as equilibrium values: $P_{CO_2} = 3.3 \times 10^{-5}$ atm., $N_{Na_2O} = 0.019$ at 1250°K. From these values one calculates: $\log K_1 = -6.2$; $\log K_2 = -9.3$ (as compared to -6.9 ± 1.2 and -9.2 ± 0.5 from the calculations in Section II), all values for 1250°K.

It should be emphasized that P_{CO_2} and b are different quantities obtained by entirely independent methods. With this in mind, it is interesting to note the similarity of the two plots Figs. 7 and 8. The numerical values for the slopes of the dashed lines are also close to equal; Fig. 7 gives a value $\alpha' = 0.019$, Fig. 8 a value $\alpha'' = 0.018$. But this quantity cannot be readily interpreted as an accommodation coefficient.

(29) P. V. Danckwerts, *Research (London)*, **2**, 494 (1949).

The experimental data indicate that, within the accuracy, the temperature coefficients, *i.e.*, the heats of reaction for reactions (R1) and (R2), are as given from the calculations in Section II. It will be seen, however, that the data scatter sufficiently to be compatible with somewhat different slopes as well. For the complete evaporation reaction (R3) high-temperature data are available for all the right-hand gaseous species, hence the present experimental data may in principle be used for a calculation of the high-temperature thermodynamic functions for sodium carbonate. But the accuracy of the data does not warrant the report of the values thus obtained at the present time.

In conclusion, it may be regarded as established that the evaporation does proceed in the general way outlined in Section III of this paper. In order to obtain numerical values of an accuracy comparable to that of the electrometric method,[13] some more experimental work is needed, which might eventually at the same time lead to an elucidation of the kinetics of the evaporation process for sodium carbonate into a vacuum.

Acknowledgments.—This work was done while the author was holding a grant from the United States International Information Administration, and he would like to express his sincere gratitude for this aid. He is also indebted for economic support from the Royal Norwegian Council for Scientific and Industrial Research.

Hearty thanks are due to Dr. Leo Brewer, in whose laboratory this work was done, and who contributed generously through valuable advice and discussions.

ATOMISTIC INTERPRETATION OF THE MELTING OF SIMPLE COMPOUNDS

By W. A. Weyl

Division of Mineral Technology, The Pennsylvania State University, State College, Pennsylvania

Received October 15, 1954

Earlier attempts to correlate the melting temperature of simple compounds with a single parameter such as character of the bond or bond strength have failed. The author has developed a physical concept which accounts for the fact that most elements are solids and that only a very few (noble gases) can form single atoms under normal conditions. This concept, the need of positive cores to be screened by electrons or anions, is used to explain the wide spread of melting temperatures of simple compounds, oxides or fluorides. The anion to cation ratio is the most important single factor. The melting points increase from fluorides to oxides, nitrides and carbides. For highly charged cations the melting point increases with increasing size of the cation (C^{4+}, Si^{4+}, Zr^{4+}, Th^{4+}) because more anions are required for screening the larger cores. Increasing the charge of the cation (Na^+, Mg^{2+}, Al^{3+}, Si^{4+}) produces two antagonistic effects: it increases the need for screening the core but it also increases the number of anions required for electroneutrality. The screening requirements depend on the sizes, charges and polarization properties of the anions and cations. There is no single parameter which controls the melting temperature but within series of compounds a plausible explanation for the melting temperatures can be derived.

I. Introduction

In order to explain the fact that most elements are solids at normal temperature, the author[1] assumes that only in the rare gas atoms are the cores well screened by the number of electrons which is required to neutralize their positive charges. All other atoms aggregate in one way or another in order to improve the screening of their cores. This can be accomplished by (1) the quantization of some electrons with respect to several cores (molecular orbitals[2] as in N_2, P_4 and S_8), by (2) the formation of an infinitely extending array of cores which are screened by mobile, quasi-free electrons (metallic state), or by (3) electron transfer which leads to

(1) (a) W. A. Weyl, *Trans. Soc. Glass Techn.*, **35**, 421, 469 (1951); (b) "Structure and Properties of Solid Surfaces," Edited by R. Gomer and C. S. Smith, The University of Chicago Press, 1953, p. 150.

(2) K. Fajans, *Chem. Eng. News*, **27**, 900 (1949).

the formation of cations and anions and surrounding the cations by anions.

The solid state is the result of two requirements, namely, that electroneutrality be achieved within the smallest possible volume and that the atomic cores be sufficiently screened. Maximum screening requires that the cores be surrounded in space by anions or by electrons. The formation of atoms at high temperatures indicates that the screening demand decreases with increasing temperature and *vice versa*. Therefore, molecules, such as SiO_2 and SO_3, with incompletely screened cations will polymerize. Such a system loses entropy in order to improve the screening of the central cores: formation of SO_4 chains or networks of SiO_4 tetrahedra.

Experimental work on the polymerization of inorganic substances, in particular on the effect of composition on the low temperature viscosity of glasses, sponsored by the Office of Naval Research, made it possible to derive some rules which govern the melting properties of simple compounds.[3]

The wide variation of inorganic compounds with respect to their melting points and their vapor pressures has challenged many scientists to speculate on the relation between these properties and their constitution. Most attempts to elucidate these relations emphasize a single parameter to account for the differences. The development of the extreme ionic viewpoint by W. Kossel (1916) led him to the concept of the "shielding of cations by anions" as an important factor which determines the volatility of compounds (1920). The influence of the electronic structure of cations on the properties of substances was recognized by Grimm (1922). The concept of the mutual deformation of ions led Fajans (1925) to his theory of chemical binding forces and to an explanation of the lower melting points of silver halides as compared with sodium halides. N. V. Sidgwick (1929) attributes the gaseous nature of SiF_4, PF_5 and SF_6 to their covalency and the high melting points of NaF, MgF_2 and AlF_3 to their ionic character. According to L. Pauling, however, covalency in this series starts with AlF_3 rather than with SiF_4. V. M. Goldschmidt (1926) demonstrated the importance of the "valence sum" as a factor which affects the melting temperature of ionic crystals.

A. E. Van Arkel (1949) tried to use the extreme ionic viewpoint and the concept of shielding in order to explain the volatility of compounds but reached the conclusion that this approach is not satisfactory. This failure is due to his emphasizing the sizes and charges of the ions without giving proper consideration to the electronic structures of the ions and their mutual polarization.

These different concepts indicate that no single parameter can account for the melting temperatures of simple inorganic compounds.

II. The Discontinuity of the Melting Process

One is accustomed to think of the forces which the ions of a crystal exert upon one another as functions of those electrical fields which are characteristic for them when they are in their equilibrium positions. Elastic deformation, compressibility, stress-optical phenomena, etc., are measured under conditions in which atoms are moved only a very short distance from their equilibrium positions. The melting process, however, involves motions of the ions which go far beyond the stage where one can apply Hooke's Law or where one can extrapolate from infinitely small distortions of the lattice to the actual event.

One can describe the forces acting in a NaCl crystal by a series of terms which are the result of attractions and repulsions between the ions

$$\Sigma = F_{Na^+-Cl^-} - F_{Na^+-Na^+} - F_{Cl^--Cl^-} \ldots .$$

The geometry of the NaCl crystal keeps the second term, $-F_{Na^+-Na^+}$, small because the cations are not close neighbors. The magnitude of the third term, $-F_{Cl^--Cl^-}$, is also small because of the polarizability of the anion. The values of these terms change drastically when the crystal reaches its melting point. The value of $-F_{Na^+-Na^+}$ increases because the sodium ions become more and more exposed to the field of adjacent sodium ions. This leads to a point where an occasional Na^+ ion will pass close to another Na^+ ion, thus causing a widening of the volume element surrounding this couple. This widening further enhances disorder and introduces a discontinuous change. The NaCl structure expands in a discontinuous fashion with the absorption of heat (latent heat of fusion). The melting point of the NaCl crystal is characterized by a thermal energy which makes it possible for the Na^+ ions not only to pass one another as in diffusion and electrical conductivity, but also to remain close neighbors for some time. The number of Na^+ ions which can be found in close proximity to other Na^+ ions increases with increasing temperature and, as a result, the thermal expansion of the fused salt exceeds that of the crystal (formation of "holes").

The probability of the cations to remain close neighbors introduces a discontinuous change of the volume. The melting point of a substance resembling NaCl depends, therefore, on the energy which is necessary to overcome the cation–cation repulsion. The magnitude of this repulsion decreases with (1) decreasing field strength of the cation, *i.e.*, decreasing charge and increasing radius, (2) increasing polarizability of the cation as determined by its size and electronic configuration, and (3) increasing ratio of the number of anions to cations.

III. Factors Determining the Melting Points of Simple Compounds

In the following paragraphs the chief factors which determine the cation–cation repulsion and, with it, the melting temperatures will be discussed.

1. Charge of the Cation (V. M. Goldschmidt's Model Structures).—The most obvious factor which determines the repulsive forces between two cations is the magnitude of their charges. The role of the "valency" of the elements in similar structures has been used by Goldschmidt[4] in the de-

(3) E. C. Marboe and W. A. Weyl, Office of Naval Research Tech. Report No. 56, Contract No. N6 onr 269 Task Order 8, NR 032-264 and NR 032-265, The Pennsylvania State University, March, 1954. Accepted for publication, *Trans. Soc. Glass Techn.*

(4) V. M. Goldschmidt, "Geochemical Distribution Laws, VIII," Skrifter utgit av Det Norske Videnskaps Akademi i Oslo, Matem. Naturvid. Klasse, 1926

TABLE I

MODEL STRUCTURES (AFTER V. M. GOLDSCHMIDT)

Formula	Weak structure Radii		M.p., °C.	Formula	Strong structure Radii		M.p., °C.
BeF_2	0.34	1.33	538	SiO_2	0.39	1.32	1710
LiF	0.78	1.33	870	MgO	0.78	1.32	2800
MgF_2	0.78	1.33	1240	TiO_2	0.64	1.32	1830
CaF_2	1.06	1.33	1360	ThO_2	1.10	1.32	3050
Li_2BeF_4	0.78 0.34	1.33	458	Zn_2SiO_4	0.83 0.39	1.32	1509
$KMgF_3$	1.33 0.78	1.33	1070	$SrTiO_3$	1.27 0.64	1.32	2050
NaCl	0.98	1.81	801	CaS	1.06	1.74	2000

velopment of his "model structures." The crystal structure is a function of the ratio, the sizes and the polarization properties of its ions, but is not strongly affected by their charges. Properties such as melting temperature and hardness, however, depend primarily on the charges because they determine the forces between the ions. Because of this relation, it is possible to construct a model of a given substance which has the same crystal structure and the same habitus but which is either "weaker" or "stronger" than the original substance because of the difference in the binding forces. As can be seen from Table I the "weak" structures have much lower melting points than their "stronger" counterparts. Even the interaction of two oxides as expressed by their phase equilibria can be modeled when the proper fluorides are chosen.[5] In all cases the fluorides as the weakened models of the oxides have lower melting points because the lower charges of their cations lower the cation–cation repulsion. In the same fashion, nitrides containing the N^{3-} ion with a threefold charge are "strengthened models" of oxides and fluorides. Their melting points are higher than those of the oxides.

2. Anion to Cation Ratio.—Let us now consider the melting temperatures of the fluorides of the second row elements (Table II). The higher melting temperature of MgF_2 (1396°) as compared with that of NaF (980°), agrees with our concept that more energy is required to move a Mg^{2+} ion past another Mg^{2+} ion than to move a Na^+ ion past another Na^+ ion. However, AlF_3 has a lower melting point than MgF_2 in spite of its containing the more highly charged Al^{3+} ion. This lowering of the melting point is due to the improved screening of the cation as the result of the increased anion to cation ratio. The last three fluorides in this row are gases because their central cores are well screened by the number of F^- ions which is needed for neutralizing the charges of the cores.

TABLE II

MELTING TEMPERATURES (°C.) OF FLUORIDES AND OXIDES OF SECOND ROW ELEMENTS

	Na^+	Mg^{2+}	Al^{3+}	Si^{4+}	P^{5+}	S^{6+}
Fluoride	980	1396	1040	Gases at ordinary temp.		
Oxide	920	2800	2030	1710	563	16.8

The melting point of a compound increases with the charge of the anion as can be seen from the melting points of the fluorides and the oxides of the second row elements (Table II). Even the sulfur compound shows a distinct tendency to polymerize and to form crystals in which the S^{6+} ions are surrounded by four O^{2-} ions.

Going from the oxides to nitrides and carbides one finds a further increase in the melting points. The highest melting compounds are carbides, silicides, borides and nitrides because the high excess charges of the C^{4-}, Si^{4-}, B^{3-} and N^{3-} ions lead to an anion to cation ratio which is very unfavorable with respect to the screening of the cations.

	SiF_4	SiO_2	SiC
M.p., °C.	−77	1710	2600

3. Size of the Cations.—The melting points of the halides (Table III) of the alkaline earths increase with increasing size of the cation. Increasing size of the cation demands either a greater number or larger sized anions for proper screening. This effect is not very strong so that other parameters, *e.g.*, the crystal structure, obscure the picture and one finds no order in the melting points of the alkaline earth fluorides or bromides.

TABLE III

MELTING TEMPERATURES (°C.) OF CHLORIDES AND OXIDES OF ALKALINE EARTHS

	Be^{2+}	Mg^{2+}	Ca^{2+}	Sr^{2+}	Ba^{2+}
Chloride	440	708	772	873	955
Oxide	2530	2800	2580	2430	1923
Ionic radius (Å.)	0.34	0.78	1.06	1.27	1.43

A much more drastic influence of the size occurs in the oxides of the general formula XO_2 (Table IV). In this series of oxides the charge of the cation and the anion to cation ratio are constant. With increasing size of the cation, however, it becomes impossible for two O^{2-} ions to provide proper screening. Only the very small core of carbons can exert such an attracting and deforming influence upon its two O^{2-} ions that it is completely screened.

TABLE IV

MELTING TEMPERATURES (°C.) OF OXIDES OF THE FORMULA XO_2

	C^{4+}	Si^{4+}	Ti^{4+}	Zr^{4+}	Th^{4+}
Oxide	gas	1710	1830	2677	3050
Ionic radius (Å.)	<0.2	0.39	0.64	0.87	1.10

4. Polarizability of the Cations.—The melting points of the alkaline earth halides fall within a relatively narrow temperature range. With increasing atomic weight and increasing number of electrons the polarizabilities of the ions increase. One can consider the polarizability of an ion as its ability to adjust its field to best suit its environment. Whereas the Mg^{2+} ion behaves as a rigid sphere, the much larger Ba^{2+} ion has an electron cloud which is not rigid but which can be deformed. As a

(5) For a review of the more recent work on Goldschmidt's Model Structure, consult E. F. Osborn, *Ceramic Age*, **60**, [5] 51 (1952).

result, two Mg^{2+} ions in close proximity repel each other more strongly than two Ba^{2+} ions within the same distance. The Ba^{2+} ions induce dipoles in each other and the ion dipole attraction lowers the repulsive forces. For this reason the melting points of the alkaline earth oxides decrease with increasing size and polarizability (Table III).

The antagonistic influences which the size of a cation and the number of its electrons exert upon the melting point of a compound make it difficult to properly evaluate the role of the polarizability in such a series. However, by comparing cations of similar size, identical charge and different electronic configuration, one can readily see that increasing polarizability decreases the melting point. The classical example is provided by the properties of the sodium halides and silver halides (Fajans[6]). In a similar manner (Tables V–VII) compounds containing cations of the noble gas-type (octet shell) are compared with others which have either a 18 shell (Zn^{2+}) or an incomplete outer electron shell (Tl^{+} and Pb^{2+}). In all cases those compounds containing the noble gas-type cations (low polarizability) have higher melting points.

TABLE V

MELTING POINTS OF RUBIDIUM AND OF THALLIUM COMPOUNDS

Compound	M.p., °C. Rubidium	Thallium
XF	760	327
XCl	715	430
XNO_3	305	206

TABLE VI

MELTING POINTS OF STRONTIUM AND OF LEAD COMPOUNDS

Compound	M.p., °C. Strontium	Lead	Compound	M.p., °C. Strontium	Lead
XO	2430	888	X_2SiO_4	>1700	743
XF_2	1190	855	$X_2B_2O_5$	1130	497
XCl_2	873	501	$X_3As_2O_8$	1635	1042
$XSiO_3$	1580	766			

TABLE VII

MELTING POINTS OF MAGNESIUM AND OF ZINC COMPOUNDS

Compound	M.p., °C. Magnesium	Zinc
XO	2800	1975
XF_2	1396	872
XCl_2	708	262
$X_3P_2O_8$	1184	900
X_2SiO_4	1900	1509

5. Polarizability of the Anions.—The concept of atoms or ions having a certain size is a useful approximation. It is not completely correct to assume that during melting two cations remain neighbors under conditions where the electron density between the ions reaches zero. The diffuse nature of the electron clouds of the anions makes that impossible. With increasing size and polarizability of the anion, the electron density between passing cations increases and lowers the repulsive forces. This influence is reflected in the melting temperatures of the sodium and potassium halides, *i.e.*, the melting points decrease with increasing size and polarizability of the anion (Table VIII).

(6) K. Fajans, "Chemical Forces and Optical Properties of Substances," McGraw-Hill Book Co., Inc., New York, N. Y., 1931, p. 66 ff.

TABLE VIII

MELTING TEMPERATURES (°C.) OF SODIUM AND OF POTASSIUM COMPOUNDS

	Fluoride	Chloride	Bromide	Iodide	Metal
Na	980	801	755	651	97.5
K	880	776	730	693	62.3

Because of the greater polarizability of the S^{2-} ion as compared with the O^{2-} ion, the melting points of sulfides are generally lower than those of oxides. In the series O^{2-}, S^{2-}, Se^{2-} and Te^{2-} one has to be cautious about drawing conclusions concerning the melting points of compounds because most selenides and tellurides and many sulfides increase their entropies by forming defective structures at temperatures far below their melting points. The compounds of Ga, B and Al with the sixth group elements show a steady drop in melting points as the anion changes from the O^{2-} ion to the much more polarizable Te^{2-} ion.

In salts containing complex anions the symmetry of this group has to be considered in addition to size and polarizability. The nitrate group NO_3^- is only slightly larger than the Cl^- ion, but due to its planar configuration nitrates have lower melting points than the corresponding chlorides

$NaNO_3$	306.8°	NaCl	801°
KNO_3	334°	KCl	776°
$AgNO_3$	212°	AgCl	455°

Perchlorates containing the symmetrical ClO_4^- group have higher melting points than chlorides because the ClO_3^- group is asymmetrical

$NaClO_4$	482°	$NaClO_3$	248°
$KClO_4$	610°	$KClO_3$	368°
$AgClO_4$	486°	$AgClO_3$	230°

6. Melting Temperatures of H^+, Li^+, Be^{2+} and B^{3+} Compounds.—From the viewpoint of the screening of cations the proton has to be treated separately. We follow the ideas of Fajans and Bauer[7] and treat the hydrogen halides as halogen ions which contain protons within their electron clouds. In the hydrogen halides, the proton, the only cation which has no electrons, penetrates into the electron cloud of the halogen ion until the attractive forces are balanced by the repulsive forces between the proton and the nucleus of the halogen.

The melting of SiF_4, PF_5 and SF_6 does not involve cation–cation repulsive forces. These molecules contain central cations which are well screened and their condensation at low temperatures involves primarily van der Waals forces. The same is true for the hydrogen compounds. Protons can be screened in two ways: they can be surrounded by anions and for this purpose it requires two anions (hydrogen bonding, liquid water and ice) or they can penetrate into the electron cloud of an anion (hydrogen halides, water molecules in the vapor state). The electronic structure of the Li^+, Be^{2+} and B^{3+} ions (helium configuration) gives these ions properties which are intermediate be-

(7) K. Fajans and N. Bauer, *J. Chem. Phys.*, **10**, 433 (1942); K. Fajans, *Ceramic Age*, **54**, 288 (1949).

tween those of the ions with neon configuration (Na^+, Mg^{2+}, Al^{3+}) and the proton. We assume that the polarization of these ions, in particular the repulsion of the 2K-electrons, exposes the nuclei to such an extent that they can penetrate partly into the diffuse electron clouds of the anions. The larger the polarizability of the anions, the greater is the deviation of the properties of Li^+, Be^{2+} and B^{3+} compounds from those expected by a comparison with Na^+, Mg^{2+} and Al^{3+} compounds.

If one plots the melting points of the alkali fluorides against the size of the cation, one obtains a straight line relation for the melting points of CsF (684°), RbF (760°), KF (880°) and NaF (980°). Extrapolating this line to the radius of the Li^+ ion one would expect LiF to melt at about 1100°. Actually LiF melts at 870°, *i.e.*, at a lower temperature than NaF. There is no straight line relationship between the melting points of those alkali halides which contain the more polarizable Cl^-, Br^- and I^- ions, but one can still see that the lithium compounds are completely out of line: their melting points are too low.

One finds the same situation for Be^{2+} compounds. The melting points of BeO and $BeCl_2$ are lower than expected from an extrapolation (Table III). Also, the melting points of B_2O_3 and B_2S_3 are very much lower than those of the corresponding aluminum compounds. The same applies to the melting points of the boron halides as compared with aluminum halides.

IV. Volume Changes during Melting

Sodium chloride expands on heating and shows a discontinuous volume increase during its melting (formation of holes in the liquid). This volume expansion as well as the higher coefficient of expansion of the fused salt as compared with the crystal can be attributed to the Na^+–Na^+ repulsion. V. Zackay[8] calculated the volume expansion of sodium and potassium halides (from the low temperature expansion) and found it to be more than 20% for the sodium salts and about 14% for the potassium salts. This agrees with the expected difference in the cation–cation repulsive forces. Most interesting is the comparatively low volume expansion (2.5%) of the two alkali metals. In accordance with our concept, Zackay[8] explains this phenomenon on the basis of a minimum repulsion between the alkali ions in the presence of the most polarizable anion, the degenerated electron gas.

(8) V. Zackay, *Trans. Soc. Glass Techn.*, **37**, (News and Rev.) 18 (1953).

V. Heat of Fusion

According to our approach, a substantial part of the latent heat of fusion is used to make it possible for one cation to pass another or to produce those "holes" in the structure which are the result of the proximity of two unscreened cations. Because of the lower polarizability of the Na^+ ion we assume that the Na^+–Na^+ repulsion is greater than the K^+–K^+ repulsion. As a result, the latent heat of fusion is higher for NaF (32.7 kilojoules/mole) than for KF (26.3). A similar relationship exists for the alkali chlorides: NaCl (30.2), KCl (23.1), RbCl (19.2); and for the nitrates: $LiNO_3$ (25.5), $NaNO_3$ (16.1), KNO_3 (10.8).

Since the mutual repulsion between cations is decreased as the polarizability of the cations increases, the replacement of a noble gas-like cation by one of the same size and charge but of higher polarizability decreases the latent heat of fusion.

NaCl	30.2	AgCl	12.8
RbCl	19.2	TlCl	16.7

Because of the different structures and the different lattice energies, this relationship cannot be expected to hold rigorously for more complicated compounds.

VI. Conclusions

The melting temperatures of inorganic compounds depend upon several factors so that it is impossible to derive general rules governing the melting points of even the simplest compounds. In properly chosen series, however, it is possible to explain the rise or fall of the melting points. These series have to be chosen so that one of the parameters dominates the melting. In the "model structures" derived by Goldschmidt the melting point increases with the valence sum. A comparison between corresponding compounds containing noble gas-type and non-noble gas-type cations reveals that the latter have the lower melting points. We have not considered gaseous or liquid compounds which have very low melting points because their condensation and melting is governed primarily by van der Waals forces.

The same concepts have been used by the author[1a] to explain the eutectic temperature and the compositions of eutectic melts of simple salts.

AN INVESTIGATION OF THE ACTIVITY OF CALCIUM CARBONATE IN MIXTURES OF FUSED SALTS[1]

BY TORMOD FORLAND[2]

Department of Mineral Technology, Pennsylvania State University, State College, Pa.

Received October 8, 1954

The aim of the present work was to investigate how the entropy of mixing and energy of mixing depend on the composition in simple mixtures of fused salts, particularly in mixtures containing cations with different number of charges. The activity of calcium carbonate in a mixture of alkali carbonates may be determined by examining the equilibrium $CaCO_3$ (in mixture) = CaO (solid) + CO_2 (gas). The systems investigated were $CaCO_3$–Na_2CO_3, $CaCO_3$–K_2CO_3 and $CaCO_3$–$(NaK)CO_3$. The measurements are discussed in connection with structural models considered for these systems.

Introduction

A fused salt is an array of positively charged cations and negatively charged anions. Due to the strong attractive forces between particles of opposite sign and the strong repulsive forces between particles of the same sign, a cation will preferentially have anions as nearest neighbors and anions will have cations as nearest neighbors. To transfer a cation from a position where it is surrounded by anions to a position where it is surrounded by cations will, for a compound like NaCl, require an energy of about 200 kcal. as may be estimated from electrostatic calculations. We may assume, therefore, that there are two kinds of positions in the fused salt, one kind for cations and one kind for anions, similar to what is known for the solid crystal.

The liquid has a larger volume than that of the crystal. This may be attributed partly to the presence of unoccupied positions in the fused salt. We also have to consider the existence of single pairs of ions of the same sign in the liquid state which will cause expansion. For a compound like NaCl the expansion on melting is more than 20%. For a compound like AgCl, the volume change on melting is less than 5%. It is also known that the small irregularities formed in the lattice of solid AgCl by heating are different from those formed in solid NaCl. This means we must be aware of the possibility that even for simple salts with the same crystal structure, the structure of the liquid state may differ.

We assume that cations and anions have different kinds of positions in fused salts. If we have a mixture of two fused salts containing two kinds of cations, we may assume that the two kinds of cations are randomly distributed over the cation positions if the cations are not very different with respect to charge, size and polarization properties. Thus, in a mixture of NaCl and KCl it is reasonable to assume that the cations are randomly distributed, whereas in a mixture of Na_2O and SiO_2, silicon and sodium will occupy different kinds of positions.

(1) Presented at the Symposium on High Temperature Chemical Reactions at the 126th Meeting of the American Chemical Society, New York, N. Y., Sept. 15, 1954.

(2) Formerly associated with The Royal Norwegian Research Council, Institute of Silicate Science, Norwegian Institute of Technology, Trondheim, Norway. At the present time employed on a contract with the Office of Naval Research Contract N6 onr 269 Task Order 8, NR 032-264, The Pennsylvania State University, State College, Pennsylvania.

Evaluation of Entropy and Energy of Mixing.—We will here consider the simple case where the ions are randomly distributed and try to evaluate the thermodynamic functions of such a system.

Entropy of Mixing.—In the system NaCl–KCl we will assume that the cations are randomly distributed over the cation positions. Therefore, the entropy of mixing for such a system will be similar to that obtained by mixing two ideal gases.

$$S = -R(n_{Na} \ln N_{Na} + n_K \ln N_K)$$

where n denotes the number of moles. N_{Na} and N_K are ionic fractions

$$N_K = \frac{n_K}{n_{Na} + n_K}$$

The partial molar entropy of one component, *e.g.*, KCl, will be

$$\bar{S}_{KCl} = -R \ln N_K$$

This is the expression for the entropy derived by M. Temkin.[3]

For a system containing cations with different numbers of charges like the system $CaCO_3$–Na_2CO_3, one may in the same way have

$$\bar{S}_{CaCO_3} = -R \ln N_{Ca}$$

Here we have assumed that the two cations are randomly distributed without respect to charge. From solid solution in crystals we know, however, that two monovalent ions may be substituted for one divalent ion and an adjacent vacant position. This model will give a different expression for the entropy

$$\bar{S}_{CaCO_3} = -R \ln \frac{n_{Ca}}{n_{Ca} + {}^1/_2 n_{Na}} = -R \ln N'_{Ca}$$

This is not strictly correct, but it is a good approximation as the coördination number of a cation to other cations in the second coördination sphere is high.[4] N' we will call the electric equivalent fraction.

Energy of Mixing.—The process of mixing will generally also involve a change in the energy of the system. Information on heat or energy of mixing is scarce in the literature. One may, however, get an idea about the heat of mixing from the phase diagrams. The deviation from ideal behavior may in simple systems be attributed to a heat of mixing. Such an estimation shows that for mixtures of alkali halides containing the same kind of anions,

(3) M. Temkin, *Acta Phys. Chim. U.R.S.S.*, **20**, 411 (1945). Compare also: H. Flood, T. Forland and K. Grjotheim, *Z. anorg. Chem.*, in press.

(4) P. J. Flory, *J. Chem. Phys.*, **10**, 51 (1942).

heat is evolved by the process of mixing. This may be attributed to a change in cation–cation repulsion by the process of mixing cations of different sizes (see Fig. 1). The left side of the figure shows the arrangements of the ions before mixing, the right side shows the arrangements of the ions after the salts are mixed. The energy due to the cation–cation repulsion is inversely proportional to the distance between the cations and it can easily be shown that this energy is higher for the unmixed system than for the mixed system. In addition, polarization will favor the mixed system. Similarly one may expect that in a system containing ions of different numbers of charges, the mixed system will have a lower energy than the unmixed system.

We will now calculate the energy of mixing for a system KCl–NaCl. To do this we will assume that the cations are randomly distributed and we will attribute a certain energy to each pair consisting of a cation and another cation in the second coördination sphere, ϵ_{KK}, ϵ_{NaNa} and ϵ_{KNa}. Assuming that each cation is surrounded by a number C of cations in the second coördination sphere, the energy of mixing will be

$$\Delta E = {}^1/_2AC(n_K + n_{Na})(N_K^2\epsilon_{KK} + 2N_KN_{Na}\epsilon_{KNa} + N^2_{Na}\epsilon_{NaNa}) - {}^1/_2AC(n_K\epsilon_{KK} + n_{Na}\epsilon_{NaNa})$$

where A is Avogadro's number. Here the pure fused component is chosen as the standard state. Differentiating this equation with respect to the component KCl we obtain

$$\bar{E}_{KCl} = N^2_{Na} \times {}^1/_2AC(2\epsilon_{KNa} - \epsilon_{KK} - \epsilon_{NaNa}) = N^2_{Na} \times b_{NaK}$$

where b_{NaK} is a constant which is equal to the energy absorbed by dissolving one mole of KCl in a large quantity of NaCl. This derivation is similar to that carried out by J. H. Hildebrand and R. J. Salstrom for the so-called "regular solutions."[5]

The system Na_2CO_3–$CaCO_3$ is a little more complicated because the number of cations surrounding a cation as next nearest neighbors will decrease as we go from Na_2CO_3 to $CaCO_3$. However, if we take this into account, we obtain the equation

$$\bar{E}_{CaCO_3} = N'^2_{Na}b_{NaCa}$$

by a somewhat similar derivation. Here N'_{Na} is the electrical equivalent fraction

$$N'_{Na} = \frac{{}^1/_2n_{Na}}{n_{Ca} + {}^1/_2n_{Na}}$$

as defined before.

We may now introduce still another kind of cation into the system by considering the system Na_2CO_3–K_2CO_3–$CaCO_3$ and derive the equation for the energy of mixing. The derivation is in principle the same as that just mentioned and the result is

$$\bar{E}_{CaCO_3} = (1 - N'_{Ca})(N'_{Na}b_{NaCa} + N'_Kb_{KCa}) - N'_{Na}N'_Kb_{NaK}$$

Here the constant b_{NaCa} is given by the heat of mixing in the binary system Na_2CO_3–$CaCO_3$ and b_{KCa} and b_{NaK} have similar meaning.

The Activity and Activity Coefficient.—We now have equations both for entropy and energy of mixing and, thus, we have an expression for the free energy or activity a of a component in a mixture. The activity, a_{CaCO_3}, of the component $CaCO_3$ in a mixture is defined by the equation

$$RT \ln a_{CaCO_3} = \bar{F}_{CaCO_3} = \bar{E}_{CaCO_3} - T\bar{S}_{CaCO_3}$$

According to Temkin

$$\bar{S}_{CaCO_3} = -R \ln N_{Ca}$$

Thus, we have

$$RT \ln \frac{a_{CaCO_3}}{N_{Ca}} = \bar{E}_{CaCO_3}$$

The activity coefficient of $CaCO_3$ may be defined as

$$\gamma_{CaCO_3} = \frac{a_{CaCO_3}}{N_{Ca}} = \frac{\bar{E}_{CaCO_3}}{RT}$$

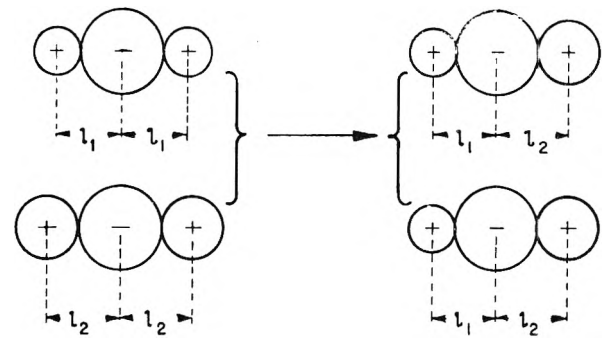

$$\frac{1}{2l_1} + \frac{1}{2l_2} > \frac{2}{l_1 + l_2}$$

Fig. 1.—Change in the cation–cation repulsion energy by the process of mixing.

Experimental

The free energy or the activity of $CaCO_3$ in a fused mixture of other salts may be determined by investigating its thermal decomposition in the mixture. An earlier investigation of this kind has been carried out by Flood, Forland and Roald.[6]

If pure calcium carbonate is heated in an atmosphere of CO_2 at normal pressure, the calcium carbonate will decompose completely into calcium oxide and carbon dioxide at a temperature of about 900°. If, however, the calcium carbonate is dissolved in a fused salt, the decomposition by heating of the calcium carbonate will proceed until a certain concentration of it is reached in the mixture and the equilibrium

$$CaCO_{3(\text{in mixture})} = CaO_{(s)} + CO_{2(gas)}$$

will be established. The concentration of calcium carbonate in a certain fused salt will depend on the temperature and the pressure of carbon dioxide above the melt. CaO was found to be insoluble in the melts investigated.

The experiments were carried out in the following manner. A platinum crucible containing weighed amounts of $CaCO_3$ and Na_2CO_3 was heated in an electric furnace at different temperatures above 900°. The temperature was kept constant within about ±0.2°. CO_2 gas at different pressures ranging from 1 to 0.1 atm. was passed through the furnace. When equilibrium had been established, air was introduced in the apparatus and the crucible was quickly removed. After cooling it was weighed again. From the weight loss, the amount of CO_2 expelled was found and from that the amount of $CaCO_3$ left was determined.

Evaluation of the Measurements.—From these equilibrium measurements the activity of calcium carbonate may be calculated. The activity of calcium carbonate in the fused mixture we denote by a_{CaCO_3} and the CO_2 pressure by p. The activity

(5) J. H. Hildebrand and R. J. Salstrom, *J. Am. Chem. Soc.*, **54**, 4257 (1932).

(6) H. Flood, T. Forland and B. Roald, *ibid.*, **71**, 572 (1949).

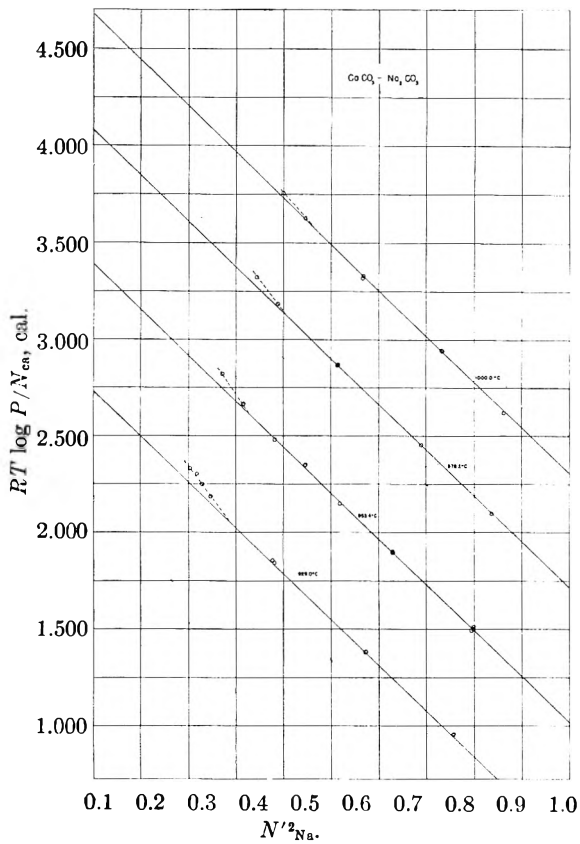

Fig. 2.—The connection between CO_2 pressure (p) and composition of the melt at different temperatures for the system $CaCO_3$–Na_2CO_3.

of solid calcium carbonate we denote by a_s and the CO_2 pressure above it by p_s. Then we have

$$\frac{a_{CaCO_3}}{a_s} = \frac{p}{p_s}$$

Now we will introduce a third state of calcium carbonate: the pure liquid calcium carbonate at the same temperature. This state we will use as the standard state for the calcium carbonate and we will denote its activity by a_{liq}. Introducing this in the above equation, we have

$$\frac{a_{CaCO_3}}{a_{liq}} \times \frac{a_{liq}}{a_s} = \frac{p}{p_s}$$

Taking the logarithm and multiplying by RT we get

$$RT \ln a_{CaCO_3} + RT \ln \frac{a_{liq}}{a_s} = RT \ln \frac{p}{p_s}$$

$RT \ln a_{liq}/a_s$ is the free energy change when calcium carbonate goes from the pure solid to the pure liquid state; that means it is the free energy of fusion, which we will denote by ΔF_f. Then we have

$$RT \ln a_{CaCO_3} = RT \ln p - RT \ln p_s - \Delta F_f$$

Further we can divide the activity into an energy term and an entropy term

$$RT \ln a_{CaCO_3} = \bar{F}_{CaCO_3} = \bar{E}_{CaCO_3} - T\bar{S}_{CaCO_3}$$

and if we use the Temkin model for the entropy, $\bar{S} = -R \ln N_{Ca}$, we get

$$\bar{E}_{CaCO_3} + RT \ln N_{Ca} = RT \ln p - RT \ln p_s - \Delta F_f$$

or

$$RT \ln \frac{p}{N_{Ca}} = \bar{E}_{CaCO_3} + RT \ln p_s + \Delta F_f$$

Here $\bar{E}_{CaCO_3}$ is the partial energy of mixing which depends upon the composition of the melt and it should be practically independent of the temperature. Further, the terms $RT \ln p_s + \Delta F_f$ are dependent only on the temperature and are independent of the composition. Therefore, if we plot $RT \ln p/N_{Ca}$ as a function of composition at different temperatures, the curves corresponding to the different temperatures should only differ in the term $RT \ln p_s + \Delta F_f$ which is independent of the composition. Therefore, the distance between two curves should be the same over the whole concentration range, if the expression for the entropy is correct. Such a plot is shown in Fig. 2 for the system Na_2CO_3–$CaCO_3$. As is seen from the figure, the experimental points fall fairly close to parallel lines. The concentration range and the temperature range are not very wide, but the use of the ionic fraction in the entropy term N_{Ca} as is shown here gives a slightly better agreement than the use of the electrical equivalent fraction N'_{Ca}.

Next we will consider the heat of mixing. The following expression for the partial heat of mixing of calcium carbonate was derived

$$\bar{E}_{CaCO_3} = N'^2_{Na} \times b_{NaCa}$$

Introducing this in the equation above, we have

$$RT \ln \frac{p}{N_{Ca}} = N'^2_{Na} \times b_{NaCa} + RT \ln p_s + \Delta F_f$$

On Fig. 2, $RT \ln p/N_{Ca}$ is plotted against N'^2_{Na} and at a constant temperature this plot gives a straight line. From its slope b_{NaCa} is found to be -2370 cal.

At the highest concentrations of $CaCO_3$, a deviation from the straight line relationship occurs. An

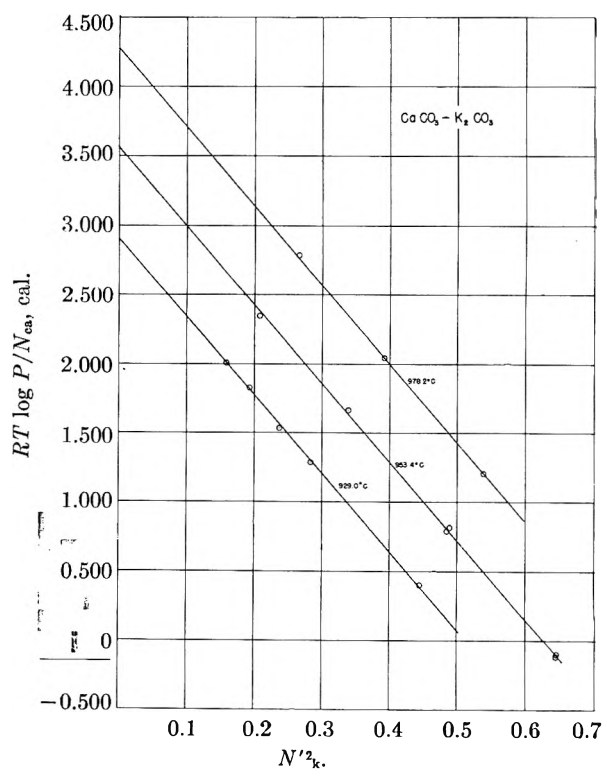

Fig. 3.—The connection between CO_2 pressure (p) and composition of the melt at different temperatures for the system $CaCO_3$–K_2CO_3.

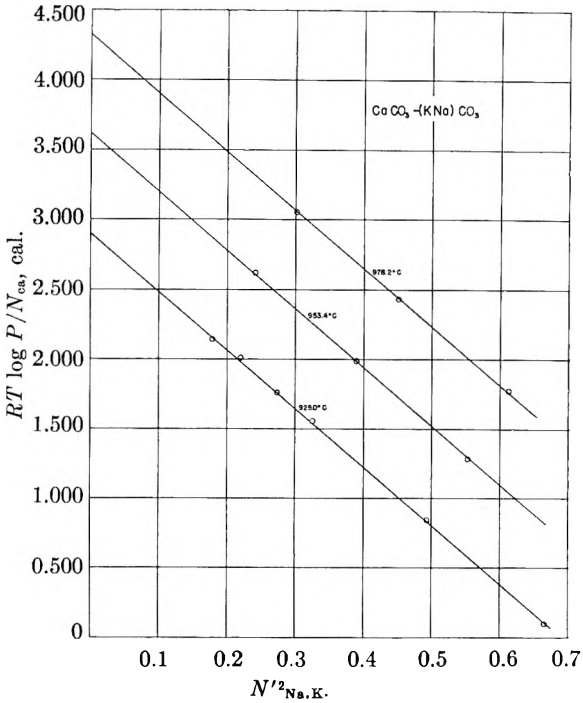

Fig. 4.—The connection between CO_2 pressure (p) and composition of the melt at different temperatures for the system $CaCO_3$-$(KNa)CO_3$.

entropy change also must take place here as the break in the curves at the different temperatures does not occur at the same composition of the melt. The deviation may be due to a change in the structure of the liquid when the $CaCO_3$ content exceeds a certain amount.

If we extrapolate the straight lines to $N'^2_{Na} = 0$, we will get the CO_2 pressure above $CaCO_3$ in our standard state which is pure liquid $CaCO_3$. The CO_2 pressure above solid $CaCO_3$ is known[7]

$$(RT \ln p_a = -44{,}284 - 6.356T \log T + 1.3 \times 10^5 T^{-1} - 10^{-3} T^2 + 58.47T)$$

From the ratio of these two pressures we may calculate the free energy of fusion ΔF_f.

The same kind of experiments have been carried out for the system K_2CO_3–$CaCO_3$. The results are shown in Fig. 3. We obtain a relationship similar to that obtained in the system Na_2CO_3–$CaCO_3$. From the slope of the straight line we obtain $b_{KCa} = -5700$ cal. As before, we can find the free energy of the standard state by extrapolating the straight lines.

A third series of experiments was carried out on the system Na_2CO_3–K_2CO_3–$CaCO_3$ having equal amounts of sodium and potassium. From the equation derived previously the partial heat of mixing for $CaCO_3$ should be

$$\bar{E}_{CaCO_3} = N'^2_{NaK}\left(\frac{b_{NaCa} + b_{KCa}}{2} - {}^1/_4\, b_{NaK}\right)$$

where N'_{NaK} is the electrical equivalent fraction of the mixed alkali. Here b_{NaCa} and b_{KCa} are known from the preceding investigations. b_{NaK} is not known, but the ions Na^+ and K^+ are very similar to one another as compared to the Ca^{2+} ion so the term

(7) T. Forland, unpublished.

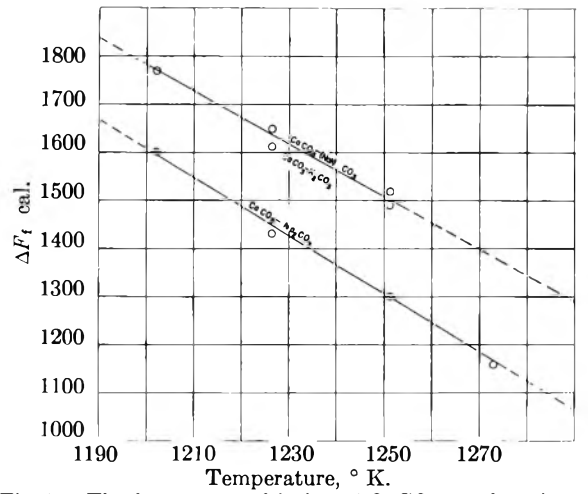

Fig. 5.—The free energy of fusion of $CaCO_3$ as a function of temperature.

$^1/_4\, b_{NaK}$ may be expected to be small compared to the other terms of the equation.

The results of these experiments are shown in Fig. 4. From the slope of the straight lines we have $b_{(NaK)Ca} = -4190$ cal. This may be compared to the middle of the b-values for the sodium system and the potassium system

$$\frac{b_{NaCa} + b_{KCa}}{2} = -4040 \text{ cal.}$$

The difference is 150 cal. If the term $^1/_4\, b_{NaK}$ were not negligible, one might expect the difference to be larger.

As mentioned before, the free energy of fusion of calcium carbonate may be obtained by extrapolating the straight lines to $N'^2_{(alkali)} = 0$. This free energy of fusion is the free energy change when calcium carbonate goes from the solid state to a liquid state which has the same structure as the calcium carbonate dissolved in the alkali carbonate. This free energy of fusion does not necessarily have to be the same as that obtained when the calcium carbonate is fused to form a pure liquid.

By plotting the free energy of fusion as a function of temperature we may find the heat of fusion and the melting point. Such a plot is shown in Fig. 5.

The heats of fusion and melting points obtained in this way are listed below:

From the system	Heat of fusion of $CaCO_3$, cal.	M. p. of $CaCO_3$, °C.
$CaCO_3$–Na_2CO_3	8800	1190
$CaCO_3$–K_2CO_3	8300	1250
$CaCO_3$–$(KNa)CO_3$		
Direct measurement at 1000 atm.		1340
Recalcd. to 1 atm.		*ca.* 1300

The data for $CaCO_3$ found by extrapolating the straight line in the system $CaCO_3$–Na_2CO_3 must correspond to a hypothetical state since a distinct deviation from the straight line was found at higher concentrations of $CaCO_3$. For the systems $CaCO_3$–K_2CO_3 and $CaCO_3$–$(KNa)CO_3$ no deviation was found within the range investigated. Therefore, the data for $CaCO_3$ obtained by extrapolation in these cases may correspond to the real fused $CaCO_3$ and may be checked against data for the pure $CaCO_3$.

The heat of fusion of $CaCO_3$ is not known, but the melting point was found to be 1340° under a CO_2 pressure of about 1000 atm. by Smyth and Adams.[8] In order to recalculate this melting point to a pressure of about 1 atm., one should know the volume change of $CaCO_3$ by melting, and this is not known. If we assume, however, a volume increase by melting of 20%, the melting point should be lowered by about 40° going from 1000 to 1 atm. This gives a melting point for $CaCO_3$ of about 1300°. This melting point is somewhat higher than the melting point obtained from the systems $CaCO_3$–K_2CO_3 and $CaCO_3$–$(KNa)CO_3$. However, measurements in progress by Drs. R. I. Harker and O. F. Tuttle[9] indicate that the decomposition of $CaCO_3$ at a certain pressure occurs at an appreciably lower temperature than that given by Smyth and Adams. This could also be an indication that the melting point of $CaCO_3$ is lower than that reported by these authors. It may here be mentioned that if we had used the electrical equivalent fraction in the entropy term, we would have found melting points of $CaCO_3$ around 1030°, which is unreasonably low.

(8) F. H. Smyth and L. H. Adams, *J. Am. Chem. Soc.*, **45**, 1167 (1923).

(9) O. I. R. Harker and O. F. Tuttle, College of Mineral Industries, The Pennsylvania State University, private communication, August, 1954.

As was mentioned earlier, the heat of solution of $CaCO_3$ in $(KNa)CO_3$ was about 150 cal. higher than the middle of the heats of solution in K_2CO_3 and Na_2CO_3. From Fig. 5 we can now see that the free energy of the standard state of $CaCO_3$ is about 180 cal. lower for the system $CaCO_3$–Na_2CO_3. This difference in standard state may to some extent explain the deviation from additivity of the heat of solution of $CaCO_3$ in the mixed alkali carbonate.

Concluding we may say that the experiments indicate that the entropy of mixing for a simple ionic mixture is given by a random distribution of ions of the same sign regardless of their numbers of charges. The energy of the mixed system may with a good approximation be expressed as a sum of energies characteristic for each pair consisting of a cation and another cation in the second coördination sphere, taking into account that the number of these neighbors may change with the composition of the mixture. Finally, structural differences for the components of a mixture may in some cases play a role.

Acknowledgment.—The author wishes to thank Professor H. Flood and Research Associate K. Grjotheim of the Institute of Silicate Science for valuable discussions.

THE DISPROPORTIONATION AND VAPOR PRESSURE OF $TiCl_3$[1]

BY MILTON FARBER AND A. J. DARNELL

Jet Propulsion Laboratory, California Institute of Technology, Pasadena, Cal.

Received September 26, 1954

The heat of reaction for the disproportionation of $TiCl_3(s)$ into $TiCl_4(g)$ and $TiCl_2(s)$ and also the vapor pressure and heat of sublimation of $TiCl_3$ have been determined by means of a molybdenum effusion cell. The temperature range of the effusion experiments was 600–740°K. A value of 38 ± 1 kcal./mole at 298°K. was obtained for the heat of reaction for the disproportionation of $TiCl_3$ The heat of sublimation of $TiCl_3$ was found to be 42 ± 1 kcal./mole at 298°K. from which an approximate boiling point of 1200°K. was estimated for $TiCl_3$. The entropy of reaction for the disproportionation of $TiCl_3$ was calculated as 38 e.u at 298°K. while the entropy of sublimation of $TiCl_3$ was 37 e.u. at 298°K. The partial pressures of $TiCl_4$ resulting from the disproportionation of $TiCl_3$ range from 0.005 mm. at 636°K. to 0.200 mm. at 732°K. while the vapor pressure of $TiCl_3$ varies from 0.0002 to 0.010 mm. over the same temperature range.

I. Introduction

A study has been made of the disproportionation and vapor pressure of $TiCl_3$ by the effusion cell method. The effusion cell was chosen for this investigation since it allows the study of the simultaneous molecular free flow of both $TiCl_3$ vapor and $TiCl_4$ vapor and the use of lower temperatures. The disproportionation of $TiCl_3$ takes place in the following manner

$$2TiCl_3(s) = TiCl_4(g) + TiCl_2(s) \qquad (1)$$

This fact has been established by an analysis of the material which was left behind after completion of the disproportionation reaction and was found to be $TiCl_2$. Therefore a determination of the $TiCl_4$-(g) pressure in equilibrium with the $TiCl_3(s)$ and $TiCl_2(s)$ yields the necessary data for the calculation of the disproportionation reaction. At the same time the determination of the $TiCl_3(g)$ pressure yields the necessary data for the calculation of heat of sublimation of $TiCl_3$.

The stipulation for employing an effusion cell is that the pressures of the $TiCl_3(g)$ and $TiCl_4(g)$ in equilibrium are low enough and thus the mean free paths high enough so that free molecular flow prevails. In practice this can be obtained in an effusion cell of the Knudsen type if the radius of the effusion hole is equal to or smaller than the mean free path.

The equation for obtaining the vapor pressure of a gas assumed to be in equilibrium with a condensed phase by means of an effusion cell was given by Knudsen[2] as

$$p = \frac{G\sqrt{2\pi RT/M}}{At} \qquad (2)$$

(1) This paper presents the results of one phase of research carried out at the Jet Propulsion Laboratory, California Institute of Technology, sponsored by the Department of Army, Ordnance Corps, and the Department of Navy, Office of Naval Research, under Contract No. DA-04-495-ORD 18.

(2) M. Knudsen, *Ann. physik*, **28**, 75 (1909).

where

G = weight of material effused
A = area of hole
T = absolute temperature
M = molecular weight of vapor
R = gas constant
t = time

However, equation 2 applies only for an orifice in an infinitely thin plate which would allow any molecule striking the hole from any solid angle to go through. When the orifice is mounted in a plate of finite thickness, it is necessary to correct for the number of molecules that are reflected from the orifice wall. Another correction to the Knudsen equation must be applied for the actual operating pressure, since the region of true molecular flow is one in which the mean free path is very large in comparison to the hole size so that no collisions take place between molecules while they are going through the hole. This correction denoted as F/F_t, has also been made by Knudsen[2] by applying an empirical relationship containing the contributions of both viscous and free molecular flow through an orifice. This correction is under 5% as long as the mean free path, L, is greater than the radius of the effusion hole.

Since the mean free path, L, has not been determined experimentally for either $TiCl_3$(g) or $TiCl_4$(g), an estimate of this quantity was made for $TiCl_4$ from critical constants as given by Skinner, Beckett and Johnston.[3] An estimate of the van der Waals b can be obtained from the critical constants by the equation

$$b = \frac{RT_c}{8P_c} \tag{3}$$

where

T_c = critical temperature in °K
P_c = critical pressure in atm

the molecular diameter δ is then given as

$$\delta^3 = \frac{3b}{2\pi N_A} \tag{4}$$

where N_A = Avogadro's number. The mean free path, L, can now be obtained from the relationship

$$L = \frac{2.33 \times 10^{-20} T}{P_{mm}\delta^2} \tag{5}$$

(where δ is in cm. and T in °K., p in mm.). The thermal expansion of the molybdenum orifices is very small, and no corrections are needed in the temperature range employed.

Applying corrections for orifice thickness and molecular collisions the effusion equation 2 employed in the experimental measurements becomes

$$p = \frac{17.14G\sqrt{T}}{K(F/F_t)At\sqrt{M}} \tag{6}$$

where p is given in mm., and all other quantities in c.g.s. units. The term K is the correction factor for orifice plate thickness. Equation 6 can be employed for calculating either the partial pressure of $TiCl_3$(g) or partial pressure of $TiCl_4$(g) by inserting the appropriate molecular weights for M and weights of effused material for G as

$$p_{TiCl_3(g)} = \frac{17.14G_{TiCl_3}\sqrt{T}}{K(F/F_t)At\sqrt{M_{TiCl_3}}} \tag{7}$$

$$p_{TiCl_4(g)} = \frac{17.14G_{TiCl_4}\sqrt{T}}{K(F/F_t)At\sqrt{M_{TiCl_4}}} \tag{8}$$

II. Experimental Method

A schematic diagram of the apparatus is shown in Fig. 1. A dry-box is mounted at the entrance end of the quartz tube since the slightest trace of moisture tends to cause $TiCl_3$ to decompose and become contaminated. The dry-box is flushed thoroughly with dry He for a considerable length of time before opening any apparatus containing $TiCl_3$. A positive pressure flow of He dried over liquid N_2 is maintained in the box at all times. Calcium hydride which removes water (equilibrium water pressure is lower than 10^{-15} mm. at 25°) is placed in a small desiccator in the dry-box. The orifice plates are also kept in a calcium hydride desiccator. The cells are placed in vacuum tight weighing bottles. The manipulation of the apparatus inside the dry-box is handled through surgeon-type gloves.

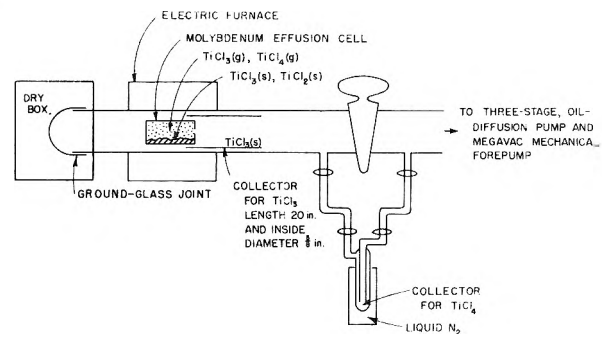

Fig. 1.—Schematic diagram of effusion cell apparatus.

The cell in Fig. 1 is located in the quartz tube inside a Pyrex sleeve which is employed for collecting the $TiCl_3$. The sleeve extends for a considerable distance beyond the end of the furnace into the cold region where the $TiCl_3$ can condense upon striking the cold wall. The plate was made long enough to collect the entire amount of $TiCl_3$ effusing through the hole. The length of the collecting tube was 20 in. with a diameter of ⅝ in. Employing the cosine law over 99% of the molecules effusing would strike the walls of the collecting tube. The furnace which is nichrome wound (600 watts) is controlled to ±1° by a Leeds and Northrup constant temperature regulator D (Series 4000). The thermocouples employed were chromel–alumel and were calibrated with a Bureau of Standards platinum–rhodium thermocouple. The thermocouples were inserted directly into the body of the cell. Calibrations were made for time necessary for the cell to reach a constant temperature. The manifold pressure was read by means of an ion gage tube and recording device. The vacuum was obtained by a Distillation Product 3-stage oil diffusion pump and a megavac fore pump which gave a vacuum of better than 10^{-6} mm.

The $TiCl_3$ employed in these experiments was made at this Laboratory[4] by a modification of the method described in the literature[5] involving the H_2 reduction of $TiCl_4$ at a temperature of 600°. The $TiCl_4$ was obtained in sealed capsules from the Bureau of Standards. By analyses the $TiCl_3$ was found to be 99% pure. Any volatile matter such as $TiCl_4$ was removed by effusion preliminary to running the experiment.

The effusion cells employed were made of either molybdenum or stainless steel with molybdenum orifice plates in four sizes which ranged from 0.020 to 0.052 in. in diameter. These materials were chosen after corrosion tests with the

(3) G. B. Skinner, C. W. Beckett and H. L. Johnston, Technical Report No. 102-AC 49/2-100-1, January 1, 1950, Cryogenic Laboratory, Department of Chemistry, Ohio State University.

(4) The $TiCl_3$ was prepared by Mr. Stephen Vango at this Laboratory in an apparatus that was a completely sealed system involving no stopcocks in which the $TiCl_4$ was introduced by vacuum distillation.

(5) W. C. Schumb and R. G. Sundstrom, *J. Am. Chem. Soc.*, **55**, 596 (1933).

compounds employed showed no reaction in the temperature range of the investigation. The variation in hole size was necessary to ascertain equilibrium at any temperature, since a criterion for equilibrium is that a change in orifice area has no effect on the pressure calculated from the effused material. The $TiCl_4$ was determined by an actual weight of the effused material while the $TiCl_3$ was dissolved in water and determined optically and checked by gravimetric analyses. The sum of the weights of the $TiCl_3$ and $TiCl_4$ effused was equal to the weight loss in the cell within the experimental accuracy. The effusion rate as a function of time was taken in order to test for the possibility of the existence of a solid solution of $TiCl_2$ in $TiCl_3$. After an initial fall off which occurred during the first few percentage decomposition the effusion rate remained constant until nearly all of the sample had been converted to $TiCl_2$ and $TiCl_4$. The fall off near the end was believed to be diffusion controlled. Table I gives the results of a typical experiment showing the rate of effusion as a function of the percentage of the sample disproportionated. The flat portion of the data was used in calculating the pressures inside the cell.

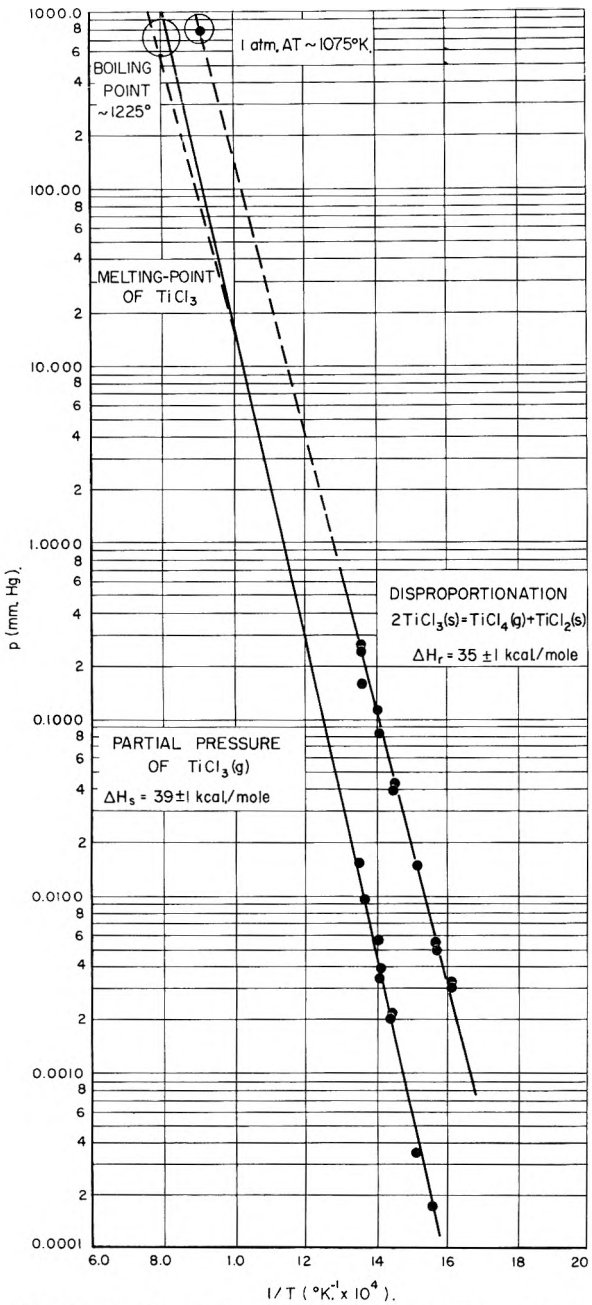

Fig. 2.—A plot of the vapor pressure of $TiCl_3$ and the pressure of TiC_4 from the disproportionation of $TiCl_3$ as a function of the reciprocal of the absolute temperature.

TABLE I

EFFUSION RATE AS A FUNCTION OF PERCENTAGE OF DISPROPORTIONATION OF $TiCl_3$

Initial wt. $TiCl_3$ sample, 1.5435 g.; temp., 710°K.; radius of orifice, 0.355 cm.

Time interval, hr.	Wt. $TiCl_4$ effused, g./hr.	% of sample disproportionated
0.5	0.142	9.48
1	.0858	18.5
1	.0870	27.7
1	.0860	36.8
1	.0877	46.0

III. Discussion of Results

The experiments were performed over a range of temperatures from 618 to 732°K. which resulted in pressures for disproportionation ranging from 0.003 to 0.250 mm. Vapor pressures of $TiCl_3$ below 636°K. were not measured. At 636°K. the measured vapor pressure of $TiCl_3$ was 0.00018 mm. and rose to 0.0093 mm. at 732°K. It was found that this temperature range was suitable for the operation of the cell in the free molecule range wherein the mean free path correction would be very small.

The calibration of the orifice areas of the effusion cell was made with mercury, since its vapor pressure has been determined by a number of investigators, and all the results were found to be in good agreement.[6] The equilibrium pressure for either $TiCl_3(g)$ or $TiCl_4(g)$ inside the cell can be calculated from equations 7 or 8 when the amount of effused material G is obtained and the correct value for KA is known. The various factors for obtaining the pressures are tabulated in Table II. This table gives the experimental data and calculations for hole size, temperatures, weights of effused material, equilibrium pressures and free energies of reaction and also the correction factors for orifice thickness and mean free path. The mean free path for $TiCl_4$ was calculated by employing equation 5 and the critical constants of reference 3 (p_c = 33 atm., T_c = 615°K.). A molecular diameter of 5.3×10^{-8} cm. was obtained from equation 4. No estimate was made for $TiCl_3$ since it contributed only a small amount to the pressure inside the cell.

From Table II it can be seen that for a given temperature two different hole sizes were chosen. Since the variation in calculated pressure with hole size was within the scatter of the data as shown in Fig. 2, it was assumed that these measured pressures were close to the equilibrium values. However, it may be of interest to mention that when an orifice of 0.052 in. in diameter was employed at the lowest temperature investigated, namely, 608°K., non-equilibrium was indicated by the deviation of pressures measured by the two orifices, and these data therefore were omitted. The free energies listed in Table II were calculated from the thermodynamic relationship

$$\Delta F = -RT \ln K \qquad (9)$$

where

$$K = P_{TiCl_4}$$

(6) K. Neumann and E. Volker, *Z. physik. Chem.*, **A161**, 33 (1932).

TABLE II

THE EXPERIMENTAL DATA AND CALCULATIONS FOR THE DISPROPORTIONATION AND VAPOR PRESSURE OF $TiCl_3$

Exp. no.	T, °K.	Length of run, hr.	Wt. of sample, g.	Wt. of effused material, g. $TiCl_4$	Wt. of effused material, g. $TiCl_3$	Radius of hole, cm., a	Thickness of hole, cm., l	Cor. area sq. cm., A	Mean free path, cm., L	Correction for a/L, F/F_t	Correction for l/a, K	p, $TiCl_4$ mm.	ΔF, kcal./mole	p, $TiCl_3$ mm.
26	615	65.00	0.498	0.078	....	0.0355	0.0254	0.00393	1.61	0.99	0.745	0.0034	15.1	....
16	618	18.50	1.048	.048	....	.0508	.0132	.00801	1.61	.99	.885	.0032	15.0	....
22	636	5.50	0.678	.0335	0.0009	.0660	.0254	.01325	0.94	.98	.834	.0047	14.8	0.00016
21	639	14.75	0.844	.058	.0018	.0508	.0254	.00801	.94	.98	.801	.0052	14.8	.00018
15	660	14.83	1.129	.077	.0013	.0355	.0132	.00393	.38	.97	.845	.0139	14.0	.00034
23	688	5.50	0.975	.0716	.0036	.0355	.0254	.00393	.135	.96	.745	.039	13.2	.00202
25	688	5.75	0.963	.182	.0078	.0508	.0254	.00801	.135	.95	.801	.043	13.2	.00199
34	706	5.20	1.669	.071	.0038	.0254	.0254	.00226	.0762	.95	.672	.081	12.5	.0050
31	712	5.00	1.090	.192	.0085	.0355	.0254	.00393	.0468	.99	745	.117	12.2	.0057
27	732	3.25	1.428	.449	.0256	.0508	.0254	.00801	.034	1.09	801	.155	12.1	.0096
29	732	5.50	0.732	.216	....	.0254	.0254	.00226	.022	1.03	.672	.225	11.4	....
33	732	2.60	1.669	.257	.0175	.0355	.0254	.00393	.019	1.03	.745	.265	11.1	.0159

The logarithm of the pressure is plotted against the reciprocal of the absolute temperature in Fig. 2. Employing the van't Hoff relationship a calculated slope of 35 ± 1 kcal. is obtained for ΔH_r for the disproportionation as given by equation 1. The heat of sublimation is obtained from the Clausius–Clapeyron equation and is found to be 39 ± 1 kcal./mole for ΔH_s of $TiCl_3$. Upon extrapolation of the vapor pressure of 760 mm. and employing an estimated heat of fusion of approximately 5 kcal./mole by employing the empirical relationship as given by Wenner,[7] an approximate boiling point of 1200°K. is obtained for $TiCl_3$.

The entropy change of the disproportionation reaction can be calculated from the second law of thermodynamics

$$\Delta S = \frac{\Delta H - \Delta F}{T} \qquad (10)$$

using an estimate of the change in enthalpy from 298°K. to the temperature range of the experiments (618–732°K.). The heat capacities C_p for $TiCl_3$(s) and $TiCl_2$(s) were estimated, respectively, as 24.8 and 18.6 cal./°/mole at 298°K. by employing Kopp's rule. The value of 22.9 cal./°/mole for heat capacity of $TiCl_4$(g) at 298°K. was taken from ref. 3. These values give −8.1 cal./°/mole for ΔC_p at 298°K. for the disproportionation reaction as given by equation 1.

mean temperature (675°K.) to 298°K.

$$\Delta S_{298}^{675} = \Delta C_p \ln \frac{675}{298} \qquad (11)$$

Equation 11 gives a value of ΔS_{298}^{675} of −6 entropy units. The value for ΔS_r at 298°K. becomes 38 entropy units. This value is in close agreement with an estimated value of 39 entropy units, which is obtained by employing Brewer's[8] data for the entropies of $TiCl_3$ and $TiCl_2$ (35 and 25 entropy units, respectively) and the value of 84 entropy units for $TiCl_4$(g) from ref. 3.

The entropy of sublimation of $TiCl_3$ can also be obtained from equation 10 after calculating the free energy from the vapor pressure data. The free energy of sublimation of $TiCl_3$ at 688°K. is 17.6 kcal./mole. The entropy of sublimation ΔS_s (in entropy units) at 688°K is

$$\Delta S_s = \frac{39{,}000 - 17{,}600}{688} = 31 \pm 1 \qquad (12)$$

An estimated entropy of sublimation of 298°K. can be obtained from Wenner's curves[7] for gaseous entropies and Brewer's value[8] for the entropy of $TiCl_3$(s). Using these data an entropy of sublimation of 37 entropy units is obtained. This value is in good agreement with the experimental value since the entropy change from 298 to 688°K. is calculated to be of the order of 6 to 8 entropy units, employing a reasonable estimate of from −8 to −10 cal./°/mole for the change in specific heats from $TiCl_3$(s) to $TiCl_3$(g). A summary of the thermodynamic data is given in Table III.

TABLE III

THERMODYNAMIC PROPERTIES OF THE DISPROPORTIONATION AND VAPORIZATION OF $TiCl_3$

Disproportionation of $2TiCl_3(s) = TiCl_4(g) + TiCl_2(s)$		Vaporization of $TiCl_3(s) = TiCl_3(g)$	
ΔH at 675°K. (kcal./mole)	35 ± 1	ΔH_s at 688°K. (kcal./mole)	39 ± 1
ΔF at 675°K. (kcal./mole)	13.5	ΔF_s at 688°K. (kcal./mole)	17.6
ΔS at 675°K. (entropy units)	32 ± 1	ΔS_s at 688°K. (entropy units)	31 ± 1
ΔC_p (cal./°/mole), approx.	−8.1	ΔC_p (cal./°/mole), approx.	−9
ΔH_{298} (kcal./mole)	38 ± 1	ΔH_{s298} (kcal./mole)	42 ± 1
ΔS_{298} (entropy units)	38 ± 1	ΔS_{s298} (entropy units)	37
ΔF^a		ΔF_s^b	

[a] $\Delta F = RT \ln K = 38{,}000 - 8.1(T - 298) - T\left(38 - 8.1 \ln \frac{T}{298}\right)$ cal./mole where T is given in °K. [b] $\Delta F_3 = RT \ln p = 43{,}000 - 9(T - 298) - T\left(37 - 9 \ln \frac{T}{298}\right)$ cal./mole where T is given in °K.

The entropy of reaction ΔS_r as calculated from equation 10 is found to be 32 entropy units in the temperature range investigated. The entropy at 298°K. can be estimated by correcting for the change in entropy from the

(7) R. R. Wenner, "Thermochemical Calculations," McGraw-Hill Book Co., New York, N. Y., 1941.

(8) L. Brewer, L. A. Bromley, P. W. Gillis and N. L. Lofgren, Met. Lab. Report CC-3585, "The Thermodynamic Properties of the Halides."

INFLUENCE OF CAPILLARITY ON THE BOILING POINT OF WATER

BY M. L. LAKHANPAL, R. K. SUD AND BALWANT RAI PURI

Department of Chemistry, Panjab University, Hoshiarpur, India

Received June 22, 1954

An apparatus for determining boiling points of capillary condensed moisture has been described. Boiling points of water held up in four different porous bodies, at different relative vapor pressures, were determined by means of this apparatus and the results obtained were compared with the theoretical values derived from thermodynamic considerations. The results offer support to the theory of capillary condensation.

There is sufficient evidence as summed up by Puri, Sharma and Lakhanpal[1] that capillary forces believed to be responsible for the adsorption of vapors by porous bodies cause considerable depressions in the freezing points of the adsorbed substances. The influence of capillarity on boiling points of adsorbates, however, does not appear to have been investigated so far. In the present paper a method for determining boiling points of water held in porous bodies has been described and the results obtained in the case of four different bodies (silica gel, sugar charcoal, a sample of bentonite and a sample of clay-loam) in equilibrium with different relative vapor pressures of water have been compared with the theoretical values.

Experimental

Apparatus.—The apparatus used in these investigations is shown in Fig. 1. It consists essentially of a manometer

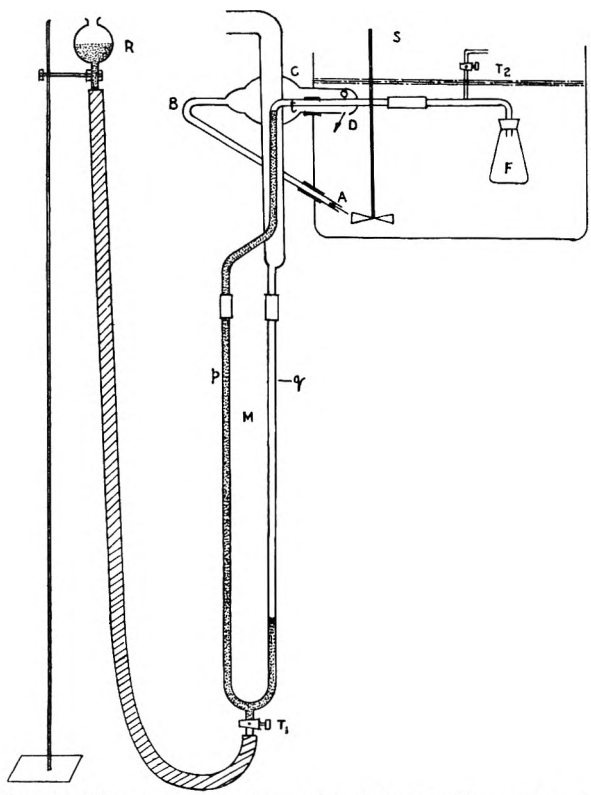

Fig. 1.—The apparatus for determining boiling point of water held in porous bodies.

M, with its limb p, communicating with the conical flask F, (40-ml. capacity) which contains the substance under examination and its limb, q, communicating directly with the atmosphere. The manometer is also connected with the reservoir of mercury R, through the stopcock T_1. The flask F is placed in an oil-bath as shown in the figure and can be connected to a vacuum pump through the stopcock T_2. The stirrer, S is worked mechanically which not only helps in keeping the temperature of the bath uniform but also pushes up the circulation of the oil through the side tube ABCD, which in its upper part CD, serves as a jacket round the tube t.

Procedure.—About 20-g. portions of the silica gel and sugar charcoal and about 40-g. portions of the samples of bentonite and clay-loam were kept in vacuum desiccators, maintained at 28 (±1°) containing sulfuric acid–water mixtures corresponding to different relative vapor pressures of water, till the equilibrium was attained. The samples were then taken for boiling point determinations, one after the other. For this purpose, the sample under examination was transferred to the flask F, so as to fill it by more than three-fourths. The reservoir R was kept quite low so that mercury in the manometer stood almost at the bottom of the two limbs p and q. The apparatus was then evacuated by working a vacuum pump at T_2 for about a minute or so. The mercury columns in p and q then stood as shown in the figure. The temperature of the oil-bath was then allowed to rise gradually and with this the vapor pressure of the system also began to increase. This resulted in the fall of mercury level in the limb p, which was made good by raising the reservoir R. This was continued and the difference of the mercury level in the two limbs, p and q, decreased progressively with gradual rise in temperature and disappeared altogether at a certain temperature. This temperature gave the boiling point of the system at the prevailing atmospheric pressure.

The vapor pressure of the system at any temperature was, obviously, given by the barometer reading less the difference between the mercury levels in the two limbs (p and q) at that temperature. By plotting vapor pressure–temperature curve of the system, it was possible to extrapolate the temperature at which the vapor pressure of the system would become equal to 760 mm. This temperature gave the boiling point of the system at the normal pressure.

The technique was tested by determining boiling points of a number of pure liquids.

Theoretical Calculation of the Boiling Point Elevation of Capillary Condensed Water.—Assuming that liquids adsorbed by porous bodies are held up by capillary forces, the lowering of vapor pressure at the meniscus will be given by the well known Kelvin equation. When a system equilibrated at a particular value of relative vapor pressure x at a temperature, T (301° in the present case) is brought to its boiling point, say T', it shall assume, as has been shown elsewhere,[1] a new relative vapor pressure, x', given by the equation

$$\log_e x' = \log_e x \times \frac{\gamma' T'}{\gamma T'} \qquad (1)$$

where γ' is surface tension of the liquid at temperature T' and can be obtained by extrapolation. The new relative vapor pressure (x') can be calculated by means of this equation. These along with the original values of vapor pressure (x) and the pore radius (r), calculated from the Kelvin equation, are given in Table I.

(1) B. R. Puri, L. R. Sharma and M. L. Lakhanpal, THIS JOURNAL, 58, 280 (1954).

TABLE I

BOILING POINT ELEVATIONS OF WATER HELD IN THE VARIOUS POROUS BODIES AT DIFFERENT RELATIVE VAPOR PRESSURES

Relative vapor pressure (x)	Corresponding capillary radius, Å.	Relative vapor pressure (x')	Theor. b.p. elevation, $\Delta T'$	Determined boiling point elevations in the case of Silica gel	Sugar charcoal	Bentonite	Clay-loam
0.970	338.6	0.994	0.2	1.0	1.0	1.0	1.0
.865	70.5	.910	2.7	3.0	3.0	4.1	3.5
.756	36.8	.836	5.2	6.7	5.7	4.7	5.5
.557	17.5	.708	10.3	10.0	9.8	11.2	10.3
.404	11.3	.574	16.7	15.5	11.5	15.0	13.5
.220	6.8	.414	27.6	23.5	20.0	22.0	24.0
.082	4.1	.259	45.4	35.0	35.0	35.5	35.0

The elevation in boiling point (ΔT) for a given value of relative vapor pressure can be obtained from the Clausius–Clapeyron equation provided ΔT is small so that the heat of vaporization (ΔH) can be taken as constant. However, for a large range of ΔT, ΔH is no longer constant. From the variations of ΔH with temperature in the case of water, the following relationship can be deduced

$$-\log_{10}\frac{p}{p_0} = 1.523 \times 10^{-2} \times \Delta T - 0.501 \times 10^{-4} \times \Delta T^2 - 1.201 \times 10^{-7} \times \Delta T^3 \quad (2)$$

Substituting the various values of x' for p/p_0, the corresponding values of ΔT were calculated.

Results and Discussion

The boiling point elevations of water held in various adsorbents at different relative vapor pressures are given in Table I. It is interesting to note that the values obtained at a given relative vapor pressure are almost identical in the case of all the adsorbents although they were of different nature and were known to differ appreciably from one another in their moisture content–vapor pressure relationships. This shows that the boiling point elevation of the sorbed water, just like its freezing point depression,[1] depends largely on the radius of the capillary pores in which it is condensed.

The theoretical values are also included in Table I. The agreement between the determined and the calculated values is seen to be quite close up to the capillary pores of radius 17.5 Å. in the case of all the adsorbents and except for sugar charcoal it is not so bad even in the case of the next lower size, *viz.*, 11.3 Å. The validity of the agreement decreases as we approach finer capillary sizes. This shows that the Kelvin equation is probably not applicable in the case of capillaries a few molecular diameters in width.[2] The probable reasons for this have been already discussed.[1] However, the fact that the results follow the Kelvin equation for an appreciable range of vapor pressure shows that probably beyond a monolayer all liquid held up in a porous body is largely due to capillary condensation.

(2) C. Pierce, J. W. Wiley and R. N. Smith, THIS JOURNAL, **53**, 669 (1949).

ON THE THERMODYNAMICS OF THE INTERACTION BETWEEN THE SOLUTES IN DILUTE TERNARY SOLUTIONS[1]

BY HAROLD L. FRIEDMAN

Contribution from the Department of Chemistry, University of Southern California, Los Angeles, Cal.

Received August 2, 1954

In widely different ternary solutions it is found that the chemical potential, μ_1, of one solute depends linearly upon the molality, m_2, of the other if m_1 and m_2 are small. The limiting value of $(\partial\mu_1/\partial m_2)_{m_1}$ as m_1 and m_2 approach zero equals $(\partial\mu_2/\partial m_1)_{m_2}$ in the same limit and is the simplest solute 1–solute 2 interaction coefficient in such a system. This coefficient may be determined by measurements of the solubility of either of the pure solutes in the ternary solution, plus certain other measurements on the appropriate binary solution, although not without an extra-thermodynamic assumption.

McKay[2] has recently shown that many useful thermodynamic relations in ternary and higher order systems may be obtained by the application of the cross-differentiation relations. In this paper McKay's results are applied to ternary systems which obey a particular activity coefficient law, which applies to such widely different ternary systems as sodium chloride–benzene–water at 25° and carbon–sulfur–iron at 1500°. The relations between various versions of this law are derived, and the procedure for the investigation of solute–solute interaction in these systems by solubility measurements is discussed.

Preliminaries.—The application of the cross-differentiation theorem is simplest if concentrations are expressed in mole ratios or molalities. m_1 and m_2 will represent solute molalities in a ternary phase and μ_1 and μ_2 the chemical potentials[3] of the solutes. γ_1 and γ_2 are activity coefficients defined relative to hypothetical 1 molal standard states of the respective solutes in the pure solvent. ν_1 and ν_2 are the

(1) This research was supported by the U. S. Atomic Energy Commission.

(2) H. A. C. McKay, *Trans. Faraday Soc.*, **49**, 237 (1953).

(3) $\mu_i = \bar{F}_i$ in G. N. Lewis notation, the partial molal Gibbs free energy

numbers of particles produced by the dissociation of a molecule of the respective solutes at high dilution. Then for either solute

$$\mu_i = \mu_i^0 + \nu_i RT \ln \gamma_i m_i \quad (1)$$

The cross-differentiation relation leads to[2]

$$(\partial\mu_1/\partial m_2)_{m_1} = (\partial\mu_2/\partial m_1)_{m_2} \quad (2)$$

and therefore

$$\nu_1(\partial \ln \gamma_1/\partial m_2)_{m_1} = \nu_2(\partial \ln \gamma_2/\partial m_1)_{m_2} \quad (3)$$

The usual relations between the partial derivatives of several variables, two of which are independent, are also required. In the dilute ternary solutions discussed here, the solutes will be designated as components 1 and 2, and are both supposed to be at concentrations of the order of one molal or less.

The Limiting Interaction Coefficient.—The salting out of a non-electrolyte (component 1) from aqueous solution by the addition of an electrolyte (component 2) is usually found to be accurately described by the Setschenow equation[4]

$$\ln (m_{1s}/m'_{1s}) = m_2 \times \text{const.} \quad (4)$$

where m_{1s} and m'_{1s} are the solubilities of the non-electrolyte in the pure solvent and in solution containing electrolyte at molality m_2.[5] Similar solubility relations are shown by many ternary systems of importance in metallurgy,[6,7] although in these cases the subscripts of eq. 4 merely designate the respective components, without necessarily implying electrolytic behavior for either. It seems then, that eq. 4 expresses a law which is valid for a variety of ternary systems. In order to express this law in a more general form, it is convenient to first rephrase eq. 4. We define a *solubility interaction coefficient*

$$k_1 \equiv -(\partial \ln m_1/\partial m_2)_{\mu_1} \quad (5)$$

This coefficient corresponds to the constant of eq. 4 if μ_1 is the chemical potential of pure phase 1, for then $m_1 = m_{1s}'$. However, the coefficient may be evaluated at any other μ_1 value which it is experimentally feasible to hold constant. The conditions for k_1 and the constant of eq. 4 to be exactly the same are discussed in a later section.

It is apparent that in any dilute ternary system there is a second solubility interaction coefficient

$$k_2 = -(\partial \ln m_2/\partial m_1)_{\mu_2} \quad (5')$$

In some cases both constants can be evaluated experimentally, and then the relation between them is of interest, as discussed below.

By change of variables, eq. 5 becomes

$$k_1 = (\partial\mu_1/\partial m_2)_{m_1}/m_1(\partial\mu_1/\partial m_1)_{m_2} \quad (6)$$

or

$$(\partial\mu_1/\partial m_2)_{m_1}/\nu_1 RT = (\partial \ln \gamma_1/\partial m_2)_{m_1} = k_1[1 + m_1(\partial \ln \gamma_1/\partial m_1)_{m_2}] \quad (7)$$

Thus to the extent that eq. 4 is valid and $m_1(\partial \ln \gamma_1/\partial m_1)_{m_2}$ is small (or independent of m_2), μ_1 depends linearly upon m_2, or

$$(\partial\mu_1/\partial m_2)_{m_1} = \text{constant} \quad (8)$$

This sort of interaction, with m_1 fixed either at m_{1s}, the solubility of 1 in pure solvent, or at another constant value, has been observed in the dilute region in several ternary liquid metallic solutions at high temperatures[8] as well as in ternary amalgams (*e.g.*, Na–K–Hg) at room temperature.[9] It can be deduced from the equations proposed to describe the behavior of ternary mixtures of liquid organic compounds[10] and ternary regular solutions[11] that eq. 8 applies to the dilute regions of these systems too. Therefore 4 and 8 are alternative expressions for a limiting law which is applicable to a wide range of ternary systems.

A third expression for this law is given by eq. 9[4,12,13]

$$\ln \gamma_1 = a_{11}m_1 + a_{12}m_2 + b_{11}m_1^2 + b_{12}m_2^2 + c_1m_1m_2 + \ldots \quad (9)$$

for if m_2 is sufficiently small, $(\partial \ln \gamma_1/\partial m_2)_{m_1}$ is independent of m_2, as required by eq. 8. Although 9 is an unnecessarily restrictive statement of the general law, it makes it clear that the simplest interaction coefficient is

$$\lim_{\substack{m_1=0 \\ m_2=0}} (\partial\mu_1/\partial m_2)_{m_1} \quad (10)$$

which is designated the *limiting interaction coefficient*, and is equal to $\nu_1 RT\, a_{12}$ if eq. 9 is valid. This limiting interaction coefficient is symmetrical in the components, as may be seen by comparison with eq. 2. Therefore, if eq. 9 is valid, and if an analogous relation holds for the activity coefficient of the other component

$$\ln \gamma_2 = a_{21}m_1 + a_{22}m_2 + \ldots \quad (11)$$

then

$$\nu_1 a_{12} = \nu_2 a_{21} \quad (12)$$

Equation 9 also leads to an insight into a class of dilute ternary solutions to which (8) does not apply. If component 1 is an electrolyte and the solvent is water, we may write

$$\ln \gamma_1 = F(\sqrt{I}) + a_{11}m_1 + a_{12}m_2 + \ldots \quad (13)$$

Here I is the ionic strength. If component 2 is not an electrolyte, this solution will obey the general law, but if component 2 is also an electrolyte, then I is a function of m_2 as well as m_1, and eq. 13 is no longer consistent with (8), even in the limit of low m_1 and m_2. Ternary solutions in which both solutes are electrolytes exhibit a more restricted sort of regular behavior.[14]

An appropriate generalization would seem to be that the law of eq. 8 is valid if components 1 and 2 are solutes at low concentration in a multicompo-

(4) F. A. Long and W. F. McDevit, *Chem. Revs.*, **51**, 119 (1952).

(5) In this discussion of solubility, and those which follow in this paper, it is assumed that the solubility of a solid or a liquid is being measured. If one of the solutes of the ternary solution is a gas when pure, then its solubility at constant partial pressure (constant μ) can be obtained and handled by the equations employed here. However, a more powerful way to proceed would be to measure the solubility of the gas (component 1) over a range of partial pressures as well as a range of m_2, to allow the direct calculation from the data of the derivative of (8) or (10).

(6) See, for example, L. S. Darken and R. W. Gurry, "Physical Chemistry of Metals," McGraw-Hill Book Co., Inc., New York, N. Y., 1953, pp. 134, 135.

(7) J. Chipman, *Disc. Faraday Soc.*, **4**, 23 (1948).

(8) J. A. Kitchener, J. O. Bockris and D. A. Spratt, *Trans. Faraday Soc.*, **48**, 608 (1952).

(9) K. Schug and H. L. Friedman, unpublished observations.

(10) R. R. White, *Trans. Am. Inst. Chem. Engrs.*, **41**, 555 (1945).

(11) J. H. Hildebrand and R. Scott, "Solubility of Non-electrolytes," Reinhold Publ. Corp., New York, N. Y., 1952, p. 202.

(12) Ref. 6, eq. 15-9.

(13) G. Scatchard in "Proteins, Amino Acids and Peptides," E. J. Cohn and J. T. Edsall, Reinhold Publ. Corp., New York, N. Y., 1943.

(14) H. S. Harned and B. B. Owen, "The Physical Chemistry of Electrolytic Solutions," Reinhold Publ. Corp., New York, N. Y., 1950, Chap. 14.

nent system in which long range interactions are not important in determining the activities of *both* of these components. In comparing eq. 8 with Henry's law, it should be noted that Henry's law deals with the first-order effects of concentration upon activity, neglecting the second-order effects implied in the use of activity coefficients. On the other hand, eq. 8 describes a general behavior of the activity coefficients, or essentially second-order effects, arising from solute–solute interaction. Henry's law fails for solutes which dissociate in the observable low concentration region, while eq. 8 fails under the more subtly defined condition discussed above.

Aside from the problem of formulating the observed regularity in ternary solutions, there is the matter of choosing the solute–solute interaction coefficient which is most suitable for comparison from system to system, for the calculation of the entropy and enthalpy of the interaction from temperature coefficient data, or for interpretation in terms of solution structure and molecular interactions. It seems clear that of the constant of eq. 4, k_1, $(\partial \ln\gamma_1/\partial m_2)_{m_{1s}}$, and the limiting interaction coefficient, only the last is independent of m_{1s}, a quantity which enters not as an intrinsic property of the system, but as a result of the use of the solubility method for the investigation of the free energy relationships. In the past, careful workers, employing the solubility method, have chosen systems in which all of these coefficients are equal. The solubility method is so often the most convenient method for the investigation of solute–solute interaction that it seems of use to discuss its application to systems less ideally suited to it.

Experimental Aspects.—A determination of the limiting interaction coefficient in dilute ternary solutions may proceed by measurements of the solubility of either of the solutes, depending on which is most convenient. Assuming that the solubility of 1 is measured, the determination may consist of the following steps.

(1) $\ln m'_{1s}$ is plotted as a function of m_2. If the data are suitable, and eq. 8 applies to the system, then the slope (approx. $-k_1$) will be constant from $m_2 = 0$ well up into the experimentally accessible range. Omitting this step, as is sometimes done[8,15] sacrifices an opportunity to judge the consistency of the data. However, the slope of this graph is not generally exactly equal to $-k_1$, because what is measured in general in a solubility experiment is not the solubility of pure component 1 in the ternary solution, but the distribution of component 1 between two phases, one consisting of nearly pure component 1 (phase a) and the other consisting chiefly of component 3 (phase b).

By expressing $\ln m_1^b$ as a function of m_2^b and μ_1

$$d \ln m_1^b = (\partial \ln m_1^b/\partial m_2^b)_{\mu_1} dm_2^b + (\partial \ln m_1^b/\partial \mu_1)_{m_2^b} d\mu_1 \quad (14)$$

we can obtain a relation between the slope of the graph and k_1

$$[d \ln m_1^b/dm_2^b] = -k_1 + [d\mu_1/dm_2^b]/[\partial\mu_1/\partial \ln m_1^b]_{m_2^b} \quad (15)$$

(15) A. P. Altshuller and H. E. Everson, *J. Am. Chem. Soc.*, **75**, 4823 (1953).

Often it will suffice to prove that the correction term in (15) is negligible compared to k_1, and in such cases the ideal-dilute solution approximation (*i.e.*, activity coefficients equal to unity) will be adequate for the estimation of the correction term from measured concentrations. In more difficult cases it would be appropriate to formulate the solute activity coefficients as in eq. 9 and 13, using estimated or independently measured values of the coefficients. For the ideal-dilute solution approximation we have

$$(\partial\mu_1/\partial \ln m_1^b)_{m_2^b} = \nu_1^b RT \quad (16)$$

$$d\mu_1/dm_2^b = (\partial\mu_1/\partial m_2^a)_{m_3^a} \times dm_2^a/dm_2^b + (\partial\mu_1/\partial m_3^a)_{m_2^a} dm_3^a/dm_2^b \quad (17)$$

$$(\partial\mu_1/\partial m_2^a)_{m_3^a} = -RTM_1\nu_2^a \quad (18)$$

$$(\partial\mu_1/\partial m_3^a)_{m_2^a} = -RTM_1\nu_3^a \quad (19)$$

$$dm_3^a/dm_2^b = -(\nu_1^b \times dm_1^b/dm_2^b + \nu_2^b)M_3m_3^a/\nu_3^a \quad (20)$$

M_1 and M_2 are the kilogram-molecular weights of the respective components. Equation 20 is obtained from the condition of equilibrium for transfer of component 3 from phase a to phase b. Then this approximation yields

$$k_1 = -(d \ln m_1^b/dm_2^b) + (\nu_2^a/\nu_1^b)M_1 \times dm_2^a/dm_2^b - M_1M_3m_3^a(dm_1^b/dm_2^b - \nu_2^b/\nu_1^b) \quad (21)$$

Evidently the first and second correction terms in (21) arise from the solubilities of components 2 and 3, respectively, in phase a.

(2) The limiting value of k_1 as $m_2 = 0$ may be combined with $(\partial \ln \gamma_1/\partial m_1)_{m_2}$ according to eq. 7 to yield $(\partial \ln \gamma_1/\partial m_2)_{m_{1s}}$. The subscript is written as m_{1s} in this case to emphasize that the solubility procedure described determines $(\partial \ln \gamma_1/\partial m_2)_{m_1}$ for this particular value of m_1, *i.e.*, for the saturation concentration of component 1 in the absence of component 2. Since the k_1 employed is valid for $m_2 = 0$, $(\partial \ln \gamma_1/\partial m_1)_{m_2}$ may be evaluated from data for the binary 1–3 system. In general, $(\partial \ln \gamma_1/\partial m_1)_{m_2=0}$ is a function of m_1, so the value at m_{1s} should be used. If this derivative is not a function of m_1, then it reduces to $\ln \gamma_1/m_1$ and the correction involved in this step (for the variation of m_1 in the measurement of k_1) reduces to the self-interaction correction of Long and McDevit.[4]

(3) The limiting interaction coefficient may be determined from $(\partial \ln \gamma_1/\partial m_2)_{m_{1s}}$ only if the dependence of this quantity upon concentration (m_1) is known. There is no way to obtain this dependence if only solubility measurements are available for the ternary system, so in this step some sort of assumption must be made. For one thing, it may be hoped that if m_{1s} is small enough so that the $\ln \gamma_1$ in the binary 1–3 system may be expressed without the use of terms in eq. 9 higher than the first power, then the higher order interaction terms will not be important either. It seems unlikely that this assumption will always be valid, but it may be tested in a particular case by proceeding both from measurements of k_1 and k_2. In the case of salt–non-electrolyte–water mixtures, the limiting interaction coefficient with a given non-electrolyte ought to be an additive property of the ions of the electrolytes investigated.

Relation between the Solubility Interaction Coefficients.—McKay concluded,[2] in the present terminology, that $\nu_1k_1 = \nu_2k_2$, but his application of the

thermodynamic relations was not exact in this instance. The exact relation between k_1 and k_2 may be obtained by calculating the limiting interaction coefficient from each of them and equating the resulting expressions. This reduces to McKay's relation as m_{1s} and m_{2s} both become very small.

THE SOLUBILITY OF BONE MINERAL. I. SOLUBILITY STUDIES OF SYNTHETIC HYDROXYLAPATITE[1]

BY GEORGE J. LEVINSKAS[2] AND W. F. NEUMAN

School of Medicine and Dentistry, University of Rochester, Rochester, N. Y.

Received August 6, 1954

By means of high speed centrifugation, which achieves an efficient separation of the basic calcium phosphates from aqueous solutions, the problem of the solubility of the bone mineral has been reinvestigated using a relatively pure sample of crystalline hydroxylapatite. The steady state was approached satisfactorily from undersaturation and supersaturation. A number of variables: time, solid/solution ratio, *p*H, Ca/P ratio, etc., were studied. The solubility (in water containing traces of chloroform) of hydroxylapatite at 1 g./l., 24°, $\mu = 0.165$ (NaCl), *p*H $\simeq$ 7.0 averaged 1.23 and 0.711 $\times 10^{-4}$ *M* for Ca and P, respectively. This crystalline solid exhibited incongruent solubility, *i.e.*, the solutions gave a higher Ca/P ratio than that present in the solid phase in most instances.

Numerous conflicting studies of the solubility of bone mineral have been reported.[3-22] Not one of these studies has offered conclusive evidence that the system under study was at equilibrium or even reversible. By means of high speed centrifugation, which achieves an efficient separation of the basic calcium phosphates from aqueous solutions, the problem has been reinvestigated. Evidence is presented that the system, under the conditions of the present study, is reproducible and reversible. If not at final equilibrium, the system at least attains the same end-point whether approached from supersaturation or undersaturation.

Experimental

Materials.—Because bone mineral itself is variable in composition and requires drastic treatment for its isolation, a relatively pure sample of commercial hydroxylapatite, the prototype mineral of bone,[23,24] was used throughout the study. This particular preparation has been very carefully characterized by X-ray diffraction, electron micrographs, surface area measurements, etc.[25] Its composition on analysis[25] was as follows[27]: calcium, 38.0 ∓ 0.2%; phosphorus, 17.7 ∓ 0.2%, sodium, <0.01% and carbon dioxide 0.86 ∓ 0.02%. The molar Ca/P ratio was 1.66, theoretically correct for pure hydroxylapatite.

Except for the hydroxylapatite, reagent grade chemicals were employed. Distilled water was first boiled to remove dissolved CO_2 and thereafter all transfers and operations were carried out under an atmosphere of nitrogen. To minimize bacterial growth, 6–7 ml. $CHCl_3$ per liter of solution was used. This procedure was successful as shown by the absence of bacterial colonies in sterile protein broth inoculated with the contents of control flasks.

Procedure.—Hydroxylapatite, dried overnight at 115° was weighed into glass-stoppered erlenmeyer flasks; a volume of CO_2-free saline to give a solid/solution ratio of 1 g./l., unless otherwise stated, was added under nitrogen; and the flasks were sealed with paraffin and parafilm. Three different saline solutions were used: initially 0.10 *N* NaCl, later 0.165*N* NaCl and finally 0.165 *N* KCl. The flasks were immersed in a water-bath at either 37 or 24° and rotated at 21.6 r.p.m. After a suitable interval, customarily 10 days, the contents of the flasks were allowed to settle and the *p*H of the supernatant liquid was determined with a Cambridge electron-ray, Model R, *p*H meter. After centrifugation in a Spinco Model L centrifuge at 30,000 r.p.m. (approximately 80,000 × gravity) the supernatant liquid was analyzed for calcium[28] and phosphorus.[29]

Results

Reproducibility.—In preliminary experiments, the analyses of duplicate samples frequently gave widely divergent results. This variability was eliminated by two precautions: the addition of $CHCl_3$ to prevent bacterial growth and high speed centrifugation to ensure complete removal of suspended solids. A few of the earlier reports[11,16,17] commented on the problems of bacterial contamination. Colloidal suspensions of hydroxylapatite which resist ordinary centrifugation have

(1) Abstracted from the Ph.D. Thesis of George J. Levinskas, June, 1953, University of Rochester.

(2) Atomic Energy Commission Predoctoral Fellow, 1949–1952.

(3) N. Bjerrum, Paper read at the Nordic Scientist Meeting in Helsingfors, August 11, 1936. Translated from the report of the meeting, 344.

(4) C. Blarez, *Compt. rend.*, **103**, 264 (1886).

(5) A. A. Browman, Doctoral Thesis, Univ. of Chicago, 1953.

(6) F. K. Cameron and L. A. Hurst, *J. Am. Chem. Soc.*, **26**, 885 (1904).

(7) H. Danneel and K. W. Frohlich, *Z. anorg. allgem. Chem.*, **188**, 14 (1930).

(8) Y. Ericsson, *Acta Ondont. Scandinavica*, **8**, Supplement 3 (1949).

(9) I. Greenwald, *J. Biol. Chem.*, **143**, 703 (1942).

(10) E. Hayek, F. Müllner and K. Koller, *Monatsh.*, **82**, 959 (1951).

(11) L. E. Holt, Jr., V. K. LaMer and H. B. Chown, *J. Biol. Chem.*, **64**, 509 (1925).

(12) P. Jolibois and J. Maze-Sencier, *Compt. rend.*, **181**, 36 (1925).

(13) H. Kleinmann, *Biochem. Z.*, **196**, 98 (1928).

(14) R. Klement and R. Weber, *Ber.*, **74B**, 374 (1941).

(15) R. Kunin, K. L. Elmore and D. L. Johnson, basic region of the system calcium oxide–phosphorus pentoxide–water (unpublished results).

(16) A. C. Kuyper, *J. Biol. Chem.*, **159**, 417 (1945).

(17) M. A. Logan and L. W. Kane, *ibid.*, **127**, 705 (1939).

(18) M. A. Logan and H. L. Taylor, *ibid.*, **125**, 377 (1938).

(19) C. L. A. Schmidt and D. M. Greenberg, *Physiol. Rev.*, **15**, 297 (1935).

(20) J. Sendroy, Jr., and A. B. Hastings, *J. Biol. Chem.*, **71**, 783 (1927).

(21) J. Sendroy, Jr., and A. B. Hastings, *ibid.*, **71**, 797 (1927).

(22) R. Warrington, *J. Chem. Soc.*, **26**, 983 (1873).

(23) S. Eisenberger, A. Lehrman and W. D. Turner, *Chem. Revs.*, **26**, 257 (1940).

(24) W. F. Neuman and M. W. Neuman, *ibid.*, **53**, 1 (1953).

(25) W. F. Neuman, ed., Atomic Energy Report, UR-238 (1953).

(26) M. L. Washburn and M. J. Shear, *J. Biol. Chem.*, **99**, 21 (1932).

(27) The CO_2 determinations were performed by Miss B. J. Mulryan and the Na analyses by Mr. W. R. Stoll, by gravimetry and flame photometry respectively.

(28) J. H. Roe and B. S. Kahn, *J. Biol. Chem.*, **81**, 1 (1929).

(29) C. H. Fiske and Y. SubbaRow, *ibid.*, **66**, 375 (1925).

also been noted previously.[7,12,13,14] In this study, three methods for separating solid from solution were tried: ultracentrifugation; the use of dialysis tubing; and filtration through very fine-pore, sintered glass filters. Of the three methods, ultracentrifugation proved most reliable. Dialysis bags frequently developed small, unseen tears during agitation. Only a few, selected sintered glass filters gave reproducible results. Under ideal conditions, however, all three methods gave comparable values. It seems most improbable that this agreement was fortuitous; rather, it is most likely that all three methods effectively remove all suspended solid and the results of analyses represent true solution values.

Time to Attain Equilibrium.—It may be questioned whether the hydroxylapatite/water system ever attains a final equilibrium in the strict thermodynamic sense because the mineral phase undergoes spontaneous recrystallization.[30] Earlier workers in an attempt to reach a steady state have equilibrated their samples for as long as 19 months.[31] For practical purposes, a reproducible end-point was reached promptly and remained unchanged, within experimental error, from one to 77 days. Perhaps the reason such long equilibration periods were necessary in earlier studies is that the solid phase employed was not an aged, crystalline preparation as used here.

Reversibility.—Many attempts have been made to reach the same solubility end-point from both supersaturation and undersaturation conditions. Only two[8,16] were claimed to be successful. In these instances, the variability of the results left much to be desired.

Because, as shown later, the solubility results are dependent on many variables difficult to control, it was possible only after exhaustive study to select the conditions under which true reversibility could be attained. For example, the *p*H, the solid/solution ratio, the composition of the crystalline surfaces, and the ionic strength must be nearly identical in the final state whether initial conditions were undersaturated or supersaturated. The results of the reversibility experiments are given in Table I. For comparison, the results of the two earlier investigations[8,16] and the data in Table I are presented graphically in Fig. 1.

Solid/Solution Ratio.—Any substance exhibiting a definitive K_{sp} dissolves to give solution values at equilibrium that are independent of the amount of solid phase used. In Table II are the results obtained when the solid/solution ratio was varied from 0.01 to 100 g./l. Comparison of the results of the present study with those of earlier investigations[24] is difficult, yet a general relationship clearly exists: with increasing amounts of solid, the concentration of dissolved calcium rises sharply; at low solid/solution ratios, the dissolved phosphate parallels that of calcium but decreases sharply at higher solid solution ratios.

Common Ion Effects.—One would expect that addition of calcium ion to the solution before equilibration would depress the solution of phosphate ions and, conversely, addition of phosphate ions would suppress the solution of calcium ions. Such a common ion effect has been observed[3,18,19,21] although quantitative agreement is lacking. A series of flasks were prepared containing 1 g. of hydroxylapatite per liter of 0.165 *N* NaCl. Additions of $CaCl_2$ or NaH_2PO_4 were arranged to give the following initial concentrations of Ca/P (γ/ml.):

(30) W. F. Neuman and B. J. Mulryan, *J. Biol. Chem.*, **195**, 843 (1952).

(31) H. Bassett, *J. Chem. Soc.*, **111**, 620 (1917).

TABLE I

EQUILIBRIUM APPROACHED FROM UNDERSATURATION AND SUPERSATURATION

10 grams of solid per liter of solution; initial solution 0.16 *N*, composed of 0.15 *N* KCl plus 0.01*N* K barbital–barbituric acid buffer; equilibrated 10 days at 24°.

Before equilibration			After equilibration		
*p*H	*M* Ca/l. (× 10⁴)	*M* P/l. (× 10⁴)	*p*H	*M* Ca/l. (× 10⁴)	*M* P/l. (× 10⁴)
		Undersaturation			
7.42	0	0	7.30	3.02	1.35
7.42	0	0	7.33	2.94	1.33
7.42	0	0	7.27	2.82	1.44
		Supersaturation			
7.43	4.42	2.11	7.28	3.27	1.28
7.43	4.42	2.11	7.28	3.12	1.33
7.43	4.42	2.11	7.27	3.14	1.33

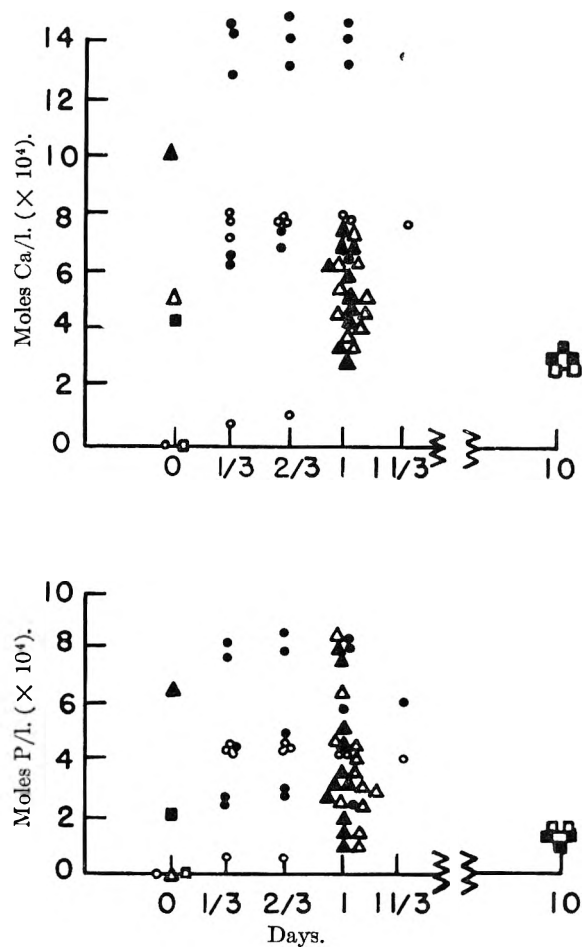

Fig. 1.—A comparison of undersaturation and supersaturation experiments. Data from Ericsson designated by circles, from Kuyper by triangles, from the present study by squares. Open figures indicate that the final state was approached from undersaturation, solid figures from supersaturation.

TABLE II

EFFECT OF SOLID TO SOLUTION RATIOS ON THE DISSOLUTION OF HYDROXYLAPATITE

Equilibrated 10 days at 24° in 0.165 *N* NaCl				Equilibrated 10 days at 24° in 0.165 *N* KCl			
G. solid/l.	Final *p*H	*M* Ca/l. (× 10⁴)	*M* P/l. (× 10⁴)	G. solid/l.	Final *p*H	*M* Ca/l. (× 10⁴)	*M* P/l. (× 10⁴)
100	6.58	15.89	0.968	100	6.70	10.97	1.16
99.8	6.51	15.74	0.995	99.8	6.62	11.35	1.14
30.3	6.74	8.33	1.10				
30.4	6.61	8.61	1.16				
10.1	6.99	4.49	1.09	10.0	6.75	3.42	1.48
9.91	6.84	4.57	1.18	10.1	6.80	3.32	1.28
				5.00	6.83	2.67	1.35
				5.02	6.77	2.56	1.39
				3.01	6.78	1.93	1.13
				3.02	6.73	1.96	1.19
2.96	6.82	2.38	1.03				
2.97	6.83	2.41	0.995				
				1.05	6.63	1.21	0.730
				1.00	6.90	1.14	0.739
0.976	7.15	1.34	0.749				
.808	6.63	1.09	.594				
.296	7.16	1.01	.542				
.297	6.73	1.07	.578				
.109	6.73	0.666	.381				
.100	6.58	.756	.387				
.0349	6.70	.579	.303				
.0289	6.84	.549	.276				
.0114	6.27	.509	.262				
.0109	6.40	.489	.224				

1000/0, 100/0, 10/0, 0/0, 0/10, 0/100, 0/1000. After 10 days of equilibration at 24°, the results given in Table III were obtained. A reciprocal relation between calcium and phosphate was observed but it did not conform to any known principle of solubility. One interesting correlation to be noted is that the addition of calcium ions depressed the equilibrium *p*H while addition of phosphate ions raised the *p*H.

TABLE III

EFFECT OF COMMON IONS ON THE DISSOLUTION OF HYDROXYLAPATITE (ULTRACENTRIFUGATION EXPERIMENTS)

1 gram solid per liter 0.165 *N* NaCl; equilibrated 9⅓ days at 24°

Initial concn. *M*/l. (× 10⁴)		Final concn. *M*/l. (× 10⁴)		Final
Ca	P	Ca	P	*p*H
25.0	...	25.4	0.144	6.27
25.0	...	22.2	0.159	6.32
2.50	...	3.17	0.465	6.68
2.50	...	3.17	0.400	6.76
0.250	...	1.38	0.629	6.80
0.250	...	1.24	0.604	6.58
...	...	1.14	0.697	6.69
...	...	1.21	0.675	6.95
...	0.322	1.02	0.891	6.87
...	0.322	1.13	0.849	6.84
...	3.22	0.594	3.21	7.24
...	3.22	0.760	3.20	7.29
...	32.2	0.178	32.9	7.86
...	32.2	0.163	32.0	7.90

Effect of *p*H.—To test the effect of varying *p*H, small amounts of HCl or NaOH were added to the saline solutions before equilibration with the hydroxylapatite. The results, given in Table IV, show that the mineral phase exerted a buffer-like action causing the *p*H to shift toward neutrality during equilibration. The quantities of calcium and phosphate which were dissolved decreased markedly as the *p*H increased. The only general relationship between *p*H and solubility collected from the literature has been given by Hodge.[32] His composite curve can be described by the relation $[Ca^{++}]/[H^+] \simeq K$. This empirical rule also describes the results of the present study as shown in Fig. 2. The

TABLE IV

EFFECT OF *p*H CHANGES ON THE DISSOLUTION OF HYDROXYLAPATITE

1 gram solid per liter 0.165 *N* NaCl; equilibrated 10⅓ days at 24°

*p*H		*M* Ca/l. (× 10⁴)	*M* P/l. (× 10⁴)
Initial (calcd.)	Final		
2.01	5.85	69.	40.3
2.01	5.67	70.7	42.9
2.82	6.22	11.3	6.16
2.82	6.34	11.8	6.26
3.30	6.68	4.62	2.25
3.30	6.68	4.62	2.18
5.00	6.88	1.26	0.646
5.00	6.54[a]	1.29	0.646
...	6.82	1.36	0.739
...	6.78[a]	1.23	0.649
9.00	6.81	2.26	1.14
9.00	6.87	1.70	0.891
10.00	6.80	0.821[b]	0.526
10.00	6.83	1.03	0.613
10.70	8.16	0.211	0.381
10.70	7.54	0.203	0.381
11.00	8.50	0.108	0.381
11.00	8.59	0.139	0.381

[a] Questionable reading. [b] Approximate value.

(32) H. C. Hodge, "Metabolic Interrelations," Josiah Macy Jr., Foundation, New York, 3rd Conference, 1951, p. 190.

reciprocal relation between calcium and hydrogen ions has been attributed to a mole for mole exchange process occurring at the crystal:solution interface[25] and explains the *p*H changes described above.

Calcium:Sodium Exchange.—In most of the experiments described above, NaCl was used to maintain a constant ionic strength. It seemed advisable to reinvestigate the extent to which sodium ion influences solubility. Accordingly, a series of flasks were prepared with varying amounts of hydroxylapatite and with KCl as the supporting electrolyte in the solution. These data, with comparable results using NaCl, are given in Table V. The principal effect of sodium ion was to increase the amount of calcium displaced or dissolved from the crystals. Slight compensatory changes were observed in the amounts of phosphate dissolved. These results are consistent with subsequent studies which have shown that sodium ions can, to a limited extent, displace surface calcium ions in hydroxylapatite by a mole for mole exchange process.[33]

TABLE V

EFFECT OF SODIUM ION ON THE DISSOLUTION OF HYDROXYLAPATITE

Equilibrated 10 days at 24°

G. solid/l.	0.165 *N* NaCl solutions Final *p*H	*M* Ca/l. (× 10⁴)	*M* P/l. (× 10⁴)	0.165 *N* KCl solutions Final *p*H	*M* Ca/l. (× 10⁴)	*M* P/l. (× 10⁴)
100	6.58	15.89	0.968	6.70	10.97	1.16
30	6.74	8.33	1.10			
10	6.99	4.49	1.09	6.75	3.42	1.48
5				6.83	2.67	1.35
3	6.82	2.38	1.03	6.78	1.93	1.13
1	7.15	1.34	0.749	6.63	1.21	0.730
0.3	7.16	1.01	0.542			
0.1	6.73	0.666	0.381			
0.03	6.70	0.579	0.303			
0.01	6.27	0.509	0.262			

Discussion

There has been considerable disagreement as to the chemical nature of the bone mineral.[24] It is not surprising, therefore, that its solubility has remained controversial.[32] The solubility properties of the bone mineral are important physiologically, however, for many theories regarding the calcification process postulate a *precipitation*. In addition, some rules of solubility, however complex, must govern the rapid interchange and turnover of bone mineral in the presence of fluctuating serum levels of calcium and phosphate.

The purpose of the present study was to re-examine the problem, starting with a well-defined material. The first criterion established was the attainment of a reproducible system, one that could be duplicated regularly. The agreement of the three different procedures for separating the solid from the solution: ultracentrifugation, sintered glass filters, and dialysis tubing, are conclusive proof that the solutions did not include suspended matter.

The second criterion was the demonstration of the attainment of equilibrium. The consistent solution values obtained with varying time and the comparable results of the undersaturation and supersaturation experiments meet the usual requirements of equilibrium state. However, there is reason to doubt that true thermodynamic equilibrium was attained. For present purposes, it is sufficient that a reproducible steady state was realized.

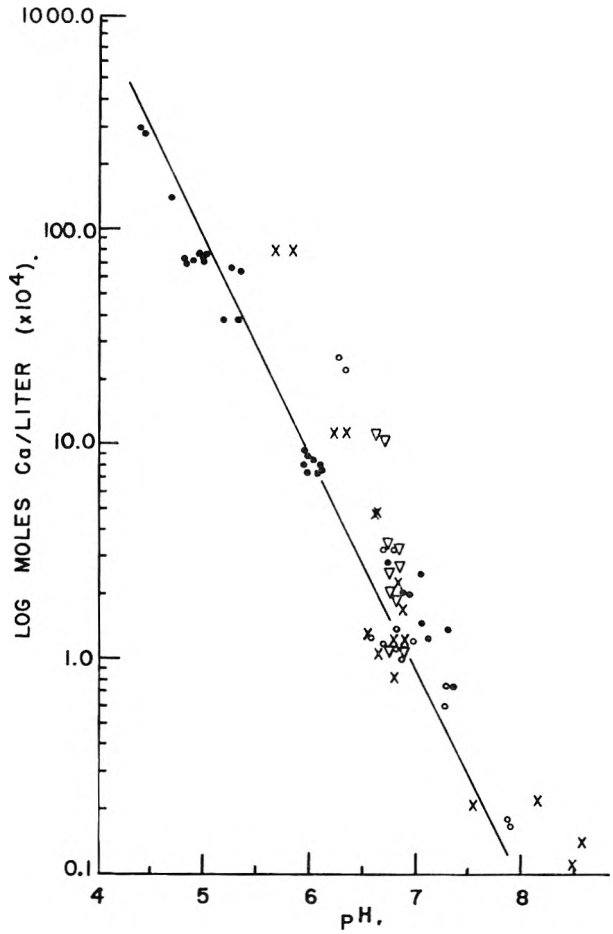

Fig. 2.—The general interrelation between calcium concentration and *p*H. The line is that predicted by Hodge's empirical rule (see text). Data from Ericsson designated by solid circles; data from common ion experiments by open circles; varying *p*H experiment by ×; from varying solid/solution experiment by triangles.

Having met these two criteria, a range of widely varying conditions were investigated, a range sufficiently wide to encompass the scattered observations of previous investigators.

The most significant finding was that solubility varied with the amount of solid phase added to a given volume of solution. This oft-observed phenomenon, in the present instance, is real evidence that the hydroxylapatite lattice exhibits incongruent solubility; it does not conform to a solubility product. This is not surprising since the solid phase is not of constant composition.[24]

The common ion effect, too, supports this same conclusion. There was no simple relation between calcium and phosphate concentrations after equilibration.

The effect of varying *p*H was consistent with the idea of incongruent solubility. While there was considerable variation, the data were best approxi-

(33) Wm. Stoll, *Federation Proc.*, **13**, 306 (1954).

mated by Hodge's empirical rule, $[Ca^{++}]/[H^+] \simeq K$, a relation that cannot be derived from solubility product considerations.

In an absolute sense it is important that the concentrations of calcium and phosphate dissolved were roughly *one tenth* those observed *in vivo*. It is clear that it is the presence of ions "foreign" to the hydroxylapatite lattice that determine the solubility of bone mineral in the living animal. The increased solubility in solutions containing sodium ion as compared with potassium solutions is evidence derived from the present study. A similar effect has been observed for citrate[16] and bicarbonate.[8] It is reasonable to suppose that magnesium[24] and ester phosphate compounds[34] also increase the solubility of bone mineral.

(34) V. D. DiStefano and W. F. Neuman, *J. Biol. Chem.*, **200**, 759 (1953).

THE COMPLEX CONDUCTIVITY OF A SUSPENSION OF STRATIFIED PARTICLES OF SPHERICAL OR CYLINDRICAL FORM[1]

BY HUGO FRICKE

Walter B. James Laboratory for Biophysics, Biological Laboratory, Cold Spring Harbor, N. Y.

Received August 16, 1954

A theoretical expression is derived for the complex conductivity of a dilute suspension of spheres or cylinders (arranged perpendicularly to the field), composed of concentric or coaxial layers of conducting dielectrics. The expression is also valid at higher volume concentrations, provided the average polarizing field acting on a suspended particle equals the average polarizing field in the suspending medium, *i.e.*, it has the value underlying the derivation of the well known Clausius–Mosotti form conductivity equation for a suspension of homogeneous particles.[7] The suspension is equivalent to a ladder type network of complex conductances, each of which is the product of the complex conductivity of the associated phase of the system and a purely geometric factor. The effect of volume concentration in the spherical expression was found in good agreement with existing observations on the permittivity of suspensions of various species of biological cells.

The dielectric properties of suspensions of heterogeneous particles have already been studied theoretically on some simple cases,[2-5] treated particularly as basis for the dielectric analysis of biological cell material. Because of the experimental development of this field in the ultrahigh frequency region, it has become desirable to extend the theory and the following generalization of an earlier model was worked out to meet this need. The problem considered is that of the complex conductivity, in an alternating field, of a suspension of spheres or cylinders, built up of any number of concentric or coaxial layers of conducting dielectrics. The axes of the cylinders are perpendicular to the field.

When the suspended particles are homogeneous, the complex conductivity $k^{(1)} = \sigma^{(1)} + j(\epsilon^{(1)}/2)f$ of the suspension can be represented by formula (1) below,[6,7] in which $k_0 = \sigma_0 + j(\epsilon_0/2)f$ and $k'_1 = \sigma'_1 + j(\epsilon'_1/2)f$ are the complex conductivities of suspending and suspended phases and v is the fractional volume of the suspended phase. The terms σ and ϵ represent conductivity (in the C.G.S. system) and dielectric constant, f is the frequency in cycles/sec., and $j = (-1)^{1/2}$.

Formula (1) rests on firm theoretical basis only when the volume concentration is vanishingly small. At higher volume concentrations, its derivation requires the assumption, for which no strict proof has yet been given, that the average polarizing field acting on a particle equals the average polarizing field in the suspending medium.[7] For spheres, this means that the particles are assumed to be in the Lorentz field. For higher volume concentrations, this requirement limits the possible theoretical validity of the formula to uniform suspensions of identical particles but, when care has been taken to approximate this condition, the formula has been found to agree well with experimental observations on spherical systems, up to concentrations near total packing[8,9]

$$(k^{(1)} - k_0)/(k^{(1)} + xk_0) = v(k_1' - k_0)/(k_1' + xk_0) \quad (1)$$

The formula contains a form factor x, the value of which is $x = 2$ for spheres, $x = 1$ for cylinders.[6,7]

The formula can be written

$$k^{(1)} = x(1 - v)k_0/(x + v) + [(1 - v)(x + v)/(1 + x)^2vk_0 + (x + v)^2/(1 + x)^2vk_1']^{-1} \quad (2)$$

which shows that $k^{(1)}$ can be represented by a network of three complex conductances—*viz.*, those represented by the different terms of formula (2)—each of which is proportional to the complex conductivity of the associated phase of the system and a purely geometric factor. The network is shown in Fig. 1a, with

$$X_0 = x(1 - v)k_0/(v + x) \quad (3)$$

$$Y_0 = (1 + x)^2vk_0/(1 - v)(v + x) \quad (4)$$

$$X_1' = (1 + x)^2vk_1'/(v + x)^2 \quad (5)$$

The problem of the conductivity of a system composed of a compound spherical conductor, built up of a spherical core (radius a_2, conductivity k_2') surrounded by a shell (radius $(a_1 - a_2)$, conductivity k_1), placed in a conducting medium in a constant field, was treated by Maxwell,[6] who showed that the sphere is electrically equivalent to a homogeneous sphere of radius a_1 and con-

(1) Aided by a contract between the Office of Naval Research and the University of Pennsylvania, N.R. 119-289.

(2) H. Fricke, *Phys. Rev.*, **26**, 678 (1925).

(3) H. Fricke and S. Morse, *J. Gen. Physiol.*, **9**, 153 (1925).

(4) K. S. Cole, *ibid.*, **12**, 29 (1928).

(5) H. Fricke, *J. Appl. Phys.*, **24**, 644 (1953).

(6) J. C. Maxwell, "A Treatise on Electricity and Magnetism," 2nd Ed., Clarendon Press, Oxford, 1881, p. 402.

(7) H. Fricke, *Phys. Rev.*, **24**, 575 (1924).

(8) H. Fricke and S. Morse, *ibid.*, **25**, 361 (1925).

(9) H. Fricke, THIS JOURNAL, **57**, 934 (1953).

ductivity k_1'' given by the following formula with $x = 2$

$$k_1'' = k_1[(xk_1 + k_2')a_1^{x+1} - x(k_1 - k_2')a_2^{x+1}]/[(xk_1 + k_2')a_1^{x+1} + (k_1 - k_2')a_2^{x+1}] \quad (6)$$

The formula was derived for the real case, but is valid for complex variables.

The corresponding cylindrical case can be dealt with in a similar manner, whereby formula (6) is obtained with $x = 1$.

By replacing k_1' of formula (2) by k_1'', we obtain the conductivity $k^{(2)}$ of a dilute suspension of the compound particles. The formula thus obtained is valid also at higher volume concentrations, provided the local field can be obtained in the manner stated above. It follows that $k^{(2)}$ can be represented by the network of Fig. 1a, when X_0 and Y_0 are calculated from formulas (3) and (4) as before, while X_1' is calculated from formula (5) after k_1' has been replaced by k_1''.

Formula (6) can be written

$$k_1'' = xk_1(a_1^{x+1} - a_2^{x+1})/(xa_1^{x+1} + a_2^{x+1}) + [(xa_1^{x+1} + a_2^{x+1})(a_1^{x+1} - a_2^{x+1})/(x+1)^2(a_1a_2)^{x+1}k_1 + (xa_1^{x+1} + a_2^{x+1})^2/(x+1)^2(a_1a_2)^{x+1}k_2']^{-1} \quad (7)$$

This formula shows that k_1'' can be represented by a network similar to that of Fig. 1a and by making use of this it will be recognized that $k^{(2)}$ can be represented by the network of Fig. 1b with $s = 2$. The network is composed of five complex conductances, including X_0 and Y_0 as given above and

$$X_1 = x(1+x)^2(a_1^{x+1} - a_2^{x+1})vk_1/(x+v)^2(xa_1^{x+1} + a_2^{x+1}) \quad (8)$$

$$Y_1 = (1+x)^4(a_1a_2)^{x+1}.vk_1/(x+v)^2(a_1^{x+1} - a_2^{x+1})(xa_1^{x+1} + a_2^{x+1}) \quad (9)$$

$$X_2' = (1+x)^4(a_1a_2)^{x+1}vk_2'/(x+v)^2(xa_1^{x+1} + a_2^{x+1})^2 \quad (10)$$

The field inside the core of a suspended compound sphere or cylinder, composed of any number of concentric or coaxial layers, is constant and parallel to the external field. The treatment given can therefore be extended to this general case and we find that the conductivity $k^{(s)}$ of a suspension of spheres or cylinders composed of s sections can be represented by the ladder-type network of Fig. 1b and expressed by the continued fraction

$$k^{(s)} = X_0 + \cfrac{1}{Y_0^{-1} + \cfrac{1}{X_1 + \cfrac{1}{Y_1^{-1} + \cfrac{1}{\ddots + \cfrac{1}{X_m + \cfrac{1}{Y_m^{-1} + \cfrac{1}{\ddots + \cfrac{1}{X_s'}}}}}}}} \quad (11)$$

in which each one of the complex conductances X_m and Y_m is the product of the complex conductivity of the associated phase of the system and a purely geometric factor. The values of X_0, Y_0, X_1 and Y_1 have already been given. For $m \geqq 2$; $s \geqq 2$

$$X_m = (xv_1k_mc_m/b_m) \prod_{n=2}^{n=m} (x+1)^2(a_{n-1} \times a_n)^{x+1}/b^2{}_{n-1} \quad (12)$$

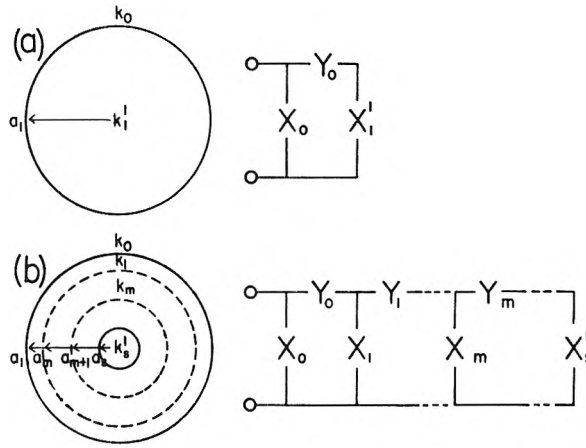

Fig. 1.—Electric diagrams of suspensions of (a) homogeneous and (b) stratified spheres and cylinders. The values of the complex conductances X_m and Y_m are given in the text.

$$Y_m = (v_1b_mk_m/c_m) \prod_{n=2}^{n=m+1} (x+1)^2(a_{n-1} \times a_n)^{x+1}/b^2{}_{n-1} \quad (13)$$

$$X_s' = v_1k_s'' \prod_{n=2}^{n=s} (x+1)^2(a_{n-1} \times a_n)^{x+1}/b^2{}_{n-1} \quad (14)$$

Where

$$v_1 = (1+x)^2 \times v/(x+v)^2 \quad (15)$$

$$b_m = xa_m^{x+1} + a_{m+1}^{x+1} \quad (16)$$

$$c_m = a_m^{x+1} - a_{m+1}^{x+1} \quad (17)$$

The case of a homogeneous sphere or cylinder covered with a thin, relatively poorly conducting homogeneous membrane (thickness t_1) is calculated from formula (11) with $s = 2$ and

$$X_1 = 0 \quad (18)$$

$$Y_1 = (1+x)^2va_1k_1/t_1(v+x)^2 \quad (19)$$

$$X_2' = (1+x)^2vk_2'/(v+x)^2 \quad (20)$$

Two special cases are considered: (1) The conductance of the membrane is negligible and the conductivities k_0 and k_2' are real

$$\sigma^{(2)} = R_0^{-1} + R_i^{-1}(2\pi R_iC_mf)^2/(1 + (2\pi R_iC_mf)^2) \quad (21)$$

$$\epsilon^{(2)} = 4\pi C_m/(1 + (2\pi R_iC_mf)^2) \quad (22)$$

where

$$R_0 = (v+x)/(x(1-v)\sigma_0 \quad (23)$$

$$R_i = (1-v)(v+x)/(1+x)^2v\sigma_0 + (v+x)^2/(1+x)^2v\sigma_2' \quad (24)$$

$$C_m = (1+x)^2a_1v\epsilon_1/4\pi t_1(v+x)^2 \quad (25)$$

(2) The conductance and admittance of the membrane are negligible

$$\epsilon^{(2)} = x(1-v)\epsilon_0/(v+x) + (1+x)^2a_1v\epsilon_1/t_1(v+x)^2 \quad (26)$$

The low frequency electric behavior of suspensions of spherical biological cells can generally be represented by the simple model just considerd.[10-17] We shall use this material for a prelimi-

(10) H. Fricke, *Nature*, **172**, 731 (1953).
(11) H. Fricke, *Phys. Rev.*, **26**, 682 (1925).
(12) H. Fricke, *Physics*, **1**, 106 (1931).
(13) H. Fricke and H. J. Curtis, *Nature*, **134**, 102 (1934)
(14) H. Fricke and H. J. Curtis, *ibid.*, **135**, 436 (1935)
(15) K. S. Cole, *J. Gen. Physiol.*, **15**, 641 (1932)
(16) K. S. Cole, *ibid.*, **18**, 877 (1935).
(17) K. S. Cole and R. H. Cole, *ibid.*, **19**, 609 (1936)

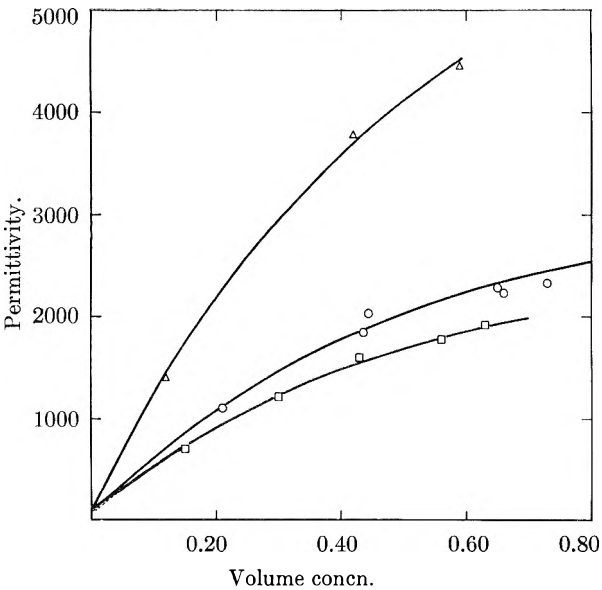

Fig. 2.—Dielectric constant of biological cell suspensions of different volume concentrations: ○, spherical rabbit erythrocytes (4.7 μ dia); □, *sacch. cerevisiae* (5.5 μ dia); △, rabbit leucocytes (dia. 10.5 μ); solid curves, calculated from formula (26) in the text.

nary test of the validity of the theoretical treatment in the high volume concentration region. In Fig. 2 are recorded observed dielectric constants[10] of suspensions of different volume concentrations of three species of (approximately) spherical cells of this type (the erythrocytes, which are normally flat discs, were transformed to spheres by chemical treatment, as described in ref. 10), measured at 16 kc./sec., at which frequency the admittance of the membrane of all these cells is negligible compared with that of the cell interior. Formula (26) may therefore be applied with $x = 2$, and the solid curves were calculated by adjusting, for each species of cell, the constant parameter of this formula to give the best fit with the experimental points. The dielectric constants of the suspending salt solutions were practically equal to the dielectric constant of water $\epsilon_0 = 80$ (21°). The agreement with the experimental points is satisfactory, over the whole range of volume concentrations studied, which for the case of the erythrocytes extended to total packing. Further experimental support is thus obtained for the validity of the Lorentz internal field in spherical suspensions, in which the suspended particles are so nearly alike as was the case in these experiments.

STUDIES ON COÖRDINATION COMPOUNDS. XI. FORMATION CONSTANTS OF SOME TERVALENT IONS AND THE THORIUM(IV) ION WITH THE ACETYLACETONATE ION[1]

BY REED M. IZATT,[2] W. CONARD FERNELIUS, C. G. HAAS, JR., AND B. P. BLOCK

Contribution from the College of Chemistry and Physics, The Pennsylvania State University

Received August 16, 1954

Stepwise, thermodynamic formation constants have been determined in water at 30° for the reaction of the acetylacetonate ion with La^{3+}, Nd^{3+}, Sm^{3+}, Eu^{3+}, Y^{3+}, Sc^{3+}, In^{3+}, Al^{3+}, Th^{4+}, Ga^{3+} and Fe^{3+} (listed in order of increasing values of the first formation constants). The determinations were made potentiometrically using glass and saturated calomel electrodes. A method is given which enables one to make the Ga^{3+}, Al^{3+} and Th^{4+} determinations without the interference of hydrolysis. In the case of iron a platinum electrode in the presence of Fe^{2+} and Fe^{3+} was used to measure Fe^{3+} activity, and a correction was made for the hydrolysis of the Fe^{3+} ion. Plots of the logarithm of the first formation constant *vs.* (1) electronegativities (in the case of Pr^{3+}, Y^{3+}, Sc^{3+}, Al^{3+}, Ga^{3+}, In^{3+} and Fe^{3+}), (2) third ionization potentials (in the case of La^{3+}, Ce^{3+}, Y^{3+}, Sc^{3+}, Al^{3+}, Ga^{3+}, In^{3+} and Fe^{3+}) and (3) atomic number (in the cases of La^{3+} and the rare earths) are straight lines.

Introduction

Previous investigators[3-6] have attempted to establish general relationships between the stability of metal chelate species and other significant properties of the metal ion. For the metal derivatives of dibenzoylmethane,[5,7] a plot of the logarithm of the first formation constant, log K_{f_1}, (measured in 75 volume per cent. dioxane at ionic strength ~0 and $t = 30°$) *vs.* the electronegativity[8] of the metal ion, X_M, gives a series of straight lines, one for each charge type. Since only three tervalent ions had previously been studied, the present investigation was undertaken to extend the knowledge of the behavior of such ions. Acetylacetone, HCh, was chosen as the chelating agent and water as the solvent in order to have smaller formation constants and thus to permit the study of a larger number of ions.

Experimental Procedure

Weighed quantities of Nd_2O_3 (99.9%, pure, Research Chemicals, Inc., Burbank, California, Lot No. 222), Sm_2O_3 (99% pure, Lindsay Light and Chemical Co., W. Chicago, Ill., Code No. 822) and Eu_2O_3 (Dr. L. L. Quill, Michigan State College) were dissolved individually in known amounts of standard $HClO_4$. The $Sc(ClO_4)_3$ solution was prepared

(1) From a dissertation presented by Reed M. Izatt in partial fulfillment of the requirements for the degree of Doctor of Philosophy, August, 1954.

(2) Mellon Institute of Industrial Research, Pittsburgh 13, Pennsylvania.

(3) M. Calvin and N. C. Melchior, *J. Am. Chem. Soc.*, **70**, 3272 (1948).

(4) A. E. Martell and M. Calvin, "Chemistry of the Metal Chelate Compounds," Prentice-Hall, Inc., New York, N. Y., 1952, pp. 181–206.

(5) L. G. Van Uitert, W. C. Fernelius and B. E. Douglas, *J. Am. Chem. Soc.*, **75**, 2736, 2739, 3862 (1953).

(6) R. M. Izatt, W. C. Fernelius and B. P. Block, THIS JOURNAL, **59**, 80 (1955).

(7) L. G. Van Uitert, Ph.D. Thesis, The Pennsylvania State University, 1952.

(8) M. Haissinsky, *J. phys. radium*, [8] **7**, 7 (1946).

from $Sc_2(SO_4)_3$ (Fordomes Trading Co., Arlington, N. J.) by adding $BaCO_3$, filtering and adding a known volume of standard $HClO_4$. The Sc^{3+} was determined by precipitating the oxide with ammonia, filtering, igniting and weighing as Sc_2O_3. The $La(NO_3)_3$ solution was prepared by dissolving C.P. $La(NO_3)_3$ (Eimer and Amend) in water. The La^{3+} was determined by precipitating the oxide with ammonia, filtering, igniting and weighing as La_2O_3. Weighed quantities of Y (King Products Co., Arlington, N. J.), In (Fordomes Trading Co.), Ga (King Products Co.), and Fe wire (99.8% pure, Merck) were dissolved in known amounts of standard $HClO_4$. The Fe^{2+} was partially oxidized to the Fe^{3+} state with 30% H_2O_2 and the Fe^{2+} determined by titration with standard $KMnO_4$. A standard $Th(NO_3)_4$ solution was prepared by dissolving $Th(NO_3)_4 \cdot 4H_2O$ (Hooper Chemical Co., Rutherford, N. J.) in water; Th^{4+} was determined by precipitating $Th(C_2O_4)_2$, igniting it, and weighing the ThO_2. The acetylacetone, HCh, (Eastman Kodak Co.) was shown to be pure by checking the refractive index (reported 1.45178, observed 1.4518).

Although, as will be shown in the discussion, the same procedure was not followed in every determination, the general procedure was as follows. Solutions containing at least four equivalents of HCh to one of metal ion were diluted to 100 ml. with water, and titrated with standard NaOH (0.1 to 1.0 N depending on the metal ion concentration). A glass electrode (Beckman, Type E. No. 1190–80), a saturated calomel electrode (Beckman No. 1170), and, in the case of iron, a platinum electrode were placed in the solution. A Beckman Model G pH meter was used to measure pH and e.m.f. The meter was checked periodically against Beckman pH 4.01 and pH 6.98 buffer solutions. The solutions were stirred continuously, and the temperature was maintained at 30.0 ± 0.1° during the titrations. Sufficient time was allowed between successive additions of base to obtain constant pH readings. The titrations were continued until precipitation occurred. An inert atmosphere of nitrogen in the titration flask was maintained during the iron determination.

Calculations.—The constants were calculated as described previously.[9] Three sets of $\bar{n}$ and $[Ch^-]$ (Ch^- = acetylacetonate ion) values were taken at or near $n = {}^1/_2$, 1.5 and 2.5, except in the case of Th^{4+}, where additional values were taken at $\bar{n} \sim 3.5$. An extension of the equations developed by Block and McIntyre[10] gave expressions for $N = 4$. In cases where precipitation occurred before $\bar{n} \sim 2.2$, two values were taken in the $\bar{n}$ range of 1 to 2 and no third constant was calculated.

The constants are tabulated in Table II. In the cases of La^{3+}, Eu^{3+} and Ga^{3+} two determinations were made at different $[M^{3+}]$. From previous determinations of the Ce^{3+} and Pr^{3+} values[9] the precision of the rare earth and Y^{3+} values reported in this paper is estimated to be approximately ±0.10 in the log for K_{f_1} and ±0.15 in the log for K_{f_2} and K_{f_3}. The Sc^{3+}, In^{3+}, Al^{3+} and Ga^{3+} values are of somewhat less precision, probably about ±0.20 in the log, and the Fe^{3+} values are least well known, the precision being about ±0.3 in the log.

Discussion

Because of the hydrolysis of several of the metal ions studied, the determination of $\bar{n}$ and $[Ch^-]$ values in those cases presented considerable difficulty. Hydrolysis of the metal ion releases protons to the solution, and it is necessary either (1) to be certain that a negligible concentration of protons is being released or (2) to correct in some manner for the protons released, if their contribution to the total $[H^+]$ is appreciable. Three methods were utilized to achieve (1) and (2). These methods are given below using as examples the metal ions involved. It is recognized that the ions discussed below are all hydrated; however, for simplicity and because the exact degree of hydration is not known no further mention is made of hydration in the discussion.

Estimation of Degree of Hydrolysis by Calculation.—Hydrolysis "constants"[11] $Q_{n_{hyd}}$, for the reaction

$$M^{n+} \rightleftharpoons M(OH)^{(n-1)+} + H^+ \qquad (9)$$

have been reported by Moeller[12] for $M^{n+} = In^{3+}$ by Sidall and Vosburgh for $M^{n+} = Fe^{3+}$ [13] and by Kilpatrick and Pokras for $M^{n+} = Sc^{3+}$.[14]

To determine if the concentration of protons released is negligible, one may take the values for the molarity quotients, Q_{f_1} and Q_{f_2}, which are calculated in the case of M^{3+}, assume that the only species containing M^{3+} are $M(OH)^{++}$, M^{3+}, MCh^{++} and MCh_2^+ and at experimental points along the titration curve calculate the approximate $[M(OH)^{++}]$. An equation may be set up with $[M(OH)^{++}]$ as the single unknown by suitable combination of equations 1, 2 and the equations

$$Q_{1hyd} = \frac{[M(OH)^{++}][H^+]}{[M^{3+}]} \quad \text{and} \quad [M_T] = [M(OH)^{++}] + [M^{3+}] + [MCh^{++}] + [MCh_2^+]$$

to give

$$[M(OH)^{++}] = \frac{Q_{1hyd}[M_T]}{Q_{1hyd} + [H^+] + Q_{f_1}[H^+][Ch^-] + Q_{f_1}Q_{f_2}[H^+][Ch^-]^2} \qquad (10)$$

Listed in Table I are data from two experimental points (in the case of In^{3+}), and one experimental point (in the case of Fe^{3+}), together with the approximate value of $[M(OH)^{++}]$ as calculated from (10). It is seen that the approximate $[M(OH)^{++}]$ is small compared to $[In_T]$ and $[H^+]$ in the In^{3+} determination and to $[Sc_T]$ and $[H^+]$ in the Sc^{3+} determination, but large compared to $[Fe_T]$ and $[H^+]$ in the Fe^{3+} determination. Since $[Fe(OH)^{++}]$ is already appreciable at pH 2.37, hydrolysis is obviously important at higher pH values. Precipitation occurred in the In^{3+} and Sc^{3+} determinations at $\bar{n} \sim 1.9$, so it was not necessary to calculate $[M(OH)^{++}]$ at higher pH values in these cases.

Correction for Fe^{3+} Hydrolysis.—From the value given in Table I the $[Fe(OH)^{++}]$ could be as much as one-tenth of the total iron concentration. The exact amount of the hydrolyzed species was determined as follows. In the discussion below only the initial two steps are considered in the Fe^{3+} hydrolysis since it was found experimentally that the correction for the second step is very small and consequently the third should be negligible. Since

(9) R. M. Izatt, C. G. Haas, Jr., B. P. Block and W. C. Fernelius, THIS JOURNAL, **58**, 1133 (1954).

(10) B. P. Block and G. H. McIntyre, Jr., *J. Am. Chem. Soc.*, **75**, 5667 (1953).

(11) Some of the literature values used for hydrolysis equilibrium constants are molarity quotients rather than true activity constants. Practically, it matters little which type of value is employed, since the use of concentrations rather than activities for the hydrolysis calculations will introduce only a second-order error. Accordingly, in the subsequent treatment of hydrolysis, all equilibrium constants are considered as molarity quotients.

(12) T. Moeller, *J. Am. Chem. Soc.*, **63**, 1206 (1941).

(13) T. H. Sidall and W. C. Vosburgh, *ibid.*, **73**, 4270 (1951).

(14) M. Kilpatrick and L. Pokras, *J. Electrochem. Soc.*, **100**, 85 (1953).

TABLE I

DATA AT 2 EXPERIMENTAL POINTS (IN THE CASES OF In^{3+} AND Sc^{3+}) AND 1 EXPERIMENTAL POINT (IN CASE OF Fe^{3+}) USED TO CALCULATE VALUES OF $[M(OH)^{++}]$ FROM EQUATION (10)

	In^{3+}		Fe^{3+}	Sc^{3+}	
$\bar{n}$	0.446	1.713	0.694	0.596	1.73
pH	2.69	3.99	2.37	2.03	3.35
$[H^+]$	2.29×10^{-3} M	1.16×10^{-4} M	4.63×10^{-3} M	1.11×10^{-2}	5.28×10^{-4}
$[Ch^-]$	1.39×10^{-8} M	2.67×10^{-7} M	1.89×10^{-10} M	2.44×10^{-8}	3.12×10^{-7}
$[M_T]$	4.88×10^{-3} M	4.70×10^{-3} M	2.47×10^{-3} M	1.03×10^{-2}	9.75×10^{-3}
$[M\,OH^{++}]$	1.5×10^{-5} M	1.3×10^{-5} M	2.5×10^{-4} M	5.4×10^{-6}	5.4×10^{-6}
Q_{f_1}	4.44×10^{7}		7.2×10^{9}	3.67×10^{7}	
Q_{f_2}	7.64×10^{6}		8.1×10^{8}	7.94×10^{6}	
Q_{1hyd}	1.2×10^{-5}		6.5×10^{-3}	1.2×10^{-5}	

each Fe^{3+} which forms one of the hydroxo species or which coördinates with HCh releases protons, the following equation may be written

$$[H^+] = [Fe(OH)^{++}] + 2[Fe(OH)_2^+] + [FeCh^{++}] + 2[FeCh_2^+] + 3[FeCh_3] + [Ch^-] \quad (11)$$

Molarity quotients may be written for the equilibria

$$Fe^{3+} \rightleftharpoons Fe(OH)^{++} + H^+; \quad Q_{1hyd} = \frac{[FeOH^{++}][H^+]}{[Fe^{3+}]}$$

$$Fe(OH)^{++} \rightleftharpoons Fe(OH)_2^+ + H^+; \quad Q_{2hyd} = \frac{[Fe(OH)_2^+][H^+]}{[FeOH^{++}]}$$

Then, when one replaces the concentrations of the hydroxide complexes of iron in (11) by their equivalents in terms of Q_{1hyd}, Q_{2hyd}, $[H^+]$ and $[Fe(H_2O)_x^{3+}]$ one obtains

$$[H^+] = \frac{Q_{1hyd}[Fe^{3+}]}{[H^+]} + \frac{2Q_{1hyd}Q_{2hyd}[Fe^{3+}]}{[H^+]^2} + [FeCh^{++}] + 2[FeCh_2^+] + 3[FeCh_3] + [Ch^-] \quad (12)$$

Measurement of $[Fe^{3+}]$ would enable one to calculate the contribution of the hydroxo species to the total acidity of the solution, provided Q_{1hyd} and Q_{2hyd} are known. A value for Q_{1hyd} has been given. T. V. Arden[15] has reported the value 4.2×10^{-4} for Q_{2hyd} in $SO_4^=$ solution, ionic strength not given.

Since the standard oxidation potential of the ferrous–ferric couple is known accurately[16] and the couple is known to be reversible, one may calculate the $[Fe^{3+}]$ from the e.m.f. of a Pt electrode in a solution containing a known concentration of ferrous ions, and the appropriate activity coefficient. Contributions from the $FeCh^+$ species may be calculated from the formation constant of Fe^{2+} with HCh which has been reported in a previous paper.[6]

Adjusting Conditions to Minimize Hydrolysis.— A treatment similar to the above for the Ga^{3+} and Th^{4+} ions would be expected to yield results intermediate between Fe^{3+} and In^{3+} since the first hydrolysis quotients for Ga^{3+} [17] and Th^{4+} [18] are 3.7×10^{-4} and 5×10^{-5}, respectively. The corresponding value for Al^{3+} is in some doubt since it is reported that dimerization occurs. Brosset[19] has summarized the work which has been done on the Al^{3+}–H_2O system and reports values for the quotients involving the dimerization.

A method for determining the K_{f_n} values for the above three ions with Ch^- was used in which experimental conditions were adjusted so hydrolysis would be minimized. This was necessary because some degree of hydrolysis from each of the above ions is likely and there is no known couple involving the M^{n+} for which an E^0 value is accurately known to enable one to correct for any hydrolysis. The following method was used. A perchlorate solution of the M^{n+} has a certain pH due to hydrolysis. The addition of standard $HClO_4$ to the solution causes the pH to decrease. Since the equilibrium for the hydrolysis is shifted toward the hydrated metal ion by the added acid, a point will be reached after sufficient acid has been added at which the observed pH equals the pH calculated from the concentration of added acid. At this point contribution to the total $[H^+]$ from hydrolysis is negligible. To this solution one may now add a concentrated standard HCh solution (to keep pH change due to dilution small). Any lowering of the pH is caused by protons which are released by the HCh; hence, the difference between the pH at x ml. HCh and at 0 ml. of HCh is a measure of the Ch^- chelated to the metal ion. Since the $[Ch^-]$ is approximately 10^{-9} M, it is negligible in these calculations. After the desired amount of HCh has been added, the regular titration with base is performed (as has been described under Experimental). One is now certain that appreciable hydrolysis does not occur until the pH has reached a value somewhat above the pH value previously established as that at which negligible hydrolysis occurs. In all three of the above cases, values of $\bar{n} = 1/2$ were obtained at pH values below the pH at 0 ml. of HCh. Since there is no known way of determining exactly where the hydrolysis becomes appreciable, the K_{f_n} values above $\bar{n} = 1$ may be somewhat in error.

Kraus and Holmberg[18] were able to obtain the same constant for the hydrolysis of Th^{4+} in the presence of either Cl^- or ClO_4^-. This fact would indicate that the formation of chloro complexes in this system is not appreciable. Since NO_3^- is intermediate in its complexing abilities between the above two ions, the value reported here should not be materially affected by the presence of NO_3^- rather than ClO_4^-.

Kraus and Holmberg[18] found hydrolysis to be negligible in Th^{4+} solutions, ($[Th^{4+}] = 10^{-2}$ to 10^{-3} M) below pH $\sim$ 3.0. This is in agreement

(15) T. V. Arden, *J. Chem. Soc.*, 350 (1951).

(16) W. M. Latimer, "Oxidation Potentials," 2nd Ed., Prentice-Hall Inc., New York, N. Y., 1952, p. 223.

(17) T. Moeller and G. L. King, THIS JOURNAL, **54**, 999 (1950).

(18) K. A. Kraus and R. W. Holmberg, *ibid.*, **68**, 325 (1954).

(19) C. Brosset, *Acta Chem. Scand.*, **6**, 910 (1952).

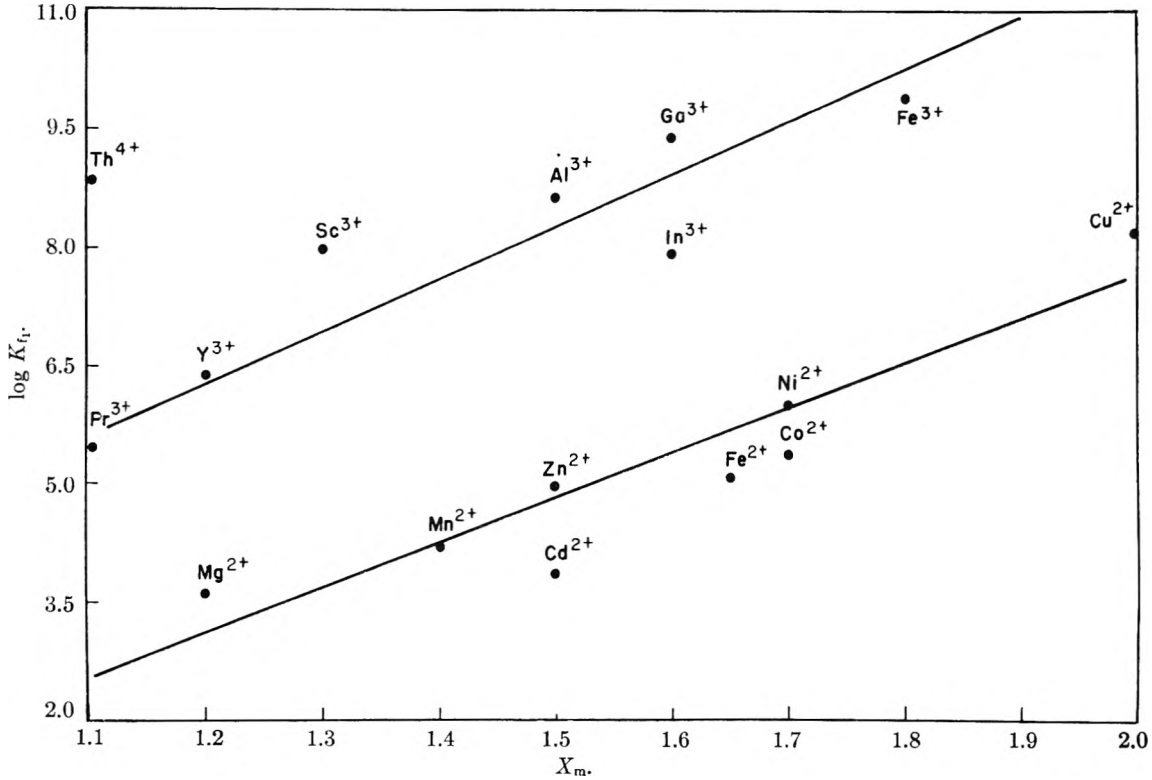

Fig. 1.—Plot of log K_{f_1} for several bi- and ter-valent metal ions with the acetylacetonate ion *vs.* the electronegativity of the respective metal ion; temp. = 30°.

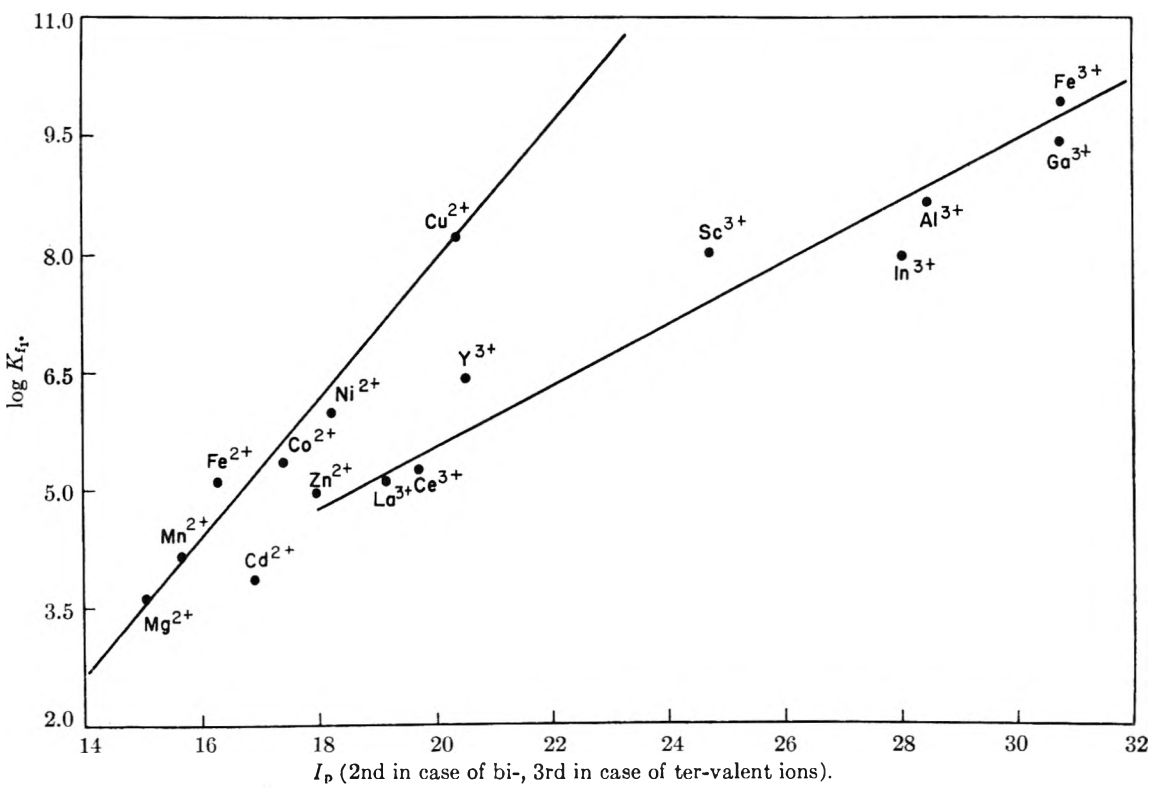

Fig. 2.—Plot of K_{f_1} for several bi- and ter-valent metal ions with the acetylacetonate ion *vs.* the ionization potential, I_p, (2nd in the case of bi-, 3rd in the case of ter-valent ions), of the respective gaseous atoms; temp. = 30°.

with the present study inasmuch as it was found that with $[Th^{4+}] = 4 \times 10^{-3}$ *M* the observed *p*H became equal to the *p*H at approximately 3.

The values given in Table II for the reaction of Th^{4+} with Ch^- agree well with those previously determined by Rydberg[20] who used radioactive tracer techniques to measure the Th^{4+} distribution

(20) J. Rydberg, *Acta Chem. Scand.*, **4**, 1503 (1950).

between an aqueous HCh solution and benzene, and by Van Uitert[7] who determined the constants potentiometrically.

TABLE II

LOG K_{f_n} VALUES FOR THE REACTION OF SEVERAL TERVALENT METAL IONS AND Th^{4+} WITH THE ACETYLACETONATE ION AT 30°

M^{n+}	$[M^{n+}]$, M	log K_{f_1}	log K_{f_2}	log K_{f_3}	log K_{f_4}
La^{3+}	1×10^{-3}	5.1	3.8	3.0	...
	1×10^{-2}	5.1	3.9	2.8	...
Nd^{3+}	1×10^{-3}	5.6	4.3	3.2	...
Sm^{3+}	1×10^{-3}	5.9	4.5	3.2	...
Eu^{3+}	7×10^{-4}	6.0	4.5	3.5	...
	7×10^{-3}	6.1	4.6	3.4	...
Y^{3+}	1×10^{-3}	6.4	4.7	2.8	...
Sc^{3+}	1×10^{-2}	8.0	7.2	ppt.	...
In^{3+}	5×10^{-3}	8.0	7.1	ppt.	...
Al^{3+}	4×10^{-3}	8.6	7.9	5.8	...
Ga^{3+}	1.6×10^{-3}	9.3	8.3	6.1	...
	3.2×10^{-3}	9.5	8.4	5.7	...
Fe^{3+}	2.5×10^{-3}	9.8	9.0	7.4	...
Th^{4+}	4×10^{-3}	8.8	7.4	6.3	4.2

In Fig. 1 is shown a plot of log K_{f_1} *vs.* X_M, for several ter- and bi-valent ions.[8] The log K_{f_1} values for the bivalent ions were reported in a previous paper.[6] The linearity in the case of the tervalent metal ions is in agreement with earlier results although the present data are more numerous and reliable.

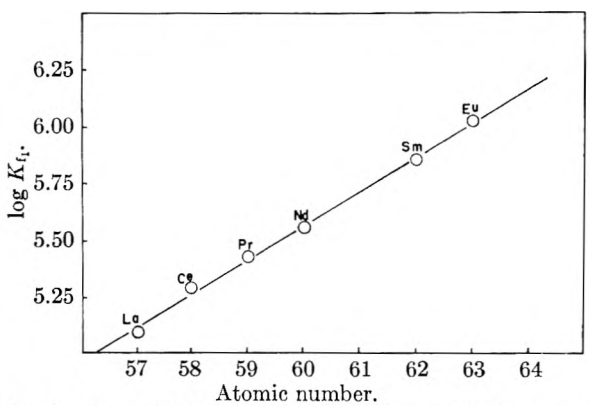

Fig. 3.—Plot of log K_{f_1} for La^{3+} to Eu^{3+} with the acetylacetonate ion *vs.* Z, the atomic number; temp. = 30°.

When log K_{f_1} *vs.* X_M is plotted in the case of Th^{4+}, it is seen that the point lies considerably above the M^{3+} line. It would be interesting to obtain log K_{f_1} values for other M^{4+} species and see whether they also obey a linear relationship when plotted against X_M.

(21) G. Herzberg (translated by J. W. T. Spinks), "Atomic Spectra and Atomic Structure," Dover Publications, New York, N. Y., 1944, pp. 200–201.

In Fig. 2 is shown a plot of log K_{f_1} *vs.* the ionization potential[21] of the gaseous atom (2nd in case of bi-, 3rd in case of ter-valent ions) for several bi- and ter-valent metal ions with HCh. Linear relationships exist for each charge type.

The linear relationships involving X_M and 3rd I_p show in a qualitative fashion a direct relation between these properties of the metal ion and the energy of the metal ligand bond. This same relationship has previously been shown to exist in the case of the bivalent metal ions[6] with the exception of Hg^{2+} and Be^{2+}.

A plot of log K_{f_1} *vs.* atomic number for the elements La^{3+} through Eu^{3+} shows that nearly constant differences between successive log K_{f_1} values exist for these ions (approx. 0.15 ± 0.03)(Fig. 3). The difference of 0.29 unit between the values for Nd^{3+} and Sm^{3+} is exactly enough so that prometheum, element 61, can fit into this series. The values for Ce^{3+} and Pr^{3+} have been given in a previous paper.[9] If this linear relationship between log K_{f_1} and atomic number continues through the remainder of the rare earth series, then on the basis of atomic radii (Dy = 1.07 Å., Y = 1.06 Å., Ho = 1.05 A.),[22] Y^{3+} would be expected to have a log K_{f_1} value between those of Dy^{3+} and Ho^{3+} (6.49 and 6.64). The observed value is 6.35.

Marked differences exist in the solubilities of the species formed during the course of the Al^{3+}, Ga^{3+} and In^{3+} determinations. No precipitation was observed during the course of the Al^{3+} and Ga^{3+} determinations. The final *p*H values were 8.42 (4 equivalents of NaOH per Al^{3+} added) in the case of $[Al^{3+}] = 4 \times 10^{-3}$ M and 8.22 (3.5 equivalents of NaOH per Ga^{3+} added) in the case of $[Ga^{3+}] = 3.2 \times 10^{-3}$ M. In the case of In^{3+}, precipitation occurred at *p*H 4.2 after 2.8 equivalents of NaOH per equivalent of In^{3+} had been added ($[In^{3+}] = 5 \times 10^{-3}$ M).

Steinbach and Freiser[23] have recently made determinations involving the use of HCh as an extraction agent for Ga^{3+}, Al^{3+} and In^{3+}. They found the order of extraction to be Ga > Al > In as the *p*H increased. Since the *p*H at which the complex is extracted is a function of the stability constant, this is also the order of stability. This order is the same as that given in Table II for these ions.

Acknowledgment.—The authors gratefully acknowledge financial support of this work by the Atomic Energy Commission through Contract Number AT(30-1)-907. The authors also appreciate the loan of several grams of Eu_2O_3 by Dr. L. L. Quill of Michigan State College.

(22) V. M. Goldschmidt, "Geochemische Verteilungsgesetze der Elemente," **8**, 69 (1926); *Ber.*, **60**, 1263 (1927).

(23) J. F. Steinbach and H. Freiser, *Anal. Chem.*, **26**, 375 (1954).

A NEW HIGH-TEMPERATURE REACTION CALORIMETER. THE HEATS OF MIXING OF LIQUID LEAD-TIN ALLOYS

BY O. J. KLEPPA

Institute for the Study of Metals, The University of Chicago, Chicago, Illinois

Received August 19, 1954

A new reaction calorimeter for temperatures up to 500° is described. The calorimeter is particula rly suited for the study of heats of mixing and heats of solution in alloy systems. The calorimeter is quasi-isothermal. The change in temperature of the calorimeter during a reaction is determined by comparison with that of a surrounding jacket which has a large heat capacity compared to the calorimeter proper. The jacket is maintained at constant temperature i n the furnace by introducing a large thermal lag between the controlled heating system and the jacket. The calorimet er has been used for a redetermination of the heats of mixing of liquid lead–tin alloys. Results are presented for 350 and 4 50°.

Introduction

During recent years metallurgists, physicists and chemists have shown greatly increased interest in the thermochemistry of alloys. An indication of this is the appearance during the past decade of several monographs wholly or largely devoted to the field.[1-4] Another indication is the fairly large number of recent experimental investigations, both of solid and liquid alloys, which have contributed much new and significant information.

Most of these investigations have been based on the equilibrium methods of chemical thermodynamics, among which the e.m.f. cell method and the vapor pressure method are particularly well known. There has, on the other hand, been little activity in the field of alloy calorimetry, in spite of the fact that calorimetric methods are very simple and also quite suitable for the study of metallic interaction.

The early calorimetric work has been adequately discussed by Weibke and Kubaschewski.[1] Here we shall give only a brief outline of this work as well as references to some recent investigations.

The first studies of the heats of formation of alloys were based on solution calorimeters using inorganic solvents and operating at room temperature or at slightly elevated room temperature.[5,6]

Some improvement in accuracy was achieved by measuring the heat effects in direct combination experiments. Notable contributions along this line were those of Körber and co-workers,[7] of Kawakami,[8] and of Kubaschewski and Walter.[9]

In very recent years improved high temperature reaction calorimeters have been constructed in the U. S. A. by McKisson and Bromley[10] and by Ticknor and Bever.[11] In the present communication the development of a new high temperature reaction calorimeter is reported. This calorimeter is designed to meet some of the needs for more and better data on the heats of formation and heats of mixing in alloy systems. The present paper also gives results obtained for the heats of mixing of liquid lead–tin alloys. Results for other systems involving both liquid and solid alloys will be presented in other communications.

(1) F. Weibke and O. Kubaschewski, "Thermochemie der Legierungen," Springer-Verlag, Berlin, 1943.

(2) O. Kubaschewski and E. L. Evans, "Metallurgical Thermochemistry," Academic Press, Inc., New York, N. Y., 1951.

(3) C. Wagner, "The Thermodynamics of Alloys," Addison-Wesley, Boston, Mass., 1952.

(4) J. Lumsden, "The Thermodynamics of Alloys," Institute of Metals Monograph #11, London, 1952.

(5) M. Herschkowitsch, *Z. physik. Chem.*, **27**, 151 (1898).

(6) W. Biltz and G. Hohorst, *Z. anorg. Chem.*, **121**, 1 (1922); W. Biltz, G. Rohlffs and H. U. v. Vogel, *ibid.*, **220**, 113 (1934).

(7) F. Körber, *Stahl und Eisen*, **56**, 1401 (1936).

(8) M. Kawakami, *Z. anorg. Chem.*, **167**, 345 (1927); *Science Rept. Tohoku Imp. Univ.*, [I] **16**, 915 (1927); [I] **19**, 521 (1930).

(9) O. Kubaschewski and A. Walter, *Z. Elektrochem.*, **45**, 631 (1939).

(10) R. L. McKisson and LeRoy A. Bromley, *J. Metals*, **4**, 33 (1952).

(11) L. B. Ticknor and M. B. Bever, *ibid.*, **4**, 941 (1952).

Principle of the Calorimeter

The central part of the present calorimeter (Fig. 1) is a hollow cylindrical constant-temperature jacket enclosed in a large resistance-heated furnace. The temperature of this surrounding furnace is maintained constant by means of a commercial temperature controller. By inserting a considerable amount of thermal insulation material between the jacket and heating system the constant temperature of the jacket is ensured. The actual heat effects occur in a removable crucible inside a cylindrical calorimeter block located in the central chamber of the jacket. The temperature measurement is by means of a multiple junction differential thermocouple (thermel) with one set of junctions in the central block, the other set in the surrounding jacket.

The calorimeter is calibrated electrically. During experiments the whole assembly is maintained in an atmosphere of argon gas. Through a central "funnel" extending from the top of the constant temperature jacket to the outside of the furnace insulation and normally closed by removable plugs, crucible and samples can be introduced or removed without serious disturbance of the thermal equilibrium in the assembly.

In designing the apparatus an attempt was made to improve on the precision of earlier work by striving for an estimated accuracy of the order of $\pm 1\%$ in the actual experimental determinations. This goal has on the whole been achieved. The equipment is designed for operation below 500°. This limit in temperature is due to the extensive use of aluminum in the construction. By replacing aluminum with more heat-resistant alloys, the upper limit in temperature may be pushed substantially upward. A new apparatus, suitable for operation at higher temperatures, will be described in a later communication.

Calorimeter Construction and Operation

Furnace and Control System.—The furnace is heated by heavy Nichrome heating coils. The principal part of the furnace core consists of a 20-inch section of heavy steel pipe, about 12″ i.d. There are, in addition, top and bottom main heaters which have separate electrical connections and are

mounted in recesses in steel end plates. By adjusting the ratio of the heat inputs of the end plate heaters to that of the main cylindrical heater the temperature differential between top and bottom of the constant temperature jacket described below can be reduced to the order of 0.1°. The temperature of the furnace system is maintained constant by means of a Leeds-Northrup Micro-Max Controller-Recorder sensitive to ±1°. The hot junction of the chromel–alumel control couple is located close to the main cylindrical heating coil, while the cold junction is maintained in a dewar flask completely immersed in a room temperature thermostat. The controller coil which compensates for room temperature fluctuations is removed. The controlled load is applied through an auxiliary heating coil, wound outside and insulated from the main heater.

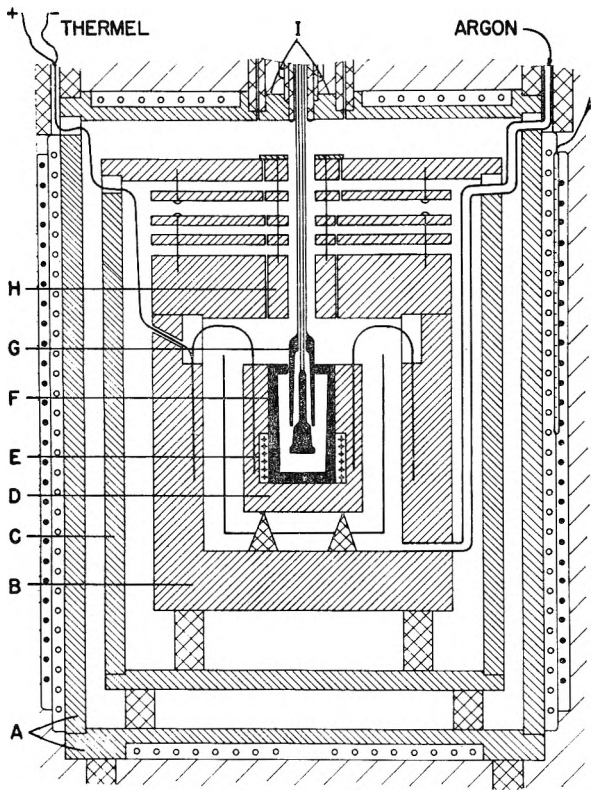

Fig. 1.—Central part of calorimeter assembly: A, furnace core with main heaters; B, constant temperature jacket; C, heavy shield; D, calorimeter block; E, calibration heater; F, removable crucible; G, charging and stirring device; H, inner plug; I, part of outer plug.

As a considerable fraction of the heat loss from the furnace occurs through the bottom and particularly through the top of the furnace system, it would have been very desirable to furnish these heaters with separate control systems. However, as control facilities suitable for this purpose were not available to the author, the heat inputs to these heaters are stabilized by means of a Sola Constant Voltage Transformer. In spite of these precautions it is never possible completely to remove long-term temperature fluctuations in the furnace system. These fluctuations can be easily detected by the very slight drift of the equilibrium deflection in the differential thermocouple–galvanometer system described below. As it was found that these fluctuations are particularly noticeable during the summer months, they are presumably due to a large extent to the effect of variations in room temperature on the heat losses through the top and bottom of the furnace assembly.

Constant Temperature Jacket and Shielding Assembly.—In the present apparatus the constant temperature jacket is made from 2S-Aluminum, is 7″ o.d. and about 12″ high (including a heavy lid). The internal chamber is 4.5″ in diameter and about 7″ high. The over-all heat capacity of the jacket is about 3000 cal./degree. The jacket is mounted on a stainless steel plate resting on supports made from alundum tubing. In the walls of the jacket near the inner surface of the cavity are located eight thermocouple wells which extend to depths varying from 4″ to 11″ below the top of the jacket. The constant temperature jacket is insulated from the heating system by a heavy shielding assembly which encloses the jacket completely. The main part of this assembly is a 16-inch section of heavy steel pipe of about 10″ o.d. The top and bottom of the assembly are closed by aluminum and stainless steel plates, respectively. The whole assembly rests on supports made from alundum tubing. The total heat capacity of these heavy shields is about 5000 cal./degree. In addition to the heavy steel shield, two lighter shields made from 1/8″ aluminum sheets are inserted in the space between the main shield and the jacket and between the shield and the furnace core. This latter space, with the exception of the top section, is also filled with Vermiculite insulating material. In order to reduce radiative heat transfer, most exposed steel surfaces are covered by foil or thin sheets of aluminum.

Calorimeter Block.—The central, cylindrical calorimeter block is made from 2S-Aluminum and has an outside diameter of 3″ and a height of 5″. It contains a removable graphite crucible, ~1.3″ i.d., 2″ o.d. and 4″ high. The heat capacity of the block assembly is about 250 cal./degree. The calorimeter block has eight thermocouple wells located symmetrically around the central axis. In the annular space between the block and the jacket there is a double radiation shield made from aluminum foil.

Differential Temperature Measuring System.—This device consists of a 16-junction thermel in connection with a sensitive galvanometer. The junctions are imbedded in alundum cement for electrical insulation. In the early work the couples were made from silver–constantan. It was found, however, that these couples did not stand up too well under extended service at the higher temperatures, and they were therefore replaced by chromel–alumel couples, made from #22 wire. The heavy wire was chosen in order to secure long-time uninterrupted service. A rough calculation shows that less than 1% of the total heat leak between jacket and block is due to the thermel.

The terminal leads of the thermel are insulated with ceramic beads and glass fiber insulation and are brought out of the furnace assembly through special channels in the multiple enclosure system. Special precautions were taken in order to prevent undesired contacts with the many metal parts. Through a thermally insulated double pole double throw knife switch the thermel is connected to a sensitive low resistance galvanometer. A decade resistance box in the circuit permits selection of a suitable galvanometer deflection for each experiment. With the chromel–alumel couples the usual resistance has been 100–150 ohms. With a resistance of 100 ohms in the circuit, a galvanometer deflection of 1 mm. at 1 meter corresponds to a temperature difference between block and jacket of the order of 0.001°.

The knife switch permits convenient determinations of the galvanometer zero by closing the galvanometer circuit without inclusion of the thermel. Because the galvanometer is used as a straightforward deflection instrument, such determinations are carried out several times during any one calorimetric experiment.

Electrical Calibration System.—The calibrating heater is wound non-inductively on a cylindrical core inside the central calorimeter block. Adequate insulation of the Nichrome heating wire is ensured by means of asbestos paper, porcelain beads and alundum cement. The total resistance of the heater is about 41 ohms and is measured by a Mueller bridge. The four nickel wires connecting the heater with the outside of the furnace are carefully insulated. The d.c. current flowing through the heater is supplied by two well-charged 6-volt lead storage batteries and is measured by the potential drop over a known manganin resistance outside the furnace system. A Rubicon portable precision potentiometer is used. When the storage batteries have been discharged through a 41-ohm dummy heater for a period of 10–15 minutes, it is found that the current is constant to better than 0.05% throughout the heating period (100–300 sec.). The heat input is timed by a Meylan precision stopwatch which permits reading to 0.05 sec. The watch is checked from time to time against an electrical chronometer.

It is estimated that the maximum uncertainty in the determination of the heat supplied to the calorimeter during a calibrating experiment is of the order of 0.2–0.3%.

Protective Atmosphere System.—During experimental runs the central part of the apparatus is flushed by a stream of argon gas. The gas is conducted into the central chamber through a stainless steel tube at a rate of 250–300 cc. per minute (measured at room temperature). Allowing for gas expansion this should ensure a flushing of the central chamber approximately once every three minutes.

Oxygen is removed from the argon by the method of Meyer and Ronge.[12] The gas is dried by passing through successive tubes containing $CaSO_4$, $Mg(ClO_4)_2$ and P_2O_5. This should provide a gas containing oxygen and water vapor at partial pressures of the order of 10^{-7} atm. In spite of these precautions it is found that the very reactive liquid metals are not completely protected against oxidation. This is presumably largely due to the fact that the furnace assembly does not provide a complete enclosure due to the various channels for electrical leads, introduction of samples, etc. It is found, however, that some additional protection is obtained by maintaining the liquid metal under a thin cover of wood charcoal. The heat generated through the reaction between the reactive impurities in the protective atmosphere and the metal and/or carbon is always negligible.

General Experimental Procedure.—The graphite crucible, which fits snugly into the central bore of the calorimeter block, is introduced through the "funnel" which connects the central chamber with the outside of the furnace. This funnel is normally closed by means of two "plugs." The inner plug is made from aluminum and stainless steel and closes the constant temperature jacket and shielding assembly. The outer plug is primarily made from refractories and thermal insulating materials and completes the heat insulation on the top of the furnace. Both plugs have a central bore $^3/_4$" in diameter which serves as a small "funnel" for the charging and stirring device. When the calorimeter is in operation, the upper part of this smaller funnel is closed by means of a refractory plug which has a small central bore of $^9/_{32}$" diameter. This allows space for the two concentric refractory tubes which connect the stirring and charging device with the outside of the calorimeter.

Under normal operations, the graphite crucible is preheated in a separate furnace to a temperature somewhat above that of the calorimeter, charged with one of the two reacting metals, and then quickly introduced into the calorimeter. In this way it is possible to introduce the charged crucible with minimum disturbance of the thermal equilibrium in the system. During the early operation of the calorimeter the system was allowed to regain equilibrium overnight after introduction of the charged crucible. Later, however, it was found to be possible to match the temperature of the central block within a few degrees, and the waiting period has been cut to three hours.

Toward the end of this waiting period the second metal or alloy sample is introduced by means of the special charging and stirring device. This device consists of two concentric graphite pieces, attached to two concentric refractory tubes. The lower parts of the two graphite pieces are tapered to form a male–female joint, providing an enclosed annular space of about 0.5" o.d. and about 0.25" i.d. By displacing the inner refractory tube with respect to the outer one, the tapered joint can be opened and the sample (which until now was contained in the annular space) is discharged into the crucible. This device has been found to work well both with liquid samples and with solid samples in the shape of ring sections.

The charging and stirring device is preheated for about 10 minutes in the upper part of the furnace proper before it is introduced into the central part of the apparatus. Under these conditions a minimum of disturbance of the thermal equilibrium in the system occurs and the calorimeter is ready for operation a few minutes later.

The stirring which is required in order to obtain a completely homogeneous liquid mixture is achieved by operating the stirring device as a plunger in the liquid metal bath. For this purpose the stirrer is connected to a motor operated cam. The vertical displacement of the stirrer is about 4 cm. and the stirring rate 4 cycles per min.

Under these conditions it was found that most mixing processes in samples of 5–25 cc. of metal were completed within 15–30 min., about 5 min. of which are due to lags in the calorimeter block. No significant change in the length of the reaction period is observed when the rate of stirring is moderately increased.

(12) F. R. Meyer and G. Ronge, *Z. angew. Chem.*, **A183**, 177 (1938).

Calculation Procedures

The Constant Temperature Jacket.—The design of the present calorimeter is based on the early work of A. Tian[13] on multiple enclosure thermostats. Tian's ideas have previously served as the basis for microcalorimeters operating at room temperature.[14,15] However, to the knowledge of the author, no really serious attempt has been made to apply these principles in high temperature calorimetry. As the considerations involved may prove important in future constructions of constant temperature systems for elevated temperatures, a brief outline of the calculations will be given.

If a thermostat consists of a central body (or a liquid bath) surrounded by one or more complete enclosures (heavy shields) thermally insulated from the central body and from each other, the temperature fluctuations of the central body may be reduced substantially by locating the control devices in the outer enclosure.

Let us assume that the temperature oscillations in the outer enclosure (the heating-control enclosure) are sinusoidal and thus given by the expression

$$T_1 = T + \frac{E}{2}\sin 2\pi\nu t \qquad (1)$$

Here T is the mean temperature of the enclosure, T_1 is its instantaneous temperature, E is the amplitude of the oscillations, while ν is the frequency of the oscillations. Let K_{12} be the coefficient of heat transfer between the two outer enclosures, namely, the heat transferred per unit time per degree temperature difference. The heat conducted from the first to the second enclosure serves to change the temperature of the latter according to the well-known differential equation

$$K_{12}(T_2 - T_1) = -C_2\frac{dT_2}{dt} \qquad (2)$$

Here C_2 is the total heat capacity of the second enclosure and T_2 is its instantaneous temperature. We have disregarded the small heat loss from the second to a possible third enclosure. For T_2 we have the well-known solution

$$T_2 = T + \frac{E'}{2}\sin(2\pi\nu t - \varphi) \qquad (3a)$$

where

$$tg\varphi = 2\pi\nu\frac{C_2}{K_{12}} \qquad (3b)$$

$$E' = E\cos\varphi \cong \frac{E}{tg\varphi}\left(\varphi \text{ near } \frac{\pi}{2}\right) \qquad (3c)$$

In the present apparatus the first complete enclosure consists of the heater core, the second is the main heavy shield of the shielding assembly, which has a heat capacity C_2 of about 5000 cal./deg. The frequency of the on-off controller system is about 6/hr. K_{12} with air insulation only was calculated to be about 3500 cal./deg. hr. at 500°, while K_{12} with Vermiculite insulation would be about 2000 cal./deg. hr. If we adopt the conservative figure of 3000 cal./deg. hr. for our mixed air–Vermiculite system, we get $E' \cong 0.03°$ for $E = 2° (\pm 1°)$.

(13) A. Tian, *J. chim. phys.*, **20**, 132 (1923).
(14) A. F. H. Ward, *Proc. Cambridge Phil. Soc.*, **26**, 278 (1930).
(15) A. V. Hill, *Proc. Roy. Soc. (London)*, **111B**, 106 (1932).

A similar argument may now be applied to the heat transfer between the second and third enclosure, which in the present case is the constant temperature jacket. We recall that $C_3 = 3000$ cal./deg., while K_{23}, the coefficient of heat transfer between the heavy shield and the jacket, is about 2500 cal./deg. hr. We thus find that the amplitude of the oscillations of the constant temperature jacket have been reduced to less than 0.001°. In fact, this figure would be even smaller if we take into account the light aluminum shields which have been disregarded in the calculations.

It should be stressed that in these calculations we have assumed the idealized case that the temperatures of the various enclosures are truly uniform, and that the control system extends over the complete surface of the outer enclosure. We have also disregarded possible drift in the mean temperature T with time.

In any practical case these ideal conditions will of course never be completely satisfied. However, in the course of the operation of the present apparatus it has been established beyond doubt that under normal experimental conditions the drift in jacket temperature due to "external" causes is always extremely small compared to the over-all temperature change of the calorimeter block during any calorimetric experiment.

Evaluation of Experimental Data.—The evaluation of calorimetric data from actual experimental observations aims at a determination of the corrected temperature change in any particular experiment.[16] If the total heat effect in the calorimetric experiment is ΔH, and the heat capacity of the calorimeter is C, we have for the corrected temperature change

$$\frac{\Delta H}{C} = \Delta T + \eta'$$

Here ΔT is the rise in calorimeter temperature during the reaction period (x-period), while η' is the temperature loss in the same period due to the exchange of heat between the calorimeter and the surroundings.

In the present calorimeter all temperature observations are differential, as we can only observe $\theta = T - T_0$, where T_0 is the temperature of the jacket. During any calorimetric experiment, heat flows from the calorimeter to the jacket and to some extent also from the jacket to the surroundings. T_0 is therefore not quite constant, and a somewhat detailed study of the evaluation procedure may therefore be justified.

The differential equation for the rate of change in calorimeter temperature is

$$C\frac{dT}{dt} = \frac{dH}{dt} + K(T_0 - T) \qquad (4)$$

Here dH/dt is the rate of heat input (through chemical reaction or electrical energy), while K is the coefficient of heat transfer between jacket and calorimeter. Similarly, we have for the jacket temperature

$$C_0\frac{dT_0}{dt} = -K(T_0 - T) + K_{10}(T_1 - T_0) \qquad (5)$$

(16) See, *e.g.*, W. P. White, "The Modern Calorimeter," Chemical Catalog Co., New York, N. Y., 1928.

K_{10} is the coefficient of heat transfer between the jacket and the surrounding enclosure which has the temperature T_1. Let us first consider the simple case $K_{10}(T_1 - T_0) = 0$. In practice this might be achieved by making the enclosure surrounding the jacket serve as an adiabatic shield for the jacket. Under these conditions we get from eq. 4 and 5

$$\frac{d\theta}{dt} = \frac{1}{C} \times \frac{dH}{dt} - K\left(\frac{1}{C} + \frac{1}{C_0}\right)\theta \qquad (6)$$

Solving for $\Delta H/C$ we get

$$\frac{\Delta H}{C} = \Delta\theta + K\left(\frac{1}{C} + \frac{1}{C_0}\right)\int_0^t \theta\, dt \qquad (7)$$

Thus

$$\eta = K\left(\frac{1}{C} + \frac{1}{C_0}\right)\int_0^t \theta\, dt \qquad (7a)$$

The quantity $\Delta\theta$ is observed directly. The effective heat leak modulus $K((1/C) + (1/C_0))$ is determined by means of the two usual rating periods ($dH/dt = 0$) immediately before and after the reaction period. The integral in η is evaluated by a graphical integration of the observed $\theta - t$ curve for the reaction period, t.

It may be noted that eq. 7 is valid for any calorimeter provided $K_{10}(T_1 - T_0) = 0$, irrespective of the heat capacity of the jacket. It generally pays, however, to make C_0 large compared to C in order to make the effective heat leak modulus as small as possible. For the truly isothermal calorimeter $C_0 \sim \infty$, $\Delta\theta = \Delta T$, and $\eta = K/C\int_0^t \theta\, dt$. In the present calorimeter $C_0/C \sim 12$, which gives an effective heat leak modulus of $13/12\ (K/C)$. This modulus depends on the geometry of the system and on the condition of the various surfaces and radiation shields. The actual values of k/c at 350 and 450° were about 0.014 and 0.017 min.$^{-1}$, respectively.

In our apparatus $K_{10}(T_1 - T_0)$ is not zero, and T_1 may vary in some manner with time due to the temperature fluctuations of the furnace assembly. A completely realistic estimate of the errors in the calculation procedure is therefore not possible. By making the simplifying assumptions that T_1 is constant and that the calorimeter assembly is in thermal equilibrium at the onset of an experiment, the author has estimated that the error introduced in the corrected temperature change if calculated by the outlined method should be of the order of 0.2% or less.

The need for application of a correction term of this order of magnitude is completely removed if the time–temperature curve of the calorimetric experiment proper is duplicated during the subsequent electrical calibration. Although such a duplication is never complete, the over-all systematic error may actually be reduced in this manner to a fraction of the calculated amount.

So far we have neglected the possible effect on the calorimetric measurements of a general lack of thermal equilibrium in the calorimeter–jacket–furnace assembly. Such a lack of equilibrium may be due to imperfections in the furnace control system itself or may arise from the manipulation of the equipment. As a result of such disturbances the temperature of the jacket may vary with time. Unfortunately, these variations in jacket tempera-

ture will normally be much too small to be determined by a thermocouple lodged in the jacket itself. They can, however, be spotted indirectly through the drift of the equilibrium temperature as indicated by our differential thermocouple system.

It is obvious that large drifts or erratic fluctuations of jacket temperature make operation of the calorimetric apparatus impossible. Generally, however, the drift in jacket temperature during the limited time required for a calorimetric experiment is very slow and apparently at a uniform rate. It is found that experiments carried out under such conditions are in good agreement with other experiments carried out when no drift in jacket temperature is indicated. The most significant effect of such drift on the actual measurements appears to be a slight variation of the calibration data. It may be concluded, therefore, that a slight uniform drift in jacket temperature does not significantly affect the usefulness of the calorimeter. It should be stressed, however, that under these conditions it is particularly important to duplicate the calorimetric experiment proper during the electrical calibration.

Example of Application

Heats of Mixing of Liquid Lead–Tin Alloys.—In the present series of experiments the integral heats of mixing of liquid lead–tin alloys were measured at 350 ± 2° and at 450 ± 2°. The over-all temperatures were determined by a chromel–alumel thermocouple calibrated at the melting point of zinc (419.4°). Although the experimental temperature fluctuated somewhat over extended periods of time, a change of the order of ±2° has no detectable effect on the measured heats of mixing (see below). The metals used were of 99.9+% purity as determined by semiquantitative spectrographic analysis.

The experiments were carried out in the manner outlined previously, with the following modifications: In these runs the charged crucible was always left in the calorimeter overnight in order to let the system regain thermal equilibrium completely. In most runs a second sample of pure metal was added to the alloy formed in the first experiment. The integral heat of mixing for the final alloy composition was then calculated by adding the heat effects obtained in the two consecutive experiments. The results are tabulated in Tables I and II and are plotted *versus* composition in Fig. 2. As the heats of mixing from the combined experiments are more uncertain than the other results, they are identified in the tables by the second digit of the run number (*e.g.*, A2). They also have a short vertical bar through the experimental point in the figure.

It will be noted that for this system the heat of mixing is essentially independent of temperature, at least in the range 350 to 450°. We may therefore compare our results with Kawakami's calorimetric data for 350° and with Elliott and Chipman's e.m.f. data for 500°.[17] As the system lead–tin does not lend itself to investigation by the more accurate direct e.m.f. method, Elliott and Chipman's data were derived indirectly from a study of the ternary system tin–lead–cadmium. It will be found from Fig. 1 that the present investigation indicates 10–15% larger heats (ΔH) of mixing than these earlier studies. It is unfortunate that the present work on lead–tin cannot be compared directly with accurate equilibrium data. For other binary systems such comparisons will be presented in a later communication.

(17) J. Elliott and J. Chipman, *J. Am. Chem. Soc.*, **73**, 2682 (1951).

Table I

Molar Integral Heats of Mixing of Pb(l)–Sn(l) at 350 ± 2°

Run No.	Total moles	Composition x_{Sn}	ΔH^M, Joule/mole	$\Delta H^M/x_{Sn}x_{Pb}$ Joule
J1	1.4429	0.0452	261.8	6066
H1	1.5857	.0494	288.0	6133
I1	1.6282	.0496	285.8	6062
E1	1.1061	.0838	475.6	6194
J2	1.5066	.0856	467.4	5974
I2	1.7098	.0949	516.3	6009
H2	1.6707	.0977	534.0	6058
F1	1.0240	.1300	690.9	6107
E2	1.1981	.1542	781.1	5989
F2	1.1643	.2346	1037	5773
G1	0.7674	.3002	1197	5698
G2	0.9983	.4621	1373	5523
B2	1.2756	.7347	1068	5479
K2	1.0102	.8182	816.1	5486
A2	1.0511	.8390	763.8	5655
B1	1.1077	.8461	720.9	5465
D2	1.3618	.8931	536.6	5621
K1	0.9121	.9062	474.6	5583
A1	0.9664	.9126	460.4	5772
D1	1.2915	.9417	308.2	5614

Table II

Molar Integral Heats of Mixing in Pb(l)–Sn(l) at 450 ± 2°

Run No.	Total moles	Composition x_{Sn}	ΔH^M, Joule/mole	$\Delta H^M/x_{Sn}x_{Pb}$, Joule
H1	1.6897	0.0438	257.9	6155
G1	1.3469	.0479	281.6	6175
F1	1.2146	.0617	353.3	6107
B1	1.0546	.0827	464.9	6133
G2	1.4176	.0954	519.5	6020
H2	1.7925	.0986	531.8	5982
A1	0.8697	.1077	590.8	6148
F2	1.2919	.1178	625.3	6018
B2	1.1583	.1647	806.7	5864
C1	0.7775	.1821	848.5	5697
A2	1.0022	.2257	1005	5748
D1	0.5864	.3017	1217	5779
C2	.9308	.3168	1197	5532
E1	.5222	.3534	1290	5645
E2	.6970	.3756	1350	5405
L2	.7622	.5742	1354	5538
M1	.5294	.6579	1228	5457
K2	1.0511	.7235	1080	5398
L1	0.5877	.7447	1053	5537
K1	0.8914	.8532	693.2	5534
J2	1.1912	.8830	575.8	5572
I1	1.0112	.9188	414.2	5555
J1	1.1216	.9377	328.4	5621
N1	1.3799	.9606	211.3	5586

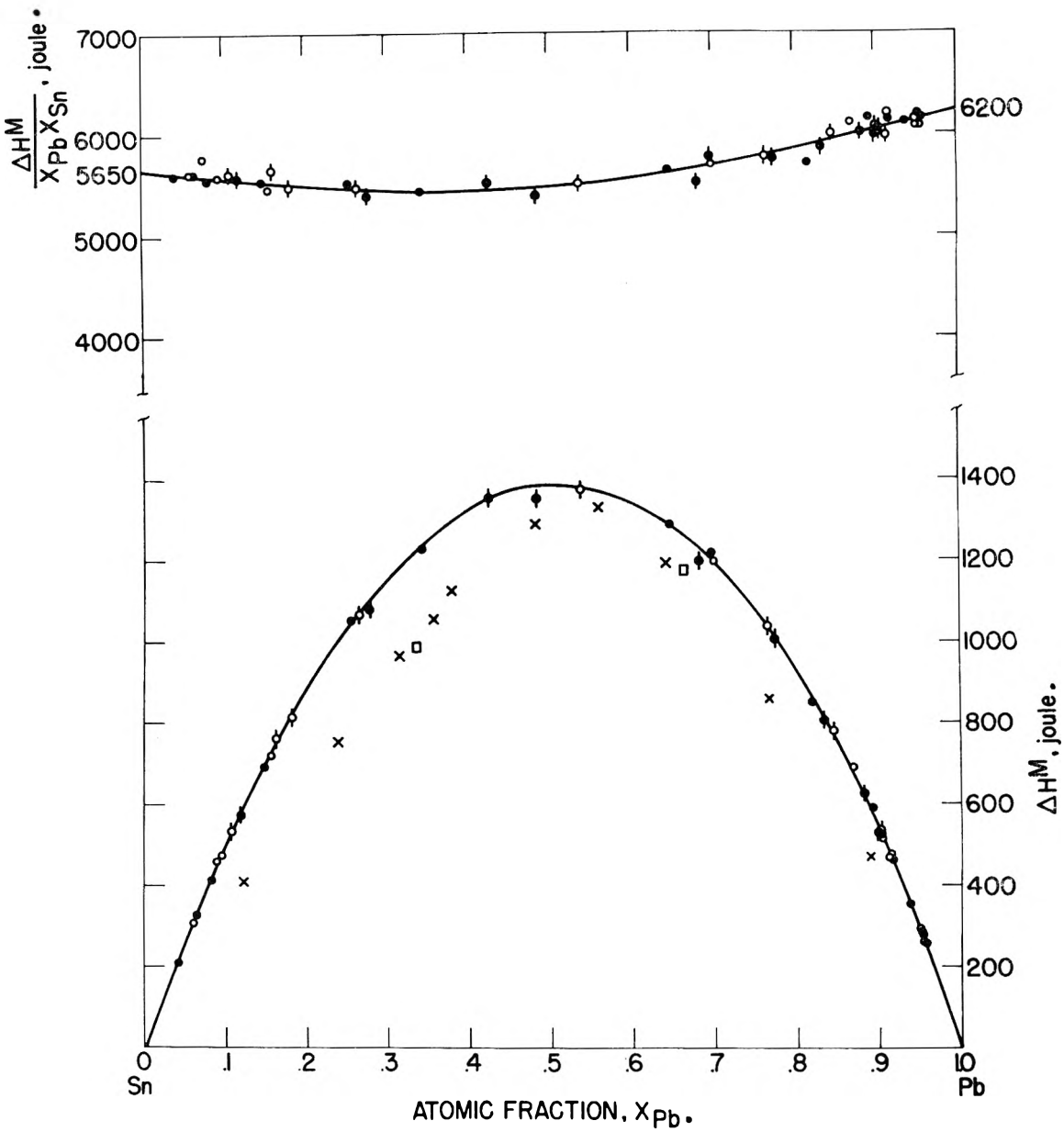

Fig. 2.—Heats of mixing of Sn(l)-Pb(l): ×, Kawakami, calorimetric, 350°; □, Elliott and Chipman, e.m.f. (indirect), 500°; ○—○, this study, 350°; ●—●, this study, 450°.

In the tables and in Fig. 1 are recorded both the molar heat of mixing, ΔH^M, and the quantity $\Delta H^M/x_{Sn}x_{Pb}$. This latter quantity is very useful for evaluation of the experimental precision. It will be noted that while the observed values of ΔH^M range from about 200 to 1400 joule/mole, the corresponding values for $\Delta H^M/x_{Sn}x_{Pb}$ fall in the range 5400 to 6200 joule. When this quantity is plotted, the observed results thus become comparable in magnitude. The plot shows that most of the experimental points deviate from the smoothed mean curve by less than 1% (~60 joule), while the maximum deviation is about 200 joule or about 3%. The plot of $\Delta H^M/x_{Sn}x_{Pb}$ is particularly valuable for determination of the relative partial molal heat contents ($\bar{L}$) from integral heat of mixing data.

If we set

$$\Delta H^M = x_A\bar{L}_A + x_B\bar{L}_B = x_Ax_BF(x) \qquad (8)$$

we have

$$\bar{L}_A = x^2_B\left[F(x) + x_A\frac{dF}{dx_A}\right] \qquad (9a)$$

$$\bar{L}_B = x^2_A\left[F(x) + x_B\frac{dF}{dx_B}\right] \qquad (9b)$$

The terms in the brackets may be obtained from the curve for $F(x)$ by geometrical construction, although the procedure is less straightforward than in the simple method of intercepts applied directly to the curve for ΔH^M. In many cases, however, the suggested procedure should prove more accurate than the conventional method.

In particular we notice that for $x_A \to 0$, $F(x) \to \bar{L}_A^0$ (the relative partial molal heat content for A in its infinitely dilute solution in B). Similarly we have for $x_B \to 0$, $F(x) \to \bar{L}_B^0$. In the present case we find $\bar{L}_{Sn}^0$ (in Pb) = 6200 joule/mole while $\bar{L}_{Pb}^0$ (in Sn) = 5650 joule/mole. The difference be-

tween these two terminal values of $F(x)$ may be used as a measure for the energetic assymmetry in the binary system. This measure is considerably more sensitive than, for example, the deviation of the maximum of the ΔH^M curve from the equi-atomic composition.

Two particularly simple cases occur when we have for all concentrations

$$dF/dx = 0 \quad (a)$$

or

$$dF/dx = \text{constant} \quad (b)$$

The former case corresponds to a completely symmetrical heat of mixing curve ("regular" solution of components of similar volumes), while the second case corresponds to the case discussed very recently by Hardy[18] under the name "sub-regular" solution.

(18) H. K. Hardy, *Acta Met.*, **1**, 202 (1953).

We note that the lead–tin system does not completely fulfill any of these very simple criteria, although either of them would represent a suitable rough approximation.

Acknowledgments.—The author is indebted to Professors J. W. Stout and N. H. Nachtrieb for reading the major part of the present manuscript and particularly for suggesting valuable improvements in the part dealing with evaluation of experimental data. He also wishes to acknowledge that the forged section of 2S-Aluminum which was used for making the thermostat jacket was a gift from the Aluminum Company of America through Dr. W. L. Fink.

This work was supported in part by the Office of Naval Research through Contract No. N-6ori-02004 with the University of Chicago.

THE INTERACTION OF PAIRS OF GAS ATOMS WITH SURFACES[1,2]

BY MARK P. FREEMAN[3] AND G. D. HALSEY, JR.

Department of Chemistry, University of Washington, Seattle, Washington

Received August 24, 1954

The interaction of rare gases with high surface area powders has been measured in the temperature range where the important contributions come from isolated atoms and isolated pairs of atoms only. The pair term governs the variation of the apparent volume of the system with pressure. The experimental values of dV/dP are compared with a crude model based on hard sphere repulsion between the surface and the atoms, and a cube law attraction between each atom and the surface. There are no adjustable parameters. The agreement between calculated and observed slopes is adequate. The systems studied are argon and neon on saran charcoal, argon on carbon black, and krypton on alumina.

Introduction

The problem of adsorption at an interface can be treated, in principle, from the same standpoint as the theory of a bulk liquid. That is, relationships can be written down that would ultimately yield a distribution function for the adsorbed molecules. Wheeler[4] has pointed out how such a calculation can be made and Ono[5] has presented some theoretical solutions. However, as Wheeler has shown, the application of this theory to the usual adsorption isotherm, even with certain approximations, involves very lengthy numerical computations.

Steele and Halsey[6] have analyzed the interactions of gas atoms with surfaces in the temperature region above the critical point of the adsorbate where the only important interactions are between isolated gas atoms and the surface. In the present paper the experiments and the analysis are extended to the next higher order interaction, that between two gas atoms and the surface. Wheeler has pointed out that this case can be written down explicitly. The gas itself in the absence of a surface will be assumed to remain effectively ideal.

Development of the Mixed Third Virial Coefficient.—We shall follow in outline the simple treatment of Mayer and Mayer.[7] The total potential energy, U, due to interactions can be written as the sum of interaction energies, u_i, between each molecule and the surface and the interaction energies, u_{jk}, between two molecules in the gas

$$U = \sum_{i=1}^{N} u_i + \sum_{j>k}^{N} \sum_{k=1}^{N-1} u_{jk} \quad (1)$$

We now define two functions

$$f_i = \exp\{-u_i/kT\} - 1 \quad (2)$$

and

$$f_{jk} = \exp\{-u_{jk}/kT\} - 1 \quad (3)$$

Then

$$\exp\{-U/kT\} = \prod_{i=1}^{N} (1 + f_i) \prod_{N \geq j \geq k \geq 1} (1 + f_{jk}) \quad (4)$$

The second product can be expanded to give

$$\exp\{-U/kT\} = \prod_{i=1}^{N} (1 + f_i) \left[1 + \sum_{N \geq j \geq k \geq 1} f_{jk} + \sum\sum f_{jk} f_{j'k'} + \dots \right] \quad (5)$$

This expression is then integrated over the coördi-

(1) This research was partially supported by Contract AF19(604)-247 with the Air Force Cambridge Research Center.

(2) Presented at the 126th National Meeting of the American Chemical Society, New York City, N. Y., September 12–17, 1954.

(3) Presented in partial fulfillment of the requirements for the Ph.D. degree.

(4) A. Wheeler, 120th National Meeting, American Chemical Society, New York City, N. Y., September 3–7, 1951.

(5) S. Ono, *Memoirs of the Faculty of Engineering, Kyushu Univ.*, **10**, 195 (1947); *J. Chem. Phys.*, **18**, 397 (1950); *Mem. Fac. Eng., Kyushu Univ.*, **12**, 9 (1950); *J. Phys. Soc. Japan*, **6**, 10 (1951).

(6) W. A. Steele and G. D. Halsey, Jr., *J. Chem. Phys.*, **22**, 979 (1954).

(7) J. E. Mayer and M. G. Mayer, "Statistical Mechanics," John Wiley and Sons, Inc., New York, N. Y., 1940, p. 263.

nates, τ_i, of all the particles throughout the available volume, V_{geo}, to yield the configuration integral

$$Q_\tau = \int_{V_{geo}} \cdots \int \prod_{i=1}^{N} (1 + f_i)\, d\tau_1\, d\tau_2 \ldots d\tau_i \ldots d\tau_N + \int_{V_{geo}} \cdots \int \prod_{i=1}^{N} (1 + f_i) \left[\sum_{N \geq j \geq k \geq 1} f_{jk} + \sum\sum_{jk\ j'k'} f_{jk} f_{j'k'} + \cdots \right] d\tau_1 \ldots d\tau_N \quad (6)$$

We now define two integrals

$$B_{AS} = \int_{V_{geo}} f_i\, d\tau_i \quad (7)$$

$$C_{AAS} = \int\int_{V_{geo}} (1 + f_1)(1 + f_2) f_{12}\, d\tau_1 d\tau_2 \quad (8)$$

Notice that if the proper irreducible integral (ref. 7, p. 287)

$$C'_{AAS} = \int_{V_{geo}} \int f_1 f_2 f_{12}\, d\tau_1 d\tau_2 \quad (9)$$

is defined, then

$$C_{AAS} = C'_{AAS} + (2B_{AS} + V_{geo})\beta \quad (10)$$

where

$$\beta = \int_{V_{geo}} f_{12}\, d\tau_2 \quad (10a)$$

However, if the gas is ideal, β is negligible and it is immaterial whether C_{AAS} or C'_{AAS} is evaluated since they are equal. We shall therefore not break down the contribution in C_{AAS}. Note that it is analogous to a gaseous mixed third virial coefficient between two atoms of a species A and one of B.

In terms of these defined integrals, the integration leads to

$$Q_\tau = (V_{geo} + B_{AS})^N \left[1 + \frac{N(N-1)}{2} \frac{C_{AAS}}{(V_{geo} + B_{AS})^2} + \cdots \right] \quad (11)$$

Ursell[8] has shown that for large N this type of expansion is correctly approximated by the form

$$\log Q_\tau = N \log (V_{geo} + B_{AS}) + \frac{N^2}{2} \frac{C_{AAS}}{(V_{geo} + B_{AS})^2} \quad (12)$$

from which

$$P = kT \frac{\partial \log Q_\tau}{\partial V_{geo}} = \frac{NkT}{(V_{geo} + B_{AS})} - N^2 \frac{kT\, C_{AAS}}{(V_{geo} + B_{AS})^3} \quad (13)$$

The area is held constant during this differentiation. This corresponds to holding the quantity of the second component (the solid surface) constant. Also, the integral C_{AAS} has been treated as if it were independent of volume, whereas eq. 10 indicates that only the proper irreducible integral C'_{AAS} is truly independent. Thus, a term proportional to β has been neglected. This neglect is possible because the relatively low pressure and small volume compared to the large surface area used in our experiments make contributions from bulk gas imperfections totally negligible.

It is convenient to express the experimental results in terms of the apparent volume of the system as defined by the ideal gas law, rather than the number of molecules N

$$V = N(kT/P) \quad (14)$$

If we make this substitution in (13), we find

$$P = \frac{kT(B_{AS} + V_{geo})^2}{V\, C_{AAS}} - \frac{kT(B_{AS} + V_{geo})^3}{V^2 C_{AAS}} \quad (15)$$

At zero pressure V becomes its limit, V_0, and we find

$$V_0 - V_{geo} = B_{AS} \quad (16)$$

the expression used by Steele and Halsey.[6]

In the experiments reported here, we have measured the slope dV/dP, which by differentiation of (15) is

$$dV/dP = 1/(dP/dV) = V^3 C_{AAS}/\{2kT(V_{geo} + B_{AS})^3 - kTV(V_{geo} + B_{AS})^2\} \quad (17)$$

Near zero pressure where V approaches $V_{geo} + B_{AS}$, (17) becomes

$$dV/dP\big|_{P=0} = C_{AAS}/kT \quad (18)$$

This is the result we require.

Crude Model for C_{AAS}.—We shall extend the crude model of Steele and Halsey[6] in as simple a way as possible in order to compute the integral C_{AAS}. We shall retain the assumption that at the hard sphere distance D_{GS} the solid–gas interaction is ϵ^* and that this energy then falls off with the third power of the distance. We shall assume in addition that the gas atoms have a hard sphere diameter for self repulsion D_{GG} and that other than this they do not interact. Thus f_{12} (see eq. 3) is -1 when the spheres overlap and zero elsewhere. We shall therefore perform our integration between the limits of contact of the sphere with the value -1 for f_{12}. D_{GG} and δ, the ratio between D_{GS} and D_{GG}, are the only new parameters we introduce.

The coördinate system we use is as follows (Fig. 1): z_1 and z_2 are the perpendicular distances of the atoms from the surface; L is the distance between these perpendiculars; and the angular orientation of gas atom 2 with respect to gas atom 1 we denote by θ, a cyclic coördinate. If for $d\tau_1$, we use $dA\, dz_1$ and for $d\tau_2$ we use $L\, dL\, d\theta\, dz_2$, then the integral (see eq. 2, 8) becomes (remembering $f_{12} = -1$)

$$C_{AAS} = -\int_A \int_{z_1} \int_\theta \int_{z_2} \int_L \exp\{\epsilon_1/kT + \epsilon_2/kT\}\, L\, dL\, d\theta\, dz_2\, dA\, dz_1 \quad (19)$$

where the limits of z_1 are from D_{GS} to $V_{geo}/A \sim \infty$, z_2 goes from D_{GS} to $z_1 + D_{GG}$ when $D_{GS} > (z_1 - D_{GG})$ and otherwise the lower limit is the latter expression, L goes from 0 to $\sqrt{D^2_{GG} - (z_1 - z_2)^2}$, and θ from 0 to 2π.

If the integral is rewritten in terms of reduced lengths where D_{GG} is 1 (see Fig. 1) and the ratio D_{GS}/D_{GG} is δ, then the integral becomes

$$C_{AAS} = -D^4_{GG} \int_A \int_{\sigma_1} \int_{\sigma_2} \int_{\sigma_L} \int_\theta \exp\left\{\frac{\delta^3 \epsilon^*}{kT}(1/\sigma_1^3 + 1/\sigma_2^3)\right\} \sigma_L\, d\sigma_L\, d\theta\, dA\, d\sigma_2\, d\sigma_1 \quad (20)$$

where $\epsilon^*/z^3_i = -\epsilon_i/D^3_{GS}$ and the limits are now: σ_1 goes from δ to V_{geo}/AD_{GG}; σ_2 goes from δ when δ is greater than $\sigma_1 - 1$ and otherwise from $\sigma_1 - 1$ to $\sigma_1 + 1$; θ's limits are as before; and σ_L goes

(8) See R. H. Fowler, "Statistical Mechanics," Cambridge University Press, Cambridge, 1936, p. 241.

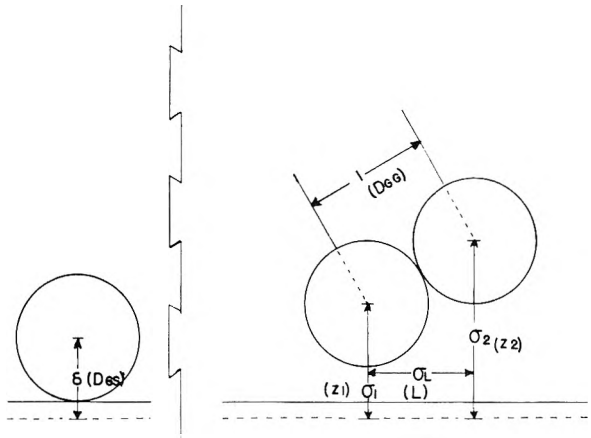

Fig. 1.—Schematic representation of the coördinate system.

from 0 to $\sqrt{1 - (\sigma_1 - \sigma_2)^2}$. After the analytic integrations are performed, we have

$$C_{AAS} = -2\pi A D_{GG}^4 \int_{\sigma_1} \int_{\sigma_2} \frac{\sigma^2 L}{2}\Big|_{\sigma L} \exp\{\delta^3\epsilon^*/kT(1/\sigma_1^3 + 1/\sigma_2^3)\}\, d\sigma_1\, d\sigma_2 \quad (21)$$

which becomes

$$C_{AAS} = -\pi D^4_{GG} \int_{\sigma_1} \exp\{\delta^3\epsilon^*/kT\sigma_1^3\} \int_{\sigma_2} \exp\{\delta^3\epsilon^*/kT\sigma_2^3\} \sqrt{1 - (\sigma_1 - \sigma_2)^2}\, d\sigma_1\, d\sigma_2 \quad (22)$$

This integral was evaluated graphically.

The dimensionless quantity log $\{-C_{AAS}/AD^4_{GG}\}$ is plotted as a function of ϵ^*/kT for various values of the parameter δ in Fig. 2. This reduced form of representation will be employed below to compare the experimental data with the results of the crude theory.

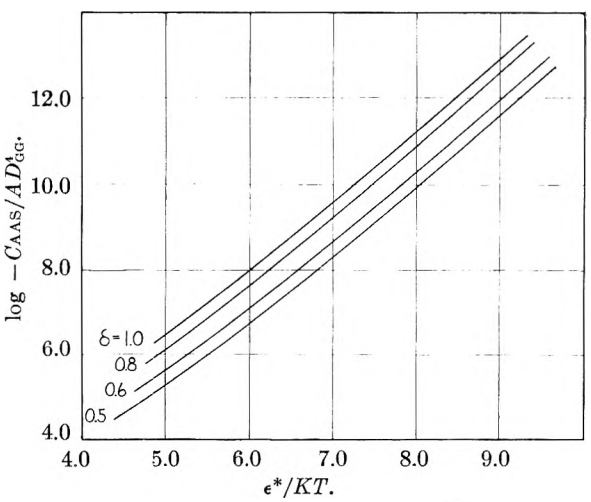

Fig. 2.—Calculated values of log (C_{AAS}/AD^4_{GG}) for various values of the parameter δ.

Experimental Results.—The apparatus and general procedure have been described in a previous paper.[6] The rare gases were obtained in sealed bulbs from the Air Reduction Company. In the earlier paper the data consisted of isosteres, performed over a range of temperatures such that the quantity ϵ^*/kT varied from unity to a maximum of about six. Over this range, when the total pressure is about 200 mm., the apparent volume was shown to be effectively independent of pressure. In the present work the temperature range has been extended down to an ϵ^*/kT value of about eight. Over this range the apparent volume becomes a linear function of pressure. Therefore V was determined as a function of P, and the results fitted to a straight line by the method of least squares. The slope of this line, dV/dP, was then compared with the calculated values of C_{AAS} by means of eq. 18.

In Fig. 3 the experimental data for krypton on alumina are shown; it is clear from these data, which are typical, that the degree of experimental accuracy is not high. The hysteresis shown on reversing the order of taking the points is within the experimental error, however, which confirms the applicability of an equilibrium theory to these measurements. The crudeness of the theory, the uncertainty in the assignment of a value to D_{GG}, and the absence of any adjustable parameter combine to make the degree of accuracy adequate.

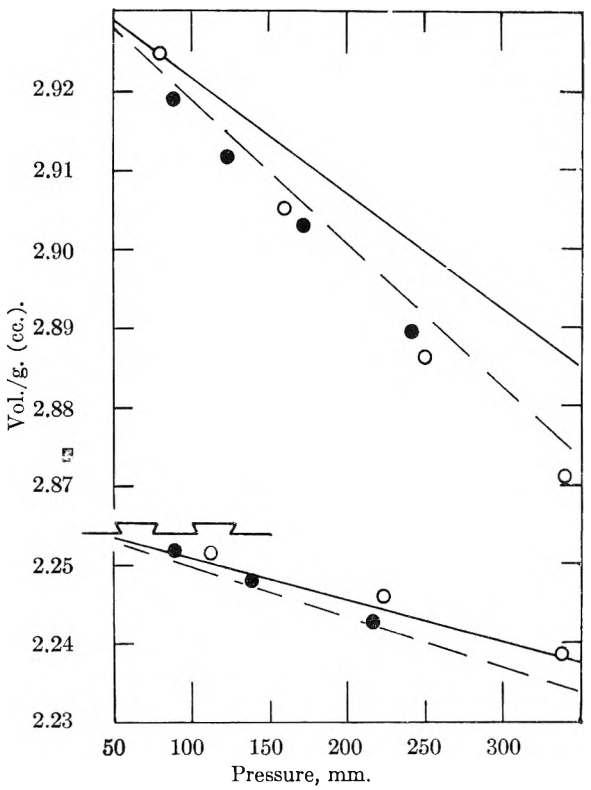

Fig. 3.—Interaction of krypton with alumina at 0° (top) and 30.2°: ○, increasing pressure; ●, decreasing pressure; ——, theoretical slope based on viscosity D_{GG}; ------, theoretical slope based on critical volume D_{GG}.

The solids have been investigated previously; the carbon black and alumina are described,[6] and the high surface area saran charcoal is described.[9] The parameters used for calculating C_{AAS} are given in Table I; all values are from the previous work except D_{GG}. For this distance the tabulated values[10] of hard sphere diameters estimated from viscosity data have been used. In the case of krypton

(9) W. A. Steele and G. D. Halsey, Jr., THIS JOURNAL, **59**, 57 (1954).

(10) Joseph O. Hirschfelder, R. Byron Bird and Ellen L. Spotz, *Chem. Revs.*, **44**, 205 (1949).

Table I

Adsorbent	Gas	ϵ^*, kcal.	A, m.²/g.	D_{GG}, Å.	D_{GS}, Å.
Carbon black	Argon	4.34	262	3.42	2.75
Alumina	Krypton	3.46	141	3.61	1.99
				(3.96)[a]	
Saran S-85	Argon	3.66	1030	3.42	2.90
	Neon	1.28	1135	2.80	2.55

[a] Calculated from the critical volume.

we have also made calculations using the rather widely differing value based on critical volume to illustrate the effect of uncertainties in D_{GG}.

In Fig. 3 the calculated slopes are drawn in with the intercept defined by the least-square line. The agreement is surprisingly good. In Fig. 4 the data for argon on carbon black are compared with the

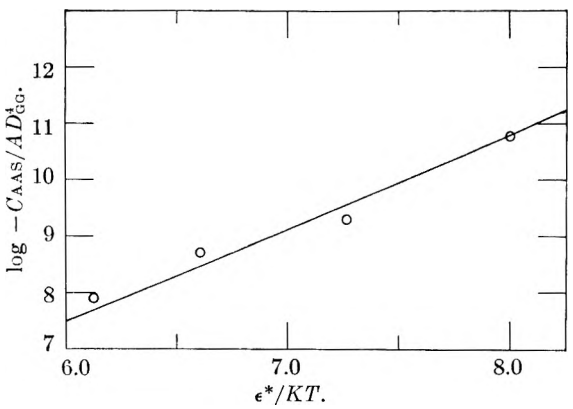

Fig. 4.—Reduced plot of data for argon on carbon black compared with theoretical line.

theoretical line in reduced form. It is clear that the temperature dependence of C_{AAS} is correctly accounted for by the theory. The results for neon and argon on saran charcoal are similarly presented in Fig. 5. The numerical comparison of the least-squares slopes and the theory is given in Table II.

Conclusions.—If one considers the crudeness of the model, the close agreement between theory and experiment found here is surprising. A similar (and

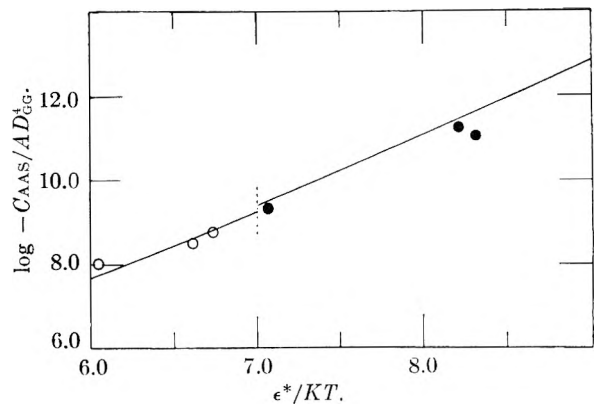

Fig. 5.—Argon (left) and neon (right) on Saran charcoal.

Table II

Adsorbent	Gas	Temp., °C.	Slope (cc./g.)mm.Hg × 10^4 Calcd.	Obsd.
Carbon black	Argon	0.00	62.1	60.2
		27.71	13.1	16.4
		57.85	5.29	6.82
		84.3	2.25	2.70
Alumina	Krypton	0.00	1.51	2.17
			(1.84)[a]	
		30.2	0.528	0.528
			(0.635)[a]	
Saran S-85	Argon	0.00	34.0	32.1
		5.09	26.4	24.2
		31.0	10.1	13.6
	Neon	−195.7	806.0	538.0
		−194.7	679.0	645.0
		−182.1	87.3	83.4

[a] Based on D_{GG} calculated from the critical volume.

apparently fortuitous) agreement has been observed with the crude theory for B_{AS}.[9] The introduction of a Lennard-Jones potential between the gas atom and the surface led to less reasonable values for the area than did the crude theory. It is possible that refinements in the model for C_{AAS} will cause similar difficulties. It is clear, however, that the theory of imperfect gases is suitable for the interpretation of the interaction of gases with solids.

THE VAPOR PRESSURE OF IRON(II) BROMIDE

By R. O. MacLaren and N. W. Gregory

Contribution from the Department of Chemistry, University of Washington, Seattle, Washington

Received August 30, 1954

The vapor pressure of $FeBr_2$ has been measured using the effusion, transpiration and diaphragm methods, covering the temperature interval 350 to 900°. The accommodation coefficient is found to be unity.

In connection with equilibrium studies on the iron–bromine system, it became necessary to know the vapor pressure of $FeBr_2$. We have made measurements between 400 and 640° using the transpiration method with argon as the carrier gas. The quantity of $FeBr_2$ transported was determined by a colorimetric technique which enabled convenient determination of vapor pressures as low as 10^{-3} mm. At the lower temperatures results have been compared with data obtained by the effusion method (350–445°). Pressures were also measured between 600 and 900° in a quartz diaphragm gage. An independent determination of the triple point was made by differential thermocouple cooling curve analysis.

Experimental

$FeBr_2$ was prepared by reaction of anhydrous bromine with iron powder (Eimer and Amend, electrolytic). The product was sublimed as Fe_2Br_6 in a bromine atmosphere at 450°; the condensate, a mixture of iron(II) and iron(III) bromides, was then heated at 120° *in vacuo* to decompose

the iron(III) phase and $FeBr_2$ finally sublimed *in vacuo* at 520°. Four independently prepared samples (typical analysis: % Fe, 25.94 (theo. 25.90); % Br 74.08 (74.10)) were used in the various experiments.

Transpiration.—A schematic diagram of the Pyrex glass apparatus is shown in Fig. 1. For experiments above 550° the transpiration chamber A was constructed of quartz. Prior to each experiment the argon was passed through liquid potassium (at 80°) at M to assure the absence of water vapor, bromine and oxygen. The purified gas was condensed in B with liquid nitrogen (v.p. of argon 209 mm. at −196°); the nitrogen was then replaced by liquid oxygen (v.p. of argon 1015 mm. at −183°). Flow through the vaporization chamber was induced by opening stopcocks C connecting with the argon collecting tube D immersed in liquid nitrogen. The flow rate was regulated between 12 and 40 ml./min. by changing capillary orifices at E. The argon collected during a given experiment was vaporized and its pressure measured in the calibrated flask F; it was then returned to storage to be recycled in the next experiment.

Before introduction of the argon, the transpiration chamber was evacuated and baked out and $FeBr_2$ sublimed in from the sublimation tube G, subsequently removed. The furnace, preheated to operating temperature, was placed around A and flow of argon begun after the temperature had stabilized (two to five minutes). Above 550° flow was reversed (from D to B) through stopcock H during the temperature equilibration period to minimize diffusion of $FeBr_2$ into the collector tube. The temperature was controlled within ±2° and measured with three calibrated chromel–alumel thermocouples spaced around the apparatus. A smaller furnace K, kept within 10° of the main furnace, was used to preheat the carrier gas.

The transported $FeBr_2$ was removed from the collector tube L in a dry-box and the quantity determined colorimetrically as the iron(II) complex with *o*-phenanthroline by a method similar to that described by Hiskey,[1,2] using a Beckman (DU) spectrophotometer at wave length 510 mμ, an absorption maximum of the complex. Quantities of $FeBr_2$ as small as 0.8 mg. may be determined easily, enabling pressures as low as 10^{-3} mm. to be measured conveniently. Above 650°, the amount of $FeBr_2$ collected was sufficient to determine by dichromate titration. The duration of the various transpiration experiments ranged from 30 to 130 minutes.

Diaphragm Gage.—Above 625° direct measurement of the vapor pressure was made in a quartz diaphragm of the Daniels type.[3] Deflections of a slender quartz pointer (20 cm. long), sealed to the diaphragm, were observed through a 40-power microscope giving a sensitivity of about 1 mm. The gage, volume approximately 35 ml., was connected by graded seals and waxed ground-glass ball joints to the vacuum line and mercury manometer. It was used as a null point instrument, the zero position determined before and after a series of measurements. No irreversible shift in null point was noted; appreciable pressure differentials were not allowed to develop at high temperatures.

Measurements were made on three independent samples of 1.10, 0.72 and 0.10 g. of $FeBr_2$, sublimed into the gage under high vacuum after outgassing at 900°. The desired temperatures were produced by an electric furnace with independent elements at top, bottom and sides in which the currents could be adjusted to keep the temperature uniform throughout (maximum variation ±2°). Measurements were made varying the temperature in a comparatively random manner. Small residual gas corrections (determined from measurements below 600°) were necessary in two of the three series (2.0 mm. and 4.0 mm. at 800°K.).

Effusion.—Measurements from 350° to 445° were made in four different cells to determine the magnitude of the accommodation coefficient of $FeBr_2$.

	Cell length, cm.	Cell diameter, cm.	Orifice diameter, cm.	Orifice thickness, cm.	K
1	3.5	1.7	0.037	0.0175	0.67
2	3.5	1.7	.0839	.02	.81
3	3.5	1.7	.137	.005	.96
4	4.5	2.5	.50	.050	.86

The factor K was evaluated as discussed by Whitman[4] to correct for the effect of the geometry of the cells on molecular flow. Cells 2 and 3 were constructed of nickel; 1 of monel (a slight reaction of copper in the monel with $FeBr_2$ was indicated by the appearance of a small amount of insoluble material with the effused $FeBr_2$ which appeared to be cuprous bromide). The fourth cell was made of Pyrex glass. The metal cells were equipped with tight fitting screw caps; orifices were made with drills and machined to the indicated thickness on a lathe. The glass orifice was prepared by grinding a hole in a piece of Pyrex plate with a brass sleeve and tapering the outside with a tapered rod (carborundum used as abrasive).

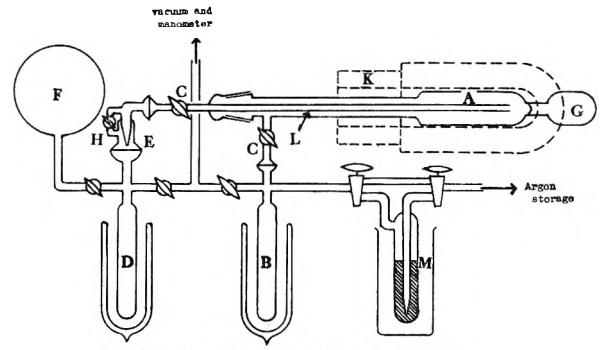

Fig. 1.—Transpiration apparatus.

Sublimed $FeBr_2$ was added to the metal cells (in a dry-box) which were then placed in a glass tube (30 mm. diameter) and attached to the vacuum line. The temperature was determined by a thermocouple placed in direct contact with the metal, the leads coming out through a wax seal at the cold end of the tube. The furnace was preheated to the desired temperature and slipped over the tube to initiate the run. A time–temperature curve was plotted to determine the actual period of effusion. $FeBr_2$ leaving the cell condensed on the glass surface just outside the furnace. It was removed in the dry-box and determined colorimetrically. At the higher temperatures, direct titration could be used for the larger quantities collected from the glass cell. With the glass cell, the effused material was removed after cracking the glass tube between the orifice and the condensation zone in the dry-box. A steel ball was placed over the orifice while resealing prior to a subsequent run. A summary of the effusion results follows

Effusion cell	Temp., °K.	Time, min.	Quantity $FeBr_2$ effused, mole	P_{mm}
4	623	1124	3.28×10^{-5}	2.16×10^{-6}
3	658	1247	2.70×10^{-5}	1.54×10^{-4}
4	666	230	9.82×10^{-5}	2.73×10^{-4}
2	668	408	5.73×10^{-6}	3.24×10^{-4}
1	682	891	4.13×10^{-6}	6.78×10^{-4}
3	688	95	9.18×10^{-6}	7.55×10^{-4}
1	699	542	5.56×10^{-6}	1.51×10^{-3}
2	707	129	9.86×10^{-6}	1.82×10^{-3}
1	711	363	6.58×10^{-6}	2.72×10^{-3}
3	712	131	4.05×10^{-5}	2.45×10^{-3}
4	717	87	4.24×10^{-4}	3.09×10^{-3}
2	718	124	1.85×10^{-5}	3.58×10^{-3}

The triple point of $FeBr_2$ was confirmed by differential thermocouple cooling curve analysis. A 1.5-g. sample was placed in a 12-ml. quartz tube provided with a thermocouple well, degassed at 400° in high vacuum before sealing, and compared against a similar tube filled with NaCl. The triple point was indicated by a sharp break in the potential difference–time curve.

Results and Discussion

The results obtained by the various methods are shown in Fig. 2. The straight lines correspond to the equations

(1) C. F. Hiskey, *Anal. Chem.*, **21**, 1440 (1949).

(2) C. F. Hiskey, J. Rabinowitz and I. G. Young, *ibid.*, **22**, 1464 (1950).

(3) F. Daniels, *J. Am. Chem. Soc.*, **50**, 1115 (1928).

(4) C. I. Whitman, *J. Chem. Phys.*, **20**, 161 (1952).

Method	Temp., range, °C.	$\log_{10} P_{mm} = -\frac{A}{T} + B$ A	B	ΔH, kcal.
$FeBr_2(s) = FeBr_2(g)$				
Transpiration	(400–689)	10,294	12.045	47.1 ± 0.5
Effusion	(350–445)	10,300	11.88	47.1 ± 1
Diaphragm	(620–689)	12,100	13.90	55 ± 10
$FeBr_2(l) = FeBr_2(g)$				
Diaphragm	(689–909)	6,912	8.450	31.6 ± 1

The transpiration data are shown as open circles, diaphragm as solid circles, and effusion as half filled circles. The diaphragm data extend below the triple point, although the experimental uncertainty, indicated by the length of the vertical lines, is a large fraction of the total pressure in this range. Fifty-seven measurements were made with three independent samples in the diaphragm gage. Only one of the series is shown in Fig. 2 for simplicity. The equations for the transpiration data and the diaphragm measurements in the liquid range were obtained by a least squares treatment. The average of the absolute deviations of log $P_{expt.}$ from log $P_{calc.}$ were 1.08% (tr.) and 0.75% (D).

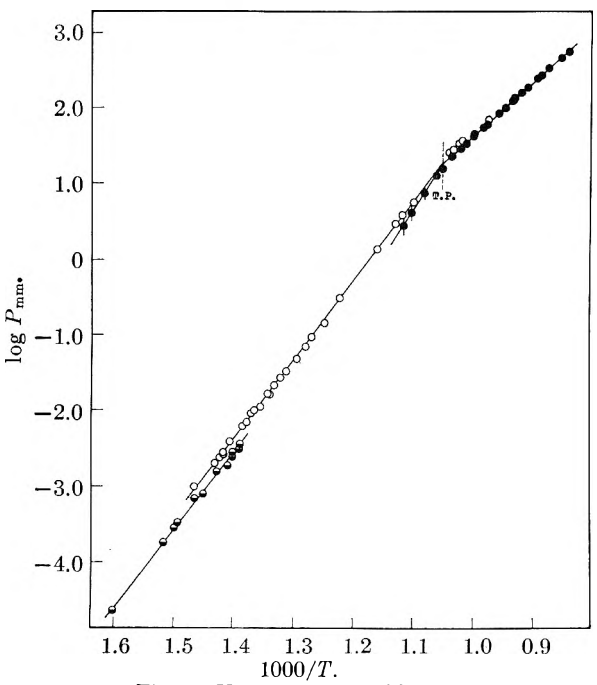

Fig. 2—Vapor pressure of $FeBr_2$.

Data from all four effusion cells are shown. The excellent agreement of values from the various cells indicates that the accommodation coefficient may be taken as unity, and the steady state effusion pressures as equilibrium pressures.

The present study is believed to be the first in which a direct comparison of vapor pressures measured by effusion and transpiration has been possible without the uncertainty associated with extrapolation. The effusion pressures are found to be only 70% of the transpiration values (diaphragm pressures about 85%). This deviation, while not extremely large, seems appreciably beyond experimental error. Several possible causes have been considered, none of which suggests a satisfactory explanation for the difference. The transpiration experiments gave consistent results with various flow rates (from 12 to 40 ml./min.) indicating that diffusion did not contribute materially to the quantity of $FeBr_2$ collected. Transpiration pressures would appear high if the argon–$FeBr_2$ mixtures were appreciably non-ideal. Pressures were calculated from the number of moles transported, assuming perfect gas behavior. Significant argon–$FeBr_2$ interaction seems unlikely at the pressures and temperatures involved, however. At partial pressures of the order of 10^{-3}–10^{-2} appreciable interaction of $FeBr_2$ molecules is not expected; molecular flow is assumed in the effusion cell. The effect of the pressure of argon on $FeBr_2$ crystals would only be expected to increase the vapor pressure by about 1%. The presence of polymerized groups would influence calculated effusion and transpiration pressures in the same way. Comparison of pressures based on the molecular formula $FeBr_2$ with those actually measured in the diaphragm gage indicates that the monomer is the principal species throughout the entire temperature range studied. Diaphragm and transpiration values could be made to agree near the melting point if one assumed the vapor to contain 5–15% dimer. However, evidence for further association at lower temperatures is not observed. Effusion and diaphragm values appear to correlate well assuming no appreciable concentration of dimer.

The heats of sublimation from all methods agree well within experimental error. Taken with the heat of vaporization a value of 15 ± 2 kcal. is obtained for the heat of fusion, somewhat higher than expected.[5] The triple point of 691°, calculated from the vapor pressure equations, is slightly above the previously reported melting point of 684°,[7] but agrees well with 689 ± 2° obtained by the differential thermocouple cooling curve analysis. An estimated heat of fusion of 11 ± 3 kcal. was obtained by comparing the areas under the differential cooling curves for NaCl and $FeBr_2$ over their respective melting ranges. The boiling point of $FeBr_2$, obtained by extrapolation of diaphragm pressures, is 967°.

No evidence for disproportionation of $FeBr_2$ into iron and iron(III) bromide was observed. Such a reaction would have been readily detected in transpiration or effusion experiments.

We wish to acknowledge support of this work by the Office of Ordnance Research, U. S. Army.

(5) L. L. Quill, "Chemistry and Metallurgy of Miscellaneous Materials: Thermodynamics," National Nuclear Energy Series IV-Vol. 19B, McGraw-Hill Book Co., New York, N. Y., 1950, p. 202.

(7) A. Ferrari, A. Celeri and F. Giorgi, *Atti accad. nazl. Lincei*, **9**, 782, 1134 (1929).

NOTES

CHLORIDE UPTAKE BY ION-EXCHANGE MEMBRANES IN DIFFERENT CHLORIDE SOLUTIONS

By N. Krishnaswamy

Division of Plastics and Polymers, National Chemical Laboratory of India, Poona, India.

Received August 17, 1954

In an earlier communication[1] the method of preparation of synthetic cation-exchange membrane discs has been described along with their Donnan diffusion properties in sodium chloride solutions. It was decided to extend the study to different salt solutions in order to observe the effect of ionic charge, ionic size and valency on the Donnan diffusion properties of the cation-exchange membranes. For this purpose Disc 63 (a phenolsulfonic acid–formaldehyde condensation product) and Permionic CR-51 (sample obtained from Ionics Inc., U.S.A., with their Bulletin No. 1) were chosen and this note describes the results obtained in sodium chloride, barium chloride and hydrochloric acid solutions.

Experimental

The membranes were completely converted to the sodium, barium and hydrogen forms for estimation of the chloride uptake at different external concentrations of sodium chloride, barium chloride and hydrochloric acid, respectively. The amount of chloride absorbed was determined by the procedure described earlier.[1] In the acid cycle the acidity was determined by titration with standard sodium hydroxide solution.

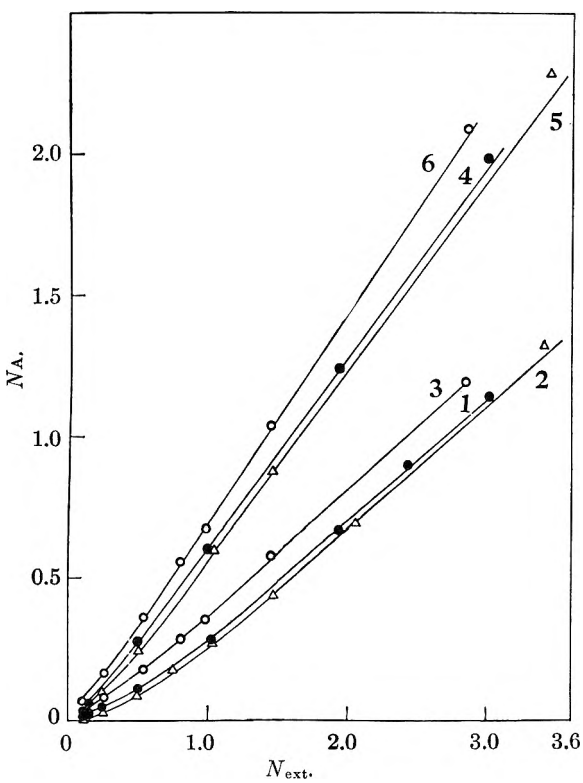

Fig. 1.—Relationship between normality of chloride absorbed (N_A) and the external chloride concentration (N_{ext}) in different solutions: 1, CR 51 in NaCl; 2, CR 51 in HCl; 3, CR 51 in $BaCl_2$; 4, Disc 63 in NaCl; 5, Disc 63 in HCl; 6, Disc 63 in $BaCl_2$.

(1) N. Krishnaswamy, *J. Sci. Ind. Res. (India)*, **13B**, 722 (1954).

Results

From the dimensions of the membranes measured in the different solutions the concentration of chloride absorbed by the resin phase (N_A) was calculated.

Figure 1 shows the relationship between the normality of chloride absorbed (N_A) and the external chloride concentration (N_{ext}).

Figure 2 reveals the variation of the ratio N_A/N_{ext} with the external concentration N_{ext} for the two samples in different solutions.

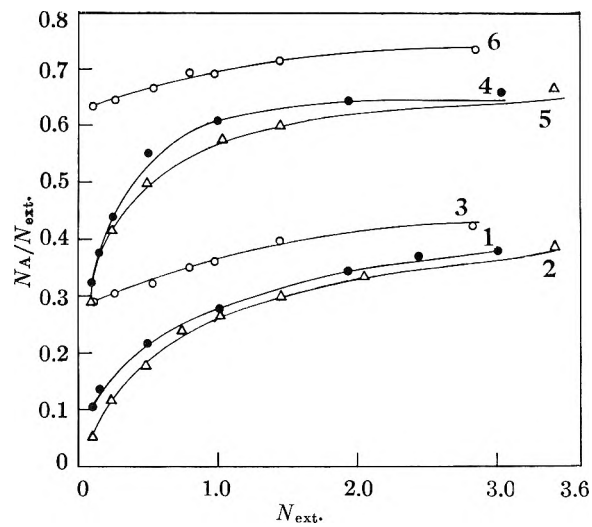

Fig. 2.—N_A/N_{ext} *vs.* N_{ext}: 1, CR 51 in NaCl; 2, CR 51 in HCl; 3, CR 51 in $BaCl_2$; 4, Disc 63 in NaCl; 5, Disc 63 in HCl; 6, Disc 63 in $BaCl_2$.

It is seen that the chloride uptake in barium chloride solution by both the samples differs from the chloride absorbed in sodium chloride and hydrochloric acid solutions. Thus, curves 3 and 6 in Fig. 2 are seen to differ from the others and the trend of these two curves in the dilute concentration range (up to 1.0 N) indicates less of variation in chloride uptake by changing the external concentration.

Further work is in progress with other salt solutions of alkali and alkaline earth metals to evaluate the Donnan diffusion characteristics.

THE DENSITY OF *n*-OCTANE AND 2,2,3,3-TETRAMETHYLBUTANE AT LOW TEMPERATURES

By G. J. Rotariu, D. W. Fraga and J. H. Hildebrand

Department of Chemistry and Chemical Engineering, University of California, Berkeley, California

Received August 16, 1954

The measurements here reported were made in order to extend to low temperatures the compari-

son between the molal volumes of *n*-octane and 2,2,3,3-tetramethylbutane, discussed by Hildebrand before the Faraday Society.[1] Our figures were obtained by weighing known masses of the solid substances under liquid nitrogen, under methyl alcohol at the sublimation temperature of CO_2, and, in the case of the $C_2(CH_3)_6$, under cold water and under liquid hydrogen. The density of n-C_8H_{18} at liquid hydrogen temperature, 0.948, is known through the observations of Heuse.[2]

Materials.—"Synthetic" *n*-octane from the Matheson Co. was used without further purification. The $C_2(CH_3)_6$ was vacuum distilled from material generously furnished by Dr. G. Calingaert, of purity stated as 99.69%, and melting point 100.69°.

Procedure.—Samples were either frozen about a copper wire or in a heavy copper cup. Each sample was thoroughly degassed in the liquid state, and moisture was carefully excluded. Details can be furnished upon request. The densities of liquid hydrogen and methyl alcohol at the temperatures used were determined by weighing a 10-g. brass weight immersed therein.

Results are given in Table I.

TABLE I

DENSITIES OF n-C_8H_{18} AND $C_2(CH_3)_6$

Octane	Immersing liquid	t, °C.	Density	Av.
n-C_8H_{18}	N_2	−195.8	0.919, 0.917, 0.910	0.915
	CH_3OH	− 75.0	.860, .855	.857
$C_2(CH_3)_6$	H_2	−252.8	.932	.932
	N_2	−195.8	.893, .911, .897, 0.903	.901
	CH_3OH	− 73.8	.850, .844	.847

From these densities and those at higher temperatures obtained by Timmermans[3] for n-C_8H_{18}, and by Seyer, Bennett and Williams[4] for $C_2(CH_3)_6$, we calculated the molal volumes of these two octanes plotted[1] in Fig. 1.

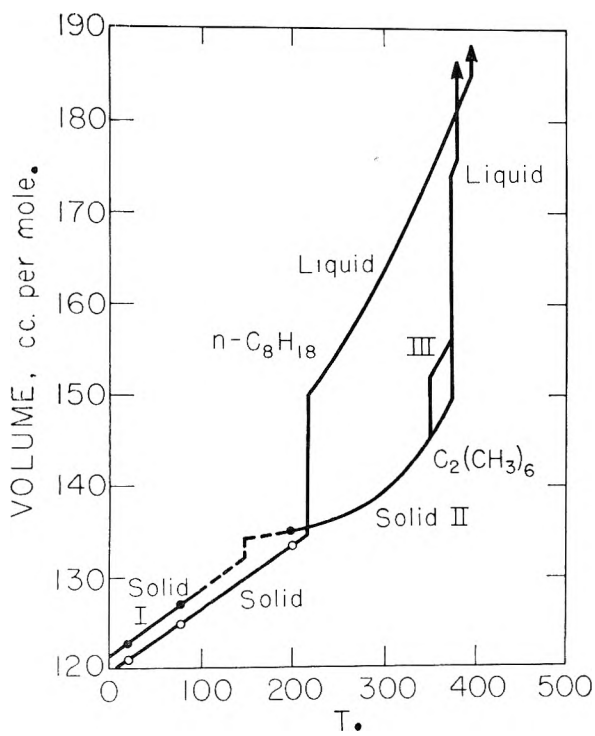

Fig. 1.

It is noteworthy that although the more symmetrical octane occupies a larger volume at low temperatures, as would be expected by analogy with the relative packing of spheres and rods, the reverse is true with their liquids. There is an interesting parallelism between the volume of $C_2(CH_3)_6$ and its entropy in the same range, from the measurements of Scott, Douslin, Gross, Oliver and Huffman.[5]

This work was supported in part by the Atomic Energy Commission.

(1) J. H. Hildebrand, *Faraday Society Disc.*, **15**, 9 (1953).

(2) W. Heuse, *Z. physik. Chem.*, **A147**, 266 (1930).

(3) J. Timmermans, "Physico-Chemical Constants for Pure Organic Compounds," Elsevier Pub. Co., Inc., New York, N. Y., 1950, p. 86.

(4) W. F. Seyer, R. B. Bennett and F. C. Williams, *J. Am. Chem. Soc.*, **71**, 3447 (1949).

(5) D. W. Scott, D. R. Douslin, M. E. Gross, G. D. Oliver and H. M. Huffman, *ibid.*, **74**, 883 (1952).

THE SOLUBILITY OF CHLORINE IN CARBON TETRACHLORIDE

BY THOR L. SMITH[1]

Contribution from Experiment Station, Hercules Powder Company, Wilmington, Delaware

Received August 30, 1954

Theories concerning solubility of non-electrolytes have been developed, primarily, by Hildebrand[2] and associates. To test and develop these theories, solubility data are needed of non-electrolytes in various solvents and over wide temperature ranges.

Some years ago the solubility of chlorine in carbon tetrachloride at 0, 19 and 40° was measured by Taylor and Hildebrand.[3] These data are still used in discussing solution theories,[4] since no additional solubility data have been reported.

In this paper, the solubility of chlorine in carbon tetrachloride from 40 to 90° is given. It appears that the solubility at 40° reported by Taylor and Hildebrand is slightly low. Our results combined with their solubility data show that the solutions

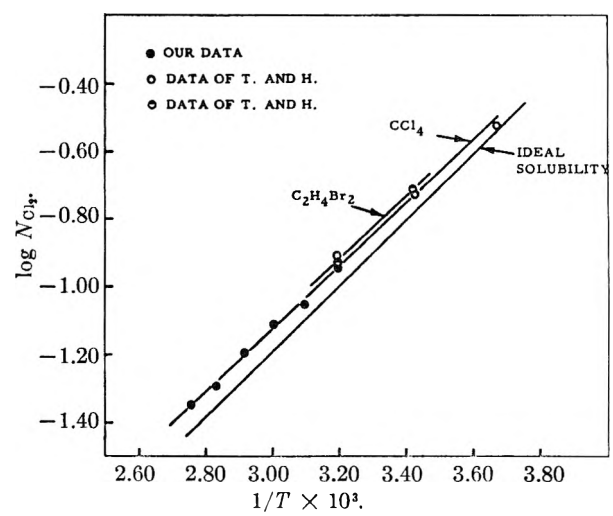

Fig. 1.—Solubility of chlorine in carbon tetrachloride and ethylene bromide.

(1) Jet Propulsion Laboratory, California Institute of Technology, Pasadena, California.

(2) J. H. Hildebrand and R. L. Scott, "Solubility of Non-electrolytes," Third edition, Reinhold Publ. Corp., New York, N. Y., 1950.

(3) Nelson W. Taylor and J. H. Hildebrand, *J. Am. Chem. Soc.*, **45**, 682 (1923).

(4) J. Chr. Gjaldbaek and J. H. Hildebrand, *ibid.*, **72**, 609 (1950).

deviate from ideality less than was previously assumed. Also, the solubility curves for chlorine in carbon tetrachloride and in ethylene bromide, shown in Fig. 1, are parallel instead of crossing as shown earlier.[4]

TABLE I

SOLUBILITY OF CHLORINE IN CARBON TETRACHLORIDE

Temp., °C.	Total pressure (atm.)	Moles Cl_2/(kg. soln.)/(atm. Cl_2)	N_{Cl_2}/Atm. Cl_2
40	2.02	0.797	
	2.36	0.789	
		Av. 0.793	0.115
50	2.02	0.590	
	2.36	0.602	
		Av. 0.596	0.0875
60	2.02	0.522	
	2.36	0.522	
		Av. 0.522	0.0771
70	2.36	0.417	
	2.36	0.433	
		Av. 0.425	0.0632
80	2.36	0.340	
	2.70	0.329	
		Av. 0.335	0.0502
90	2.70	0.296	0.0444

Experimental.—The solubilities were determined using a two-bulb glass apparatus with a pressure stopcock and a spherical joint between the upper and lower bulbs. The upper bulb was partially filled with distilled carbon tetrachloride and heated for several minutes in a hot bath (130–140°) in order to degas the solvent and sweep the air out of the bulb. A 20% solution of potassium iodide was added to the lower bulb which was then weighed and attached to the upper bulb. The apparatus was connected to a cylinder of chlorine (The Matheson Company) and immersed in a thermostat regulated to ±0.1°. After flushing the connecting tubing with chlorine several times, the apparatus was agitated by hand until the total pressure in the system, measured with a calibrated Bourdon gage, remained constant. The stopcock was then turned, allowing a sample of saturated chlorine solution to flow into the potassium iodide solution. The lower bulb was detached and weighed. The amount of iodine liberated by the chlorine was determined by titrating with standard sodium thiosulfate solution using starch solution as the end-point indicator.

Discussion.—The results of the solubility measurements are given in Table I. The total pressures at which the measurements were made are given along with chlorine solubilities expressed both as moles of chlorine/1000 grams of solution/atmosphere chlorine partial pressure and as mole fraction of chlorine/atmosphere chlorine partial pressure. The partial pressures of carbon tetrachloride were calculated from the vapor pressure of carbon tetrachloride[5] assuming Raoults law, and the partial pressures of chlorine were obtained by difference.

Figure 1 shows our solubility data along with the solubility data of Taylor and Hildebrand[3] for chlorine in carbon tetrachloride and in ethylene bromide. Also shown are the ideal solubilities, f/f^0, calculated previously.[3]

It appears that the two solubility lines do not intersect, as previously reported,[3,4] and consequently the chlorine–carbon tetrachloride solutions show less deviation from ideality above 40° than predicted by an extrapolation of the earlier data.

(5) J. Timmermans, "Physico-Chemical Constants of Pure Organic Compounds," Elsevier Publishing Co., New York, N. Y., 1950, p. 225.

EXCHANGE BETWEEN HEAVY WATER AND CLAY MINERALS[1]

BY JOSEPH A. FAUCHER[2] AND HENRY C. THOMAS
Department of Chemistry, Yale University, New Haven, Conn.

Received September 20, 1954

Water associated with a clay mineral may either be an integral part of the crystal lattice, as OH groups, or bound more or less loosely to the clay in a variety of ways. We report here experiments of a somewhat preliminary nature on exchanges between the water of clays and added deuterium oxide done in the hope of adding to our knowledge on the nature of clay water and the intimacy of its contact with the structural hydroxyl groups.

The exchange of deuterium oxide directly with the hydroxyl groups of two clay minerals has been studied by McAuliffe, Hall, Dean and Hendricks[3] who found with kaolinite and halloysite complete and rapid H–D exchange with surface OH groups and a slow diffusion into the lattice at elevated temperatures. These workers used clay intensively dried *in vacuo*. The present work was done with air-dried material, *i.e.*, with material containing much free water, and the exchange results correlated with weight-loss curves done at temperatures up to 800°.

Experimental

The procedure for most of the exchanges was as follows. About 0.5 g. of clay of known water content was accurately weighed into a small glass centrifuge tube, heavy water added, and the tube again weighed. The tube was tightly closed, shaken vigorously and allowed to stand overnight. After more shaking the tube was centrifuged and the supernatant liquid (about 0.5 g.) removed. The water mixture was distilled in a short-path molecular type still, used merely for ease in handling the small samples, closed to the outer atmosphere through a drying tube. The distillates were analyzed by means of a Zeiss dipping refractometer equipped with the auxiliary prism for small samples. Temperature control for the refractometer was provided by a water-bath at 30.00 ± 0.03°. The instrument was set against water, taking $n = 1.33196$ at 30°. Our stock of 99.65% D_2O gave a reading corresponding to $n = 1.32754$ for pure D_2O. Luten[4] gives 1.32760 for pure D_2O at 30°. Compositions of mixtures were computed taking the refractive index as a linear function of mole fractions, according to Luten an excellent approximation. Two synthetic mixtures of H_2O and D_2O gave results within the error of reading the instrument, about 0.00002 in n. This instrumental uncertainty entails gross errors in the analysis of mixtures of low H_2O content, hence our experiments were done with as large a ratio of clay to added D_2O as could be conveniently handled. Even so, the determination of small exchanges is subject to large error.

Weight loss curves on the minerals were obtained simply by heating samples in platinum crucibles in a regulated muffle furnace for periods of 12–24 hours at each temperature. Temperatures were measured on a thermocouple placed near the crucibles.

(1) Contribution No. 1248 from the Sterling Chemistry Laboratory of Yale University, New Haven, Connecticut.

(2) 22 Hamilton Place, Garden City, N. Y.

(3) C. D. McAuliffe, N. S. Hall, L. A. Dean and S. B. Hendricks, *Proc. Soil Sci. Soc. Amer.*, **12**, 119 (1947).

(4) D. B. Luten, *Phys. Rev.*, **45**, 161 (1934).

Results and Discussion

Kaolinite.—American Petroleum Institute Reference Clay No. 4, Macon, Georgia. The clay lost 1.3% at 60°, 2% at 400°, 3% at 450°, 13% at 500°, and a total of 14.7% on ignition, the curve showing the familiar sharp rise corresponding to the destruction of the mineral. With heavy water no exchange outside the error of our determination was found. The surface moisture and exposed OH groups undoubtedly exchanged, but according to McAuliffe, *et al.*,[3] the magnitude of this effect corresponds to our experimental error in this region. We also observed no significant exchange on heating the clay–D_2O mixture at 200° for a day in a Parr bomb.

Halloysite.—A.P.I. No. 13, Eureka, Utah. The heating curve was similar to that obtained by Ross and Kerr[5] and showed an initial rapid loss of 6% up to 60°, a gentle rise to 9.5% at 400°, a steep rise to 19% at 500°, followed by a gentle rise to 20.7% at ignition temperature. The exchange results on this material show points of considerable interest. (In the following discussion results of the exchange experiments will be given in terms of the percentage of water in the mineral apparently coming to equilibrium with the added D_2O, designated % E.W. Thus complete exchange on the halloysite would give 20.7% E.W.) At room temperature the average of eight experiments gave 12.5% E.W., the range of the experiments being 11.8–13.3%. Experiments done in the Parr bomb at 200° gave 17.0% E.W. (six determinations between 15.8 and 18.6%). At room temperature no significant difference in the extent of exchange was observed on increasing the time of contact to 48 hours. At 200° contact for 24 hours gave 15.8 and 16.0%; contact for 96 hours gave 18.0 and 18.6%. These results may be explained if we suppose, as appears reasonable from the structure of the mineral, that in halloysite, in addition to the relatively small amount of surface hydroxyl, all interlayer water together with three-quarters of the water of constitution (*i.e.*, those hydroxyl groups in contact with the interlayer water) are exchangeable. We suppose further, in analogy with the results on kaolinite, that in completely dehydrated metahalloysite no water of constitution is exchangeable. Assuming ideal formulas, we compute from the weight loss data that our clay can be considered as a mixture of 39.3% completely dehydrated metahalloysite and the remainder completely hydrated halloysite. We are thus led to a calculated value of 13.7% E.W., to be compared with the average experimental value of 12.5%. If in addition we suppose that under pressure at 200° metahalloysite is rehydrated, we compute for the high temperature limit 17.5% E.W., in agreement with the experimental finding. This discussion must be considered as tentative only, particularly as regards the assumed rehydration of metahalloysite.

Attapulgite.—A.P.I. No. 26, Quincy, Florida. The heating curve obtained is entirely different in character from those of the other clays, being always convex upward. It shows an initial sharp rise to 6% at 60°, followed by a nearly linear increase to 15.5% at 500°, finally reaching 16.7% at ignition temperature. The shape of this curve allows no differentiation between various "kinds" of water in the mineral. This is borne out, although somewhat roughly, by the exchange results, which gave 14.0, 14.9, 17.2, 18.9 % E.W. These results are consistent with the structure assigned to attapulgite by Bradley[6] which implies an intimate contact between the hydroxyl groups and the water present in the channels of the crystal.

Chabazite.—For comparison with the results on attapulgite similar experiments were done with a sample of finely ground chabazite. The heating curve is very similar to that of attapulgite and showed a total water content of 21.8%. After 24-hour contact with D_2O at room temperature two experiments showed complete exchange, again indicative of the intimate contact between OH groups and intra-lattice H_2O.

Montmorillonite. A.P.I. No. 23, Chambers, Arizona.—The weight loss curve showed the characteristic two-step form, the first step corresponding to a loss of 17%, followed by a relatively sharp rise to 21.1% on ignition. Five exchange experiments at room temperature with contact times from 24 to 120 hours gave 19.7% E.W. (range 19.4–20.0%). A single experiment with contact time 5 min. gave 18.9%, indicating that the exchange is very rapid, as was to be expected. These results imply that only 93% of the total water of the mineral exchanges with added D_2O. To confirm this result in a less ambiguous manner the following experiment was done. About 8 g. of clay was washed four successive times with 99% D_2O over a period of two days. The final wash liquid, after centrifuging and distilling, showed 1.5 mole % H_2O. The wet clay was quickly transferred to a large nickel boat and placed together with a thermocouple in a long combustion tube. Dry nitrogen (from a sulfuric acid bubbler and two magnesium perchlorate tubes) was passed slowly over the clay as it was gradually heated in a furnace. Water was condensed from the effluent gas in a cooled U-tube, protected from the outside air by magnesium perchlorate. During the first stage the tube was gradually heated to 150°, at which point the U-tube was emptied. This water also contained 1.5 mole % H_2O. A second sample was collected between 150 and 180°, which showed 7.3% H_2O. At this point a clay sample was removed from the boat which on ignition showed 5.5% of volatile matter remaining. From the heating curve this is seen to be largely OH water. A dry U-tube was put in place, and the clay heated rapidly to 800°. About 0.4 ml. more water was collected which contained 52 mole % H_2O.

These experiments are best interpreted in terms of the now generally accepted structure of montmorillonite in which no OH groups are exposed to interlayer water. The heating experiment alone does not rule out a modified Edelmann–Favajee structure in which part of the OH water is exchangeable. Although the data are not of sufficient precision to permit of a definite conclusion, it appears

(5) Ross and Kerr, U. S. Geological Survey, Professional Paper 165-E. 1931.

(6) W. F. Bradley, *Am. Min.*, **25**, 405 (1940).

reasonable that the increase in the H_2O content of the water evolved up to 180° is due to an increased rate of diffusion through the lattice. The final water collected up to 800° now necessarily contains much exchanged D_2O.

For an excellent summary, with references, of present ideas on montmorillonite structure and with important confirmatory evidence see Karsulin and Stubican.[7]

A single experiment at room temperature on a sample of bentonite from Clay Spur, Wyo., showed the E.W. to be 94% of the total water in agreement with the above experiments.

This work was done under the auspices of Brookhaven National Laboratory, Upton, New York, to which it is a pleasure to acknowledge our indebtedness.

(7) M. Karsulin and Vl. Stubican, *Monatsh.*, **85**, 343 (1954).

LIGHT SCATTERING FROM CRYSTALLIZING POLYMERS

BY FRASER P. PRICE

General Electric Research Laboratory, The Knolls, Schenectady, N. Y.

Received September 24, 1954

Crystallizable high polymers when cooled from above the melting point frequently developed crystalline regions in the form of spherulites. While the nature of these structures is still not completely elucidated, and therefore is still the subject of much investigation,[1,2] almost certainly they are not single crystals in the usual crystallographic sense. The investigations of spherulite structure have, thus far, been confined to examination with light or electron microscopes. Both these techniques are incapable of examining the crystals in the very early stages of their formation.

This note describes a brief and very cursory light scattering investigation of crystal development in polychlorotrifluoroethylene. This technique affords a means of examining the crystalline regions very close to their beginning. The results were somewhat unexpected and hence, in spite of their brevity, are deemed worthy of presentation.

Experimental

Polychlorotrifluoroethylene was obtained from M. W. Kellogg Company of Jersey City, N.J., under the trade name Kel-F. The material was from the same batch on which previous investigations of spherulite formation had been made.[3]

Measurements were carried out in a light scattering apparatus which permitted observation of scattered light down to within about 2° of the primary beam. Light of wave length 4358 Å. was used. The polymer sample, a 0.012 in. thick pressed sheet, was clamped to an electrically heated hot stage of low heat capacity mounted normal to the light beam. The low heat capacity of the hot stage made it possible to heat and cool the polymer very rapidly (250 to 150° in 30 sec.). The temperature was controlled to ±3° by a thermocouple-actuated relay system. It was necessary to clean the polymer sheet very carefully to eliminate bubbles from decomposing lint at the elevated temperatures.

After the polymer sheet had been placed in the apparatus, the temperature was raised to 250° for five minutes. The temperature was then allowed to drop rapidly to a predetermined fixed value below the melting point. Measurements of scattered light were made with the photometer at 4 and 16° with respect to the primary beam. Since the refractive index of the amorphous polymer was found to be 1.427 these angles correspond to scattering angles of 2.80 and 11.13° within the sample. The scattered light from the melted sheet was subtracted from that of the crystallizing sheet to correct for the small scattering from foreign particles in the matrix. The light from the melted sheet was never more than few per cent. of that from the crystallizing sheet, and the hot stage itself showed no variation in scattered light with changing temperature.

Results and Discussion

If one considers a block of material composed of small well separated regions of one refractive index imbedded in a matrix of different index of refraction, then from the theory of light scattering[4] it is possible to define an average square distance, ρ^2, within the small regions as

$$\overline{\rho^2} = \frac{\Sigma n_i V_i^2 \overline{r_i^2}}{\Sigma n_i V_i^2} = \frac{3\lambda^2}{4\pi^2} \frac{D-1}{DS_2^2 - S_1^2} \qquad (1)$$

where

$\overline{\rho^2}$ = mean square radius of the scattering regions
n_i = no. of particles of ith kind
V_i = vol. of particles of ith kind
$\overline{r_i^2}$ = mean square distance from center of gravity in scattering particles of ith kind
λ = wave length of light in the matrix
$D = \left(\frac{\text{light scattered at } 4°}{\text{light scattered at } 16°}\right)\left(\frac{1 + \cos^2 11.13°}{1 + \cos^2 2.80°}\right)$
$S_1 = 2 \sin 1.40°$
$S_2 = 2 \sin 5.57°$

Equation 1 was derived assuming no secondary scattering. If a Lambert type law is assumed for diminution of the scattered light due to secondary scattering, then since the path lengths for the 16 and 4° scattered light differ by only 4% only a negligible change in D would result. The inclusion of this correction will affect the quantitative but not the qualitative aspects of the conclusions presented below.

Figure 1 shows D as a function of time for the sample of polychlorotrifluoroethylene quenched from 250° to various crystallization temperatures. Even though the light scattered at a given angle increased with time, these results show that D and hence the root mean square radius decreased with increasing time.

It is surprising that the average size decreased as crystallization proceeded. This might result from any one of three causes; first the average shape of the scattering regions might change in such a way as to produce a decrease in the radius; second the crystallites might actually break up under the stress induced by volume changes resulting from crystallization; third, and most probable, the crystallites might be nucleated faster than they can grow. It is reasonable to expect that large crystallites would appear rapidly from the liquid magma because, in this state, the long chains are relatively free to move about and to line up with each other. As the crystallization proceeds, however, because

(1) A. Keller, *et al.*, *Nature*, **169**, 913 (1952); **171**, 170 (1953); *J. Polymer Sci.*, **11**, 215, 567 (1953).

(2) G. Schuur, *ibid.*, **11**, 325 (1953).

(3) F. P. Price, *J. Am. Chem. Soc.*, **74**, 311 (1952).

(4) P. Debye, THIS JOURNAL, **51**, 18 (1947).

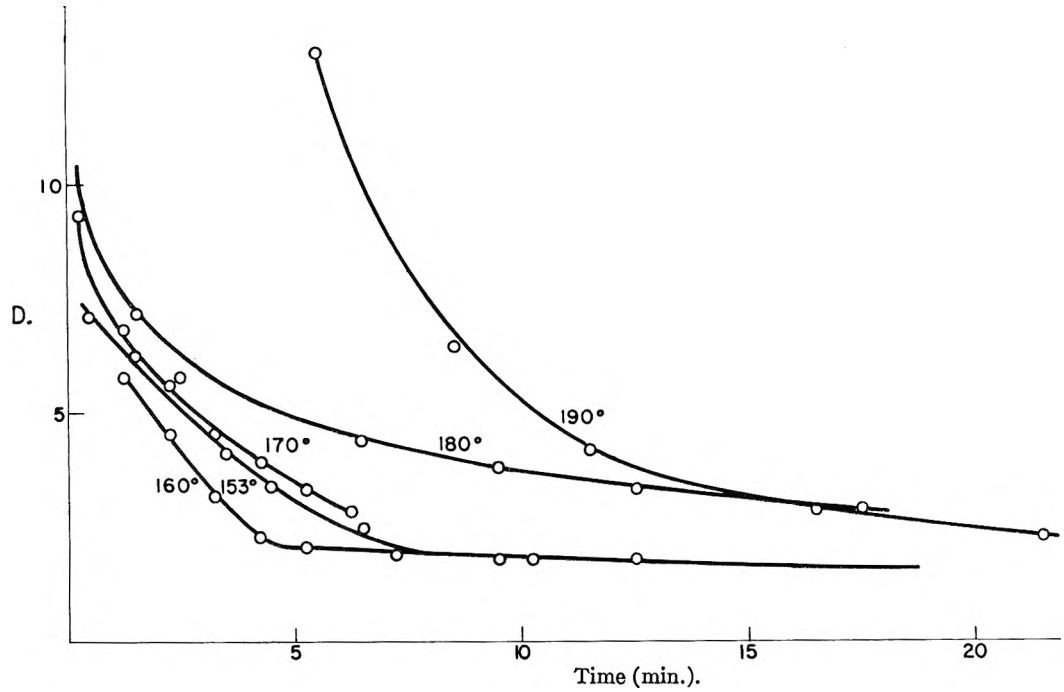

Fig. 1.—Dissymmetry, D, as a function of time for several growth temperatures.

the previously crystallized portions of some of the chains tend to freeze in the chain entanglements, the remainder of the molecules must crystallize much more slowly into smaller crystallites. Therefore, one would expect that the few crystallites formed initially would be quite large, while those formed later would never attain this size. This mechanism has already been suggested for polyethylene.[5] If, in addition, the nucleation rate were high compared to the growth rate, then the fractions of crystallites in the smaller size groups would become larger causing the average size to decrease. The phenomenon of decreasing D with increasing time has also been observed for crystallizing polyethylene.[6]

It will be noted from Fig. 1 that the time rate of change of D and hence size is a maximum at a growth temperature of about 160°. The 153° and the 170° runs both show at a given time, higher values of D and hence larger values of $(\overline{p^2})^{1/2}$ than does the 160° run. This observation is in accord with the prediction made previously[3] that there should be a maximum in the growth rate as the temperature is lowered.

The results presented in Fig. 1 indicate that the scattering regions have dimensions in the range of 0.4 to 0.7 μ. Spherulites in this material attain sizes approaching 200 μ in radius. The light scattered by such single particles, scattering as units, is probably small. It has been shown[3] that the crystallinity in this material as detected by X-rays develops at a much greater rate than does that determined from spherulite volumes. The present investigation shows rates of crystallization which approximate the rates of the spherulite growth rather than the rates of the crystallization detected by X-rays. Therefore, the crystallites that the light-scattering method detects are probably those which compose the spherulites and certainly are not the same ones detected by X-rays.

(5) M. Dole, *et al.*, *J. Chem. Phys.*, **20**, 781 (1952).
(6) Private communication from F. Bueche.

ORDER THESE SPECIAL PUBLICATIONS FOR YOUR PERMANENT RECORDS

Selected For Reprinting Solely On The Basis Of Their Importance To You

UNIT OPERATIONS REVIEWS

1st Annual Review	$0.50
2nd Annual Review	0.50
4th Annual Review	0.50
5th Annual Review	0.50
6th Annual Review	0.50
7th Annual Review	0.75
8th Annual Review	0.75
9th Annual Review	0.75

FUNDAMENTALS REVIEWS

1st Annual Review	0.75
2nd Annual Review	0.75

UNIT PROCESSES REVIEWS

1st Annual Review	0.50
2nd Annual Review	0.50
5th Annual Review	0.75
6th Annual Review	0.75
7th Annual Review	1.50

MATERIALS OF CONSTRUCTION REVIEWS

2nd Annual Review	0.75
3rd Annual Review	0.50
4th Annual Review	0.75
5th Annual Review	0.75
6th Annual Review	0.75
7th Annual Review	0.75

ANALYTICAL CHEMISTRY REVIEWS

2nd Annual Review	1.50
3rd Annual Review	1.50
5th Annual Review	0.75

RESOURCES SYMPOSIA

Southwest	0.50
Far West	0.50
New England	0.75
Mid Atlantic	0.75
Rocky Mountain—Part 1	0.75
East North Central States	0.75

MISCELLANEOUS REPRINTS

Raman Spectra	0.35
Corrosion Testing in Pilot Plants	0.25
Atmospheric Contamination and Purification Symposium	0.75
Titanium Symposium	0.50
Absorption and Extraction Symposium	0.75
Adsorption Symposium	0.50
Careers in Chemistry & Chemical Engineering	1.00
Information Please Symposium	0.50
Dispersion in Gases	0.50
Statistical Methods in Chemical Production	0.50
Liquid Industrial Wastes Symposium	0.75
Nucleation Phenomena	0.75
Chemical Facts and Figures—1952	1.00
Corrosion Data Charts	0.75
Synthetic Fibers	1.00
Chemical Progress in 1952	0.75
Chemical Facts and Figures	1.50
Process Kinetics Symposium	0.75
X-Ray Symposium	0.75
Emulsion Paints	0.75
Industrial Process Water Symposium	0.75
Symposium on Pilot Plants	0.75
Symposium on Boiler Water Chemistry	0.75
Flow through Porous Media	0.75
Process Instrumentation Symposium	0.75
First Air Pollution Review	0.50
Synthetic Detergents Symposium	0.75

ADVANCES IN CHEMISTRY SERIES

No. 4, Searching the Chemical Literature	2.00
No. 5, Progress in Petroleum Technology	3.00
No. 6, Azeotropic Data	4.00
No. 7, Agricultural Applications of Petroleum Products	1.50
No. 8, Chemical Nomenclature	2.50
No. 9, Fire Retardant Paints	2.50
No. 10, Literature Resources for Chemical Process Industries	6.50
No. 11, Natural Plant Hydrocolloids	2.50

MISCELLANEOUS

Seventy-Five Eventful Years (History of the ACS)	5.00
Chemistry—Key to Better Living	4.00
Combination of Seventy-Five Eventful Years and Chemistry—Key to Better Living	7.50
List of Periodicals Abstracted by Chem. Abs.	3.00
Faculties, Publications, and Doctoral Theses in Chemistry and Chemical Engineering at U. S. Universities	2.00
10 Years Numerical Patent Index (1937–1946)	6.50
27 Year Collective Formula Index	80.00
2nd Decennial Index to Chemical Abstracts	100.00
3rd Decennial Index to Chemical Abstracts	150.60
4th Decennial Index to Chemical Abstracts	120.60

[Supply of the above items is limited, and each will be sold only until present stock is exhausted.]

Order from: Special Publications Department, American Chemical Society
1155 Sixteenth Street, N.W., Washington 6, D. C.